Studies on the Eukaryotic Chaperonin CCT

by

Mikayala D. A. King

A thesis submitted to the University of Kent for the Degree of PhD in Biochemistry in the Faculty of Science, Technology and Medical Studies.

September 2003

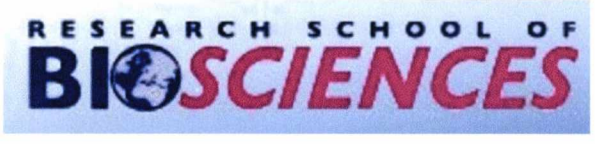

Declaration

No part of this thesis has been submitted in support of an application for any degree or qualification of the University of Kent or any other university or institute of learning.

Mikayala D. A. King

April 2004

Acknowledgements

I would like to thank my supervisor, Dr. Martin Carden, for his help and support and for giving me the opportunity to work on this project. I would also like to thank Dr. Anne Roobol for her help, support and unnerving ability to answer any question put to her, no matter how obscure and also for being an absolute pleasure to work with over the last few years.

I would also like to thank Dr. Angela Dunn for her help with all things yeast and prion and for supplying me with the yeast cells and plasmids used in this study.

I would also like to thank Judy Hardy for preparing the peptides used in this study and Brian Cover and Sarah Reed for injecting the animals used in this study and for collecting sera during antibody production.

Finally I would like to thank my friends and family for their continued support, understanding and enthusiasm for my studies.

'Many of the truths we hold to depend greatly on our own point of view.'
George Lucas 1982

Contents

Title i

Declaration ii

Acknowledgements iii

Contents v

Abbreviations xii

List of Figures xiv

List of Tables xvii

Abstract xviii

Chapter 1: Introduction

1.1 Introduction 1

1.2 The Molecular chaperones and Chaperonins 2

1.3 Group I chaperonins 3

1.4 Group II chaperonins 6

1.5 Molecular chaperonin – mediated protein folding 10

1.6 Substrate proteins of CCT 14

1.7 Other cellular functions of CCT 18

1.8 Aims 21

Chapter 2: Materials and Methods

2.1 Materials 24

2.2 Cells 25

2.2.1 Yeast cell cultures 25

2.2.2 Transformation of *Saccharomyces cerevisiae* 25

2.2.3 Bacteria 26

2.2.4 Transformation of bacteria 27

2.2.5 Animal (ND7/23) cells 27

2.2.6 Immunocytochemistry 29

2.3 Protein analysis 30

2.3.1 Mammalian tissue lysate extraction 30

2.3.2 ND7/23 cell lysate extraction 30

2.3.3 Mammalian cell lysate labelling 31

2.3.4 Yeast lysate extraction 32

2.3.5 Yeast lysate labelling 33

2.3.6 Immunoprecipitation (IP) 33

2.3.7 SUP35p sedimentation analysis 34

2.3.8 *In vitro* transcription/translations 35

2.3.9 ATP assays 36

2.4 Gels and Western Blots 37

2.4.1 SDS Poly-acrylamide gel electrophoresis (Laemli 1970) 37

2.4.2 Native Poly-acrylamide gel electrophoresis (derived from Liou & Willison, 1997) 37

2.4.3 Two-Dimensional i.e.f/PAGE (modified version of O'Farrel, 1975, described by Burland *et al*, 1983) 38

2.4.4 Gel staining 39

2.4.5 Western blotting (Tobin *et al,* 1979) 41

2.4.6 Autoradiography 41

2.5 Purification of CCT (derived from Lewis *et al* (1992) as modified by Roobol *et al*, 1995) 42

2.5.1 Sucrose gradients 42

2.5.2 Ion exchange chromatography 43

2.6 Chromatographic analysis 44

2.6.1 ATP column analysis 45

2.6.2 Superose 6 Column 46

2.7 Antibody production 46

2.7.1 Peptide Immunogens 46

2.7.2 Activated KLH Preparation (McCray & Werner 1989) 47

2.7.3 Peptide coupling 47

2.7.4 Immunization 47

2.7.5 Serum testing 48

2.7.6 Peptide Columns 49

2.7.7 Antibody affinity purification 50

2.8 PCR and Cloning 50

2.8.1 Bioinformatics and Primer design 50

2.8.3 Plasmid purification and precipitation 51

2.8.4 Sequencing 51

2.8.5 Restriction Digestion of Plasmids 52

2.8.6 Purification of redigested DNA fragments 52

2.8.7 Ligation 52

2.8.8 Screening of putative clones 53

2.8.9 PCR composition and program 53

2.8.10 Yeast plasmid shuffling 54

Chapter 3: Antibody Production

3.1 Aims 55

3.2 Introduction 56

3.2.1 Antibodies 56

3.2.2 Polyclonal antibodies 57

3.2.3 Monoclonal antibodies 58

3.2.4 Peptide specific antibodies 59

3.2.5 Uses of antibodies in research 60

3.2.6 Choice of Sequence for generating Peptide-specific antibodies 62

3.3 Results 65

3.3.1 KLH activation 65

3.3.2 Serum testing 68

3.3.3 Purification 71

3.3.4 Specificity testing 73

3.3.5 Use of anti-CCT subunit antibodies to immunoprecipitate the complex from cell lysate. 78

3.3.6 Use of GSPT1/2 antibodies in immunohistochemistry 80

3.4 Discussion 82

Chapter 4: Yeast Sup35p/CCT Interaction

4.1 Introduction 83

4.1.1 Yeast CCT 83

4.1.2 Sup35p 86

4.1.3 Prionisation 89

4.1.4 Chaperones and prionisation 91

4.1.5 CCT/Sup35p interaction 94

4.1.6 Aims and Objectives 95

4.2 Results 96

4.2.1 Demonstration of a physical interaction between CCT subunits and Sup35p influenced by both its aggregation state ([*PSI*+] vs. [*psi*-]) and N-domain. 96

4.2.2 Influence of ATP on CCT subunit/Sup35p interaction. 100

4.2.3 Influence of IP conditions on CCT subunit/Sup35p interaction. 104

4.2.4 Distribution of Sup35p and the CCT subunits when fractionated on a sucrose gradient. 108

4.2.5 Apportionment of Sup35p and CCT subunits when SUP35p aggregates are pelleted. 112

4.2.6 *In vitro* transcription/translation of wild type and mutant (ΔN) Sup35p. 116

4.3 Discussion 123

Chapter 5: CCT/eRF3 (GSPT1/2) Interaction

5.1 Introduction 129

5.1.1 GSPT1/2 129

5.1.2 Evidence for an interaction 132

5.1.3 I.M.A.G.E. 133

5.1.5 Aims and objectives 134

5.2 Results 135

5.2.1 Tissue distribution of GSPT1/2 135

5.2.2 Demonstration of a physical interaction between CCT subunits and GSPT1/2 138

5.2.3 Influence of ATP on CCT subunit/GSPT1/2 interaction. 140

5.2.4 Influence of RIPA detergents on CCT subunit/GSPT1/2 interaction. 142

5.2.5 Sucrose gradient analysis 144

5.2.6 I.M.A.G.E. clone sequencing 148

5.2.7 *In vitro* transcription/translation 152

5.2.8 Immunocytochemistry 155

5.3 Discussion 159

Chapter 6: CCT Disassembly

6.1 Introduction 166

6.1.1 The Disassembly of CCT 166

6.1.2 Function of CCT disassembly 168

6.1.3 Aims and objectives 170

6.2 Results 171

6.2.1 Demonstration of CCT complex disassembly 171

6.2.2 Analysis of disassembled CCT complex 176

6.2.3 Purification of individual CCT subunits 179

6.2.4 ATPase activity of individual CCT subunits 185

6.3 Discussion 189

Chapter 7: Discussion

7.1 The use of antibodies in research 193

7.2 Do CCT and eRF3 interact? 194

7.3 What is the nature of the interaction? 195

7.4 What could be the function of the interaction? 197

7.5 Does CCT disassemble? 203

7.6 What is the nature of the disassembled products? 204

7.7 What are the properties of the individual CCT subunits? 205

7.8 Conclusion 205

7.9 Further Work 206

References 208

Appendix 228

Abbreviations

3-D	Three Dimensional
5-FOA	5-fluoroorotic acid
ade	adenine
ADP	Adenosine DiPhosphate
$AmmNiSO_4$	Ammonium Nickel Sulphate
APC	Anaphase Promoting Complex
APS	Ammonium PerSulphate
ATC	AurinTriCarboxilic acid
ATP	Adenosine TriPhosphate
ATPase	Adenosine TriPhosphatase
bp	base pairs
BSA	Bovine Serum Albumin
BSE	Bovine Spongiform Encephalopathy
c-cpn	cytosolic chaperonin
CCT	Chaperonin Containing TCP-1
CJD	Creutzfeldt Jakob Disease
dH_2O	deionised water
DMEM	Dulbecco's Modified Eagle's Medium
DMF	DiMethyl Formamide
DMSO	DiMethyl SulphOxide
DNA	DeoxyRiboNucleic acid
ECL	Enhanced Chemical Luminescence
EDTA	Ethylene-Diamine-Tetraacetic Acid
eEIF	eukaryotic Elongation Factor
EF	Elongation Factor
ELISA	Enzyme Linked Immunosorbent Assay
EM	Electron Microscopy
eRF	eukaryotic Release Factor
EST	Expressed Sequence Tag
FBS	Fetal Bovine Serum
FCA	Freund's Complete Adjuvant
FPLC	Fast Performance Liquid Chromatography
g	gravity
GDP	Guanosine DiPhosphate
GSPT	G to S-Phase Transition Protein
GTP	Guanosine TriPhosphate
GTPase	Guanosine TriPhosphatase
HGMP	Human Genome Mapping Project
his	histidine
hr	Hours
HSP	Heat Shock Protein
ief	iso-electric focusing
Ig	Immunoglobulin
IMAGE	Integrated Molecular Analysis of Genomes and their Expression
IP	ImmunoPrecipitations
kan	kanamycin
KBq	KiloBequerels
KDa	Kilo Daltons
KLH	Keyhole Lympet Haemocyanin
LB	Luria Bertani
leu	leucine
mA	milliamps
mAbs	monoclonal Antibodies
MAT	Mating type
MBS	MaleimidoBenzoic acid N-hydroxy-Succinimide ester
min	minutes
mRNA	messenger RiboNucleic Acid
NCBI	National Centre for Biotechnology Information
NMR	Nuclear Magnetic Resonance
OD	Optical Density
Oligo(dT)	oligodeoxyThymine
PABP	Poly Adenine Binding Protein
PAGE	PolyAcrylamide Gel Electrophoresis
PBS	Phosphate Buffered Saline
PCR	Polymerase Chain Reaction
PhLP	Phosducin Like Protein
pI	Iso-electric point
PMSF	Phenyl-Methyl-Sulphonyl Fluoride
Poly(A)	Poly Adenine
RCC	Renal Clear Cell carcinoma

RF	Release Factor
rpm	revolutions per minute
RRF	Ribosomal Release Factor
SDS	Sodium Dodecyl Sulphate
SE	Spongiform Encephalopathy
Sec	Seconds
TAE	Tris, glacial Acetic acid, EDTA
TCP	Tailless complex polypeptide
TRiC	TCP-1 Ring Complex
trp	trypsin
ura	uracil
v/v	volume by volume
VHL	Von-Hippel Lindau protein
WD-40	Tryptophan/Aspartic acid repeat motif
w/v	weight by volume
YEPD	Yeast Extract, Peptone, D-glucose
YNB	Yeast Nitrogen Base
YPDS	Yeast Extract, Peptone, D-glucose, Sorbitol

List of Figures

Figure 1.1 The molecular chaperonin GroEL **page 4**

Figure 1.2 A single subunit from the molecular chaperonin GroEL **page 4**

Figure 1.3 Subunit orientation in one of the eight membered rings according to Liou & Willison (1997) **page 7**

Figure 1.4 Diagram of CCT subunit δ **page 8**

Figure 1.5 Mechanism of GroEL-mediated protein folding **page 9**

Figure 1.5 The structure of the actin bound CCT complex as revealed by cryoelectron-microscopy **page 12**

Figure 2.1 SDS-PAGE analysis of the fractions obtained from a 10-40% sucrose gradient **page 43**

Figure 2.2 Peptides designed for the construction of antibodies **page 45**

Figure 2.3 Primers designed for PCR and sequencing **page 50**

Figure 3.2 Peptides chosen for the generation of antibodies **page 57**

Figure 3.3 Elution profile of activated KLH after passage through a Pharmacia FPLC fast desalting column **page 64**

Figure 3.4 Diagram of standard antibody **page 66**

Figure 3.4 Diagram showing the chemistry of activating KLH **page 67**

Figure 3.4 Western blots of *S. cerevisie* cell lysate, probed using various concentrations of serum from rabbit immunized with KLH conjugated Cct1p C-terminal peptide **page 69**

Figure 3.5 Western blots of *S. cerevisiae* (Cct1-8 and Sup35p) and ND7/23 (GSPT1/2) cell lysates, probed using various concentrations of serum from animals immunized with KLH conjugated peptides from each of the yeast CCT subunits, yeast Sup35p and murine GSPT1/2 **page 70**

Figure 3.6 Diagram showing the chemistry of coupling synthetic peptide with an N-terminal cysteine residue to the Sulfolink® coupling gel **page 72**

Figure 3.7 Dot blot of purified Cct1 antibody fractions **page 73**

Figure 3.8 Western blots of ND7/23 (GSPT1/2) and *S. cerevisiae* (Cct1-8 and Sup35p) cell lysates, probed using various concentrations of affinity purified antibody raised against C-terminal peptides from yeast CCT subunits, yeast Sup35p and murine GSPT1/2 **page 74**

Figure 3.9 Silver stains of *S. cerevisiae* and ND7/23cell lysates subjected to two-dimensional i.e.f./PAGE **page 76**

Figure 3.10 Western blots of ND7/23 (GSPT1/2) and *S. cerevisiae* (Cct1-8 and Sup35p) cell lysates subjected to two-dimensional i.e.f./PAGE **page 77**

Figure 3.11 Autoradiographs of immunoprecipitated CCT from *[psi⁻]* yeast cell lysates **page 79**

Figure 3.12 Immunocytochemistry of GSPT1/2 **page 81**

Figure 4.1 The structures of both Sup35p and EF-Tu **page 88**

Figure 4.2 N domain of Sup35p **page 91**

Figure 4.3 Map showing the interactions predicted by functional computer algorithms **page 94**

Figure 4.4 Western blots of immunoprecipitated CCT from both *[PSI⁺]*, *[psi⁻]* and ΔN yeast cell lysates **page 97**

Figure 4.5 Autoradiographs of immunoprecipitated CCT from *[PSI⁺]* and *[psi⁻]* yeast cell lysates **page 99**

Figure 4.6 Coomassie stain of immunoprecipitated CCT from *ΔN* yeast cell lysate **page 100**

Figure 4.7 Autoradiographs of immunoprecipitated CCT from both *[PSI⁺]*, *[psi⁻]* yeast cell lysates in the presence of ATP **page 101**

Figure 4.8 Coomassie stain of immunoprecipitated CCT from *ΔN* yeast cell lysate **page 102**

Figure 4.9 Anti-Sup35p western blots of immunoprecipitated CCT from *[PSI⁺]*, *[psi⁻]* and ΔN yeast cell lysates **page 103**

Figure 4.10 Autoradiographs of immunoprecipitated CCT from both *[PSI⁺]*, *[psi⁻]* and ΔN yeast cell lysates **page 105**

Figure 4.11 Coomassie stain of immunoprecipitated CCT from *ΔN* yeast cell lysate **page 106**

Figure 4.12 Western blots of immunoprecipitated CCT from both *[PSI⁺]*, *[psi⁻]* and ΔN yeast cell lysates **page 107**

Figure 4.13 Coomassie Stained SDS-PAGE gels of sucrose gradient fractions of yeast cell lysate from both *[PSI⁺]* and *[psi⁻]* cells **page 109**

Figure 4.14 Western blots of sucrose gradient fractions of yeast cell lysate from both *[PSI⁺]* and *[psi⁻]* cells **page 110**

Figure 4.15 Coomassie stained SDS-PAGE gels of yeast cell lysate, from both *[PSI⁺]* and *[psi⁻]*cells, centrifuged to separate soluble and insoluble proteins **page 113**

Figure 4.16 Western blots of yeast cell lysate from both *[PSI⁺]* and *[psi⁻]* cells, centrifuged to separate soluble and insoluble proteins **page 114**

Figure 4.17 Graph to show percentage of total protein found in insoluble fraction of protein in *[PSI⁺]* and *[psi⁻]* yeast cell lysates **page 115**

Figure 4.18 Map of pBluescript plasmid containing the GSPT2 full length gene under the control of the T7 promotor. **page 116**

Figure 4.19 A Gel to show the products of the digestion of the *ΔN* and *SUP35* plasmids **page 117**

Figure 4.19 B Gel to show the products of the digestion of the re-isolated, sub-cloned *ΔN* and *SUP35* plasmids **page 117**

Figure 4.20 Autoradiographs of native PAGE gels of *in vitro* transcription/translation reaction samples **page 119**

Figure 4.21 Diagram showing the possible orientation of interaction between Sup35p and CCT **page 120**

Figure 4.22 Graph of the densitometry of the CCT band on autoradiographs of native PAGE gels of *in vitro* transcription/translation reaction samples **page 121**

Figure 4.23 Autoradiographs of SDS-PAGE gels of *in vitro* transcription/translation reaction samples **page 126**

Figure 4.24 Order of CCT subunits in the yeast complex, based on that proposed for the mammalian complex **page 128**

Figure 5.1 Protein sequence alignment of Human GSPT1, Murine GSPT1 and 2, and Yeast Sup35p **page 130**

Figure 5.2 Western blots of various tissue samples from a euthanised male rat **page 136**

Figure 5.3 Western blots of immunoprecipitated CCT from ND7/23 cell lysates **page 139**

Figure 5.4 Autoradiographs of immunoprecipitated CCT from ND7/23 cell lysate **page 141**

Figure 5.5 Western blots of immunoprecipitated CCT from ND7/23 cell lysate **page 143**

Figure 5.6 Western blots of sucrose gradient fractions of ND7/23 cell lysate **page 146**

Figure 5.7 Western blots of immunoprecipitated CCT from sucrose gradient fractions containing both CCT subunits and GSPT1/2 **page 147**

Figure 5.8 Sequence of the I.M.A.G.E. clone 533932 **page 150**

Figure 5.9 Sequence of the I.M.A.G.E. clone 586105 **page 151**

Figure 5.10 Autoradiograph of SDS-PAGE gel of *in vitro* transcription/translation reaction samples of GSPT2 **page 153**

Figure 5.11 Autoradiograph of native PAGE gels of *in vitro* transcription/translation reaction samples of GSPT2 **page 154**

Figure 5.12 Immunocytochemistry of GSPT1/2 and either CCTβ or actin **page 156**

Figure 5.13 Western blots of immunoprecipitated CCT from ND7/23 cell lysates **page 158**

Figure 5.14 Order of subunits in the CCT complex as proposed by Liou & Willison, (1997) **page 162**

Figure 5.15 Diagram of the proposed model for CCT/eRF3 interaction **page 164**

Figure 6.1 CCTα (*green*) and CCT β (*gold*) subunits superimposed to demonstrate the differences in size of the variable sized loop on different subunits **page 167**

Figure 6.2 Comparison between the order of ATPase activity found amongst the yeast CCT subunits and the ease with which mammalian subunits are able to leave the complex **page 167**

Figure 6.3 Autoradiographs of immunoprecipitated CCT from ND7/23 cell lysate **page 172**

Figure 6.4 Autoradiograph of immunoprecipitated Cctα from ND7/23 cell lysate **page 174**

Figure 6.5 Autoradiograph of immunoprecipitated Cctα from ND7/23 cell lysate **page 175**

Figure 6.6 Silver stains of fractions eluted from a superose 6 gel filtration column **page 177**

Figure 6.7 Western blots whole lysate and CCTβ depleted lysate were also probed for the presence of CCTβ to ensure complete clearance. **page 179**

Figure 6.8 Silver stain of CCT containing sucrose gradient fractions passed over an ATP column **page 180**

Figure 6.9 Dot blots of CCT containing sucrose gradient fractions resolved over an ATP column in the presence of K^+ ions. **page 182**

Figure 6.10 Percentage density of each fraction eluted from the ATP column when probed for the different CCT subunits. **page 183**

Figure 6.11 Graph of luminescence counts per second for differing concentrations of ATP using the ATP-Lite™ Luminescence ATP detection assay system **page 186**

Figure 6.12 Bar chart to show the different ATPase activities of four of the CCT subunits and the whole complex **page 187**

Figure 6.13 The order of ease with which CCT subunits are able to leave the 16mer complex **page 189**

Figure 6.14 Schematic diagram of the proposed disassembly cycle of the CCT double ring complex **page 191**

Figure 7.1 Order of CCT subunits in the yeast complex, based on that proposed for the mammalian complex by Liou & Willison, (1997) **page 200**

Figure 7.2 Diagram of the proposed model for CCT/eRF3 interaction **page 202**

Figure 7.3 The order of ease with which CCT subunits are able to leave the 16mer complex **page 203**

List of Tables

Table 2.1 Components of *in vitro* translation reactions **page 34**

Table 2.2 PCR Reaction Componants for Taq DNA polymerase **page 53**

Table 3.1 Predicted properties of all eight CCT proteins and Sup35p from yeast and GSPT1 and 2 from mouse **page 68**

Table 4.1 Different nomenclature for the mammalian and yeast CCT proteins and genes **page 84**

Abstract

CCT (chaperonin containing TCP-1) is a barrel-shaped chaperone complex (16-mer) of eight different subunits, organised in two rings. CCT is essential in folding the cytoskeletal proteins actin and tubulin but also interacts with a wider range of proteins. A strong functional link was predicted by bioinformatics (Marcotte *et al.* Nature 402 p83 1999) with yeast Sup35p, a model prion-like protein in yeast, which is the eukaryotic translation release factor 3 (eRF3). Sup35p shares 43% amino acid similarity with its mammalian homologue named G to S-phase transition protein 1 (GSPT1). In mammalian systems there are two GSPT homologues GSPT1 and GSPT2. Unlike Sup35p, GSPT aggregation is unknown and it lacks the N-terminal repeats implicated in Sup35p prionogenesis. In this study a non-substrate like interaction has been demonstrated between Sup35p/GSPT and CCT. This interaction has been demonstrated both *in vitro* and *in vivo* by a number of methods. The nature of the interaction indicates that sub-16mer complexes of CCT are involved as opposed to the whole complex. The presence of these microcomplexes has been both implied and demonstrated in a study of the disassembly process of CCT. It has been demonstrated that the CCT complex disassembles in a single ring mediated manner and requires the presence of both ATP and K^+ ions. The order in which the CCT subunits are able to leave the complex appears to be related to the size of a variable loop as reported by Roobol *et al* (1999) and not to their individual ATPase activities. The ATPase activities of four of the subunits are reported and vary enormously. It is proposed that the function of the CCT/eRF3 interaction is to couple translation termination and protein folding in the cytosol, a process not previously put forward involving these proteins.

Chapter 1: Introduction

1.1 Introduction

In order to be biologically active, proteins must adopt a three dimensional structure giving rise to a unique shape made up of individual units of ordered structure. Small changes in this structure can have major effects on the function of the protein and many disease states can be attributed to incorrectly folded proteins. The most obvious are the neurodegenerative prion diseases, which include Creutzfeldt Jakob Disease (CJD), Bovine Spongiform Encephalopathy (BSE), Scrapie and Kuru. It appears that these diseases are caused by the misfolding of a native protein within the neuronal cells of the brain and nervous tissue of the affected individual (Cohen, 1999). These diseases are rare. However, the misfolding of proteins has been shown to be a factor in other, more common, diseases such as cystic fibrosis (Johnston, Ward & Kopito, 1998), Huntington's disease (Ho *et al,* 2001) and Alzheimer's disease (Bellotti *et al*, 1999).

Although a great deal is now known about the structure of proteins, with the aid of tools such as X-ray Crystallography, Nuclear Magnetic Resonance (NMR) and cryo-electron microscopy, little is known about how the final conformation of proteins is achieved by the cell. Early work on the folding of proteins, especially ribonuclease, introduced the concept that the final conformation of a protein is entirely consequent to its amino acid sequence provided a protein is folding at infinite dilution (Anfinsen, 1973). However, this is not always possible in the high protein concentrations of protein found within the cellular environment where many partially folded proteins may be present in high concentrations (Anfinsen, 1973). Studies on protein folding mechanisms have revealed a group of proteins involved in the folding pathway,

which help to overcome this problem by providing an environment of infinite dilution within the cell, termed the molecular chaperones. The first to be identified was nucleoplasmin, a nuclear protein required for the assembly of nucleosomes from DNA and histones (Laskey *et al*, 1978). Since then, these chaperones have been found in all cells including bacteria, archaea and in all cellular compartments of eukaryotes including chloroplasts and mitochondria. The term has been used to encompass most proteins involved in the folding of other proteins, and includes an extensive number of heat shock proteins whose synthesis is increased greatly under stress conditions when proteins are damaged and denatured. It therefore seems feasible that a study of these chaperones, and more specifically those found in eukaryotic cells, may hold the key to understanding the mechanisms involved in giving rise to disease states due to misfolded proteins and may afford clues to future therapies for sufferers.

1.2 The Molecular chaperones and chaperonins

Molecular chaperones are defined as a class of unrelated protein families which act as catalysts in the non-covalent assembly of proteins *in vivo* (Ellis & Hemmingsen, 1989). This includes the correct folding of newly synthesised proteins, the assembly of oligomeric structures, changes in the folding or association of proteins during their normal functions and the repair of proteins damaged after stresses such as heat shock (Ellis, 1996).

The above definition of a molecular chaperone meant that a large number of proteins could be included. For this reason a distinction was made between the different types of chaperone and the term chaperonin was introduced (Hemmingsen *et al*, 1988). A chaperonin is defined as a member of a sequence-related molecular

chaperone family, that exhibits a characteristic multi-subunit toroidal structure and functions to assist protein folding, in all types of cell, by binding to non-native forms of proteins (Ellis, 1996). This family of chaperones was further subdivided into two groups, group I is the GroEL subclass found in bacteria, chloroplasts and mitochondria and group II is the TCP-1 subclass found in archaea and the eukaryotic cytosol.

1.3 Group I chaperonins

GroEL was first identified as a mutant in *Escherichia coli* cells incapable of producing bioactive λ phage particles; the phage heads formed aggregates or 'monsters' thus implicating GroEL in a protein assembly role. A mutation in the 5th cluster of genes (E) of the bacterium encoding a long form (L) of a protein resulted in a partial curing of this phenomenon hence the name GroEL (Gro from phage growth) (Georgopoulos, *et al*, 1973; Sternberg, 1973). It was later found that GroEL was an abundant heat shock protein, constituting 1% of total cellular protein, which increased in abundance, to 10% of total cellular protein, under heat shock conditions (Fayet *et al*, 1989).

GroEL is an 800KDa oligomeric protein assembly consisting of two rings stacked on top of each other; each ring contains seven identical 57KDa subunits (see figure 1.1), with each subunit in the top ring positioned slightly clockwise of its counterpart in the other ring (Braig *et al*, 1995; Xu *et al*, 1997). This structure forms a cylinder with a central cavity measuring 45Å in diameter (Hutchingson, *et al,* 1989; Zwickl, *et al*, 1990; Saibil, *et al*, 1993; Braig, *et al*, 1994; Chen, *et al*, 1994).

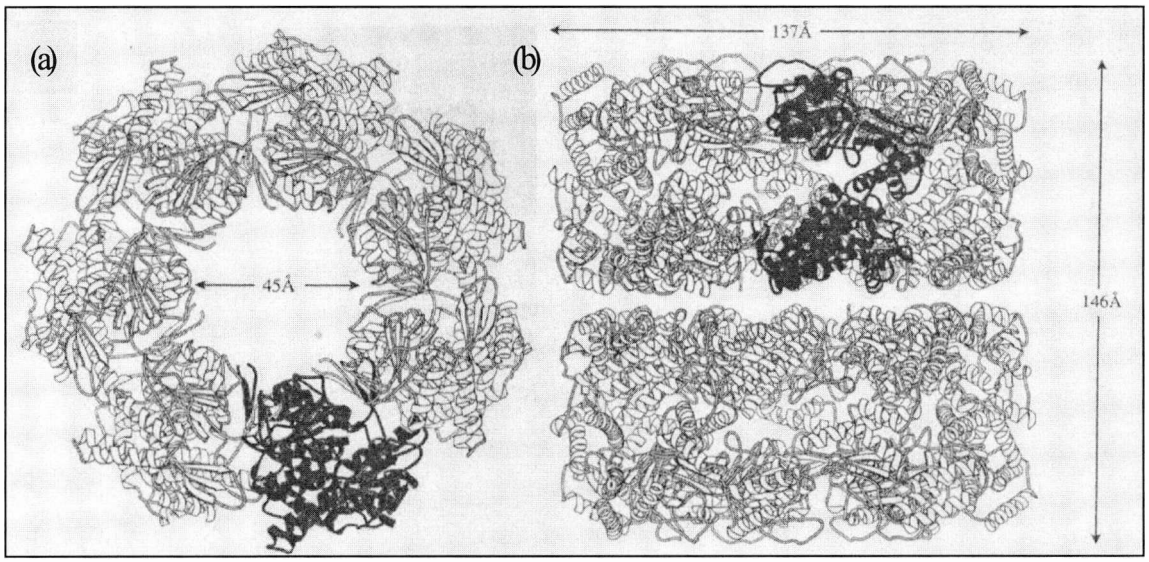

Figure 1.1 The molecular chaperonin GroEL. (a) Top view showing 45 Å cavity in the centre of the cylinder. (b) Side view showing the double ring structure. The darkened areas show the position of a single subunit (Weissman *et al*, 1997).

Each GroEL subunit consists of three domains, the apical domain, found at the top or bottom of the completed cylinder, the equatorial domain, where the two rings meet in the oligomeric structure, and the intermediate domain, a hinge-like region which connects them (Braig, *et al*, 1994) (see figure 1.2).

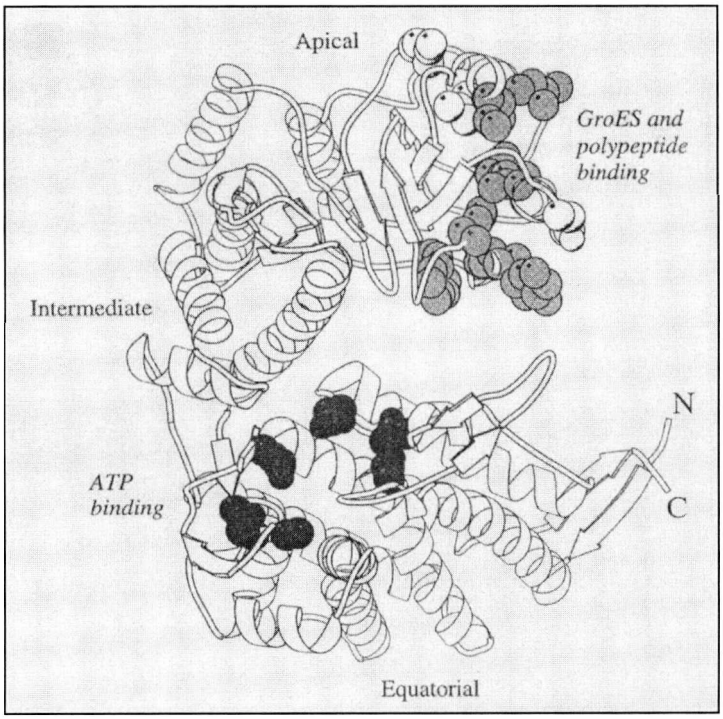

Figure 1.2 A single subunit from the molecular chaperonin GroEL showing the positions of the apical, intermediate and equatorial domains, the ATP binding site, as well as the GroES and polypeptide binding sites (Weissman *et al*, 1997).

The assembled cylinder binds ATP in the seven ATP binding sites located in the equatorial domains of the subunits (Boisvert *et al*, 1996) (see figure 1.2), in one ring at a time (Jackson *et al*, 1993). Once bound, the ATP is then hydrolysed in a reaction dependent upon Mg^{2+} and K^{+} ions (Vitanen *et al* 1990; Todd *et al*, 1993). It is thought that this ATP hydrolysis reaction is responsible for the release of bound substrate by the cylinder (Buchner *et al*, 1991; Martin *et al*, 1991; Vitanen *et al,* 1991). The binding of ATP to the subunits within one ring of the complex is positively co-operative, whereas negative co-operativity of ATP binding between the two rings means that ATP binding in the second ring is inhibited (Yifrach & Horovitz, 1994, 1995; Burston *et al*, 1995). This pattern of co-operativity allows the two rings to act sequentially with one ring hydrolysing ATP and sequestering folding substrate at a time (Rye *et al*, 1997; Kad *et al*, 1998). A major role of this process is also to stabilise the binding of the co-chaperonin GroES (Jackson *et al*, 1993; Martin *et al*, 1993; Todd *et al*, 1993).

GroES is a homo-heptamer of 10KDa subunits, encoded by the groE operon that also encodes GroEL in a polycistronic gene, which binds to GroEL to form a lid on the cavity within the ring. Once bound the GroES forms a dome roughly 30Å high on top of the GroEL cylinder (Hunt & Deisenhofer, 1997). GroES is an essential protein and a deficiency in its yeast homologue, hsp10, results in defective polypeptide folding in the mitochondrial compartment (Hohfeld & Hartl, 1994). Although GroEL can function without GroES, the folding process for proteins requiring the presence of GroES is extremely slow when compared to the spontaneous folding of these proteins or that which occurs in the presence of GroES (Martin *et al*, 1991; Vitanen *et al*, 1991). However, a distinction can be made between proteins that cannot fold without GroEL and those which are assisted by

GroEL, with the total number of cellular proteins falling into these categories being approximately 10% (Houry *et al*, 1999).

1.4 Group II chaperonins

Three independent lines of investigation led to the discovery of the cytosolic chaperonin containing TCP-1 or CCT (also known as TCP-1 complex, cytosolic chaperonin (c-cpn), chromobindin A or TRiC). The mouse t-complex polypeptide 1 (TCP-1) gene was found to be upregulated during spermatogenesis (Dudley *et al*, 1984; Silver *et al*, 1987; Willison *et al*, 1990) and this gene and its human homologue were cloned (Willison *et al*, 1986, 1987; Kirchoff & Willison, 1990; Kubota *et al*, 1992). Subsequently this polypeptide was identified as a component of a 20S particle - the chaperonin containing TCP-1 (Lewis *et al*, 1992). Second, studies on the archaebacterial heat shock response yielded a protein with *in vitro* chaperonin activity (Phipps *et al,* 1991, 1993; Trent *et al*, 1991) that also showed great (and closest) identity with the eukaryotic TCP-1 (Trent *et al*, 1991). Finally, rabbit reticulocyte lysate, programmed with actin or tubulin mRNAs, showed an association between the newly synthesised protein and a high molecular weight complex within the lysate (Gao *et al*, 1992; Yaffe *et al*, 1992), which was found to be CCT.

Studies on this chaperonin have revealed, in part, its structure and it appears in some ways similar to that of GroEL. CCT is an oligomeric complex of 950Kda and consists of two eight membered rings stacked directly on top of each other to form a cylinder (Lewis *et al*, 1992; Gao *et al*, 1992; Frydman *et al*, 1992). However, the subunits which form the rings are different, and it is thought that one of each of the eight different subunits make up each ring, in a particular order, (Liou & Willison,

1997) (see figure 1.3). Seven of the subunits (CCTα, β, γ, δ, ε, ζ, η) are present in equimolar amounts, but the other subunit (CCTθ) is around half-molar (Rommelaere *et al*, 1993; Kubota *et al*, 1994; Creutz *et al*, 1994; Hynes *et al*, 1996). This does suggest that both rings may not be identical, in that 15 or 14 subunit complexes may be formed (Yokota *et al*, 2001), and this could have implications for the mechanism of CCT-mediated protein folding. Indeed there is evidence that the composition of the CCT complex changes during the cell cycle, being deficient in some subunits (mainly α and δ) at metaphase and having the full complement of subunits at S-phase (Yokota *et al*, 2001). It should also be noted that CCT from testis contains one or two extra, testis-specific subunits, depending on species, related to CCTζ (Kubota *et al*, 1997).

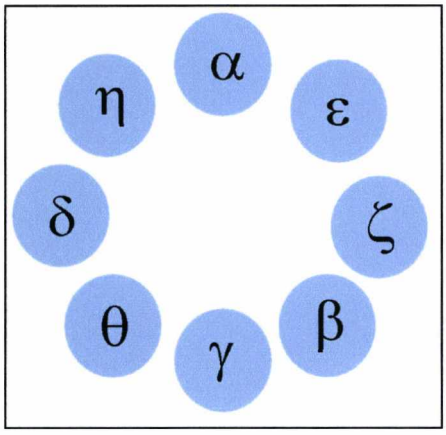

Figure 1.3 Subunit orientation in one of the eight membered rings according to Liou & Willison (1997).

The subunits of CCT range in size from 57 to 61Kda and can be separated by two dimensional gel electrophoresis as they have differing pIs, ranging from 6.25 to over 7.2 (Kubota & Willison, 1997). Each of the subunits of CCT is arranged in a similar way to those of GroEL (see figure 1.4), having large, globular apical and equatorial domains with a hinge-like intermediate domain (Willison & Horwich, 1996).

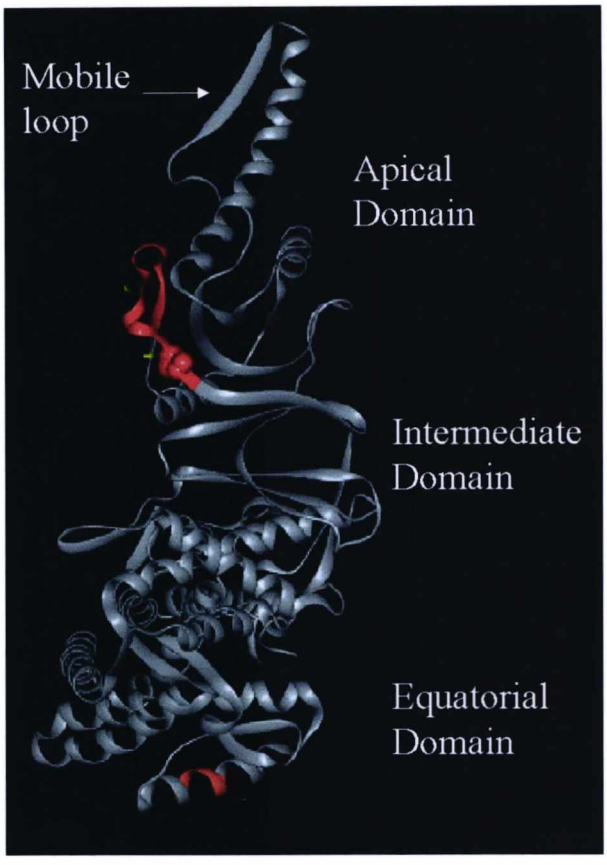

Figure 1.4 Diagram of CCT subunit δ showing the three domains and the mobile loop structure, which is thought to take the place of a co-chaperone (Llorca *et al*, 1999).

It is proposed that the polypeptide-binding sites are located within the apical domain so that, in the double ring structure, polypeptide binds towards the ends of the 60Å cavity (Willison & Horwich, 1996). This process appears to be subunit specific, with substrate binding specifically to certain subunits and not others (see figure 1.5) (Llorca *et al*, 1999, 2000), this is shown further when the sequences of the subunits are compared (when CCT subunits are aligned using multalign http://prodes.toulouse.inra.fr/multalin/multalin.html (Corpet, 1988)). The subunits share a high degree of sequence homology in the majority of the sequence but the apical domains are very different (Kim, Willison & Horwich, 1994) suggesting different peptides, or parts of peptides, bind to different subunits. Putative binding motifs for substrate have been located on the inner surface of the apical domains of

the subunits where the structure mainly consists of loops, which are ideal for recognising different structural motifs on substrate polypeptides (Pappenberger *et al*, 2002). The apical domains of the CCT subunits contain a relatively high number of charged residues when compared to GroEL, where these areas are mainly hydrophobic (Fenton *et al*, 1994) and therefore more likely to bind to hydrophobic patches on unfolded proteins, however, the purpose of this difference is as yet unknown.

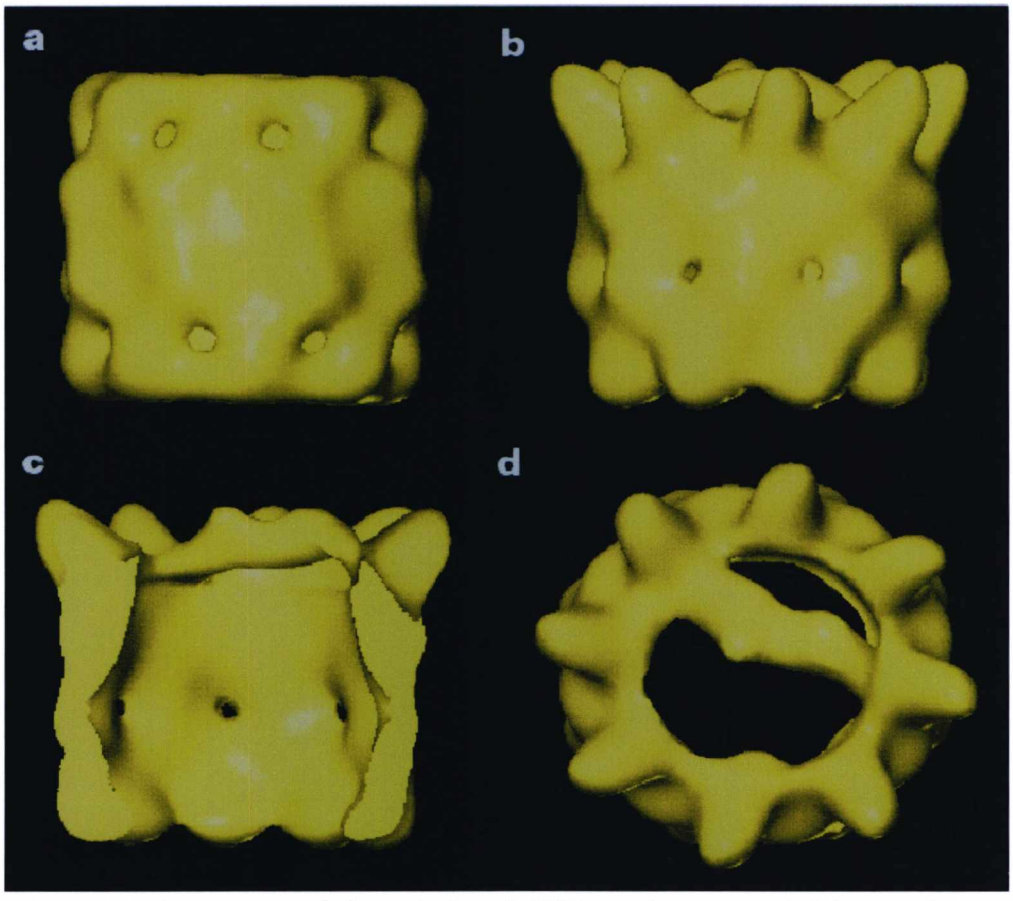

Figure 1.5 The structure of the actin bound CCT complex as revealed by cryoelectron-microscopy. **(a)** shows the unbound CCT complex, **(b)** shows the actin bound CCT complex from the side, **(c)** shows the complex in cut away to show the position of the bound actin within the cavity, and **(d)** shows the complex from the top showing the specific binding nature of actin. Taken from Llorca *et al* (1999).

Like GroEL, CCT has ATPase activity and a group of residues, including GDGTT, is conserved between the ATP binding site of GroEL monomers and a portion of the

equatorial domain of CCT subunits, suggesting that the ATP binding site is in a similar position (Willison & Horwich, 1996). Work in *Saccharomyces cerevisiae* has revealed a hierarchy in the ATP binding of the different CCT subunits within the complex (Lin & Sherman, 1997) and this order of binding is consistent with the proposed order of subunits within the two rings (Liou & Willison, 1997).

Although group I chaperonins require the presence of co-chaperonins to carry out their folding functions efficiently, no corresponding co-chaperonin has been found for the group II chaperonins. It is thought, however, that the enclosed folding cavity, created in the GroEL-GroES complex, is formed by the mobile loop protrusions of the apical domains of the subunits (see figure 1.4). In the CCT complex the mobile loops of the subunits fold over the cavity forming a lid, in much the same way as the monomers of GroES interact and form the lid for GroEL (Ditzel *et al*, 1998). In evolutionary terms it seems that the lid was incorporated into the chaperonin complex, which should increase the efficiency of the protein folding process. The cryo-electron microscopy image of CCT with actin bound to it was published (Llorca *et al*, 1999) in which ATP was not present and this suggests that nucleotide is not required for the initial binding of substrate to the CCT complex, but is required later in the folding cycle.

1.5 Chaperonin – mediated protein folding.

The steric information necessary for newly synthesised protein chains to fold correctly within cells resides solely in the primary structure of the initial translation product (Anfinsen, 1973). Most denatured proteins will refold correctly, *in vitro*, after dilution, providing the conditions approach a favourable infinite dilution environment, and there is removal of the denaturing agent from the pure protein

(Anfinsen, 1973). This information suggests that proteins are capable of forming the correctly folded end product by themselves, with no assistance from other factors, within the cell. However, the evolution of a large number of protein folding chaperones suggests otherwise. One reason for this may be that the self-folding of some proteins is inefficient (or even impossible) or they may favour aggregation over proper folding. Other factors in the cellular environment, particularly the very high concentrations of protein (200-400μg/ml), (molecular crowding), with many of these being unfolded to some extent either because they are nascent or partly unfolded during their functional cycle (Ellis, 1996), may also result in interactions which prevent correct folding of the protein.

The chaperonins appear to overcome these factors by providing a protected environment, within their central cavity, in which proteins can fold themselves, the 'Anfinsen cage' theory (Ellis & Hartl, 1999). The best characterised chaperonin folding mechanism is that of GroEL. This mechanism relies on the two rings being slightly out of step with each other. The interaction between GroEL and the polypeptide to be folded takes place between the hydrophobic surface on the apical domains of the subunits and exposed hydrophobic patches on the unfolded or partially folded polypeptide and appears to be non-specific (Fenton *et al*, 1994; Buckle *et al,* 1997; Farr *et al*, 2000). Seven ATP molecules bind to one of the rings together with the polypeptide to be folded. The substrate for GroEL folding is already partially folded, possibly by association with hsp70 which binds unfolded polypeptides, and is said to be in a 'molten globule' state, a state achieved by proteins very rapidly and spontaneously on dilution from denaturant (Martin *et al*, 1991). GroES is then able to bind to this ring, causing a large conformational change in the apical domains of the subunits in the ring, thus creating an enlarged cavity.

GroES also binds to the same hydrophobic regions of the apical domain as the substrate, thus displacing it into the central cavity. Displacement into the cavity is also encouraged by conformational changes inside the cylinder which changes the walls from hydrophobic to hydrophilic, so encouraging the release of substrate into the cavity (Wang & Weissman, 1999). The ATP molecules are then hydrolysed to ADP. Binding of ATP to the other ring then facilitates the release of the fully folded protein and GroES. The cycle then begins again with the other ring binding polypeptide and GroES (Wang & Weissman, 1999) (see figure 1.5).

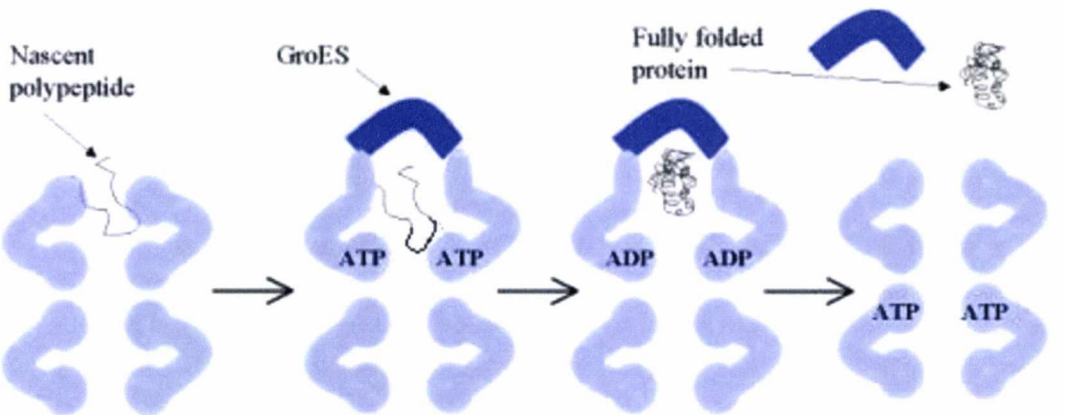

Figure 1.5 Mechanism of GroEL-mediated protein folding. Nascent polypeptide binds to one of the rings of GroEL. The binding of 7 ATP molecules and GroES follows this. The polypeptide then self-folds and the ATP is hydrolysed. Finally 7 ATP molecules bind to the other ring of GroEL and the release of GroES and the fully folded protein is triggered (Wang & Weissman, 1999).

GroEL works in this manner to assist in the folding of many different proteins including folding intermediates and it is thought that for some protein molecules to achieve a fully folded native state, several rounds of binding and release may be necessary (Hloden & Hartl, 1994). However, this concerted mechanism of folding may not represent the only folding procedure of the GroEL/GroES/ATP system. The mitochondrial enzyme aconitase requires the full GroEL machinery in order to fold properly and facilitate the binding of its metal co-factor. However, this protein is too large to be encapsulated (Chaudhuri *et al*, 2001). It is thought that this enzyme goes

through multiple rounds of binding and release in the open cavity, and is bound by GroEL until its metal cofactor binds, at which point the enzyme is released by the binding of GroES to the opposite ring (trans-folding) (Chaudhuri *et al*, 2001).

The mechanism of CCT-mediated folding was assumed to be similar to that of GroEL. However, the differences in the sequences of the apical domains of the subunits of CCT suggested that the binding of substrate was more specific than in GroEL where all the subunits are identical (Kim, Willison & Horwich, 1994). Recently this has been shown to be the case, where actin and tubulin selectively bind to only certain subunits within the CCT complex (Llorca *et al,* 1999, 2000).

The discovery of prefoldin, a chaperone molecule that appears to deliver unfolded proteins to CCT, highlighted another difference. GroEL is capable of cyclically binding native and non-native forms of actin, without folding it, thus inhibiting its folding by CCT, it appears that prefoldin is capable of selectively delivering actin to CCT in preference to GroEL, overcoming this inhibition (Vainberg *et al*, 1998). The substrate for folding by CCT also appears to be a very late folding intermediate; this can be seen from cryo-electron microscopy of actin bound to CCT where the dimentions of the substrate are very similar to the native protein (Llorca *et al,* 1999). However, it has also been demonstrated by cross-linking experiments that CCT can bind to polypeptide chains as they emerge from the ribosome (McCallum *et al*, 2000) and can bind ribosome-bound, actin nascent chains as short as 133 amino acids and luciferase nascent chains as short as 77 amino acids (Dunn *et al*, 2001).

Although there is evidence that the mechanism of CCT-mediated protein folding differs from that of GroEL there are also some similarities. The substrate binds to the apical domains of the subunits in one ring of the CCT complex within the cavity, as in GroEL (Llorca *et al*, 1999), the folding process involves rounds of binding and

release of native and non-native forms of proteins *in vitro* (Farr *et al*, 1997), although there is evidence that this may not occur *in vivo* as there is evidence that actin and tubulin remain bound to CCT throughout the folding cycle (Thlusiraman *et al*, 1999; Siegers *et al*, 1999), and the binding of ATP induces conformational changes in the apical and equatorial domains of the subunits (Llorca *et al*, 1998). However, rather than these changes providing a protected environment for proteins to self-fold in a passive manner as is the case for GroEL/GroES, it has been postulated that sequential release of substrate from subunits, consequent to the hierarchical nature of CCT subunit ATPase activity (Lin & Sherman, 1997), implies some order to which the substrate is released from its binding to the chaperone, which may impose some constraints on the ways in which the protein can fold (Llorca *et al*, 2001). Importantly there is also evidence that in the case of actin and tubulin, a crucial step in the folding pathway is the incorporation of bound nucleotide, which occurs whilst the protein is still bound to the CCT complex and stabilises the native conformation of the proteins (Llorca *et al*, 1999). Finally the hydrolysis of ATP, in the presence of K^+ ions, causes the disassembly of the complex, which may be involved in the release of the bound substrate (Roobol *et al*, 1999).

1.6 Substrate proteins of CCT

It remains the consensus amongst researchers that the main substrates of CCT are the cytoskeletal proteins actin and tubulin, which are among the most abundant proteins in eukaryotic cells. In fact it is believed that the divergence of the CCT subunits from each other, approximately two billion years ago (Kubota *et al*, 1994), was either driven by, or helped drive, the transition from prokaryotic to eukaryotic cells by allowing the development of a more sophisticated cytoskeleton (Maynard-Smith &

Szathmary, 1995) and the mechanism of division of these cells (microtubule spindle formation, cytokinesis etc).

Nevertheless, other substrate proteins have been characterised as mentioned previously, and recently with the analysis by immunoprecipitation of the entire yeast proteome (Ho *et al*, 2002; Gavin *et al*, 2002) a large number of proteins have been found to interact with CCT (see appendix), but the published data are problematic in that some probable CCT substrates were omitted as non-specific i.e. hits were too numerous. It is not yet clear whether all these interacting proteins are substrates or have other, e.g. regulatory, roles. It is now estimated that between 9 and 15% of cellular proteins are folding substrates of CCT (Thulasiraman *et al*, 1999). These figures are based on pulse-chase experiments measuring the flux of proteins through the CCT complex. These proteins all had varying dissociation kinetics suggesting differences in their folding requirements and rates (Thulasiraman *et al*, 1999). The majority of these proteins had a molecular weight of between 30 and 60KDa, much the same as those folded by GroEL (Houry *et al*, 1999), but there were other proteins found to associate with CCT in the 100 to 120KDa molecular weight range, suggesting that CCT may also assist in the folding of much larger proteins (Thulasiraman *et al*, 1999) e.g. myosin (Srikakulam & Winkelmann, 1999).

The protein substrates of CCT that have been characterised cover a range of proteins expressed in many different cell types. Much work has been done to try and identify sequence or structural motifs that mark proteins as requiring either GroEL or CCT for correct folding (Houry *et al*, 1999). It was noticed that GroEL substrates tend to have a α–helix-β–sheet-α–helix structure (Houry *et al*, 1999) and many of the substrate proteins are oligomers or oligomeric subunits (Houry *et al*, 1999). Meanwhile, many CCT substrate proteins share common characteristics such as

being either nucleotide binding proteins or having a WD-40 domain and also many of these proteins are also oligomers or oligomeric subunits (Dunn *et al*, 2001). For example, G *a*-transducin is a cytosolic protein found in the retina of the eye. It is involved in the transfer of light energy into a signalling cascade by binding to the G-protein β and γ subunits in its inactive, GDP bound, form. Light-activated rhodopsin then catalyses the exchange of GDP for GTP on the α subunit, which releases it and the signal passes to downstream components (see Wittinghofer, 1994 for review). This protein associates with CCT in rabbit reticulocyte lysate and is released upon the addition of Mg^{2+} and ATP (Farr *et al*, 1997).

Another substrate protein of CCT, requiring co-factors for its release from the complex, much like tubulin does, is the Von-Hippel-Lindau (VHL) tumour suppressor protein (Feldman *et al*, 1999). This protein regulates several mechanisms of cell proliferation including tumour formation, exit from the cell division cycle (Pause *et al*, 1998), response to hypoxia and formation of the extracellular matrix (Ohh *et al*, 1998). Mutations in VHL are associated with VHL disease, which results in renal clear cell carcinomas (RCC), pheochromocytomas, and highly vascularised tumours of the retina and cerebellum (Latif *et al*, 1993; Chen *et al*, 1995; Lineham *et al*, 1995; Maher & Kaelin, 1997). Inactivation of this protein is also reported in approximately 80% of sporadic RCC (Gnarra *et al*, 1994; Shuin *et al*, 1994). VHL functions only as part of a heterotrimeric complex with elongin BC (Kibel *et al*, 1995) and it seems that CCT mediates its incorporation into the complex as well as folding newly synthesised VHL into its correct conformation (Feldman *et al*, 1999). The release of VHL from the CCT complex requires the presence of elongin BC and is coupled to the formation of the VBC complex (Feldman *et al*, 1999). The interaction with CCT has been mapped to a 55 amino acid region of VHL (Feldman

et al, 1999) and it is the region surrounding this stretch of amino acids where most sporadic disease-causing mutations occur in the protein (Gnarra *et al*, 1994; Shuin *et al*, 1994). This suggests that lack of interaction with CCT is a factor in the disease process.

Another complex associated with the proteosomal degradation pathway of cyclins and entry into anaphase, is the anaphase-promoting complex (APC) (see Zachariae & Nasmyth, 1999 for review). The APC consists of a large complex of several different proteins, 10 or more (12 in yeast). Most of these proteins remain tightly associated throughout the cell cycle and form the core particle (Peters *et al*, 1996; Grossberger *et al*, 1999) and in addition to these, several regulatory proteins have been identified. The protein Cdc20 is one of these regulatory subunits and during the metaphase to anaphase transition, mediates the degradation of the anaphase inhibitor Pds1 (Visintin *et al*, 1997; Shirayama *et al*, 1998), the S-phase B-type cyclin Clb5 (Zachariae & Nasmyth, 1999) and the mitotic cylin Clb3 (Alexandru *et al*, 1999). By destroying its targets the APC/Cdc20 complex is involved in the anaphase checkpoint, promotes sister chromatid separation and facilitates cytokinesis, but also removes a block to chromosome replication for the next round of division (Zachariae & Nasmyth, 1999). The levels of Cdc20 rise and fall during the cell cycle and is only bound to the APC during M-phase. However, it has been demonstrated that over-expressed Pds1 is only allowed to build up in *cdc20* yeast mutants and not wild type cells (Visintin *et al*, 1997), suggesting Cdc20 is not completely lost or inactivated during the whole of the cell cycle. This leaves a question of its regulation. Recently, Cdc20 has been shown to associate with the CCT complex (Camasses *et al*, 2003). It has been found that in order for the APC/Cdc20 complex to form, Cdc20 must first associate with the CCT complex and there is a suggestion

that CCT may have a role in regulating the formation of an active complex by binding tightly to Cdc20 and only releasing it in response to some unknown signal (Camasses *et al*, 2003). Because CCT also binds cdh1 (Camasses *et al*, 2003), a regulator very much like cdc20 and VHL, but of the S-phase related SCF complex (Camasses *et al*, 2003), CCT may also have a role in the regulation of the cell cycle at G to S phase transition. Hence CCT would have a crucial role in cell cycle regulation.

1.7 Other cellular functions of CCT

Due to the complexity of its structure and its high abundance within the cell it has been speculated that the function of CCT is not only that of a folding machine for newly synthesised proteins. Indeed it is also speculated that these extra-curricular activities may not involve the whole complex but just individual subunits (Roobol *et al*,1999; Roobol & Carden, 1999).

In addition to its well characterised folding of actin and tubulin, CCT has also been implicated in cell cycle control in other ways (Dunn *et al*, 2001). This is mainly because of the interaction of CCT with Cdc20 and VHL as described earlier, but also its interaction with cdh1 and the S-phase regulator cyclin E, which requires the presence of functional chaperonin to complex with its partner, Cdk2 (Won *et al*, 1998). Cyclin E is a positive regulator of the G1-S phase transition of the cell cycle through its interaction with its binding partner Cdk2. Regulation of this process is brought about by association with inhibitor proteins or phosphorylation of cyclin E, which is then rapidly destroyed by the ubiquitination/proteosome pathway (Clurman *et al*, 1996). The overexpression of cyclin E is lethal in yeast and three CCT

subunits (β, δ and η) were found to be able to suppress this lethality (Won *et al*, 1998). It was then confirmed that cyclin E was a folding substrate of CCT and that CCT was required for the assembly of the cyclin E/Cdk2 complex (Won *et al*, 1998). It seems then that CCT may be responsible for the control of cyclin E in that it could 'hold on' to the protein, preventing its release until such time as is necessary for the cell to enter S phase. This is a similar mechanism to that proposed for the control of Cdc20 activity, where CCT is necessary for the formation of an active APC/Cdc20 complex, allowing the transition from metaphase into anaphase and cytokinesis (Bogdanova *et al*, 2002). It is thought that CCT may only release Cdc20 for formation of the APC/Cdc20 complex upon the correct signal (Camasses *et al*, 2003). Alternatively individual CCT subunits may have the regulatory role, binding to cyclin E in its folded state until association with the rest of the CCT complex results in the assembly of the cyclin E/Cdk2 complex. The latter scenario relies on there being 'free' CCT subunits available to bind to the cyclin E. This is possible, as the complex has been shown to disassemble under physiological ATP and K^+ concentrations (Roobol et al, 1999), and it is only logical to imagine that cyclin E is not released from all of the subunits under these conditions unless Cdk2 is available for binding and remains bound to three of the CCT subunits until Cdk2 is available when the rest of the CCT complex assembles and the Cdk2/cyclin E complex is formed. Indeed one of the reasons speculated upon for the disassembly of CCT is that a single ring acts as a template for the formation of the second ring from free subunits (Liou *et al*, 1998). Further to the speculation about a role for CCT in the cell cycle is its involvement in the folding of the VHL tumour suppressor protein and its assembly into a functional complex with elongin B and C (Feldman *et al*, 1999). Again it is not much of a step to imagine that the VHL protein is held by CCT until

the two elongins are available for complex formation when it is necessary for the cell to exit the cell cycle. It is intriguing to think that these processes, as well as the folding of tubulin for the cell division machinery, are linked in a way that sees CCT as a regulator of the cell cycle. Indeed a number of cancer charities have funded research into the role of CCT in the cell in the hope new drug targets can be found.

Other cellular roles for CCT and its subunits are also proposed, such as salt and osmotic-stress tolerance in higher plants (Yamada *et al*, 2002), where the α subunit has been found to be sufficient to confer this tolerance when expressed in *E. coli* (Yamada *et al*, 2002) and subunits α and ε are found to fluctuate with the prevailing light conditions (Himmelspach *et al*, 1997), suggesting a regulatory role for these subunits. As already mentioned, it has also been proposed that CCT may act as a nucleotide-loading device (Llorca *et al*, 1999). This is due to the main conformational change in the actin protein, as it is folded, being in the nucleotide-binding pocket (Llorca et al, 1999), which results in the actin then being able to bind ATP, or in the case of tubulin folding, the binding of GTP. From the same group comes the suggestion that CCT may in fact be an elaborate counting device which helps cells measure and integrate the rates of synthesis of the actins and tubulins (Willison & Grantham, 2001). Roles for CCT have also been suggested in other processes such as transcription (Soues *et al*, 2003), translation (Seixas *et al*, 2003) and viral assembly (Dunn *et al*, 2001).

Whatever other roles CCT may have in the cell, only a limited amount of information is available for the regulation of CCT, and hence regulation of its other suggested roles. Of course the regulation of CCT may be as simple as the availability of unfolded substrate or ATP within the cell, however, there is evidence for changes in the transcription rate of CCT, for example through the cell cycle (Yokota *et al*, 2001;

Bourke *et al*, 2002), but again the regulation of this control mechanism remains a mystery. With the study of CCT interacting proteins arising from the recent study of protein interactions in the yeast proteome (Ho *et al*, 2002; Gavin *et al*, 2002), it may well arise that some of these have a regulatory role. To date only one regulatory protein has been characterised and that is phosducin-like protein (PhLP) (McLoughlin *et al*, 2002). PhLP is a protein expressed in all tissues examined so far (Miles *et al*, 1993; Lazarov *et al*, 1999), and has a role in the regulation of G-protein signalling (Bauer *et al*, 1992; Lee *et al*, 1992; Hawes *et al*, 1994; Hekman *et al*, 1994; Yoshida *et al*, 1994; Schroeder & Lohse, 1996; Thibault *et al*, 1997; Thulin *et al*, 1999) and interacts with the 26S proteosomal subunit SUG1 (Zhu & Craft, 1998; Barhite *et al*, 1998). It has been found that PhLP inhibits the CCT-mediated folding of β-actin, *in vivo,* by competitively binding to the CCT complex and thus preventing the binding of its substrate (McLoughlin *et al*, 2002) and PhLP does this whilst being in a folded, active state (McLoughlin *et al*, 2002). As CCT has also been implicated in the folding of G α-transducin protein (Farr *et al*, 1997), the identification of a role for CCT in this signalling cascade may yet be clarified.

1.8 Aims

In this thesis two aspects of CCT behaviour were to be investigated, its interaction with a specific protein, eRF3 and its disassembly activity.

With the vast amount of protein interaction data emerging over the past few years (Marcotte *et al*, 1999; Overbeak *et al*, 1999; Huynen *et al*, 2000; Uetz *et al*, 2000; Ito *et al*, 2001; Tong *et al*, 2001; Gavin *et al*, 2002; Ho *et al*, 2002;), the next step is to confirm and characterise these predicted interactions. For this reason the aims of this

study encompass different proteins and their functions, but the central character is that of CCT. In order to study CCT in the yeast *Saccharomyces cerevisiae*, a complete set of antibodies to the different subunits was required. Therefore, the first aim of the project was to create these antibodies and characterise them.

The second aim of this study was to elucidate any interaction between CCT and the translation termination factor eRF3 (Sup35p in yeast and GSPT1/2 in mammals), predicted by computer algorithm (Marcotte *et al*, 1999). Translation termination initiation, in eukaryotes, requires two classes of translation termination release factor eRF1, a class I stop codon-responsive release factor, and eRF3, the class II guanine nucleotide-responsive release factor (Ebihara & Nakamura, 1999). These two proteins interact to form the translation termination complex but eRF3 has also been implicated in cell cycle control (Kikuchi *et al*, 1988). An interaction between eRF3 and CCT could have implications in this process and could have implications for the way in which we view the role of these proteins. Secondarily, if yeast eRF3 (Sup35p) was found to be a substrate of CCT, this could have implications in the mechanism of prion diseases as Sup35p is a model prion protein, forming aggregates when misfolded and seeding the formation of new aggregates when passed to an uninfected cell (Glover *et al,* 1997).

Further to this, specific antibodies raised against the C-terminal peptide of both Sup35p and GSPT1/2 were also to be constructed and characterised. This part of the project was to be carried out in both yeast and mammalian cells as a comparison of the interaction and its nature, as it could give an indication of the general importance of the interaction. For example, if it is present in yeast and not in mammals then evolution may have side-tracked the interaction as unimportant.

Finally a study on the nature of the disassembly of the CCT complex as reported by Roobol *et al* (1999) was to be carried out to hopefully clarify the mechanism of disassembly and define the functional differences between the eight subunits. This was to include attempts to purify individual subunits from the whole complex.

Chapter 2: Materials and Methods

2.1 Materials

General chemicals were analytical grade, unless otherwise stated, and were obtained from SIGMA (Missouri, USA) and GIBCO-BRL (Strathclyde, Scotland). Media ingredients were purchased from DIFCO (Michigan, USA). Water was of 'milli Q' quality (18.2mΩ cm^{-2}) throughout. DNA molecular weight markers, enzymes and PCR reagents were purchased from Promega (Southampton, England), unless otherwise stated. Oligonucleotide synthesis and DNA sequencing was by MWG-Biotech (Milton Keynes, England). Secondary antibodies were from SIGMA (Missouri, USA), unless stated otherwise. Extensive details of primary antibodies produced and used during this research are described later (section 2.7 and Chapter 3). Nitrocellulose and Nylon membranes were obtained from Amersham Pharmacia Biotech Inc (Buckinghamshire, England), as were the autoradiography and chemiluminescence films and radioactive reagents.

2.2 Cells

2.2.1 Yeast cell cultures

Three different strains of *Saccharomyces cerevisiae* were used: [1] *S. cerevisiae* 74 – D694 (*MAT a, ade 1-14, trp 1-289, his 3-Δ200, ura 3-52, leu 2-3,112, [PSI$^+$]*), [2] *S. cerevisiae* 74 – D694 (*MAT a, ade 1-14, trp 1-289, his 3-Δ200, ura 3-52, leu 2-3,112, [psi$^-$]*) and [3] *S. cerevisiae* MT700/9D (*MATα, sup35::kanMX4, SUQ5, ade2-1$_{UAA}$ his3-11,15, ura3-1, leu2-3,112*, transformed with pYK810 (a centromeric plasmid containing *SUP35* and *URA3*), (Kikuchi et al, 1988)), (all were kind gifts from Dr. Angela Dunn, University of Kent, England).

Unless otherwise stated these strains were grown either on solid YEPD media at 30°C for 36hrs or in liquid YEPD media at 30°C with 200 rpm shaking overnight.

Liquid YEPD media (1L) contained 10g yeast extract, 20g Bacto® peptone and 20g D-glucose all at pH 7.5 (with 1M HCl). For solid YEPD plates, agar, 2% w/v, was added to this media prior to sterilisation by autoclaving for 15mins.

2.2.2 Transformation of *Saccharomyces cerevisiae* (Elble, 1992)

Overnight cultures (0.5ml) were inoculated into prewarmed (30°C, 30mins) YEPD media (50ml) and incubated (30°C, 200rpm) until OD_{600} reached 0.8. Cells were harvested by centrifugation (2000g, 3mins, 4°C; Beckman GS-6R centrifuge, California, USA), washed in sterile H_2O (25ml, 0.1M) and in lithium chloride (1ml, 0.1M) and resuspended in lithium chloride (400µl, 0.1M). 50µl of this suspension was used for

each transformation. Cells were pelleted (30sec, 13000rpm, room temperature, Heraeus instruments, Biofuge pico) and polyethylene glycol (240µl, 50% w/v), LiCl (36µl, 1M), and sheared, denatured, salmon sperm DNA (25µl, 2mg/ml) were added. Plasmid (5-10µg in 50µl H_2O) was added and the cells vortexed vigorously (1min) to resuspend the pellet. The cells were incubated for 30mins at 30°C, and then heat-shocked (42°C, 20-25mins). Cells were again pelleted (30sec, 13000rpm, room temperature, Heraeus instruments, Biofuge pico), resuspended in YEPD media (1ml) and further incubated (30°C, overnight, 200 rpm shaking) before samples (100µl) of the transformed cells were plated onto YPDS (1% w/v yeast extract, 2% w/v peptone, 2% w/v glucose, 1M sorbitol, 2% w/v agar), and incubated (30°C) for 48hrs.

2.2.3 Bacteria

The DH5α strain of bacteria *Escherichia coli* was used throughout (a kind gift from Dr. Anne Roobol), stored as a stock (800µl overnight culture made 15% v/v glycerol) at –80°C. Unless otherwise stated, these were grown either on LB agar plates at 37°C overnight or in liquid LB media at 37°C, 200 rpm shaking, overnight. Liquid LB media (1L) contained 10g Bacto® tryptone, 5g yeast extract and 10g NaCl all at pH7.0 (with 5M NaOH). Agar, 2% w/v, was added to this media prior to sterilisation (by autoclaving for 15mins) for solid LB plates.

2.2.4 Transformation of bacteria (Sambrook *et al*, 1990)

A single colony of DH5α was picked from a recently made LB plate and cultured in 1ml LB overnight at 37°C (200 rpm throughout). This was used to start a 50ml culture in LB and grown to an OD_{600} of 0.6 (10^8 cells/ml). Cells were harvested by centrifugation (4000rpm, 4°C, 10min Beckman GS-6R Centrifuge, California, USA), washed in ice-cold $CaCl_2$ (0.1M, 10ml) and resuspended in 2ml $CaCl_2$ (0.1M, 0°C). 200µl aliquots were mixed gently, on ice, with 10µl DNA (50ng) for 30min. Cells were then heat shocked (42°C, 45 sec) and mixed with 800µl SOC media (2% w/v Bacto® tryptone, 0.5% w/v yeast extract, 0.05% w/v NaCl, 2.5mM KCl, 20mM $MgCl_2$, 20mM D-glucose, all at pH7.0, adjusted with 5M NaOH) and incubated (37°C, 1hr) without shaking, to recover before being plated out (100µl) onto selective media.

2.2.5 Animal (ND7/23) cells

One line of animal cells was used throughout – the ND7/23 all in one adherent cell (original cell line obtained from John Wood, Sandoz Institute for Medical Research, London): These are a mouse neuroblastoma (N18 tg 2) X rat dorsal root ganglion neurone hybrid cell line produced by PEG mediated cell fusion. They have been found to more closely resemble mouse neuronal cells than rat cells (Wainer & Heller, 1992) and express, for example, mouse rather than rat CCT proteins (Roobol *et al*, 1999a).

The basic growth medium was high glucose Dulbecco's Modified Eagle's Medium (DMEM) (SIGMA, D5648) (Dulbecco & Freeman, 1959) containing 10% v/v fetal bovine serum (FBS) (SIGMA, F4135), 100i.u./ml penicillin, 0.1mg/ml streptomycin

(SIGMA, P0781) and 2mM glutamine (SIGMA, G7513) pH7.2. Cells were grown at 37°C in a 5% CO_2 air atmosphere in T75 or T175 flasks (Starstedt, Quebec, Canada). Cells were revived from frozen stock vials (see later) by rapidly thawing a 1ml vial of $2x10^6$ cells/ml and diluting them into 9ml basic growth media (37°C) followed by centrifugation (1000rpm, 5min, room temperature, Denley BS400 centrifuge). Cell pellets were then resuspended in basic growth media (1ml) and inoculated into a T75 flask (15ml, 37°C) incubated at (37°C, 5% CO_2) for 24 hr. Once confluent, cells were diluted to maintain growth. To do this, media was removed and cells were rinsed in 1 x PBS (0.14M NaCl, 9mM Na_2HPO_4, 1.76mM KH_2PO_4, 2.68mM KCl - 5ml, 37°C) for 2min and then with 1 x trypsin EDTA (SIGMA T4174) in 1 x PBS (2ml forT75 or 3ml for T175 at 37°C for 5min). The flask was then sharply tapped to release cells and the trypsin solution quenched with an equal volume of basic growth media. An aliquot of this cell suspension was then used to inoculate fresh media (15ml for T75 or 30ml for T175 all at 37°C). A 1/25 split (150µl cell suspension from T75 flask into 15ml media) was sufficient for confluence to be regained in 3-4 days.

Fresh frozen stocks were made at the lowest possible passage number in order to maintain the line. Confluent cells were trypsinised and quenched (see above) and their numbers determined using a haemocytometer. This cell suspension was centrifuged (1000rpm, 5min, room temperature, Denley BS400 centrifuge) and the pellet resuspended in 90% v/v FBS and 10% v/v Dimethyl-suphonyl-oxide (DMSO) (SIGMA, D2650) at a cell density of 2 x 10^6 cells/ml. Aliquots (1ml) were then transferred to cryotubes (Nalge Nunc International, Denmark) and rapidly frozen to –80°C (24hr) before being transferred to liquid nitrogen for long-term storage.

2.2.6 Immunocytochemistry

ND7/23 cells were grown to confluence and trypsinised (see section 2.2.5). The cell suspension was further diluted with basic growth media (15ml (T75) or 30ml (T175), 37°C) and aliquots (1ml) placed on sterile glass coverslips (Fisher Scientific, Leicestershire, England) in the wells of a 24 well Costar plate (Greiner, Gloucestershire, England). Plates were incubated for 24hr (37°C, 5% CO_2). Spent media was aspirated and the cells washed in 2ml of 1 x PBS (37°C). The PBS was aspirated and the cells either fixed in paraformaldehyde (4% in 1 x PBS, 37°C, 15-20min) and permeabilised in either Triton X-100 (0.1% v/v in 1 x PBS, room temperature, 5min) or methanol (100%, -20°C, 5min) or fixed and permeabilised in either methanol (100%, -20°C, 5min) or methanol/acetone (1:1 mixture, -20°C, 5min). The permeabilising agent was removed, the cells rinsed in 2ml 1 x PBS and blocked in BSA (3% w/v in 1 x PBS, 0.2ml/well, room temperature, 30min). The coverslips were placed cell side down onto primary antibody (50µl, 4°C, overnight in a moist chamber), either a single antibody or a mixture of two for double labelling. The cells were washed on 5 successive drops of 1 x PBS containing 0.1% v/v TWEEN 20 (100µl, room temperature, 1min each) before being placed onto secondary antibody (50µl, diluted 1/100 in 3% w/v BSA in 1 x PBS containing 1% v/v normal goat serum (SIGMA), room temperature, 2hr), again either a single antibody or a mixture of two for double labelling. Cells were once again washed and mounted onto slides using mowiol (CALBIOCHEM) (0.1% w/v solution in 0.25% v/v glycerol, 0.1M Tris-HCl pH8.5, and 2.5% w/v p-Phenylenediamine (antifade, SIGMA)) (10µl, 4°C, overnight). The coverslips were then sealed using clear varnish,

cleaned with water and cells viewed and recorded using a confocal microscope (Leica TCS 4D) (Leica, Bensheim, Germany).

2.3 Proteins and their analysis

2.3.1 Mammalian tissue lysate extraction

Various tissue samples were removed from a euthanised male rat (dissection kindly performed by Dr Anne Roobol) and placed into liquid nitrogen. These were weighed and ground in a pestle and mortar, under liquid nitrogen, to a fine powder. Powdered tissue was then resuspended in 2ml/g lysis buffer (20mM HEPES, 5mM $MgCl^2$, 140mM KCl, 0.5% v/v Triton – X-100, 200μM PMSF (freshly added), 10μg/ml Leupeptin, 10μg/ml pepstatin A) at 4°C. This was centrifuged (13000rpm, 10min, 4°C Heraeus instruments, Biofuge pico) to remove large debris and protein concentration determined by Bradford (1976) assay with BSA as a standard. Lysates were used immediately when possible or else stored at –80°C not longer than 1 month.

2.3.2 ND7/23 cell lysate extraction

Five T175 flasks were grown to confluence and trypsinised (as in section 2.2.5 above). The suspension was centrifuged (1000rpm, 5min, room temperature, Denley BS 400 centrifuge) to pellet cells and these were washed twice in sterile 1 x PBS (first with 20ml then with 10ml). Cells were finally resuspended in lysis buffer (20mM HEPES, 5mM $MgCl_2$, 140mM KCl, 0.5% v/v Triton – X-100, 200μM PMSF (freshly added), 10μg/ml Leupeptin, 10μg/ml pepstatin A, 2ml, 4°C) and broken by pipetting the suspension up

and down several times through a 1ml pipette tip. This was centrifuged (13000rpm, 10min, 4°C Heraeus instruments, Biofuge pico) to remove cell debris and protein concentration was determined by Bradford (1976) assay with BSA as a standard.

2.3.3 Mammalian cell lysate labelling

Cells were grown to 60-70% confluence (as in section 2.2.5 above). The media was removed and labelling media (10% v/v FBS, 10% v/v regular DMEM, 2mM glutamine, 100i.u./ml penicillin, 0.1mg/ml streptomycin, 78% v/v methionine deficient DMEM (SIGMA D0422), 3700KBq 'Promix' [^{35}S] cell labelling mixture (Amersham SJQ0079, Buckinghamshire, England), 37°C) added to the flasks (5ml in T75, 10ml in T175). Cells were then incubated (37°C, 5% CO_2, 18-20hrs), harvested and lysed as above. A 1µl aliquot of the cleared lysate and post-incubation media were put into Optiphase 'Highsafe' 3 (Wallac (now Perkin-Elmer), Massachusetts, USA) (3ml) scintillation fluid and counted (Wallac (now Perkin-Elmer) 1410 Liquid scintillation counter, Massachusetts, USA) to determine specific activity.

2.3.4 Yeast lysate extraction

Cells were harvested by centrifugation (2000g, 4°C, 10mins; Beckman GS-6R centrifuge, California, USA), washed in PBS (1X PBS, 20ml, 4°C) and resuspended in PBS buffer (1X PBS, 2mM PMSF (freshly added), protease inhibitor cocktail (Roche, Mannheim, Germany), 1mM EDTA, leupeptin (2µg/ml) 200µM proteosome inhibitor MG – 132 (CALBIOCHEM, California, USA) 500µl, 4°C). 0.4mm glass beads were

added (2/3 volume) and the cells ruptured by vortexing (4°C, 5mins; 30secs on, 30secs off, but on ice). The suspension was then centrifuged (3000rpm, 4°C, 1min, Heraeus instruments, Biofuge pico) and the supernatant collected. Samples were then stored (-20°C).

2.3.5 Yeast lysate labelling

50ml yeast nitrogen base (YNB) (without amino acids or NH_4SO_4 with 5% glucose, 100μm NH_4SO_4 and amino acids added) was inoculated with approx. 200μl overnight starter culture. Cells were grown to an OD_{600} of 0.2-0.45 and 7.5 OD_{600} units of cells were harvested by centrifugation (2000g, 5 min, Beckman GS-6R centrifuge, California, USA) and the pellet resuspend in 0.5ml fresh medium but without NH_4SO_4, methionine and cysteine. 740KBq (1.4μl) 'Promix' [^{35}S] cell labelling mixture (Amersham SJQ0079, Buckinghamshire, England) was added and cells labeled for 60min (30°C, tubes agitated every minute). Labelled cells were harvested by centrifugation (30sec, room temperature, 13000rpm, Heraeus instruments, Biofuge pico) and resuspended in 200μl lysis buffer (20mM HEPES, 2mM $MgCl_2$, 140mM KCl, 1mM PMSF). Acid washed 0.4mm glass beads (2/3 volume) and 50μl lysis buffer were added and the cells ruptured by vortexing (4°C, 5mins; 30secs on, 30secs on ice). The samples were then centrifuged (30sec, room temperature, 13000rpm, Heraeus instruments, Biofuge pico) and the supernatant collected. Each 250μl sample was used for one immunoprecipitation reaction in 500μl.

2.3.6 Immunoprecipitation (IP)

0.5mg cleared cell lysate was mixed with 3μg appropriate, polyclonal, affinity-purified, antibody (stored in PBS containing 1% w/v bovine serum albumin) in a microspin column (Amersham Pharmacia Biotech Inc., Buckinghamshire, England) in a total volume of 500μl (containing 0.1% v/v Triton-X100 for 'native conditions' and 0.5% v/v Triton-X100, 1% w/v Na deoxycholate, 1% v/v nonidet P40 and 0.1% w/v SDS for 'RIPA' (denaturing) conditions) and incubated (room temperature, 100rpm shaking) for 1-2hr. 60μl of protein A suspension (Protein A-Sepaharose (SIGMA, England), made up as a 1 in 4 suspension of beads in buffer with 0.2% w/v sodium azide) was added and incubated (2hr, 4°C, 100rpm shaking). The columns were then centrifuged (1min, 4°C, 13000rpm, Heraeus instruments, Biofuge pico) and the flow through removed. The beads were then washed (2 x 500μl) in the appropriate buffer and proteins solubilised from the beads by resuspending them in 60μl 2 × SDS-PAGE sample buffer ((5X) 57.5% v/v glycerol, 0.33M Tris pH6.8, 5% w/v SDS, 10% v/v mercaptoethanol, 0.03% w/v bromophenol blue, 0.03% w/v pyronene G) and incubating for 2min in a boiling water bath. The samples were collected by centrifugation (1min, 13000rpm, room temperature, Heraeus instruments, Biofuge pico) before loading onto gels as above.

2.3.7 Sup35p sedimentation analysis

Saccharomyces cerevisiae strains 74-D694 [*PSI*$^+$] and 74-D694 [*psi*$^-$] were grown (50ml YEPD, 30°C, overnight, 200rpm shaking) to an OD_{600} of 4. Cell lysate was made (as in section 2.5.4 above) and the initial, low-speed supernatant (100μl) used in sedimentation

analysis. Samples were centrifuged at high speed (50 000rpm, 4°C, 15min, Beckman TL 100.3 rotor, Beckman TL 100 ultra centrifuge, California, USA), the supernatant removed and the pellet resuspended in an equal volume of PBS buffer.

2.3.8 *In vitro* transcription/translations

Rabbit reticulocyte TNT lysate (L4610, Promega, Wisconsin, U.S.A.) was used to perform *in vitro* transcription/translations in the presence of [^{35}S]-methionine (AG1094, Amersham Pharmacia Biotech Inc. Buckinghamshire, England) to radiolabel the products. The reaction mixture was always set up in the same way (see table 2.1) with only the added plasmid (always with a T7 promoter) being different.

Reaction component	Concentration
Plasmid	2µg
Rabbit reticulocyte lysate	50µl
Polymerase buffer	1 x
T7 Polymerase	40 units
Amino acids without methionine	20µM
Rnasin	80 units
Redivue [^{35}S] L-methionine	1480KBq (400nmol)
Add sterile milli Q H_2O to 100µl	

Table 2.1 Components of *in vitro* translation reactions.

The reaction mixture was then incubated (30°C) and at 10min intervals 2µl was removed and added to 20µl 2 x Laemmli (1970) sample buffer and 5µl removed and added to 5µl EDTA (20mM), samples were then flash frozen on dry ice. After 30min, 39µl reaction mix was removed and added to 0.85µl Aurintricarboxylic acid (ATC) (3.75mM) and samples again taken from all reactions every 10min up to 80min total time elapsed.

Laemmli (1970) samples were then loaded onto 9% SDS-PAGE gels with 4.5% stack and electrophoresed as above. 10µl native sample buffer was added to the EDTA samples and they were then loaded onto 6% native gels with 3.25% stack and electrophoresed as above. Gels were then dried and autoradiographed as above and the resultant films analysed using Bio-Rad GelDoc bioimaging system (California, USA).

2.3.9 ATP assays

ATP assays were carried out using the ATP-Lite™ Luminescence ATP detection assay system from Packard Biosciences (now Perkin Elmer, Massachusetts, USA). This assay system is based on the reaction:

$$\text{ATP} + \text{D-Luciferin} + O_2 \xrightarrow[Mg^{2+}]{\text{Luciferase}} \text{Oxyluciferin} + \text{AMP} + \text{PPi} + CO_2 + \text{LIGHT}$$

Where the light output is proportional to the ATP concentration. This assay is normally used to estimate cell viability, therefore, the assay procedure was changed slightly to modify the kit to measure ATPase activity. Samples were prepared by immunoprecipitation in the presence of ATP (10mM) to recover single CCT subunits, protein concentration was determined by comparison of a known quantity of beads to a

standard concentration of BSA by SDS-PAGE, coomassie staining and quantification using the BioRad GelDoc Bioimaging system. At time = 0 the protein was made 1mM ATP and 1µl removed and mixed with 99µl water and 50µl mammalian cell lysis solution, from the kit, in a 96 well plate (Packard Biosciences now Perkin Elmer, Massachusetts, USA), to prevent any further ATPase activity and stabilise the ATP present in the sample. After 10 and 20 min of incubation (room temperature) further 1µl samples were mixed with 99µl water and 50µl mammalian cell lysis solution. 50µl of substrate solution was then added and the wells well mixed for 5 min. The plates were then dark adapted for 10min and read in the Wallac luminometer (Wallac, now Perkin Elmer, Massachusetts, USA).

The amount of ATP used in the time indicated was determined and a specific ATPase activity calculated. This was repeated several times and an average taken.

2.4 Gels and Western Blots

2.4.1 SDS polyacrylamide gel electrophoresis (Laemmli 1970)

Protein samples with 20% v/v 5x concentrated dye mix (57.5% v/v glycerol, 0.33M Tris pH6.8, 5% w/v SDS, 10% v/v mercaptoethanol, 0.03% w/v bromophenol blue, 0.03% w/v pyronine G) were heated at 95°C for 2min and then electrophoresed (30mA, 1hr, room temperature) on a 9% acrylamide gel (0.375M Tris pH8.9, 9% w/v acrylamide:bisacrylamide (19:1), 0.1% w/v SDS, 0.1% w/v ammonium persulphate, 1% v/v TEMED), 1.5mm gel thickness, with 4.5% acrylamide stacking gel (0.125M Tris pH6.8, 4.5% w/v acrylamide, 0.1% w/v SDS, 1% w/v ammonium persulphate) in 1 x

Laemmli running buffer (1% w/v SDS, 0.25M Tris, 1.92M glycine) using the Hoeffer (California, USA) mini-gel apparatus.

2.4.2 Native polyacrylamide gel electrophoresis (derived from Liou & Willison, 1997)

Protein samples with 20% v/v 5x concentrated dye mix (250mM Bis-Tris-HCl pH7.0, 25% v/v glycerol, 10mM glutathione, 5mM methionine, 5mM cysteine, 0.15% w/v ponceau S), were electrophoresed (90v, 4hrs, 4^0C) on a 6% acrylamide gel (0.37M Tris-HCl pH8.8, 6% w/v acrylamide:bisacrylamide (19:1), 0.1% w/v ammonium persulphate, 0.1mM GTP, 1% v/v TEMED), 1.5mm gel thickness, with 3.25% acrylamide stacking gel (57.2mM Tris-HCl pH8.8, 3.25% w/v acrylamide, 0.152% w/v ammonium persulphate, 0.1mM GTP, 1% v/v TEMED), in 1x running buffer (0.25M Tris pH8.6, 1.92M glycine, 0.1mM GTP).

2.4.3 Two-Dimensional i.e.f/PAGE (modified version of O'Farrell, 1975, described by Burland *et al*, 1983)

To resolve complex mixtures of proteins the first dimension employed isoelectric focusing between pH 3.5 – pH 10 (with a shallower gradient achieved between pH 5 – pH 7, see Burland *et al*, 1983), and the second dimension was SDS poly-acrylamide gel electrophoresis.

The first dimension 'stick gels' were prepared in 1.5mm glass tubes using the Hoeffer (California, USA) system. Gel mixture was prepared (540mM Urea, 0.034% v/v

NONIDET p40, 0.07% w/v acrylamide, 0.004% w/v Bis-acylamide, 3.4% v/v Ampholine pH 5-7, 5% v/v Ampholine pH 3.5-10, made up to 5.83ml with H_2O, room temperature (30°C briefly to dissolve urea)) and degassed before being polymerised by the addition of 20µl APS (10% w/v) and 10µl TEMED. The casting apparatus was assembled according to the manufacturer's instructions and 20ml of water was layered onto the gel mixture to ensure the sticks were filled.

Samples were prepared by precipitating 3 – 6ml cell lysate, by the addition of 2 volumes acetone (-20°C) overnight at –20°C. Centrifuged (13000rpm, 15min, 4°C, Heraeus instruments, Biofuge pico) pellets were resuspended pellets in 200 – 400µl sample buffer (1mM urea, 2% v/v NONIDET p40, 5% v/v β – mercaptoethanol, 2% v/v Ampholine pH 5-7, 3% v/v Ampholine pH 3.5-10).

20µl of sample was loaded per stick and electrophoresed (500v, 3hr) with 0.08% w/v NaOH in the upper reservoir (negative) and 0.1% v/v Phosphoric acid in the lower reservoir (positive). Once electrophoresed, sticks were equilibrated in 1 x Laemmli sample buffer and loaded onto 9% SDS-PAGE gels with 4.5% stack, using 1% w/v agarose in 0.125M Tris – HCL pH 6.8 as a securing agent. The second dimension, standard SDS-PAGE, was as described (section 2.4.1).

2.4.4 Gel staining

Gels were usually stained immediately on completion of electrophoresis using Coomassie brilliant blue (0.25% w/v Coomassie brilliant blue G250, 50% v/v methanol, 10% v/v glacial acetic acid) for 30min to 1hr (room temperature, 100 rpm shaking). The

gels were then transferred to destain buffer (50% v/v methanol, 10% v/v glacial acetic acid) for several hours until bands could be clearly seen. The addition of 2cm diameter sponge pieces (retrieved from Roche enzyme packaging) enabled the destain process to be speeded up.

For more sensitive protein detection gels were stained with silver by the method of Wray *et al* (1981). Briefly, gels were soaked in 50% v/v methanol (room temperature, 200rpm, overnight) and then put into staining solution (0.8% w/v $AgNO_3$, 0.075% w/v NaOH, 0.2M NH_3) (100ml, 15min, room temperature, 200rpm). Gels were then rinsed in dH_2O (200ml, 5min, room temperature, 200rpm) and placed into 500ml developer (0.005% w/v citric acid, 0.02% v/v formaldehyde) at room temperature (400rpm) for 15min or until a yellow background was observed. Gels were then immediately put into 100ml stop solution (50% v/v methanol, 10% v/v acetic acid) for 15min at room temperature, (200rpm). Gels were then photographed using the BioRad Geldoc Imaging system (California, USA) and dried (70°C, 90min, medium ramp, ATTO Rapidry, New York, USA).

2.4.5 Western blotting (Tobin *et al,* 1979)

Protein samples were electrophoresed (section 2.4.1) and the acrylamide gel then sandwiched between blotting paper (3M Whatman) and nitrocellulose membrane ensuring all air bubbles were removed. Transfer of the proteins from the gel to the membrane took place over 1 hour (4°C, 750mA total field) in transfer buffer (39mM glycine, 48mM Tris, 0.037% w/v SDS, 20% v/v methanol). The membrane was usually then stained with Ponceau S (3% w/v TCA, 1% w/v ponceau S, 5min, room temperature,

100rpm), rinsed in dH_2O and any marker bands identified and marked with pencil. Membranes were then blocked in fat-free dried milk (5% w/v Marvel™, 1 x PBS) for 1 hour (room temperature, 100rpm). The primary antibody (diluted in fat free milk) was then added overnight (4°C, 100rpm). The membrane was then washed in stringent buffer (2% w/v NaCl, 0.1% v/v TWEEN 20, 1 x PBS) (10mins, room temperature, 100rpm) and then in fat free milk (3 x 15mins, room temperature, 100rpm). The membrane was then incubated (1hr, room temperature, 200rpm) with the appropriate secondary antibody (1/1000 dilution in fat free milk), washed in stringent buffer (10min, room temperature, 100rpm) and then washed in 1 x PBS, 0.1% v/v TWEEN 20 (4 x 10mins, room temperature, 100rpm). Antibody binding was detected using enhanced chemiluminescence substrate (equal volumes of solution 1 (2.5mM Luminol [from a 250mM stock in DMSO], 0.4mM Coumaric acid [from a 90mM stock in DMSO], 0.1M Tris-HCl pH8.5) and solution 2 (0.1M Tris-HCl pH8.5, 0.02% v/v H_2O_2)) (Rodrigues, 1999). The membrane was incubated in the substrate (5min, room temperature, 100rpm) and exposed to chemiluminescence film.

Membranes were also permanently stained using diaminobenzidine (Roobol & Carden, 1993). The membrane was incubated (10mins, room temperature, 100rpm) with 50mM phosphate (25ml pH7.4) and then with diaminobenzadine solution (0.03% w/v $AmmNiSO_4$, 0.03% w/v $CoCl_2$, 0.5mg/ml diaminobenzadine, 50mM phosphate) (25ml, 10 mins, room temperature, 100rpm). H_2O_2 (0.002% v/v) is added to the diaminobenzadine solution and the membrane incubated (25ml, room temperature, 100rpm) for 10mins. Finally the membrane was rinsed in 50mM phosphate and allowed to air dry

2.4.6 Autoradiography

For autoradiography experiments, radio-labelled proteins were electrophoresed on the appropriate acrylamide gel and stained gels were dried (70°C, 90min, medium ramp, ATTO Rapidry, New York, USA), and exposed to autoradiography film (room temperature, 1-7 days).

2.5 Purification of CCT (derived from Lewis *et al* (1992) as modified by Roobol *et al*, 1995)

2.5.1 Sucrose gradients

A 40% w/v solution of sucrose was prepared in sucrose gradient buffer (20mM HEPES-NaOH pH7.2, 90mM KCl) and 2.75ml added to a Beckman (California, USA) SW28 centrifuge tube (0.93ml for SW40) and frozen on dry ice. The solution is then diluted to 37.5% w/v using sucrose gradient buffer and a further layer added to the tubes and frozen on dry ice. This process is continued until a final, 10% w/v sucrose, layer has been added and frozen. Before use, prepared gradients were thawed at 4°C, overnight, this produces an essentially continuous gradient. Soluble cell extracts from yeast, rat testis or cultured ND7/23 (up to 4ml) were layered onto the top of thawed sucrose gradients and these were then balanced and centrifuged (25000rpm, 4°C, 18hr, acceleration setting 7, deceleration setting 0, Beckman SW40 or SW28 swing out rotor, Beckman L8-70M ultracentrifuge, California, USA). Gradients were fractionated at room temperature by lowering a 19 guage, 15cm, blunted needle into the bottom of the gradient and extracting 1 or 2ml fractions using a peristaltic pump and automated

fraction collector (Amersham Pharmacia Biotech, Buckinghamshire, England). The residual pellet was then resuspended in 1ml sucrose gradient buffer (no sucrose).

2.5.2 Ion exchange chromatography

The CCT content of sucrose gradient fractions was assessed by Coomassie-stained SDS-PAGE. These fractions were obvious (see figure 2.1) and were pooled. The pool was loaded onto a Resource Q (1ml, Amersham Pharmacia Biotech, Buckinghamshire, England, binding capacity: 25mg protein/ml matrix) ion exchange column using the Fast Purification Liquid Chromatography (FPLC) apparatus (Waters 650E, Massachusetts, USA). Fractions were eluted over a 100mM – 400mM NaCL gradient (start buffer: 20mM HEPES pH 7.6 with NaOH, 2mM MgCl2, 100mM NaCl; end buffer: 20mM HEPES pH 7.6 with NaOH, 2mM MgCl2, 400mM NaCl; flow rate of 0.5ml/min, gradient curve of 6 (linear increase in end buffer and decrease in start buffer over time), 40min).

Fractions were again analysed by SDS-PAGE and coomassie staining as above to identify fractions containing CCT. These fractions were then pooled and protein concentration was determined using the Bradford (1976) assay with BSA as a standard. CCT was then stored at $-80^{o}C$.

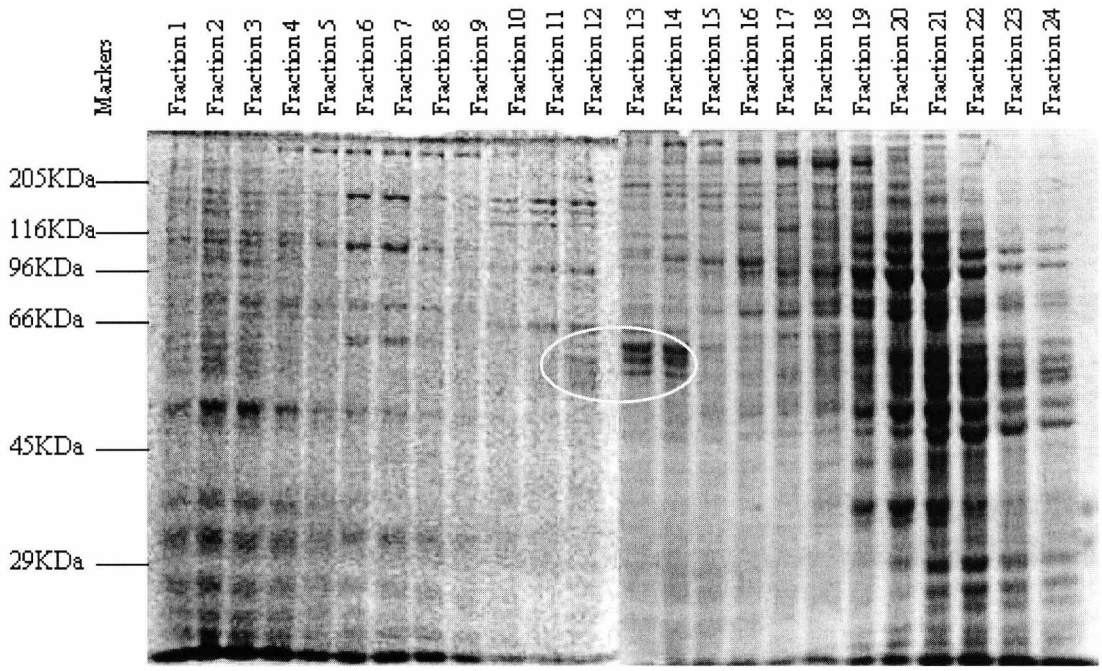

Figure 2.1 SDS-PAGE analysis of the fractions obtained from a 10-40% sucrose gradient. 'Soluble extract from rat testis was centrifuged (25000rpm, 4°C, 18hr, acceleration setting 7, deceleration setting 0, Beckman SW40 swing out rotor, Beckman L8-70M ultracentrifuge) through a 10-40% sucrose gradient and the gradient fractionated. The fractions were separated by SDS-PAGE (9% gel, 30mA, 1hr), stained using coomassie brilliant blue and visulaised using Bio-Rad bioimager. CCT is circled and appears in the 26S fractions.

2.6 Chromatographic analysis

2.6.1 ATP column analysis

A 10mm x 100mm advanced purification glass column (WAT021901, Waters, Massachusetts, USA) containing ATP immobilised on cross-linked 4% beaded agarose with a 9 atom spacer (SIGMA, A-2767) was made by swelling the lyophilised ATP-agarose in 10ml column buffer (20mM HEPES - KOH pH7.2, 10mM $MgCl_2$, 140mM KCl, 10%w/v glycerol) and then degassing the slurry for 10min using a vacuum pump. The slurry was then applied to the column and washed with several column volumes of buffer and then sealed using 2 inlet connector assemblies (WAT021904, Waters, Massachusetts, USA).

Sucrose gradient fractions containing CCT were loaded onto the column using the Fast Purification Liquid Chromatography (FPLC) apparatus (Waters 650E, Massachusetts, USA). Fractions were eluted over a 0mM – 10mM ATP gradient (start buffer: 20mM HEPES - KOH pH7.2, 10mM $MgCl_2$, 140mM KCl, 10%w/v glycerol; end buffer: 20mM HEPES – KOH pH7.2, 10mM $MgCl_2$, 140mM KCl, 10%w/v glycerol, 10mM ATP; flow rate of 0.5ml/min, gradient increase of end buffer of 2.5%/min, 40min). The column run was also carried out using NaCl in place of KCl.

Fractions were analysed by dot blotting 50µl onto nitro-cellulose and treating this as a western blot as in section 2.6.6. Fractions were also analysed by SDS-PAGE and native PAGE as above.

2.6.2 Superose 6 column

Mammalian cell lysate (15mg/ml) was prepared as above and filtered through a 0.2µm (Millipore, Molsheim, France) filter to remove any small particles.

A sample of the lysate was made 10mM ATP by the addition of a 1M stock solution of ATP. A further sample was immunoprecipitated using CCT β C-terminal antibodies in the presence of 10mM ATP and the unbound protein collected. A sample of this had the ATP removed by incubation (room temperature, 15min) with 5 units of apyrase (SIGMA, A6132).

These samples were loaded, individually, onto a Superose 6 HR 10/30 column (Amersham Pharmacia Biotech, Buckinghamshire, England) using the Fast Purification Liquid Chromatography (FPLC) apparatus (Waters, Massachusetts, USA). Fractions

were eluted using lysis buffer without Triton X-100. Fractions were analysed by SDS-PAGE and western blotting.

2.7 Antibody production

2.7.1 Peptide immunogens

Extreme C-terminal peptides approximately 15 amino acids long were identified from the predicted protein sequences of the 8 yeast CCT subunits (CCT1p-8p), Sup35p and murine GSPT1/2 in the NCBI database (fig 2.2). These peptides were synthesised (Judy Hardy, Biosciences Department, University of Kent) with an additional cysteine introduced at the N-terminus for use in conjugation and checked by mass spectroscopy (Judy Hardy, Biosciences Department, University of Kent).

Yeast CCT α	NH_2–CTVDPEPPKEDPHDH-COOH
Yeast CCT β	NH_2–CIIRARPRTANRQHM-COOH
Yeast CCT γ	NH_2–CLRVDDIVSGVRKQE-COOH
Yeast CCT δ	NH_2–CVKSILRIDDIAFSR-COOH
Yeast CCT ε	NH_2–CLKIDNVIISGKDEY-COOH
Yeast CCT ζ	NH_2–CLLRAGRSTLKETPQ-COOH
Yeast CCT η	NH_2–CMPPQGAGRGRGMPM-COOH
Yeast CCT θ	NH_2–CAPQGPRPGNWDQED-COOH
Yeast Sup35p	NH_2–CQGTTIAIGKIVKIAE-COOH
Murine GSPT1/2	NH_2–CGKVLKLVPEKD-COOH

Figure 2.2 Peptides designed for the construction of antibodies

2.7.2 Activated KLH preparation (McCray & Werner 1989)

30mg Keyhole Lympet Haemocyanin (KLH) (CALBIOCHEM, California, USA) was dialysed overnight into 1L 50mM Phosphate (pH 7.5, 4°C). 8mg MaleimidoBenzoic acid N-hydroxy-Succinimide ester (MBS,) (Pierce) (in 100µl anhydrous DiMethyl Formamide (DMF)) was added dropwise to stirred KLH solution (room temperature). The reaction mix was stirred in a stoppered vial (30min, room temperature), 100µl Glycylglycine (50mg/ml in the phosphate buffer adjusted with 1M NaOH to pH7) added to block further reaction and the mixture centrifuged (10min, room temperature, 13000rpm, Heraeus instruments, Biofuge pico) to remove large aggregates. This activated KLH was rapidly desalted over a pharmacia FPLC fast desalting column equilibrated and eluted with 50mM phosphate bufffer (pH7.5) and was stored as 3-4mg aliquots at –80°C.

2.7.3 Peptide coupling

3-6mg peptide were dissolved in 100µl 50mM phosphate buffer, adjusted to pH7-7.4 with 400mM phosphate buffer (pH 7.4). The peptide solution was mixed with 3-4mg activated KLH and stirred in the dark (room temperature, 3hr). The conjugate was dialysed into PBS (1L) overnight (4°C, with stirring) and aliquoted into appropriate immunogen doses.

2.7.4 Immunization

Brian Cover and Sarah Reed (Biological services unit, University of Kent) performed all procedures under home office license according to guidelines in the Animal Scientific Procedures Act (1986).

Primary injections of 400μg (rabbit) or 100μg (Guinea Pig) of the conjugate in Freund's complete adjuvant (FCA) are given followed by boosts of 400μg (rabbit) or 100μg (Guinea Pig) of the conjugate in IFCA at four weekly intervals. Test bleeds were carried out after the 3rd injection, and the terminal bleed was usually done after the 4th/5th injection.

2.7.5 Serum testing

Appropriate cell lysate samples were electrophoresed on a 9% SDS-PAGE gel and blotted (as in sections 2.4.1 and 2.4.6 above). Using a 'mini-blotter' (Biometra, Göttingen, Germany), a variety of concentrations of sera were incubated on the blot (4^{o}C, overnight, no shaking) and the blot developed (as in section 2.4.6 above). The terminal bleed was made when the antibody titre was such that a strong signal was obtained at a 1/1000 dilution. Screening was repeated once antibody had been affinity purified.

2.7.6 Peptide columns

3ml Sulfolink® (Pierce, Illinois, USA) coupling gel suspension was added to a small BioRad (California, USA) column and washed with 12ml coupling buffer (50mM Tris-

HCl pH8.5 containing 5mM EDTA). 3-6mg peptide was dissolved in 2ml coupling buffer and added to the column. This was mixed end over end (room temperature, 15min) in the dark and the gel allowed to settle for 30min. The column was washed with 15ml coupling buffer and 1.5ml blocking buffer (30µl β-mercaptoethanol in 5ml coupling buffer), added. This was mixed end over end (room temperature,15min), then allowed to settle for 30min. Finally the column was washed with 1M NaCl (15ml) and could be stored in 1 x PBS (with 0.02% w/v azide, 4°C) for up to ten years before use.

2.7.7 Antibody affinity purification

4-6ml serum containing 2µl each of leupeptin (5mg/ml), Pepstatin (1mg/ml in ethanol) and phenyl methyl sulphonyl fluoride (PMSF) (100mM in isopropanol) was applied to an appropriate affinity column (flow rate 15ml/h, 4°C, capacity 15mg) pre-equilibrated with 1 x PBS and the flow-through collected for assay of unbound antibody. The column was then washed (flow rate 30ml/h) with 15-30ml 1 x PBS and then 15-30ml 1 x PBS containing 1M NaCl. Bound antibody was eluted with 30ml of acidic (0.1M glycine, 0.15M NaCl, pH2.8) buffer. The fractions collected were neutralised as quickly as possible with unbuffered 2M Tris and the column neutralised by washing through 30ml 0.1M Phosphate buffer pH 7.4. The column was then washed with 1 x PBS containing 0.02% w/v NaN_3 for storage (4°C).

Neutralised fractions were assayed for antibody by spotting 2µl of each fraction onto nitrocellulose, blocking in 5% w/v fat free dried milk (Marvel™) in 1 x PBS (room temperature, 1h, 100rpm), incubating with peroxidase conjugated anti-rabbit or anti-

guinea pig secondary antibody at 1/1000 concentration (in 5% w/v Marvel™ in 1 x PBS, room temperature, 1h, 100rpm), and developed using the diaminobenzidine stain (as in section 2.2.6 above). Positive fractions were pooled and protein concentration determined by the method of Bradford (1976) before adding 1% w/v BSA and dialysis into 1 x PBS containing 0.02% w/v NaN_3 overnight. Purified antibody was stored at –20°C.

2.8 PCR, DNA Cloning and related procedures

2.8.1 Bioinformatics and primer design

Sequences for CCT subunits, eRF3 and I.M.A.G.E. (Lennon *et al*, 1996) clones were located in the National Centre for Biotechnology Information (NCBI) database (http://www.ncbi.nlm.nih.gov/) and BLAST (Altschul *et al*, 1990; http://www.ncbi.nlm.nih.gov/BLAST/). DNA translations were carried out using The Protein Machine (Flores *et al*, 1998; http://www2.ebi.ac.uk/translate/) and comparisons were performed using CLUSTALW (Thompson, Higgins & Gibson 1994; http://www.clustalw.genome.ad.jp/).

Primers were designed for sequencing of I.M.A.G.E. clones 586105 (GSPT2) and 533932 (GSPT1). These primers were also used for PCR to screen putative clones. The primers included a cytosine or guanine residue at the 3' end, where possible, with minimal sequence repeats and a cytosine and guanine content of approximately 50%. Primers used in this study are shown in figure 2.3.

T7	5' – GTA ATA CGA CTC ACT ATA GGG CG – 3'
T3	5' – AAT TAA CCC TCA CTA AAG GGA – 3'
GSPT2 F1 (5')	5' – CTT CAG CAG TCA GCT CAA CAT CCA – 3'
GSPT2 F2 (5')	5' – GAC AGG AAT GGT TGA CAG AAG GAC – 3'
GSPT2 R1 (3')	5' – GTC TAC TAA GGA GAT CAA GGC TG – 3'
GSPT1 F1 (5')	5' – CTA CTG TTA GCA TGG – 3'

Figure 2.3 Primers designed for PCR and sequencing.

2.8.2 Plasmid purification and precipitation

Plasmids were extracted using the QIAGEN (West Sussex, England) QIAfilter midiprep kit according to manufacturers instructions. Purified plasmids were quantified by spectrophotometry (OD_{260} and OD_{280}) and if the concentration was insufficient then precipitation was carried out: dilute plasmid was made 300mM sodium acetate and 2 volumes of ethanol (-20°C) added. This was then incubated at -80°C for 2 hours, the solution centrifuged (13000g, 10mins; Heraeus instruments, Biofuge pico) and the pellet washed with 70% v/v ethanol (100µl, -20°C). Excess liquid was drained from the pellet, which was then incubated (55°C, 5mins) to resuspend it in sterile dH_2O (50µl).

2.8.3 Sequencing

I.M.A.G.E. clones 586105 (GSPT2) and 533932 (GSPT1) were sent to MWG-Biotech (Milton Keynes, England) for sequencing. The initial primers were T7 and T3 (I.M.A.G.E. clones) (see figure 2.1). As sequence fragments were returned, new internal primers were designed and samples resequenced by MWG.

2.8.4 Restriction digestion of plasmids

Isolated plasmid was digested with EcoRI, XhoI, BamHI or XbaI separately or in combination. Digestion reactions were set up containing the following; 1 x restriction buffer, 1μg DNA sample, 10u restriction enzyme, 1mg/ml acetylated bovine serum albumin (BSA), to stabilize the enzyme, and nuclease free H_2O to a final volume of 20μl.

Reaction mixtures were incubated for 4hrs at 37°C, and then placed at 65°C (10mins) to denature the enzyme. Dye containing sample buffer (5 x concentrate; 15% v/v Ficoll® 400, 0.03% w/v bromophenol blue, 0.03% w/v xylene cyanol FF, 0.4% w/v orange G, 10mM Tris-HCl pH7.5, 50mM EDTA) was added to the mixtures and they were electrophoresed on a 0.7% TAE (40mM Tris, 1mM EDTA, 17.8mM glacial acetic acid) agarose (low melting point) gel (containing 0.5mg/ml ethidium bromide) (75V, room temperature). Markers and undigested DNA were also electrophoresed on the gel as controls.

2.8.5 Purification of redigested DNA fragments

Digested product was excised from a 0.7% low melting point agarose gel and purified using the Hybaid Recovery ™ DNA Purification Kit II (Middlesex, U.K.) according to the manufacturer's instructions. Once purified, DNA concentration was determined by spectrophotometry (Eppendorf BioPhotometer, Hamburg, Germany).

2.8.6 Ligation

Ligations were carried out in 5min using the Rapid Ligation Kit from Roche (Mannheim, Germany) according to manufacturer's instructions, using equimolar concentrations of plasmid and insert and transformation performed into bacteria (see section 2.2.3).

2.8.7 Screening of putative clones

Samples of putative clones were pooled (5 colonies/pool) in sterile H_2O (100µl) and boiled (100°C, 15mins) to rupture the cells. The resultant liquid (10µl) was used as template DNA for PCR using the appropriate 5' and 3' primers. Samples (20µl) were electrophoresed on a 1% TAE agarose gel (90V, room temperature).

Pools producing positive PCR results were split and the individual clones re-screened by PCR, to find the positive colonies.

2.8.8 PCR composition and program

PCR studies were carried out using Taq DNA polymerase (Promega, Southampton, England). The PCR reaction composition stayed constant (see table 2.1) with only the DNA template being variable. In every set of reactions a negative control was used which contained all reaction components (see table 2.2) except template DNA, to check for contamination. A positive control was also included, where possible, to ensure the reaction had been successful.

Reaction component	**Concentration**
dNTPs	0.05mM
PCR buffer	1X
$MgCl_2$	1.5mM
Template DNA	10ml colony mixture
Primers	10pmol (each)
Taq DNA Polymerase	2.5u (0.5µl)
Use sterile milli Q H_2O to 50µl	

Table 2.2 PCR Reaction Componants for Taq DNA polymerase.

The PCR reactions were carried out in the Perkin Elmer Genamp PCR System 2400 (Boston, Massachusetts). The PCR program involved cycles consisting of a melting phase (94°C for 30secs), an annealing phase (30secs; chosen to be 5°C below the lowest melting point of the primers) and a polymerisation phase (72°C for 1.5min) performed 35 times.

Once the cycle had reached its conclusion, samples (10µl) of the reaction mixture, with 17% running dye (40% w/v sucrose, 0.25% w/v bromophenol blue, 0.25% w/v xylene cyanol FF), were electrophoresed on a 1% TAE agarose gel (containing 0.5µg/ml ethidium bromide) (90V, room temperature) to check for product presence and contamination. DNA was visualised and photographed using the BioRad Geldoc Imaging system (California, USA).

2.9 Yeast plasmid shuffling (Kaiser *et al*, 1994)

This method allows complementing genes to be tested in a yeast strain where an essential gene has been disrupted and viability is maintained by the same gene on a plasmid containing a *URA3* selectable marker. Once transformed with the complementing gene on another plasmid, the *URA3* plasmid is lost by growing the cells on media containing 5-fluoroorotic acid (5-FOA). The gene product of *URA3*, orotidine-5'-phoshphate decarboxylase, converts 5-FOA to 5-flourouracil which is toxic to cells and hence only those cells which have lost the plasmid remain viable on this media.

S. cerevisiae strain MT700/9D containing a disrupted genomic *SUP35* gene and maintained by pYK810 plasmid containing wild type *SUP35* and *URA3* was transformed (as in section 2.2.2 above) with either wild type *SUP35* (pR-Sp) or *SUP35* with the N-terminal domain missing (ΔN) (pRΔN) (Parham *et al*, 2001) The transformants were then streaked onto 5-FOA containing plates (0.67% w/v Yeast nitrogen base (YNB), 2% w/v D-glucose, 1% w/v supplement mixture (equal quantities of all amino acids plus adenine and uracil), 1mg/ml 5-FOA, 2% w/v agar) and incubated (30°C) for 48hrs. Colonies were then replica plated onto media lacking uracil (0.67% w/v YNB, 2% w/v glucose, 1% w/v supplement mixture lacking uracil, 2% w/v agar) to ensure the *URA3* gene had been lost. Cells were then treated in the usual way.

Chapter 3: Production of New Peptide-Specific Antibodies Useful in CCT Research

3.1 Aims

One aim of my thesis research was to examine a possible interaction between CCT and a model prion, Sup35p, in yeast. The rationale for studying this interaction is given later (Chapter 4) but suitable antibodies were not available commercially and existing antibodies against murine CCT subunits did not cross-react with their yeast orthologues. It is clear from sequence data why this would very likely be the case. It was a significant effort to generate and characterise such antibodies. Because of this, and the fact that in general much of the research described in this thesis relied absolutely on using specific antibodies as tools to identify or selectively bind proteins of interest (e.g. individual CCT subunits), this chapter describes the procedures I used to generate and characterize new antibodies. To put this work in context, a short introductory section follows, intended to provide a general background to antibodies.

3.2 Introduction

3.2.1 Antibodies

Antibodies are unique proteins in that they are generated from a conserved set of genes (Harlow & Lane, 1988, Kuby, 1997) to produce a random set of molecules in any single individual, having the ability to bind practically any foreign element (antigen). The total number of antigenic determinants theoretically recognizable is estimated to be in the region of 100 million (Harris, 1991), even including lipids (Schuster *et al*, 1979). In the body, the functions of antibodies, in the humoral immune response, is to recognize and bind to 'foreign' elements found on invading organisms and to recruit other components of the immune system such as complement and macrophages, to destroy the invader (Kuby, 1997). Antibodies are able to do this by virtue of their structure, which includes 'heavy' (H) and 'light' (L) polypeptide chains, each of which have conserved (C) and variable (V) domains (see figure 3.1). These are arranged in such a way that the variable (V_H and V_L) domains are located at the extremes of two arms on a Y-shaped molecule (in IgG at least). These terminal (Fab) regions are responsible for antigen binding (bivalent in IgG) while the conserved (Fc) domains, at the stem end, are more constant in their sequence and responsible for recruiting the other elements of the immune response (Edelman, 1973) (see figure 3.1).

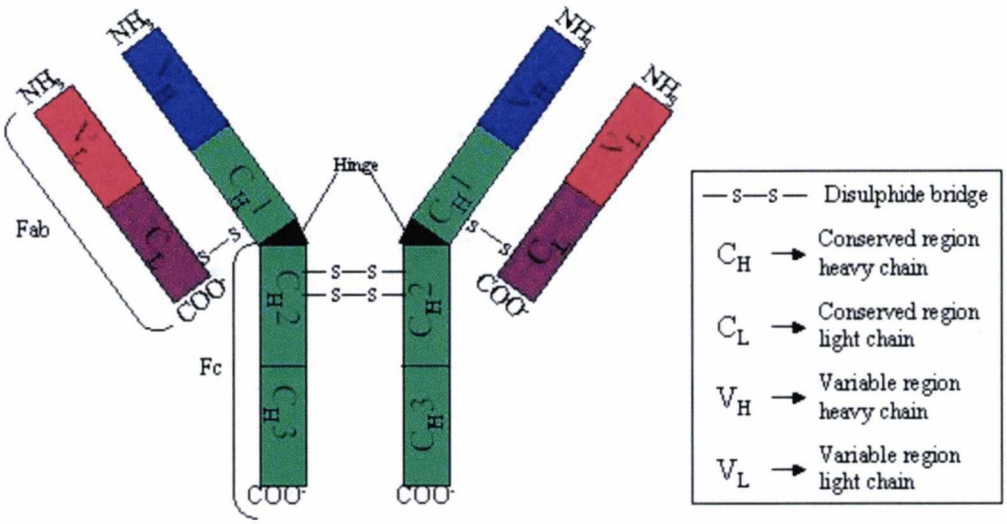

Figure 3.1 Diagram of standard antibody showing arrangement of variable and conserved heavy and light chains and the Fab and Fc regions.

The constant regions of heavy (H) and light (L) antibody chains contain determinants that distinguish the antibodies into classes, the main ones being IgA, IgD, IgE, IgG and IgM. The structure of IgA and IgM can be further modified by the addition of a 'J' chain which binds the Fc regions of two (IgA) or more (pentameric IgM) antibody units together to create multivalent antibodies (Kuby, 1997). Altogether this structure allows an antibody to bind highly specifically and tightly, by a combination of affinity, with affinity constants typically between 10^6 and 10^9 M (Harris, 1991), and avidity by virtue of its double (or more) recognition sites to its target. Since the discovery of the specific nature of the antibody, these molecules have become a powerful tool in the biochemical and cell biological study of proteins.

3.2.2 Polyclonal antibodies

When an animal is immunized with antigen (either naturally or artificially introduced), the immune response manufactures antibody by the clonal expansion of

B cells specifically carrying antibodies able to bind that antigen. This clonal expansion produces a number of different antibodies referred to as a polyclonal set of antibodies. This type of antibody response is relatively quick, easy and cheap to produce artificially. However, the antibodies generated may not be targeted to a particular part of the protein and can prove both difficult to purify and cross-reactive. Such antibodies are of limited use. Antibodies to specific target areas of a protein are more useful and easier to purify. They can be generated either by the monoclonal antibody route (Köhler & Milstein, 1975) or by use of synthetic peptide antigens (or short sequences expressed recombinantly). Both the monoclonal and peptide-specific approaches will now be described briefly.

3.2.3 Monoclonal antibodies (mAbs)

Technology now allows the production of antibodies specific to a particular region of a complex protein (Köhler & Milstein, 1975). Such antibodies can assist in the elucidation of function and structure of the target protein as they have in the case of CCT (Chapter 1 and e.g. Llorca *et al*, 1999). Monoclonal antibodies are produced artificially by selecting a particular B cell from an induced immune response and fusing it with a cancer cell (myeloma) to form a hybridoma. This conveys on the B cell immortality and allows it to be grown in culture indefinitely. In effect, usually the spleen of an immunized laboratory animal (most often a mouse) is disrupted into its individual cells and all are then fused with cultured cells from a suitable myeloma cell line. Individual hybridomas, each secreting a pure population of unique mAb of suitable specificity and affinity, must then be identified by some screening procedure and then grown (cloned) in isolation by limiting dilution. This is not a trivial undertaking. Because such antibodies are derived from a single original B cell they

are referred to as monoclonal. Monoclonal antibodies can be extremely specific and non-variable, yielding a vast number of uses. However, production of monoclonal antibodies can be a time consuming, difficult process and can prove to be expensive too. Past attempts by a previous PhD student in my supervisor's laboratory (Julie Grantham) and by a senior research fellow (Dr Anne Roobol) were both disappointing. Moreover, although purification is simple, large quantities of antibody can be difficult to produce as the method relies on the growth of hybridomas in culture rather than the production of ascites (from an animal implanted with the hybridoma cell), which is now forbidden, at least in the UK (under the Animals (Experimental Procedures) Act, 1998). The ideal alternative would be a mono-specific polyclonal antibody to synthetic peptide immunogens and my supervisor's laboratory has had considerable success using this approach.

3.2.4 Peptide-specific antibodies

Peptide-specific antibodies overcome many of the problems involved in monoclonal antibody production while still yielding antibodies that are fairly specific for particular regions of a target protein. In this method, a specific peptide, corresponding to a particular part of the target protein, is conjugated to a highly immunogenic carrier protein and is used to immunize an animal. Antibodies specific to the immunogenic peptide can quite easily be purified from other antibodies in the serum, such as those raised against the carrier protein, using a peptide-coupled affinity column. One drawback of this method can be that the antibody will recognize only the sequence of the peptide, rather than the native shape the corresponding region adopts within the protein and so are not always as specific as monoclonal antibodies. As such, they can also be quite promiscuous although neither

of these problems has been significant in quite a few cases previously. It can be argued quite strongly that the advantages of cheap, simple production and ease of purification out-weigh the disadvantages as long as these are carefully taken into account when using, and interpreting results obtained with, such antibodies.

3.2.5 Uses of antibodies in research

Due to their highly specific nature, antibodies have become useful tools in biological research. They are used for several techniques to both identify proteins and help elucidate their structure and function.

The most common techniques used are immunoblotting, enzyme linked immunosorbant assay (ELISA) and immunofluorescence. Immunoblotting (or western blotting) allows the detection of a single protein or subunit from a mixture of proteins when separated by electrophoresis and transferred to a solid support, such as nitrocellulose. The primary (protein specific) antibody is bound followed by an enzyme conjugated secondary antibody, raised against antibodies of a particular species. The enzyme linkage then allows detection of the primary antibody by producing a colour change or fluorescing when exposed to the right conditions. The ELISA technique is similar in that it allows the detection of a protein within a mixture, but this time quantitatively. There are several methods of ELISA but essentially either the protein of interest or the specific antibody is attached to the surface of wells in a multi-well plate and the protein of interest is bound by either one or two antibodies, the final one of which has an enzyme linkage. The protein is then detected using a colour change and the intensity of colour is used to calculate the concentration of the antigen present. This method has proved extremely useful in

the clinical sense to detect small quantities of hormones and other substances in blood samples. Immunofluoresence has proved useful in locating specific proteins in cells. Essentially living cells are fixed and permeabilised if looking at proteins inside the cell, and the protein specific antibody introduced. This primary antibody is then detected by the binding of a secondary antibody conjugated to a fluorophore. This fluorophore can then be detected when excited by a laser of the correct frequency and visualised under a fluorescence microscope. With the advent of different fluorophores, with different excitation frequencies, more than one protein can be detected and therefore interactions between proteins can be seen.

Immuno-electronmicroscopy can also be used to determine the position of proteins within a cell with much higher resolution. In this case either the primary or secondary antibody can be conjugated to gold particles, which are clearly visible under the EM. By using different sized gold particles the proximity of two proteins to each other can also be determined.

Immunoprecipitation is a further technique to establish interacting proteins and the conditions under which these occur. Antibody is mixed with a protein sample e.g. cell lysate and then sepharose beads conjugated to protein A or protein G are added to the mixture. Protein A binds to the Fc region of most antibodies (human IgG subclasses, IgM, IgA and IgE; and mouse IgG1 (weakly), IgG2a and IgG2b: also binds IgGs from other laboratory and domestic animals, including monkey, rabbit, pig, guinea pig, dog and cat) and protein G binds to the Fc region of IgGs from other species especially rat, these beads are then pelleted by centrifugation and washed thoroughly. Proteins bound to the beads are then eluted with either an acidic solution or 2x Laemlli (1970) sample buffer. The eluted protein can then be analysed by electrophoresis. Proteins generally detected are those targeted by the antibody and

any interacting proteins; e.g. when CCT is immunoprecipitated with antibodies directed against CCTα, the entire complex is present (Roobol et al 1999a). This method has proved extremely useful in my supervisor's laboratory and has been used to demonstrat conditions under which CCT dissassembles (Roobol et al 1999a).

Many more techniques are being discovered using antibodies and more recent developments at the University of Kent have seen antibodies produced to deliver both imaging and therapeutic agents to malignant cells in cancer victims (Dr. Peter Nicholls, personal communication). They are also being used to interfere with cellular processes in living cells and as the proteomic era takes over from the genomic, more and more uses will be found and the antibody will become even more useful.

3.2.6 Choice of Sequence for generating Peptide-specific antibodies

From the known sequence of the target protein, a peptide is chosen from the C-terminus, N-terminus or internally. Ideally; internal sequences will represent surface exposed loops in the native protein and not α-helices that, due to their structure, do not expose enough of the peptide to be useful as antibody targets. Internal sequences are most likely to yield antibodies useful on western blots of denatured protein – so-called 'sequential epitopes', while antibodies to C-termini and/or N-termini have a greater potential to recognise the native protein in applications such as immunoprecipitation (IP). This is especially likely to be so when the N- or C-termini are relatively unstructured and free, rather than tied into (bound as part of) the 3-D structure of the protein or else modified in some way (e.g. trimmed or involved in post-translational modification).

When producing peptide-specific antibodies against murine CCT proteins, C-terminal peptides have proven especially successful (Roobol *et al.*, 1995; Roobol and Carden 1999; Grantham *et al.*, 2002 and Roobol - unpublished data). This is in part because the C-terminal ends of the CCT subunit sequences are the most highly variable, unlike other regions which share much common sequence and this favours subunit specificity of the antibodies. Also, the C-terminal region seems to be accessible in the fully folded protein (Roobol *et al*, 1999a), even though its exact location is not known from homology modelling or other structural characterisations because the last 20 or so amino acids of all chaperonins examined to date are refractory to X-ray crystallography. This is thought to be due to highly flexible and/or disordered structure (Pappenberger *et al*, 2002). Another reason for choosing C-terminal sequences is that the C-terminus of TCP-1 (CCTα) is highly antigenic. A large proportion of mAbs made against a recombinantly expressed fragment of the mouse protein turned out to target this region (Harrison Lavoie *et al*, 1993; Willison & Grantham, 2001). Moreover, a very subtle change in amino acid sequence (LDD-COOH to LED-COOH) between the mouse and rat TCP-1 proteins is enough to render a particular mAb (23c) unreactive with the latter (Harrison Lavoie *et al*, 1993; Liou *et al*, 1998) and yet cross-reactive with a Golgi-associated COP protein (Harrison Lavoie *et al*, 1993; Liou *et al*, 1998), the only shared feature of which seems to be the terminal LDD-COOH sequence.

Because of these observations, C-terminal end peptides were chosen (see figure 3.2) as the most promising source for the production of specific antibodies against each of the yeast CCT proteins as well as yeast Sup35p and murine GSPT1/2 (the C-terminus of murine GSPT1 and GSPT2 being identical).

Yeast CCT α	NH_2–CTVDPEPPKEDPHDH-COOH
Yeast CCT β	NH_2–CIIRARPRTANRQHM-COOH
Yeast CCT γ	NH_2–CLRVDDIVSGVRKQE-COOH
Yeast CCT δ	NH_2–CVKSILRIDDIAFSR-COOH
Yeast CCT ε	NH_2–CLKIDNVIISGKDEY-COOH
Yeast CCT ζ	NH_2–CLLRAGRSTLKETPQ-COOH
Yeast CCT η	NH_2–CMPPQGAGRGRGMPM-COOH
Yeast CCT θ	NH_2–CAPQGPRPGNWDQED-COOH
Yeast Sup35p	NH_2–CQGTTIAIGKIVKIAE-COOH
Murine GSPT1/2	NH_2–CGKVLKLVPEKD-COOH

Figure 3.2 Peptides chosen for the generation of antibodies. All represent the extreme C-terminus of the respective proteins.

Rabbits were chosen for the production of anti-CCT antibodies as these generate a larger volume of sera and hence antibody than e.g. rats or mice. Rabbit antibodies raised against yeast Sup35p were available from Prof. Tuite (University of Kent, Canterbury, Kent), but, to prevent cross-reaction on blots of immunoprecipitations, an anti-Sup35p antibody in guinea pig was produced.

Rabbit antibodies were also produced against the murine GSPT proteins, the mammalian homologue of Sup35p. In this case cross-reaction would not be a problem since guinea pig anti-murine CCT antibodies were already present in the lab (created by Dr. Anne Roobol, University of Kent, Canterbury, Kent).

Antibodies produced were then purified and tested for specificity, before being used in later studies.

3.3 Results

3.3.1 KLH activation

Keyhole Limpet Haemocyanin (KLH) is a large five-subunit protein from the marine mollusc *Megathura crenulata.* Due to its large size and non-mammalian origin, KLH acts as a powerful adjuvant that enhances a mammalian antibody response. This makes it an ideal carrier for target peptides, which are linked to it via maleimide groups on each of the KLH subunits when the complex is activated on its numerous lysine residues.

In order to link peptides to KLH, the complex must first be activated (see figure 3.4). The procedure used was essentially as described by Werner and McCray (1989)

This activation then allows cysteine residues at the N-terminus of the synthetic peptide to be covalently attached to the maleimide groups on the KLH subunits. Once activated, the complex must be kept in the dark and frozen as quickly as possible. Activated KLH must also be 'desalted'. Therefore, the activated complex was loaded onto a Pharmacia FPLC fast desalting column equilibrated and eluted with 50mM phosphate bufffer (pH7.5), for rapid desalting and was then stored as 3-4mg aliquots at $-80^{o}C$.

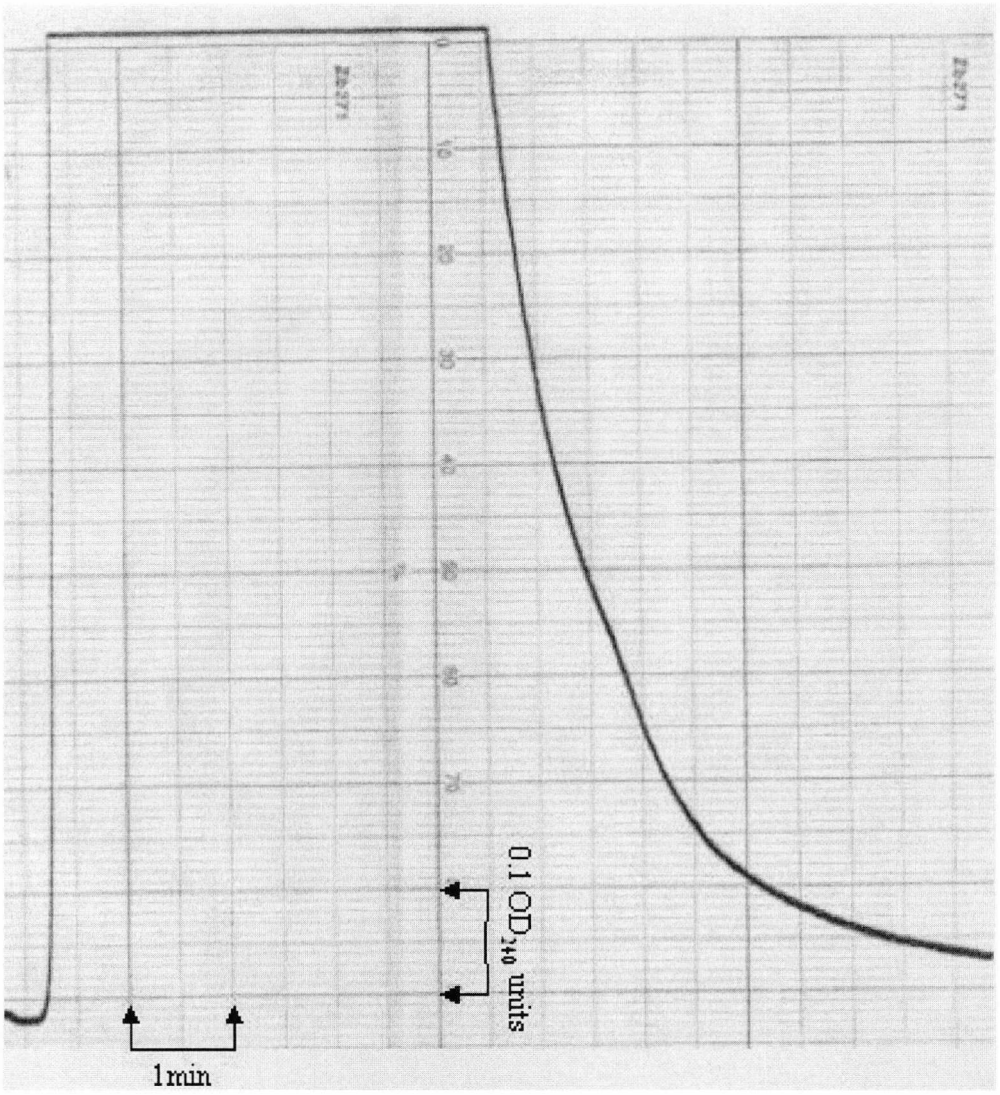

Figure 3.3 Elution profile of activated KLH after passage through a Pharmacia FPLC fast desalting column equilibrated and eluted with 50mM phosphate bufffer (pH7.5), flow rate: 0.5ml/min. Range; 0-1 OD units at 280nm: rate; 2mm/min.

Figure 3.2 shows the elution profile of activated KLH after passage through a Pharmacia FPLC fast desalting column.

The KLH was then coupled to the cysteine residue introduced at the N-terminus of the specific peptide (see figure 3.4 for chemistry of coupling).

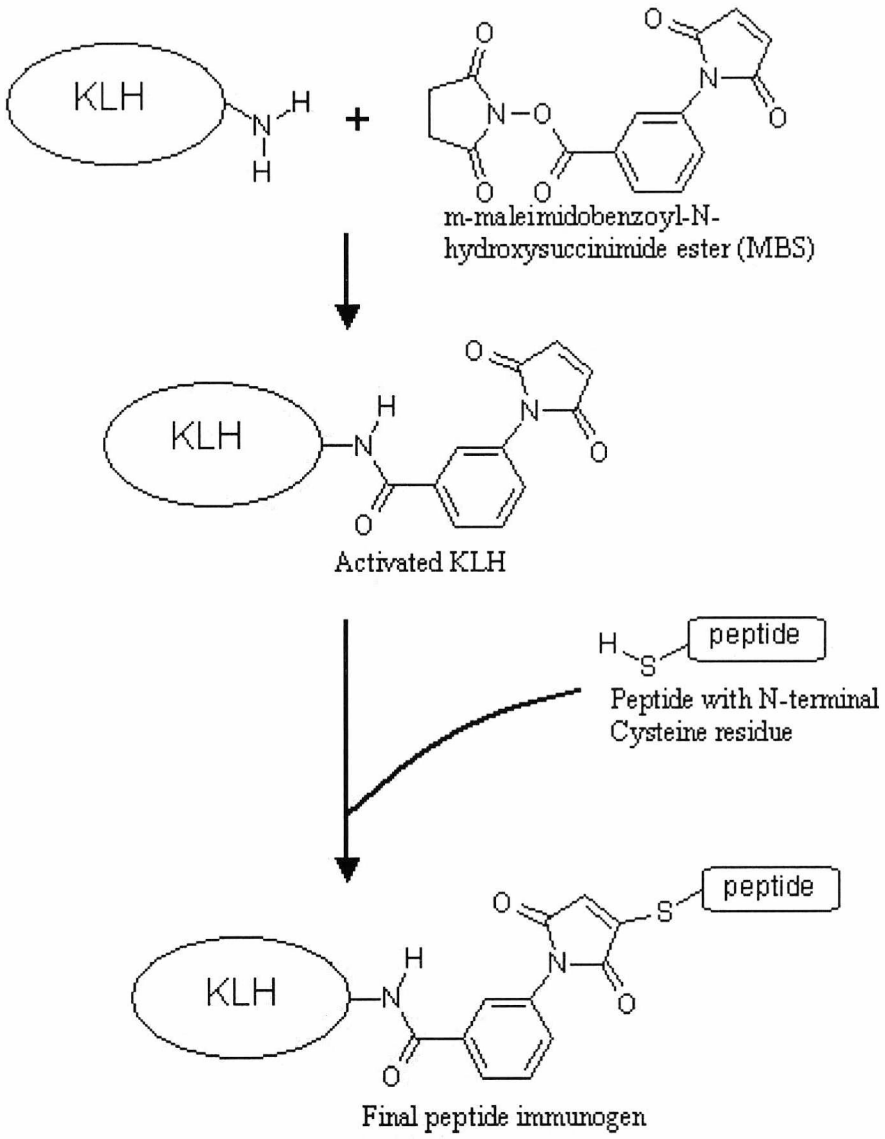

Figure 3.4 Diagram showing the chemistry of activating KLH by m-maleimidobenzoyl-N-hydroxysuccinimide ester

These constructs were then injected into either rabbit or guinea pig with TitreMax Gold® (Cytrx, Norcross, Georgia, USA) adjuvant for the initial injection and boosters (at 0.2ml/dose for rabbit and 0.1ml/dose for guinea pig). After the initial injection and 3 boosters, a sample of serum was collected (kindly carried out by Sarah Reed or Brian Cover, Biological services unit, Department of Biosciences, University of Kent), for antibody titre testing.

3.3.2 Serum testing

Following immunisation with initial and 2 monthly booster injections of immunogen a small sample of serum is taken and tested for antibody titre against the appropriate cell lysate on a western blot. Serum was diluted into fat-free dried milk (10% Marvel™ in 1 x PBS) at a range of dilutions from 1 in 20 to 1 in 1000. These dilutions were applied to a western blot using the Biometra (Göttingen, Germany) mini-blotter system and incubated overnight (4°C, without shaking) and developed in the usual way.

Positive bands were identified and compared to pre-immune sera and target proteins located by comparison to molecular weight markers and to the predicted molecular weight of the protein as shown in table 3.1.

Protein	Predicted molecular weight (KDa)	Predicted pI (unmodified protein)	Genbank Accesion no.
Cct1p	60.3	6.28	NP_010498
Cct2p	57.0	5.93	NP_012124
Cct3p	58.8	5.93	NP_012520
Cct4p	57.5	8.15	NP_010138
Cct5p	61.8	5.43	NP_012598
Cct6p	59.8	5.62	NP_010474
Cct7p	59.7	5.38	NP_012424
Cct8p	61.5	5.54	NP_012526.
Sup35p	76.6	6.42	NP_010457.
GSPT1p	68.6	5.11	NM_146066
GSPT2p	69.1	5.12	NM_008179

Table 3.1 Predicted properties of all eight CCT proteins and Sup35p from yeast and GSPT1 and 2 from mouse. Predictions were made using Yeast Protein Database (YPD) at http://www.proteome.com/databases/YPD and http://ca.expasy.org/tools/pi_tool.html

Once the target protein could be identified at a 1 in 1000 dilution of serum, the terminal bleed of the animal was made.

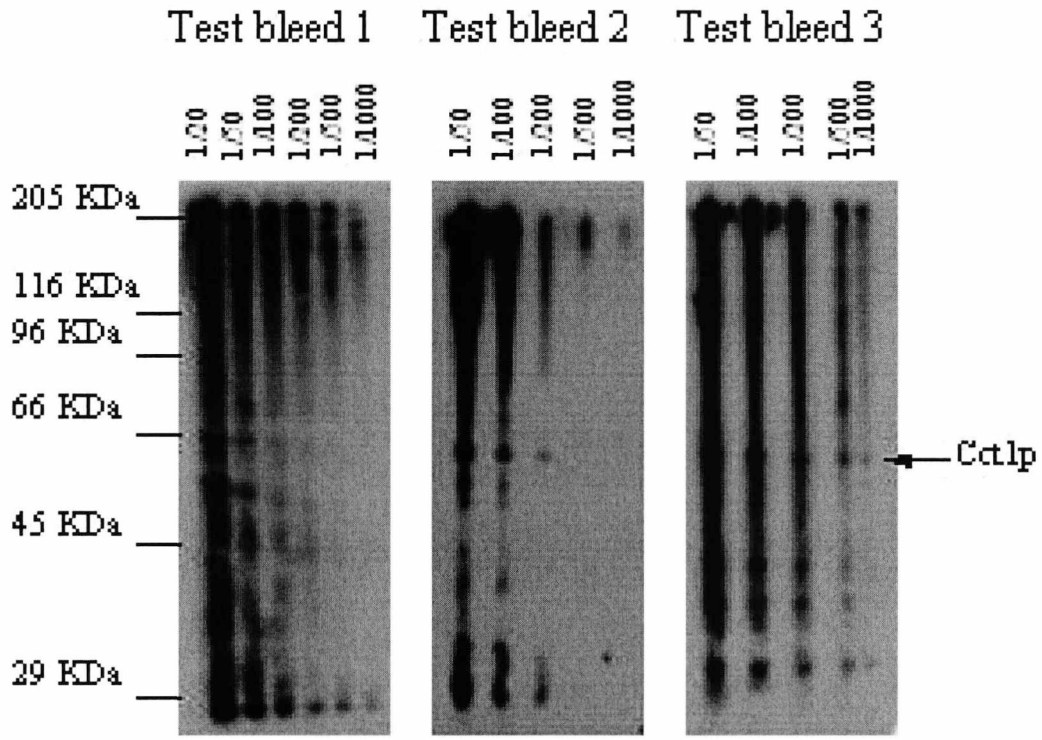

Figure 3.4 Western blots of *S. cerevisie* cell lysate, probed using various concentrations of serum from rabbit immunized with KLH conjugated Cct1p C-terminal peptide. Test bleed 1 after 3 injections, test bleed 2 after 4 injections and final test bleed (3) after 5 injections. Total cell protein (300µg) was separated by SDS-PAGE (9% gel, 30mA, 1¼hr), transferred to nitrocellulose membrane (750mA, 4°C, 1hr), blocked with 5% Marvel® and probed with various concentrations of serum, diluted in 5% Marvel®, from animals immunized with KLH conjugated peptides using the Biometra mini-blotter system.

Figure 3.4 shows the series of test bleeds carried out on rabbit MJC66 that was inoculated with KLH conjugated Cct1p C-terminal peptide. The first test bleed was carried out after the 3rd injection and the blot shows a band is detectable at the correct size at a serum dilution of 1/50. The second test bleed was carried out after the 4th injection and the blot again shows a band detected at the correct size at a serum dilution of 1/200. The third and final test bleed was carried out after the 5th injection and the blot shows the same band but detected at a serum dilution of 1/1000. After

this test bleed was carried out, Brian Cover (Biological services unit, Department of biosciences, University of Kent) made the terminal bleed of the rabbit.

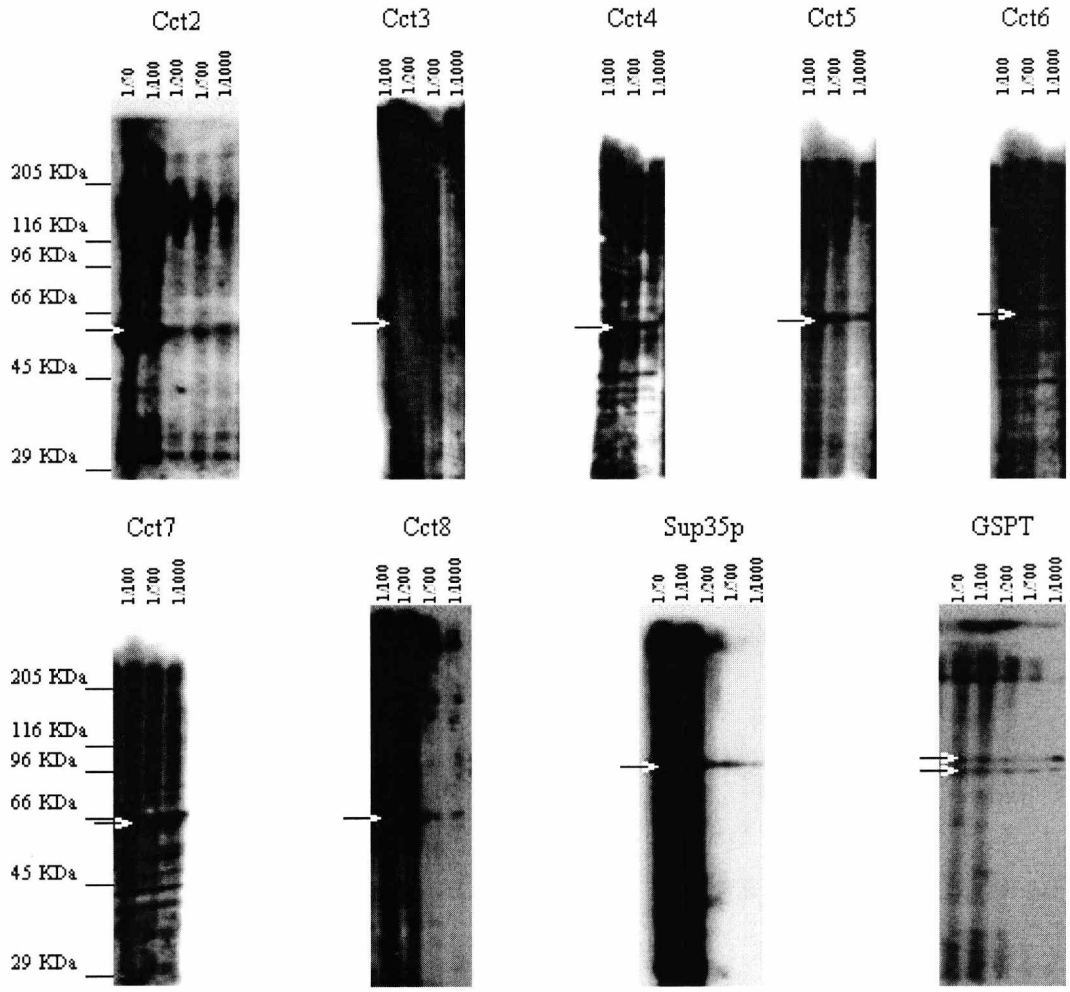

Figure 3.5 Western blots of *S. cerevisiae* (Cct1-8 and Sup35p) and ND7/23 (GSPT1/2) cell lysates, probed using various concentrations of serum from animals immunized with KLH conjugated peptides from each of the yeast CCT subunits, yeast Sup35p and murine GSPT1/2. Final test bleed before terminal bleed of animal for yeast Cct subunits, Sup35p and mammalian GSPT. Total cell protein (300µg) was separated by SDS-PAGE (9% gel, 30mA, 1¼hr), transferred to nitrocellulose membrane (750mA, 4°C, 1hr), blocked in 5% Marvel® and probed with various concentrations of serum, diluted in 5% Marvel®, from animals immunized with KLH conjugated peptides using the Biometra mini-blotter system.

Figure 3.5 shows the final test bleeds before the terminal bleed for the remaining yeast CCT subunits, yeast Sup35p and murine GSPT1/2 KLH conjugated peptides injected into rabbits or guinea pig (Sup35p). In each case a band is detected on the blot of the expected size with a serum dilution of 1/1000. In the case of GSPT two bands are detected, this is expected as the C-termini of both GSPT1 and GSPT2 are

identical and they differ only at their N-termini, with GSPT2 being shorter over all, thus indicating that this antibody can detect both forms of the protein by western blotting. Also the bands for Sup35p and GSPT1/2 appear larger than predicted, 96KDa as observed compared to 76.6 as predicted for Sup35p and 96KDa and 94KDa observed for GSPT1/2 respectively as opposed to 69.1KDa and 68.6KDa respectively as predicted. This was expected however; as it is well documented that Sup35p appears much larger on SDS PAGE analysis.

3.3.3 Purification

Once the target protein could be detected with a 1 in 1000 dilution of serum the terminal bleed of the animal was made. The antibody was then purified by affinity chromatography. The chromatography column was constructed by covalently linking the iodoacetyl group on Sulfolink® gel support (Pierce) to the sulfhydryl group on the N-terminal cysteine of the peptide (see figure 3.5 for chemistry of binding). The iodoacetyl group is on a 12 atom spacer arm to reduce steric hindrance and increase binding efficiency (Sulfolink® coupling gel manufacturers instructions).

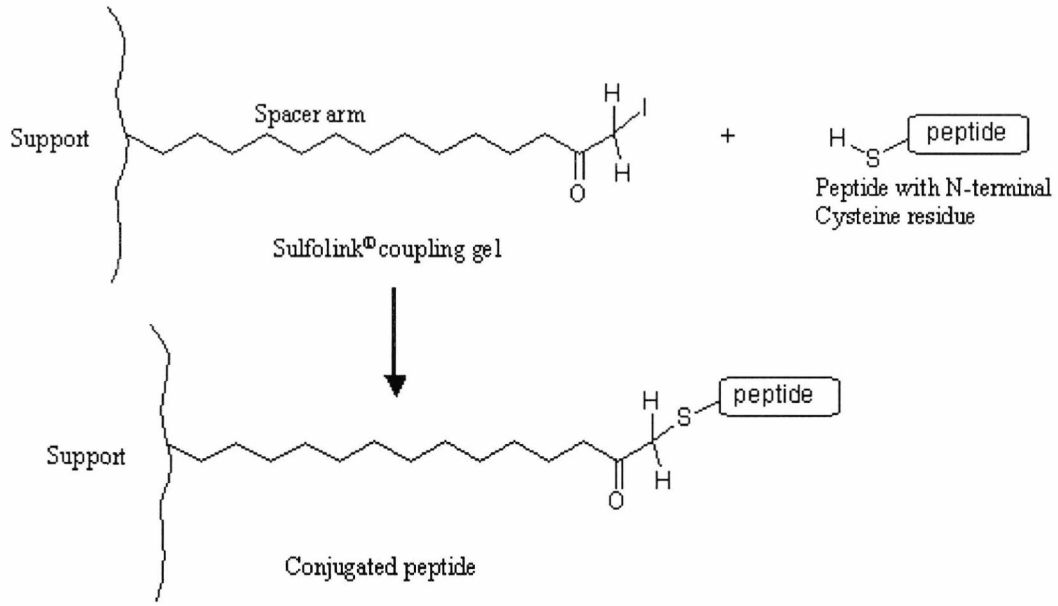

Figure 3.6 Diagram showing the chemistry of coupling synthetic peptide with an N-terminal cysteine residue to the Sulfolink® coupling gel.

Serum (4-6ml), containing protease inhibitors (see section 2.7.7), was applied to the appropriate column, the flow-through collected and the column washed with PBS and high salt (PBS with 1M NaCl). The antibody was then eluted by reducing the pH of the column (0.1M glycine, 0.1M NaCl, pH2.8) and collecting 1ml fractions (4°C and with immediate neutralisation). The fractions were then assayed for antibody content via dot blotting 2µl samples of each acid eluted fraction and the flow-through onto nitro-cellulose and developing it in the same way as a western blot (see section 2.4.6) by blocking, incubating with the appropriate secondary antibody and staining using diaminobenzidine.

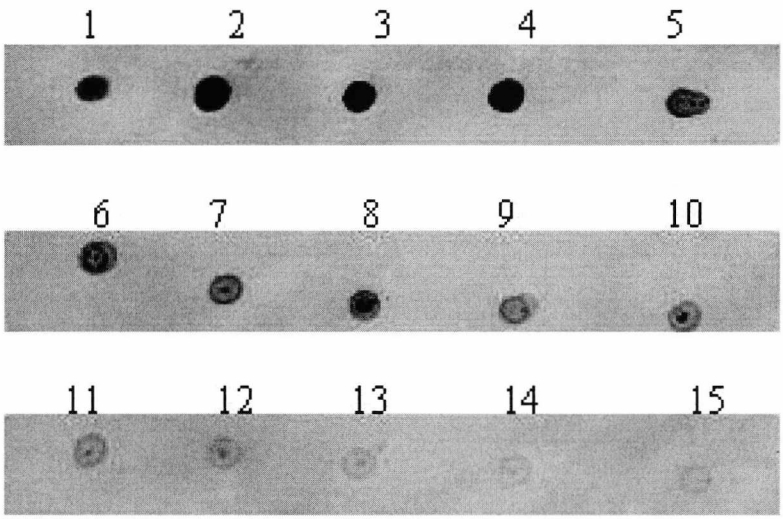

Figure 3.7 Dot blot of purified Cct1 antibody fractions. Numbers represent fraction numbers. 2µl of each fraction and flow-through was dotted onto nitrocellulose, blocked, incubated with anti-rabbit secondary antibody (1/1000 dilution) and stained with diaminobenzidine to locate antibody-containing fractions.

Figure 3.7 shows that the majority of antibody is eluted from the column in the first 4 fractions, this was true of all the antibodies purified.

3.3.4 Specificity testing

Once purified, antibody was tested for its specificity both on one-dimensional and two-dimensional PAGE western blotting. One-dimensional SDS-PAGE was carried out to ensure that the proteins identified by the purified antibodies was of the correct size and two-dimensional i.e.f./PAGE was carried out to ensure that only one protein of the correct size was identified.

Purified antibody was tested against the appropriate cell lysate on a western blot. Antibody was diluted into fat-free dried milk (10% Marvel™ in 1 x PBS) at a range of dilutions from 1 in 20 to 1 in 500. These dilutions were applied to a western blot using the Biometra mini-blotter system and incubated overnight (4°C, without shaking) and developed in the usual way. Positive bands were identified and

compared to molecular weight markers. The minimum concentration of antibody giving a clear band was used in further blotting experiments.

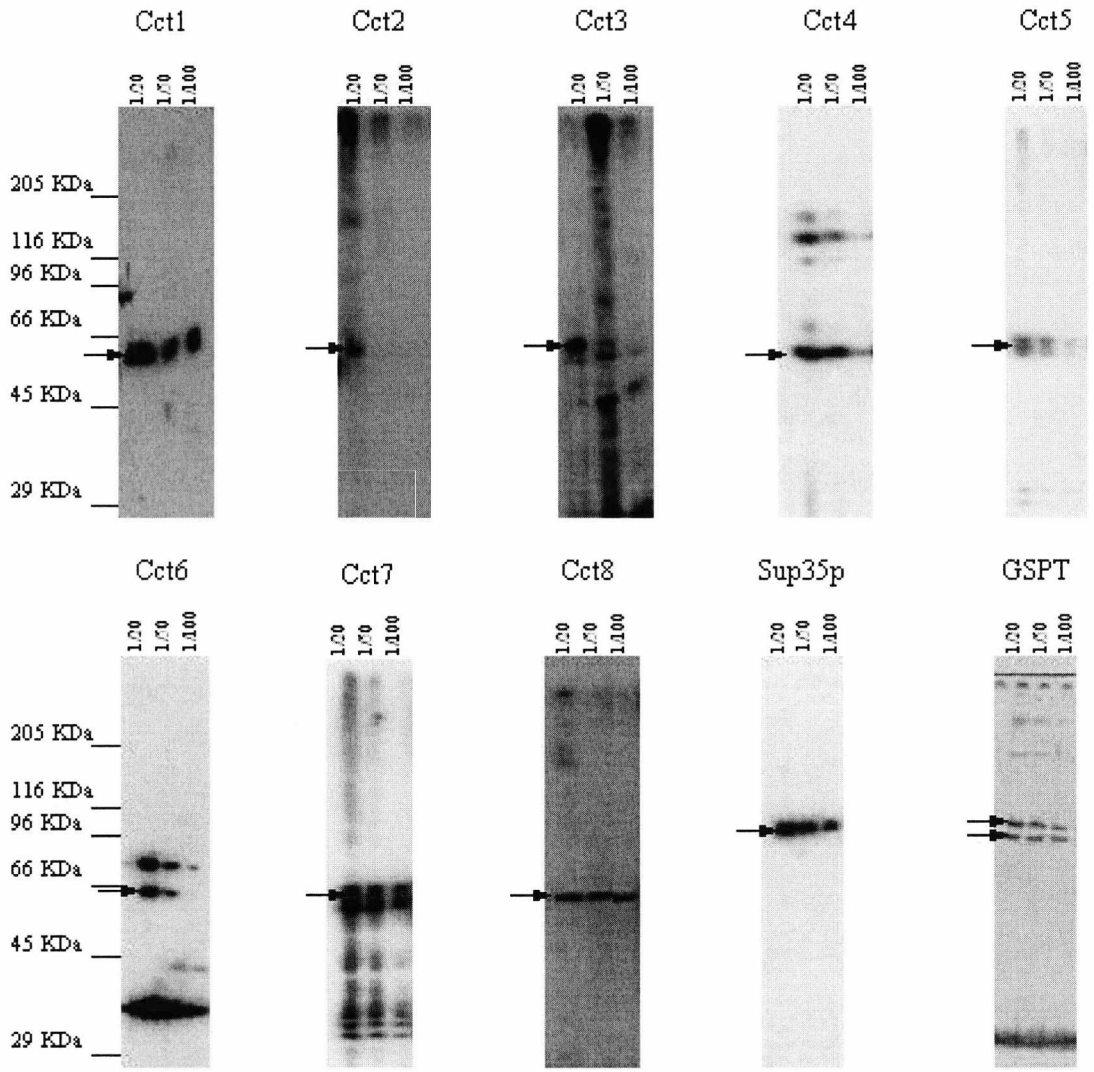

Figure 3.8 Western blots of ND7/23 (GSPT1/2) and *S. cerevisiae* (Cct1-8 and Sup35p) cell lysates, probed using various concentrations of affinity purified antibody raised against C-terminal peptides from yeast CCT subunits, yeast Sup35p and murine GSPT1/2. Total cell protein (300μg) was separated by SDS-PAGE (9% gel, 30mA, 1hr), transferred to nitrocellulose membrane (750mA, 4°C, 1hr), and probed with various concentrations affinity purified antibody, using the Biometra mini-blotter system.

Figure 3.8 shows western blots of the appropriate cell lysate tested with various concentrations of purified antibody. In all cases a band of the expected size was detected, however in some cases other bands are also visible. In most cases these are

much larger or smaller than the expected band and can therefore be easily discounted on western blot analysis, but could pose a problem for immunoprecipitation experiments. These extra bands are also much fainter than the expected band and so at low dilutions of antibody these will not even be detected. The exception to this is the larger and smaller band detected by Cct6, which both appear to be much stronger that the expected band. There are also smaller bands detected by the Cct7 antibody. Due to their ladder-like appearance and the lack of any larger bands, these could be breakdown products of Cct7p.

Purified antibody was tested against the appropriate cell lysate on a western blot, separated firstly by isoelectric focusing and secondly by SDS-PAGE, at an appropriate dilution. 1-2mg of cell lysate was precipitated using acetone, resuspended in i.e.f. sample buffer and applied to an i.e.f. stick gel before being focused by the application of 500v between acidic and alkaline electrodes (see section 2.4.3). The focused stick gel was then electrophoresed over a 9% SDS-PAGE gel before being western blotted. The blot was developed in the usual way using the previously identified concentration of antibody. Single spots or streaks were putatively identified by comparison with published two-dimensional gels. Each lysate was also subjected to two-dimensional i.e.f./PAGE and silver stained to show how well the proteins had been separated.

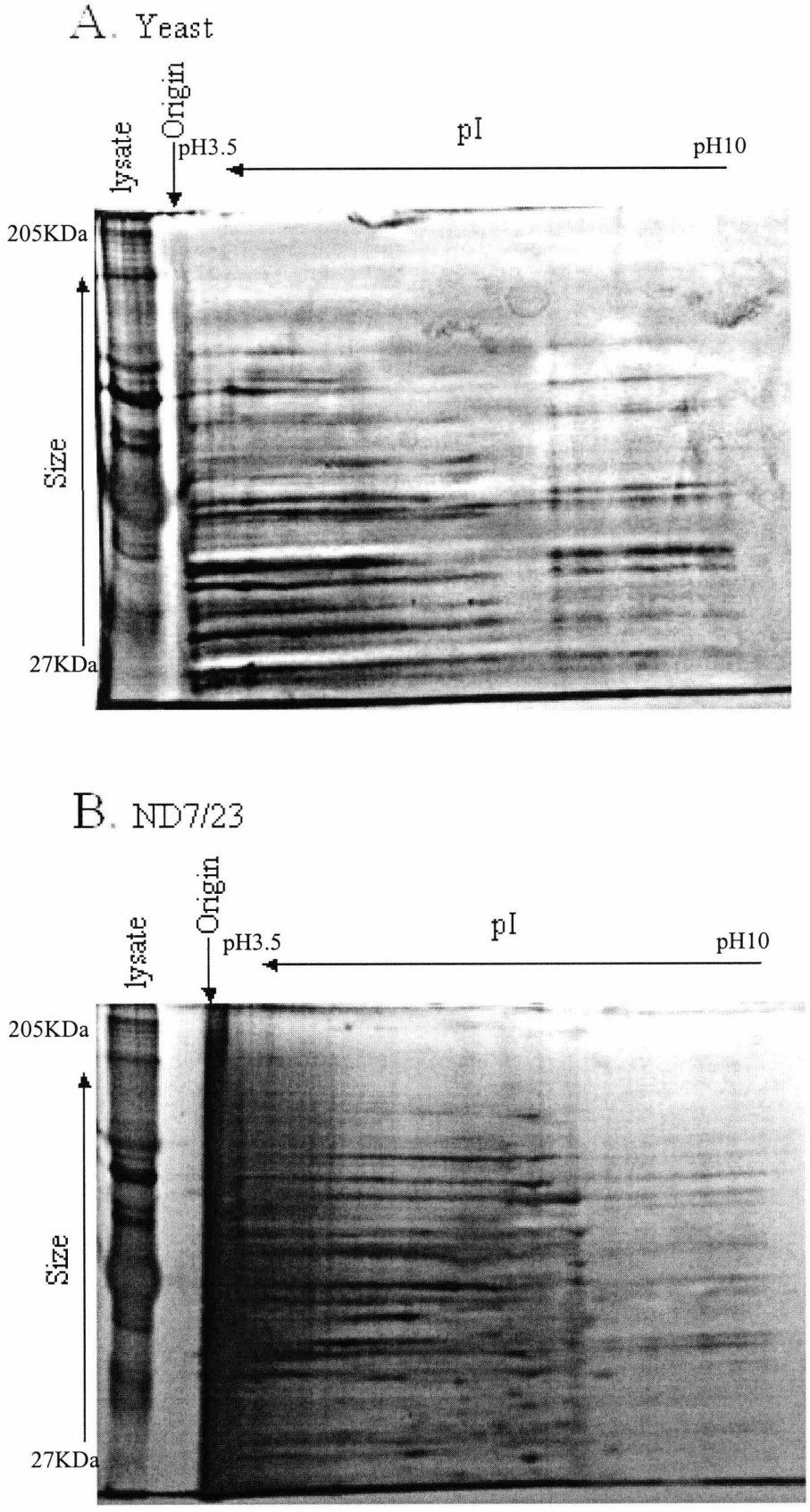

Figure 3.9 Silver stains of **A**. *S. cerevisiae* and **B**. ND7/23cell lysates subjected to two-dimensional i.e.f./PAGE. Total cell protein (10-12mg) was separated by i.e.f. (pH3.5-10, 500v, 3hr) and SDS-PAGE (9% gel, 30mA, 1hr) and silver stained.

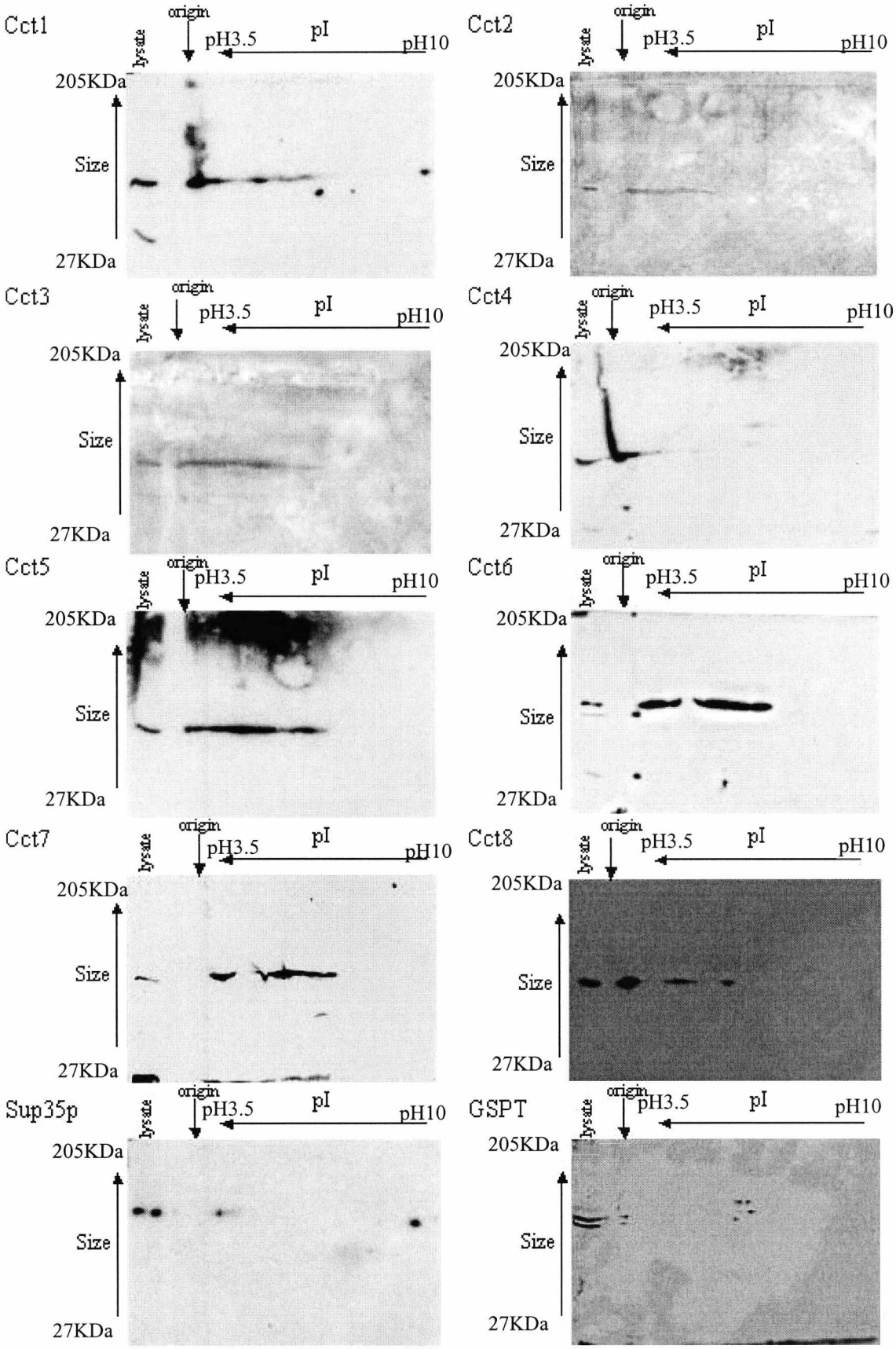

Figure 3.10 Western blots of ND7/23 (GSPT1/2) and *S. cerevisiae* (Cct1-8 and Sup35p) cell lysates subjected to two-dimensional i.e.f./PAGE, probed using appropriate concentrations of affinity purified antibody raised against C-terminal peptides from yeast CCT subunits, yeast Sup35p and murine GSPT1/2. Total cell protein (10-12mg) was separated by i.e.f. (pH3.5-10, 500v, 3hr) and SDS-PAGE (9% gel, 30mA, 1hr) and transferred to nitrocellulose membrane (750mA, 4°C, 1hr), and probed with appropriate concentrations of affinity purified antibody.

The silver stains in figure 3.9 show that rather than discreet spots, the proteins seem to have formed long streaks when analysed by i.e.f PAGE. This can be due to the sample buffer and gel mixture being warmed to 30°C for too long when dissolving the urea (Anne Roobol, personal communication). This means that, when blots of these gels are probed with antibody, instead of spots of detection, streaks are likely.

Figure 3.10 shows the two-dimensional i.e.f./SDS PAGE blots probed with purified antibody. As predicted most of the blots show streaks instead of distinct spots, however these streaks correspond to the predicted size as shown by bands detected in the cell lysate, loaded to act as a marker track, and also incorporate the predicted pI. The blots probed with anti-Sup35p and anti-GSPT1/2 antibodies do contain distinct spots and these correspond to both the predicted size and pI. The g ls and blots here are too streaked to be very informative in several cases, the exceptions being Cct1p, Cct4p, Cct8p, Sup35p and GSPT1/2. The two spots visible in the case of Cct8p may be due to different isoforms of the protein observed in mammalian extracts, possibly due to adenylation (Kubota *et al*, 1994). There is also a strong signal observed at the origin of the blot due to not all of the protein being solubilised by the i.e.f. sample buffer. The anti-Cct6p antibody, does however show a strong cross reactivity with a slightly larger protein, hypothesized to be one of the HSP70 family of proteins, but as the difference in size is easily visible the two proteins should be distinguishable in further studies using these antibodies.

3.3.5 Use of anti-CCT subunit antibodies to immunoprecipitate the complex from cell lysate.

One of the major uses the anti-CCT subunit antibodies were intended for was immunoprecipitation. The antibodies were intended to isolate the CCT complex

from whole lysate so that any interacting proteins could be detected. For this reason the antibodies were first mixed with whole cell lysate, labelled with [^{35}S] methionine and cysteine, and then the antibody/antigen complex was isolatd and washed by use of protein A bound sepharose beads. As mentioned above, protein A is able to bind the Fc portion of the antibody molecule and is therefore a useful tool for isolating bound antibody molecules. The beads were washed to remove any non-specifically binding proteins and the bound complex removed by incubation (95°C, 2min) with a 2 x concentrate of Laemmli (1970) sample buffer before being subjected to SDS-PAGE, Coomassie staining and autoradiography.

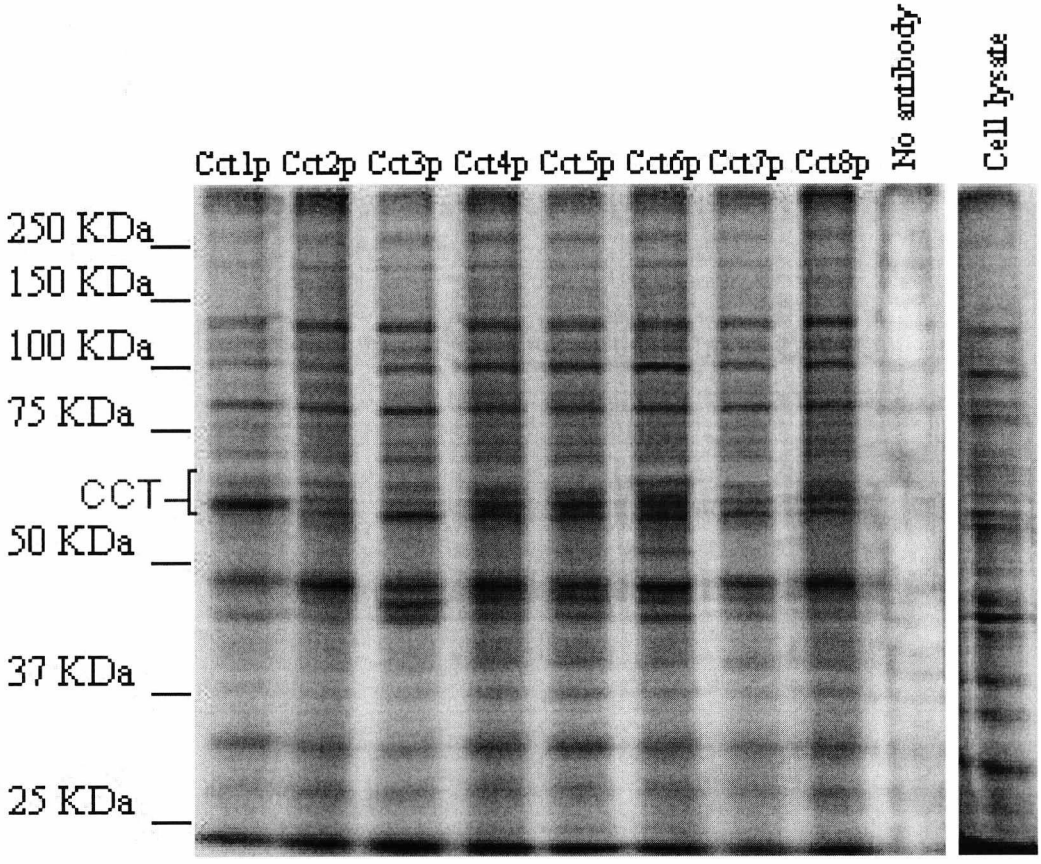

Figure 3.11 Autoradiographs of immunoprecipitated CCT from [*psi*$^-$] yeast cell lysates. Rabbit antibodies raised against the C-terminus of the yeast CCT subunits were used to immunoprecipitate the CCT complex from whole cell lysate labelled with [^{35}S] methionine and [^{35}S] cysteine. The immunoprecipitate was then electrophoresed by SDS-PAGE (30mA, 1hr), stained with coomassie brilliant blue, dried (70°C, 90min, medium ramp) and incubated with autoradiography film (7 days, room temperature).

Figure 3.11 demonstrates that the CCT complex could successfully be immunoprecipitated from whole cell lysate using the antibodies produced in this study. The CCT complex is clearly distinguishable in all of the Ips although in the case of anti-Cct1p and anti-Cct3p antibody Ips there seems to be enrichment for the targeted subunit. There are also many other proteins present in the Ips but interestingly the cross-reactive proteins found on the SDS-PAGE tests appear not to have been targeted e.g. the 70KDa protein cross reacting with Cct6p. This could be due to the motif recognized by the antibody being inaccessible in the native state of the protein and only exposed when the protein is denatured for SDS-PAGE analysis.

3.3.6 Use of GSPT1/2 antibodies in immunohistochemistry

One of the aims of further studies using the antibodies generated here was to use them to locate areas of co-localisation between CCT subunits and GSPT1/2 in mammalian cells. It was therefore necessary to test the GSPT1/2 antibody for its ability to stain fixed mammalian cells.

ND7/23 cells were grown on glass cover slips before being fixed by use of paraformaldehyde (4% in 1 x PBS, 37°C, 15-20min) and permeabilised in either Triton – X-100 (0.1% in 1 x PBS, room temperature, 5min) or methanol (100%, -20°C, 5min) or fixed and permeabilised in either methanol (100%, -20°C, 5min) or methanol/acetone (1:1 mixture, -20°C, 5min), blocked in BSA and incubated with GSPT1/2 (rabbit) antibodies. The secondary antibodies used had either rhodamine (anti-rabbit) conjugated to them to give the staining antibody a red appearance when excited by the correct wavelength laser light.

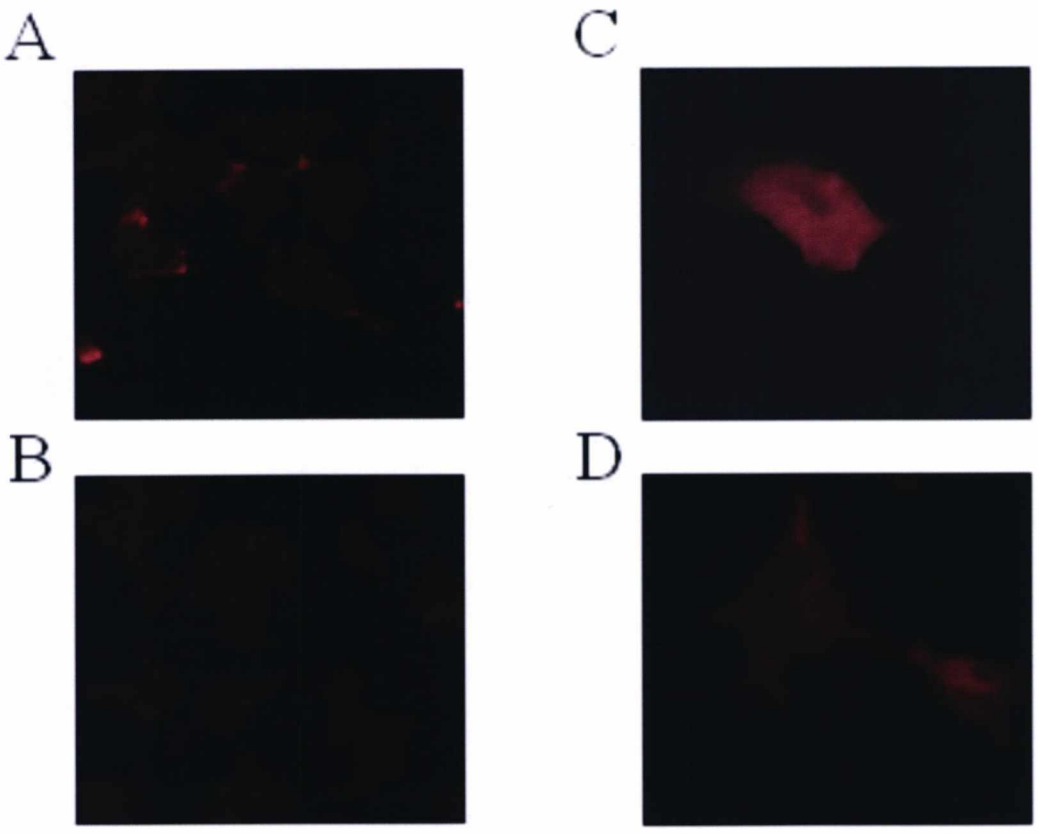

Figure 3.12 Immunocytochemistry of GSPT1/2, showing slices through the base of the cell **(A and B)** and the center of the cell **(C and D)**. ND7/23 cells were grown on glass cover slips in 24 well Costar plates. The cells were then fixed, permeabilised, blocked in BSA and incubated with GSPT1/2 antibody raised against the C-terminus in rabbit. After incubation with secondary antibody conjugated to rhodamine (anti-rabbit), cells were viewed and recorded using a confocal microscope (Leica TCS 4D) (Leica, Bensheim, Germany).

Figure 3.12 shows the localization within the cell of GSPT1/2. it can be seen that at the base of the cell the GSPT1/2 is mainly located around the periphery of the cell, whereas in the center of the cell these proteins appear to be located centrally and include staining within the nucleus. The staining surrounding the nucleus is expected as these proteins are mammalian homologues of the yeast translation termination factors and this is where most of the protein synthesis machinery is located, especially the ribosomes. As for the staining at the periphery of the cell, this is unexpected and as yet unexplained.

3.4 Discussion

This study has resulted in the production of ten peptide antibodies.

When used to probe western blots of the appropriate cell lysate it can be seen that single bands are visible, and where this is not the case other bands are not visible when the antibodies are used to probe two-dimensional blots, this could be due to the lower concentration of lysate used in these blots. The exception is the antibody raised against the C-terminus of Cct6p. This antibody exhibits very strong cross reactivity with another protein of approximately 70KDa. This will be taken into account in further studies using these antibodies and care will be taken to interpret results appropriately, especially when using the antibodies for Ip studies, although Ip data suggests that this cross-reacting protein is not bound by the antibody in its native state and hence is not targeted in Ips.

The efficacy of the purified antibodies varies wildly and some are used at very high concentrations (e.g. anti-Cct2p is used at a 1/20 dilution). This could be a result of the purification procedure and further work could have been done to optimize this, however, even at such high concentrations cross-reactivity is minimal showing that the antibody is at least extremely pure and as such is usable for further studies.

The GSPT1/2 antibody has also been shown to be effective in immunocytochemistry of cultured ND7/23 cells, localizing the proteins to protein synthesis regions of the cell as expected.

These antibodies will be used to determine any interaction between CCT and Sup35p in yeast and between CCT and GSPT1/2 in mammals.

Chapter 4: Yeast Sup35p/CCT Interaction

4.1 Introduction

This chapter presents evidence for an interaction between *Saccharomyces cerevisiae* CCT and Sup35p (eRF3). As such it is important to introduce both of these proteins and the pre-existing evidence already in existence for their interaction.

One of the most interesting properties of Sup35p is its behavior as a model prion protein and so the prion concept is also introduced as well as the evidence for the involvement of protein folding chaperones in this process.

4.1.1 Yeast CCT

Although identified in mammalian cells (Lewis et al, 1992), CCT has been found in every eukaryote examined including the yeasts *Candida albicans* (Stoldt *et al*, 1996), *Schizosaccharomyces pombe* (Stoldt *et al*, 1996) and *Saccharomyces cerevisiae* (Ursic & Culbertson, 1991). By 1996 all eight CCT genes from *S. cerevisiae* had been identified (see Stoldt *et al*, 1996, for review) using a range of approaches including, analysis of actin and tubulin folding mutants (Chen *et al*, 1994, Miklos *et al*, 1994, Ursic & Culbertson, 1991, Vinh & Drubin, 1994), similarity to Drosophila proteins (Rasmussen, 1995), sequence similarities with murine CCT genes and systematic sequencing by the yeast genome project (Miklos et al, 1994, Rasmussen, 1995, Van *et al*, 1995). To distinguish the yeast CCT genes from their mammalian equivalents, they were denoted CCT1-CCT8 (as opposed to Cctα - Cctθ in mammals) and the proteins Cct1p-Cct8p (CCTα-CCTθ) (Kubota *et al*, 1994, Stoldt *et al*, 1996) (see table 4.1).

Mammalian protein	Mammalian gene	Yeast protein	Yeast gene	Other names
CCTα	*Cctα*	Cct1p	*CCT1*	TCP1, YDR212W
CCTβ	*Cctβ*	Cct2p	*CCT2*	BIN3, TCP2, YIL142W
CCTγ	*Cctγ*	Cct3p	*CCT3*	BIN2, TCP3, YJL014W
CCTδ	*Cctδ*	Cct4p	*CCT4*	TCP4, YDL143W
CCTε	*Cctε*	Cct5p	*CCT5*	TCP5, YJR064W
CCTζ	*Cctζ*	Cct6p	*CCT6*	HTR3, TCP6, TCP20, YDR188W
CCTη	*Cctη*	Cct7p	*CCT7*	TCP7, YJL111W
CCTθ	*Cctθ*	Cct8p	*CCT8*	YJL008C

Table 4.1 Different nomenclature for the mammalian and yeast CCT proteins and genes

The relative ease of genetic manipulation in *S. cerevisiae* has been exploited in elucidating both the function and interactions of the CCT complex and its subunits. It has been shown by gene disruption experiments that all eight genes are essential in that their disruption is lethal to yeast cells (Ursic & Culbertson, 1991, Chen *et al*, 1994, Miklos *et al*, 1994, Vinh & Drubin, 1994, Li *et al*, 1994) and none can replace any of the others. Lethality could be a result of a disrupted regulatory process of central importance such as the cell division cycle (Yokota *et al*, 2001, Camasses *et al*, 2003) or merely to the general build-up of unfolded or misfolded proteins, which could push the cell into apoptosis (Frőhlich & Madeo, 2000). The effects of individual subunit disruptions have been studied by the production of conditional mutants of CCT1-4 (Chen *et al*, 1994, Miklos *et al*, 1994, Ursic & Culbertson, 1991, Vinh & Drubin, 1994, Ursic *et al*, 1994) and in all cases examples of cytoskeletal disorganization and abnormal microtubule and/or actin organization were shown (Chen *et al*, 1994, Miklos *et al*, 1994, Ursic & Culbertson, 1991, Vinh & Drubin, 1994, Ursic *et al*, 1994). These findings indicate that a chief function of CCT in *S.*

cerevisiae cells is shared with mammalian cells, i.e. the correct folding of actin and tubulin for the maintenance of a functional cytoskeleton.

The CCT proteins found in yeast are approximately 51-57% identical to each other. However, orthologs (e.g. mouse CCTα and yeast Cct1p) are 68-78% identical (Stoldt *et al*, 1996). This finding, as well as the information that over-expression of one subunit could not rescue a mutation in a second subunit (Chen *et al*, 1994, Miklos *et al*, 1994, Ursic & Culbertson, 1991, Vinh & Drubin, 1994, Li *et al*, 1994) suggest that each subunit has evolved to have a distinct function. An explanation has been offered for the separately essential natures of CCT subunits from studying the murine CCT system, where different substrate proteins were shown to bind to distinct subunits (Llorca *et al*, 1999, 2000).

Analysis of CCT subunits in *S. cerevisiae* has shown there is a certain degree of cooperativity between the subunits with regard to ATP hydrolysis. The results suggest that ATP binding occurs sequentially, in a defined order within one ring, in a positively cooperative manner in the sequence Cct1p → Cct3p → Cct2p → Cct6p, for the four subunits examined (Lin & Sherman, 1997). This sequence is consistent with the published order of subunits in the murine CCT complex (Liou & Willison, 1997). If this is taken to include all eight subunits then the order of ATP binding in the whole ring is predicted to be:

Cct1p → Cct7p → Cct4p → Cct8p → Cct3p → Cct2p → Cct6p → Cct5p →
Cctα → Cctη → Cctδ → Cctθ → Cctγ → Cctβ → Cctζ → Cctε →

So far, the only interactions to be investigated in detail in yeast are between the CCT subunits themselves and actin or tubulin. However, it has been shown in mammalian cells that CCT interacts with a variety of other proteins (see Dunn *et al*, 2001, for

review) and it seems likely this would be so in *S. cerevisiae*. Recent extensive analysis of the yeast 'interactome', both experimentally (Gavin *et al*, 2002, Ho *et al*, 2002) and bioinformatically (Eisenberg *et al*, 2000), suggest this to be the case.

4.1.2 Sup35p

In order to initiate translation termination in eukaryotes, two classes of translation termination release factor are required; the class I stop codon-responsive release factor, eRF1, and the class II guanine nucleotide-responsive release factor, eRF3 (Ebihara & Nakamura, 1999). In *S. cerevisiae* these are referred to as Sup45p and Sup35p respectively (Frolova et al, 1994, Zhouravleva et al, 1995).

Sup35p was first identified by its ability to complement a temperature sensitive *gst1* mutation in *S. cerevisiae* (Kikuchi *et al*, 1988). Sup35p was thought to have an important role in the G_1 to S phase transition in the yeast cell cycle as in the *gst1* mutant, DNA synthesis was substantially arrested (Kikuchi *et al*, 1988). At the same time Sup35p was identified as an omnipotent suppressor (see Stansfield & Tuite, 1994, for review); these are a class of nonsense suppressor, which are recessive and effective against all three nonsense codons (UAA, UGA and UAG). Mutations in the *SUP35* gene were shown to increase the amount of translational ambiguity, suggesting that Sup35p functions as a positive regulator of translational accuracy in yeast (Stansfield & Tuite, 1994).

Sup35p consists of a N-terminal prion-forming domain, a charged M (middle) domain of unknown function and a C-terminal domain that provides the translation termination activity (Ter-Avanesyan *et al*, 1993, 1994, Wilson & Culbertson, 1988). In order to function as a translation termination release factor, Sup35p forms a part of

the translation termination release factor complex together with Sup45p (Stansfield *et al*, 1995). A conserved stretch of acidic amino acids at the C-terminus of Sup45p allows Sup35p to bind to it and form the complex (Ito *et al*, 1998, Ebihara & Nakamura, 1999). Sup45p mimics the structure of tRNA (Song *et al*, 2000) and binds into the decoding, A site of the ribosome and triggers the hydrolysis of the peptidyl-tRNA bond by the ribosome, releasing the nascent peptide (see Nakamura & Ito, 1998, for review). eRF3, meanwhile, is thought to mimic either elongation factor EF-Tu or EF-G (see figure 4.1) and progresses the complex from the A site to the P site on the ribosome whilst hydrolyzing GTP, activity which requires the presence of both Sup45p and the ribosome and enhances the rate of peptidyl release (Nakamura & Ito, 1998). Although the mechanism of translation termination is well theorized, the initiation of the process has remained uncertain. Recently it has been suggested that the poly (A)-binding protein (Pab1p) is also able to bind the N and M domains of Sup35p (Cosson *et al*, 2002). This could indicate that Pab1p brings Sup35p into close proximity with the poly (A) region of the mRNA being translated, thus bringing the entire translation termination complex into the correct position to initiate translation termination (Cosson *et al*, 2002).

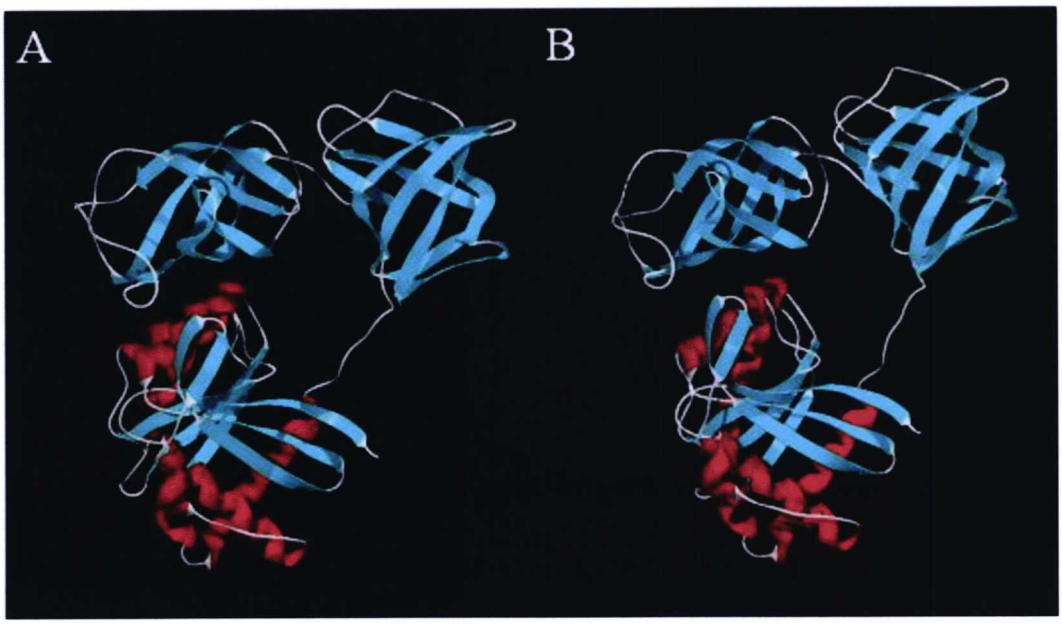

Figure 4.1 The structures of both Sup35p (A) and EF-Tu (B) modeled using Swiss model (http://www.expasy.org/swissmod/SWISS-MODEL.html). The sequences of both proteins were put into the Swiss model programme and homology modeled on known structures in the databases. β sheet is shown in blue whilst α helix is shown in red. The structures were then rendered and lit using Persistence of Vision Raytracer tool (http://www.povray.org/). The atomic coordinates are included on floppy disc.

The role of Sup35p in translation termination is well documented; however, comparisons between Sup35p and RF3 in bacteria have shown a number of differences. Firstly, the SUP35 gene is essential whilst the RF3 gene is not (Weiss *et al*, 1984). Secondly, Sup35p and Sup45p bind stably in vivo and in vitro whilst RF1 and RF3 do not (Ito *et al*, 1996). Sup35p GTPase activity requires the presence of Sup45p, RF3 activity does not (Frovola *et al*, 1996). Over expression of both Sup35p and Sup45p is required to enhance termination efficiency (Stansfield *et al*, 1995) and finally, Sup35p has a N-terminal extension which has no counterpart in RF3 (Nakamura & Ito, 1998). This all suggests that Sup35p may have a role outside translation termination (Nakamura & Ito, 1998). There is speculation that this role could be as a ribosomal release factor (RRF), as no homologous protein has been found in eukaryotes except in the mitochondria of yeast (Nakamura & Ito, 1998), or

as a proof-reading protein for the correct recognition of stop codons as well as for the differential usage of stop triplets (Stansfield & Tuite, 1994). Alternatively this extra-curricular activity may be something completely different, for example in the cell cycle, as previously suggested (Kikuchi *et al*, 1988).

4.1.3 Prionisation

One of the unusual properties of Sup35p is that it can undergo ordered, self-seeded assembly into amyloid fibers *in vitro* (Glover *et al,* 1997). These fibers are formed when the native protein is misfolded (has increased β-sheet content) and aggregates (Glover *et al,* 1997). Because of this Sup35p is considered to be a model for the processes involved in forming prion proteins of mammals (prionisation). These are thought to be the causal agents of a number of spongiform encephalopathy (S.E.) neurodegenerative diseases, including Bovine Spongiform Encephalopathy (BSE) and Creutzfeldt Jakob Disease (CJD) (see Prusiner, 1996 for review), and polyglutamine diseases e.g. Huntingtons disease as well as a number of other amyloid forming diseases e.g. systemic amyloidosis.

The term prion is derived from proteinaceous infectious particle (Prusiner, 1982) and refers to an infectious protein, encoded by a single gene, which exists in two stable conformations. Once the pathogenic, aggregation prone, form of the protein is present it becomes the dominant species by influencing the conformation of the non-infectious form of the protein, thus creating large protein aggregates which can affect the function of the cell (Telling *et al*, 1996). It has been theorized that almost any protein can form amyloid-like aggregates, under the right conditions (Goda *et al*, 2002), and therefore could be a method of protecting the cell from the early

intermediates of protein misfolding, by storing them until they can be re-folded or destroyed.

The discovery of Sup35p as a prion protein began when Cox (1965) reported the discovery of a new nonsense suppressor that was found to be metastable, appearing and disappearing in yeast strains in a pattern that defied explanation. This trait appeared to be inherited in a non-mendelian fashion, indicating that it was encoded by a non-chromosomal element and as such these strains were denoted [*PSI*$^{+}$] for the dominant nonsense suppressor and [*psi*$^{-}$] for the recessive form (Cox, 1965). Further investigation indicated that this nonsense suppressor was Sup35p (Chernoff *et al*, 1988, 1993, Doel *et al*, 1994). It was not until almost 30 years later that it was suggested that Sup35p was an ideal candidate for a prion protein (Wickner, 1994).

There are a number of proposed models for the formation of prion proteins (Caughey & Chesebro, 1997), but the defining step seems to be the formation of the infectious form of the protein in the first place. It has been shown that the aggregating form of prion protein has an increased amount of β-sheet when compared to its non-infectious partner (Cohen *et al*, 1994). This makes the protein far more prone to aggregation as the β-sheet structure allows the individual molecules to come into close proximity with each other and thus increases the likelihood of exposed hydrophobic side chains bonding to each other as well as the increased potential for hydrogen bonding and other salt bridges. The resultant structures appear to be twisted, hollow fibers (King *et al*, 1997) and can associate with a number of other proteins to form large aggregates (Caughey & Chesebro, 1997). The exact size and number of aggregates needed to 'seed' a new cell remains unknown, however, the potential for a protein to misfold and become a prion seems to depend on a region of regular glutamine containing repeats within the sequence of the protein (Glockshuber

et al, 1997). In the case of Sup35p these are located at the N-terminus and consist of 5½ repeat regions (Ter-Avanesyan *et al*, 1994) (see fig 4.2). Systematic deletion of these repeats has shown them all to be important for the stable formation of aggregates (Parham *et al*, 2001).

```
1     MSDSNQGNNQQNYQQYSQNGNQQQGNNRYQGYQAYNAQAQ/PAGGYYQNY/Q
51    GYSGY/QQGGYQQYN/PDAGYQQQYN/PQGGYQQYN/PQGGYQQQFN/PQGG/RGN
101   YKNFNYNNNLQGYQ
```

Figure 4.2 N domain of Sup35p, amino acids 1-114, showing the N-terminal repeats (in red) responsible for the prionisation of the protein.

Although the mechanism of prionisation appears to be similar, one major difference between the Sup35p prion and those of mammals is that the prionisation of Sup35p does not appear to be detrimental to the cell, except perhaps in deep stationary phase in expired medium (Chernoff *et al*, 1998, Eaglestone *et al*, 1999). This is unexpected as the SUP35 gene is essential (Nakamura & Ito, 1998) and any limit to the function of Sup35p would, logically, be expected to lead to major consequences for the cell. It seems that the only phenotypic trait of [*PSI*+] cells is an increased read-through of stop codons (Lindquist, 1997). Quite apart from this being detrimental to the cell, it has been suggested that this could give the cell an evolutionary advantage by providing a way of having two different phenotypes with only one genome (Lindquist, 1997). In fact it seems that there may be an evolutionary reason for the existence of prions, as the potential for prionisation exists in a large number of diverse proteins (Goda *et al*, 2002).

4.1.5 Chaperones and prionisation

One of the most important steps in the prionisation process is the formation of the infectious, misfolded prion protein conformation. It is likely that a protein folding

chaperone is involved in this process as it has been shown that a number of chaperones affect the prion state of Sup35p (Kushnirov *et al*, 2000) and it has also been shown that the mammalian prion protein can be converted into its β-sheet form, *in vitro,* in the presence of GroEL (DeBurman *et al*, 1997).

The maintenance and inheritance of the aggregated Sup35p form, *in vivo,* requires a moderate level of Hsp104p (Chernoff *et al*, 1995). Hsp104p functions as a molecular chaperone, but unlike other chaperones it does not prevent the aggregation of denatured proteins. However, in concert with Hsp40 and Hsp70, it can reactivate proteins that have been denatured and allowed to aggregate (Glover & Lindquist, 1998). Hsp104p appears to be most important when the rate of protein unfolding exceeds the capacity of other chaperones to prevent the accumulation of aggregates. During recovery from such severe conditions, Hsp104p promotes disaggregation of heat-damaged proteins (Parsell *et al,* 1994a). The current model for the mode of action of Hsp104p is that its hexameric structure (Parsell, Kowal & Lindquist, 1994) provides multiple sites for polypeptide substrate binding. Upon ATP binding and hydrolysis, conformational changes in Hsp104p change the positions of bound substrates relative to each other - in effect, Hsp104p acts as a molecular "crowbar" (Glover & Lindquist, 1998).

It has been proposed that when Hsp104p is present at its normally low constitutive level, it partially unfolds Sup35p or disassembles Sup35p/Sup45p heterodimers, thereby overcoming conformational or kinetic barriers to the formation of ordered Sup35p aggregates (Patino *et al*, 1996). Alternatively, Hsp104p may dissociate large, preformed Sup35p aggregates into smaller; aggregation prone particles that seed the aggregation of newly synthesized Sup35p more efficiently (Glover & Lindquist, 1998).

The other major chaperone protein known to interact with Sup35p is Ssa1p, a member of the Hsp70 family. When Hsp104p is over expressed in [*PSI*$^+$] cells it is able to cure the prion phenotype. However, when it is over expressed in conjunction with Ssa1p the curing effect is stopped (Newman *et al*, 1999). The mechanism of action of Ssa1p has not been elucidated. The usual methods of investigation are difficult as the levels of the protein can only be altered slightly before toxicity and then even the expression of many proteins is altered (Werner-Washburne et al, 1987). One theory, however, is that during stress conditions, when Ssa1p expression is induced, the physiology of the cell is such that the ability of Hsp104p to cure [*PSI*$^+$] may be affected and indeed the presence of Ssa1p interacting with Hsp104p may directly affect this ability (Serio & Lindquist, 1999).

As previously stated the type I chaperonin GroEL has been shown to assist the formation of prion fibers *in vitro* in cultured mammalian cells. Interestingly the type II chaperonin CCT has never been tested in such a system. This seems surprising, as CCT has been described as the GroEL equivalent in mammalian cells, where the PrP protein resides. However, the mammalian cell experiments required the over-expression of the relevant chaperone genes in transfected cells (DeBurman *et al*, 1997). This would prove very difficult in the case of CCT, as all eight genes would need to be transfected and over-expressed simultaneously! Unfortunately, the investigation of any interaction between CCT and the mammalian prion would be hampered by legislation surrounding the use, in the lab, of PrP (ACDP, 1998). Therefore the interaction must be investigated using a model system i.e. Sup35p in *S. cerevisiae.*

4.1.5 CCT/Sup35p interaction

Functional computer algorithms first predicted an interaction between CCT and Sup35p (Eisenberg *et al*, 2000) (see figure 4.3).

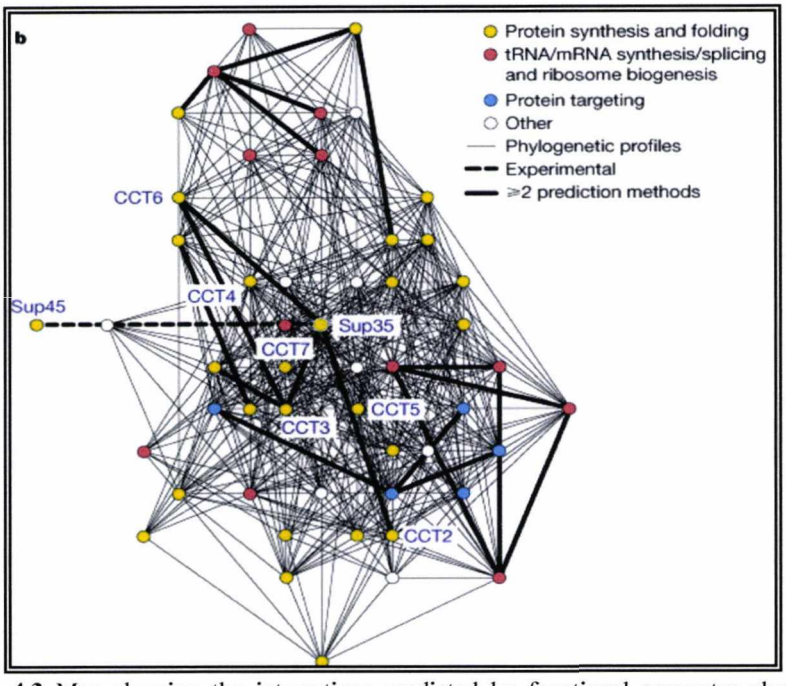

Figure 4.3 Map showing the interactions predicted by functional computer algorithms. Reproduced from Eisenberg *et al*, 2000.

The interaction was not, however, predicted by experimental means using immunoprecipitation (Gavin *et al*, 2002, Ho *et al*, 2002). Mass spectroscopy identified proteins found to co-immunoprecipitate with the targeted species and a giant map of interacting proteins produced (Ho *et al*, 2002). In this way the *S. cerevisiae* proteome was analyzed. Although the information in this map is extensive it is not conclusive as some well characterized interactions were not identified e.g. Sup35p/Sup45p and some proteins were found to be promiscuous and were found in many of the immunoprecipitations e.g. CCT8 (Ho *et al*, 2002). Such proteins were not considered further; though imposing such a cut off precludes many significant interactions of proteins that genuinely interact with a whole variety of other proteins e.g. actins and tubulins.

Further to this, an investigation into GroEL identified EF-Tu as a substrate protein (Houry *et al*, 1999) and as has been shown earlier (figure 4.1) both EF-Tu and Sup35p share a similar structure, providing further indications that an interaction between CCT and Sup35p is likely.

4.1.6 Aims and Objectives

Due to the evidence presented for an interaction between chaperones and prions and more specifically between CCT and Sup35p, I decided to investigate whether an interaction could be demonstrated biochemically.

The main aim of the investigation was to determine if there was an interaction between the CCT subunits and Sup35p and whether this interaction was different between prion positive and negative cells. Secondarily an indication of the nature of the interaction was sought. A yeast strain lacking the prion-forming N-terminal region of Sup35p was utilized to determine any interaction with this part of the protein. Also techniques were used to determine whether the interaction was with individual CCT subunits or whether the whole complex was required. I also sought to establish whether Sup35p was acting as a substrate of CCT or an associated protein.

This study employed the antibodies discussed in chapter 3.

4.2 Results

4.2.1 Demonstration of a physical interaction between CCT subunits and Sup35p influenced by both its aggregation state ([*PSI*+] vs. [*psi*-]) and N-domain.

To verify interaction between CCT subunits and Sup35p in yeast, the technique of immunoprecipitation (IP) was chosen. IP has become a useful tool when looking for interactions between proteins. Antibodies against one of the interacting proteins are used to isolate that protein from a complex mixture, such as whole cell lysate, by binding the antibody to beads via protein A, which binds the Fc portion of most (human IgG subclasses, IgM, IgA and IgE; and mouse IgG1 (weakly), IgG2a and IgG2b: also binds IgGs from other laboratory and domestic animals, including monkey, rabbit, pig, guinea pig, dog and cat) antibodies (Boyle & Reis, 1987). This allows the target protein to be isolated along with any binding partners. The only proteins left after thorough washing of the beads should be the target protein and any stably interacting proteins. The composition of IP and wash buffers may be critical determinants in preserving particular interactions. Proteins are released from the beads by incubation with a 2x concentrate of Laemmli sample buffer (Laemmli, 1970) (95°C, 2min). The resultant samples can then be electrophoresed by SDS-PAGE and western blotted. Thus, other interacting proteins can then be probed for, using specific antibody. It is important that this be raised in a different species to the antibody used for the IP because otherwise it will cross-react with the large amount of IP antibodies on the blot, masking many target and/or interacting proteins, especially in the 45-55KDa range i.e. the size of the antibody heavy chain, difficult to distinguish.

Antibodies were raised in rabbit against KLH-coupled synthetic peptides with the sequence of the C-terminus of the yeast CCT subunits (see section 2.7). These were used to IP the CCT complex from *[PSI$^+$]*, *[psi$^-$]* and ΔN (Sup35p lacking the N-terminal 114 amino acids: Parham *et al*, 2001) yeast cell lysates. Samples were electrophoresed (on SDS-PAGE), western blotted and the blots probed for Sup35p with antibody raised in guinea pig against the C-terminus of Sup35p (see section 2.7). In the same way, IPs from radiolabelled cell lysate were produced in order to show the diversity, sizes and numbers of other proteins co-immunoprecipitated with the CCT subunits.

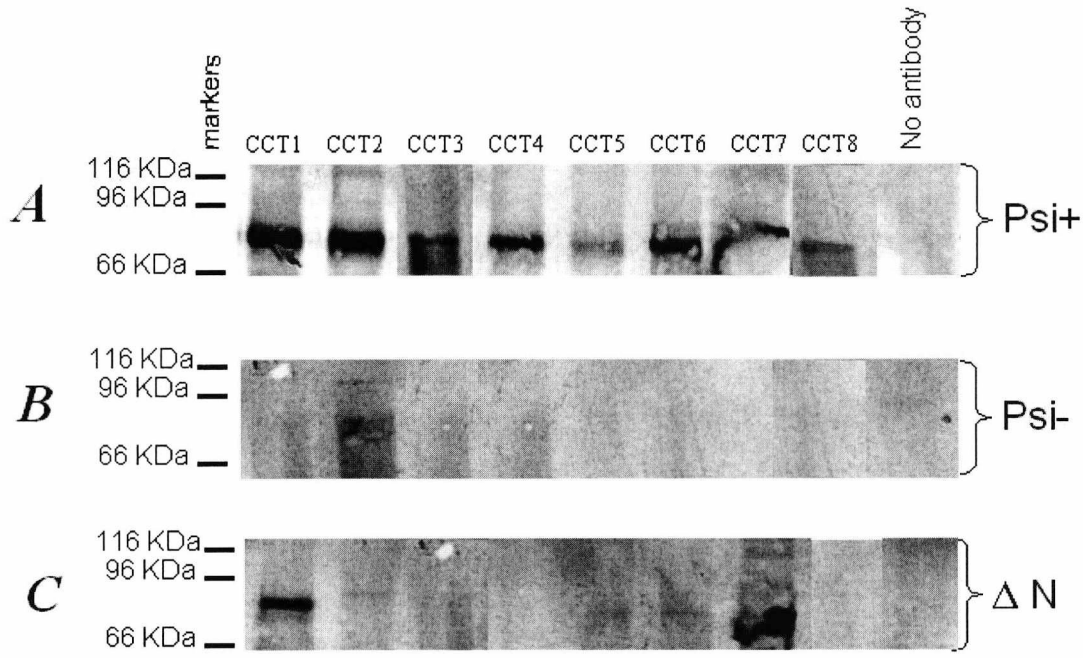

Figure 4.4 Western blots of immunoprecipitated CCT from both [*PSI*$^+$] **(A),** [*psi*$^-$] **(B)** and ΔN **(C)** yeast cell lysates. Rabbit antibodies raised against the C-terminus of the yeast CCT subunits were used to immunoprecipitate the CCT complex from whole cell lysate. The immunoprecipitate was then electrophoresed by SDS-PAGE (30mA, 1hr), western blotted (750mA, 1hr, 4°C) and probed with a guinea pig antibody raised against the C-terminus of Sup35p.

Figure 4.4 shows the results obtained by immunoblot probing of CCT subunit-targeted IPs using antibody to Sup35p. This confirms the computer based prediction of Eisenberg *et al* (2000) that Sup35p interacts with CCT subunits and that this is a

physical interaction, i.e. part of a protein complex, though not necessarily a direct binding between the two.

IP from [*psi*$^-$] cells yielded a markedly different pattern to that from [*PSI*$^+$], with much more extensive interaction when Sup35p was in the more aggregated, prion-like [*PSI*$^+$] form. The results also show, incidentally, that these CCT subunit specific antibodies do not IP Sup35p (i.e. do not cross react). Thus observations of Sup35p in IPs reflect genuine interaction.

All of the eight subunits of CCT interact with Sup35p when it is in the [*PSI*$^+$] state, although to different extents. However, only Cct2p appears to interact with Sup35p when it is in the [*psi*$^-$], non-aggregated, form. These are startling differences in the pattern of interaction and suggest that CCT may interact with Sup35p, when it is aggregated, as an oligomer (although this would mean that the antibodies vary in their efficiency at immunoprecipitating the complex, which is demonstrated by the autoradiography), while 'free' Sup35p interacts preferentially with a single, specific subunit, Cct2p.

The N-domain deletion strain (ΔN) produced a different pattern of interaction again. This Sup35p mutant is unable to form aggregates (Parham *et al*, 2001) and therefore results in the [*psi-*] phenotype when expressed in *S. cerevisiae*. In this strain CCT still interacts with Sup35p, again in a subunit specific manner but in this case Cct1p and Cct7p, with faint bands visible for Cct2p, Cct5p and Cct6p. This is different from the interaction observed with the wild type [*psi*$^-$] strain and so suggests a different means of interaction or a difference in the composition of the CCT/Sup35p complex.

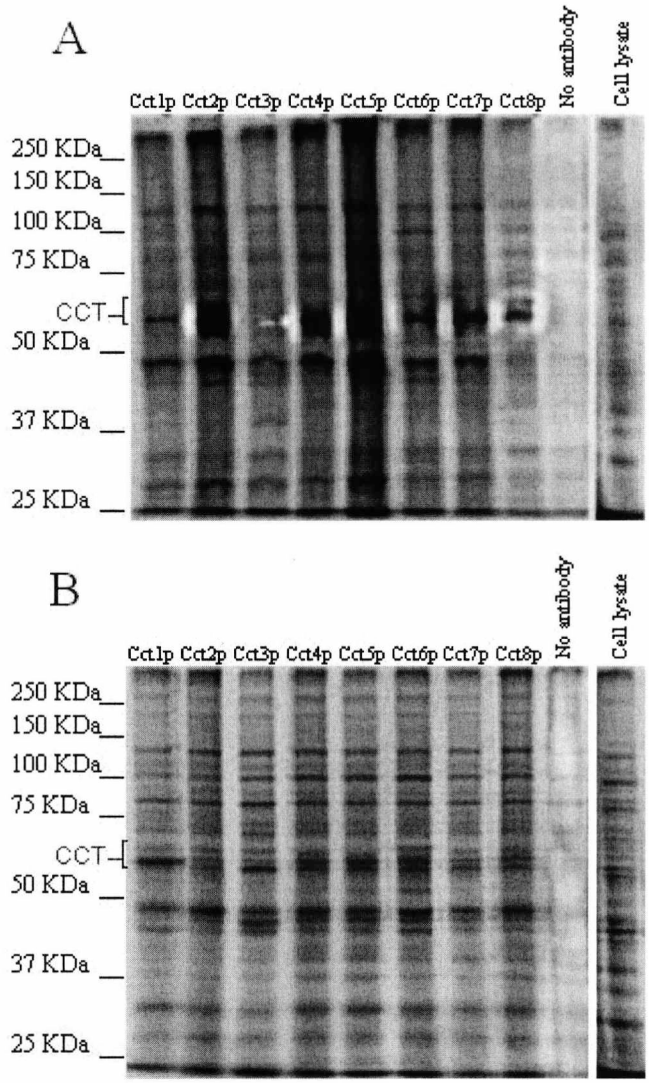

Figure 4.5 Autoradiographs of immunoprecipitated CCT from *[PSI⁺]* **(A)** and *[psi⁻]* **(B)** yeast cell lysates. Rabbit antibodies raised against the C-terminus of the yeast CCT subunits were used to immunoprecipitate the CCT complex from whole cell lysate labeled with [^{35}S] methionine and [^{35}S] cysteine. The immunoprecipitate was then electrophoresed by SDS-PAGE (30mA, 1hr), stained with coomassie brilliant blue, dried (70°C, 90min, medium ramp) and incubated with autoradiography film (7 days, room temperature).

Figure 4.5 shows autoradiographs of immunoprecipitated CCT from radiolabelled yeast cell lysate. It can be seen that the whole CCT complex is immunoprecipitated from the lysate in [*psi⁻*] cell lysates in most cases except Cct1p and Cct3p in which only the targeted subunit appears enriched. Interestingly, in the [*PSI⁺*] cell lysate the whole complex is only immunoprecipitated when Cct2p, Cct4p and Cct5p are targeted; otherwise the targeted subunit seems enriched. This appears to imply that

in the [PSI+] cell state the CCT complex is in a more disassembled state or there are more free subunits available for immunoprecipitation.

Unfortunately the growth of the ΔN cells was so severely slowed in the highly defined media required for radiolabelling that no labelling was achieved, this was also the case when label was added to rich media. For this reason the Coomassie stain of IPs from ΔN yeast lysate is included here.

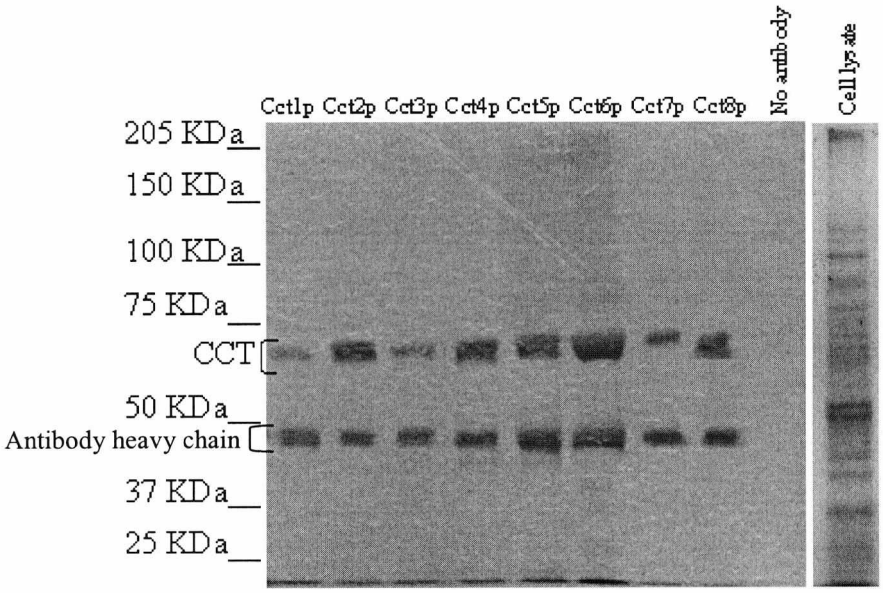

Figure 4.6 Coomassie stain of immunoprecipitated CCT from *ΔN* yeast cell lysate. Rabbit antibodies raised against the C-terminus of the yeast CCT subunits were used to immunoprecipitate the CCT complex from whole cell lysate. The immunoprecipitate was then electrophoresed by SDS-PAGE (30mA, 1hr) and stained with Coomassie brilliant blue.

Figure 4.6 shows a smudge at the size expected for the CCT complex, unfortunately, not much more can be seen from this figure except the IgG heavy chain band.

4.2.2 Influence of ATP on CCT subunit/Sup35p interaction.

In mammalian systems it has been shown that in the presence of physiological concentrations of potassium and ATP the CCT complex disassembles (Roobol *et al*, 1999) and it is generally agreed that ATP releases bound substrate (Quaite-Randall *et*

al, 1995). It was therefore decided that immunoprecipitations be conducted in the presence of potassium and ATP. The detection of co-immunoprecipitating species, under these conditions, would indicate a non-substrate interaction. Therefore the immunoprecipitations were carried out as above in the presence of 2mM ATP and 140mM KCl.

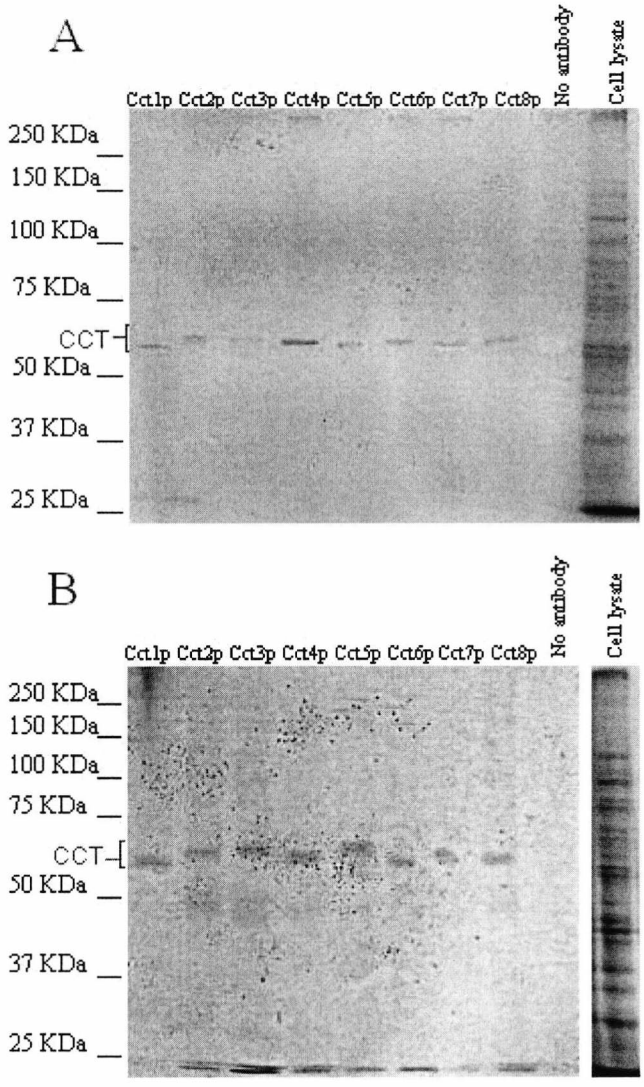

Figure 4.7 Autoradiographs of immunoprecipitated CCT from both *[PSI$^+$]* **(A)**, *[psi$^-$]* **(B)** yeast cell lysates in the presence of ATP. Rabbit antibodies raised against the C-terminus of the yeast Cct subunits were used to immunoprecipitate the CCT complex from whole cell lysate labeled with [^{35}S] methionine and [^{35}S] cysteine, in the presence of 2mM ATP and 140mM KCl. The immunoprecipitate was then separated by SDS-PAGE (30mA, 1hr), stained with Coomassie brilliant blue, dried (70°C, 90min, medium ramp) and incubated with autoradiography film (7 days, room temperature).

Figure 4.7 shows autoradiographs of immunoprecipitated CCT subunits from radiolabelled whole yeast cell lysate in the presence of 2mM ATP. This figure shows a startling difference to the IPs carried out under native conditions with hardly any other proteins brought down with the CCT. Also only individual subunits are present which is the first time that disassembly of the CCT complex under conditions of ATP and K^+ ions has been shown in yeast cells.

Again the coomassie stain of the IPs using the ΔN strain is shown, as the cells could not be radiolabelled.

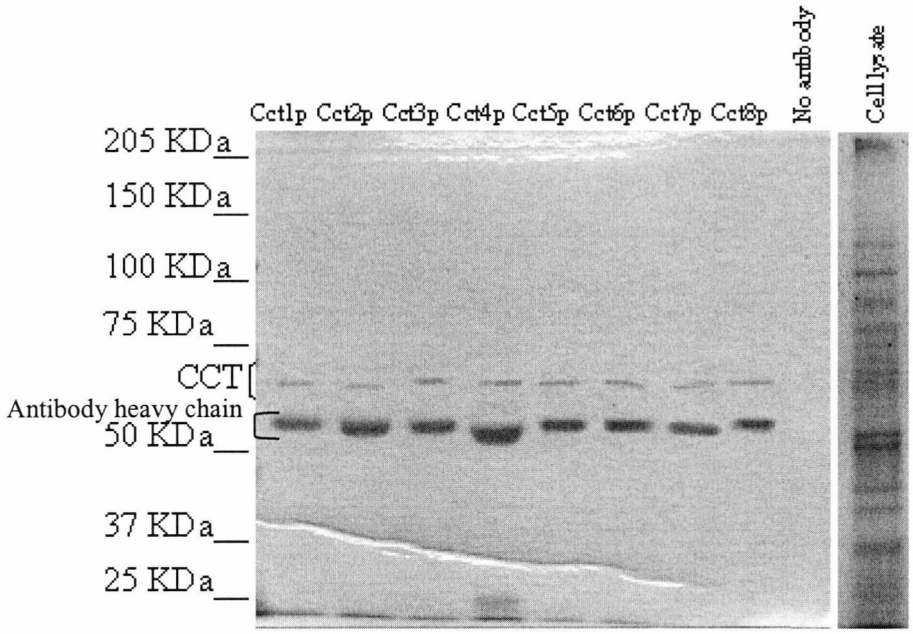

Figure 4.8 Coomassie stain of immunoprecipitated CCT from *ΔN* yeast cell lysate. Rabbit antibodies raised against the C-terminus of the yeast CCT subunits were used to immunoprecipitate the CCT complex from whole cell lysate in the presence of 2mM ATP and 140mM KCl. The immunoprecipitate was then separated by SDS-PAGE (30mA, 1hr) and stained with Coomassie brilliant blue.

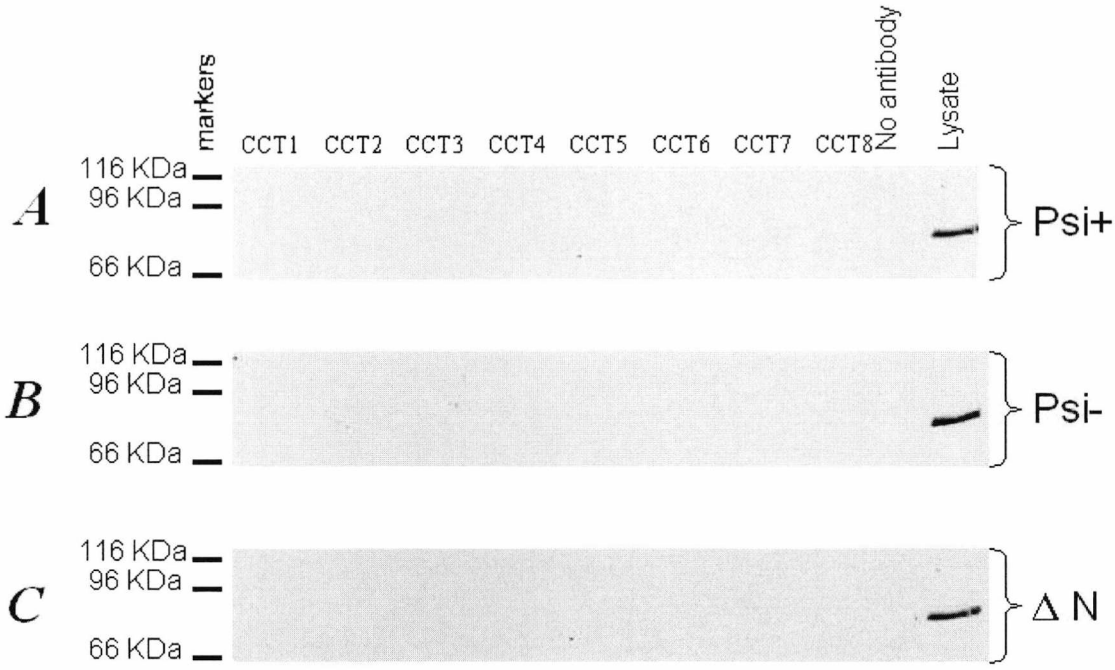

Figure 4.9 Anti-Sup35p western blots of immunoprecipitated CCT from *[PSI⁺]* **(A)**, *[psi⁻]* **(B)** and ΔN **(C)** yeast cell lysates. Rabbit antibodies raised against the C-terminus of the yeast CCT subunits were used to immunoprecipitate the CCT complex from whole cell lysate in the presence of 2mM ATP and 140mM KCl. The immunoprecipitate was then electrophoresed by SDS-PAGE (30mA, 1hr), western blotted (750mA, 1hr, 4°C) and probed with a guinea pig antibody raised against the C-terminus of Sup35p.

The observations in figure 4.9 show that Sup35p is undetectable by western blotting in the IPs of all yeast strains tested.

This indicates that the presence of ATP and potassium disrupts the interaction of CCT and Sup35p, demonstrated above, whether with the complex or individual subunits. This may indicate that Sup35p is a substrate of CCT and in the presence of ATP and potassium it is released as the CCT complex disassembles. Alternatively, the major conformational changes that occur in the CCT complex during ATP hydrolysis (Llorca *et al,* 1998) may simply disrupt any interaction. This could give an indication that Sup35p contacts the CCT subunits in either their equatorial or apical domains, as these are the areas of maximum change during ATP hydrolysis (Llorca *et al,* 1998). Incidentally, conformational changes in lone subunits during ATP hydrolysis has not been shown, therefore these data could offer a clue that these changes do occur in individual subunits as well as the complex.

4.2.3 Influence of IP conditions on CCT subunit/Sup35p interaction.

In mammalian systems it has been shown that in the presence of mildly denaturing detergents (RIPA buffer) the CCT complex is disrupted into its individual subunits (Roobol & Carden, 1999). However, substrate can remain bound to these subunits and this has been used to infer that these are the subunits to which that substrate binds in the whole complex (Hynes & Willison, 2000). Detection of Sup35p in RIPA IPs might be useful in establishing whether Sup35p behaves like a substrate and reveal the subunits to which it binds within the complex. Therefore the immunoprecipitations were carried out as above under RIPA conditions i.e. containing 1% v/v Triton-X100, 1% w/v Na deoxycholate, and 0.1% w/v SDS.

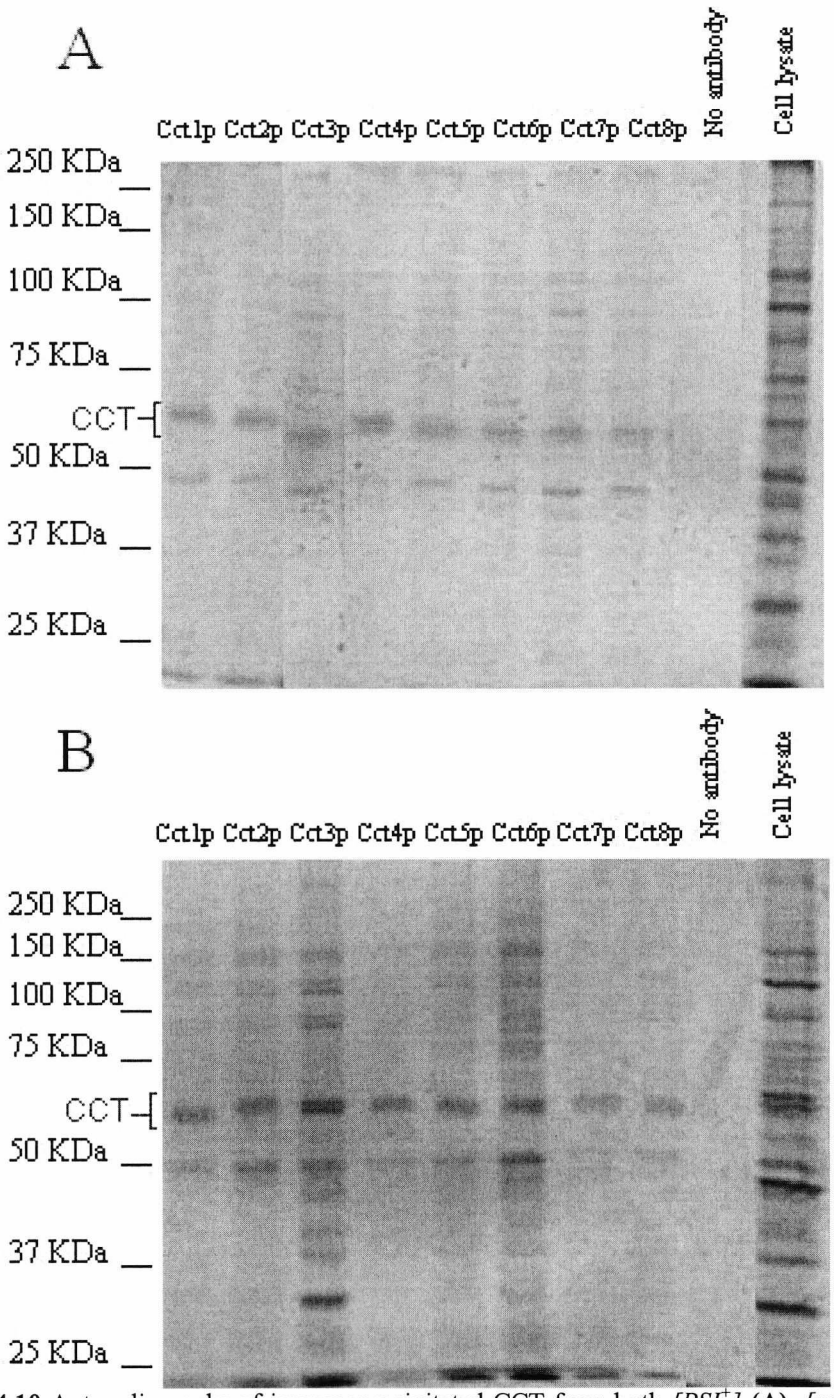

Figure 4.10 Autoradiographs of immunoprecipitated CCT from both *[PSI$^+$]* **(A)**, *[psi$^-$]* **(B)** and ΔN **(C)** yeast cell lysates. Rabbit antibodies raised against the C-terminus of the yeast CCT subunits were used to immunoprecipitate the CCT complex from whole cell lysate labeled with [^{35}S] methionine and [^{35}S] cysteine, in the presence of RIPA conditions (0.5% Triton-X100, 1% Na deoxycholate, 1% nonidet P40 and 0.1% SDS). The immunoprecipitate was then electrophoresed by SDS-PAGE (30mA, 1hr), stained with coomassie brilliant blue, dried (70°C, 90min, medium ramp) and incubated with autoradiography film (7 days, room temperature).

Figure 4.10 shows the autoradiographs of immunoprecipitated CCT subunits from radiolabeled yeast cell lysates carried out under RIPA conditions. It can be seen that

once again only individual CCT subunits are isolated but this time a number of other proteins are also visible in the IPs. It has been shown that under these conditions, substrate proteins remain bound to the individual CCT subunits (Hynes & Willison, 2000), which implies that these other proteins are substrates of the CCT complex.

Again the coomassie stain of the ΔN IPs is shown.

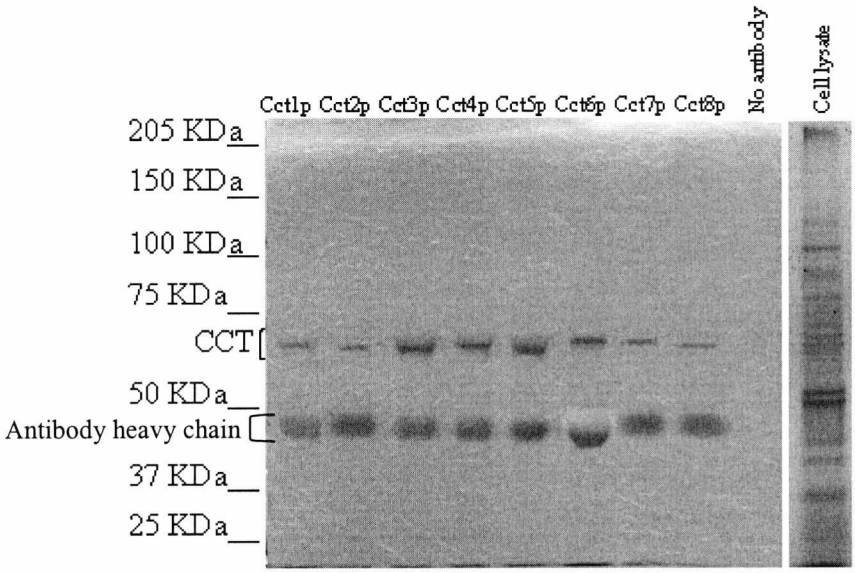

Figure 4.11 Coomassie stain of immunoprecipitated CCT from *ΔN* yeast cell lysate. Rabbit antibodies raised against the C-terminus of the yeast CCT subunits were used to immunoprecipitate the CCT complex from whole cell lysate, in the presence of RIPA conditions (0.5% Triton-X100, 1% Na deoxycholate, 1% nonidet P40 and 0.1% SDS). The immunoprecipitate was then electrophoresed by SDS-PAGE (30mA, 1hr) and stained with coomassie brilliant blue.

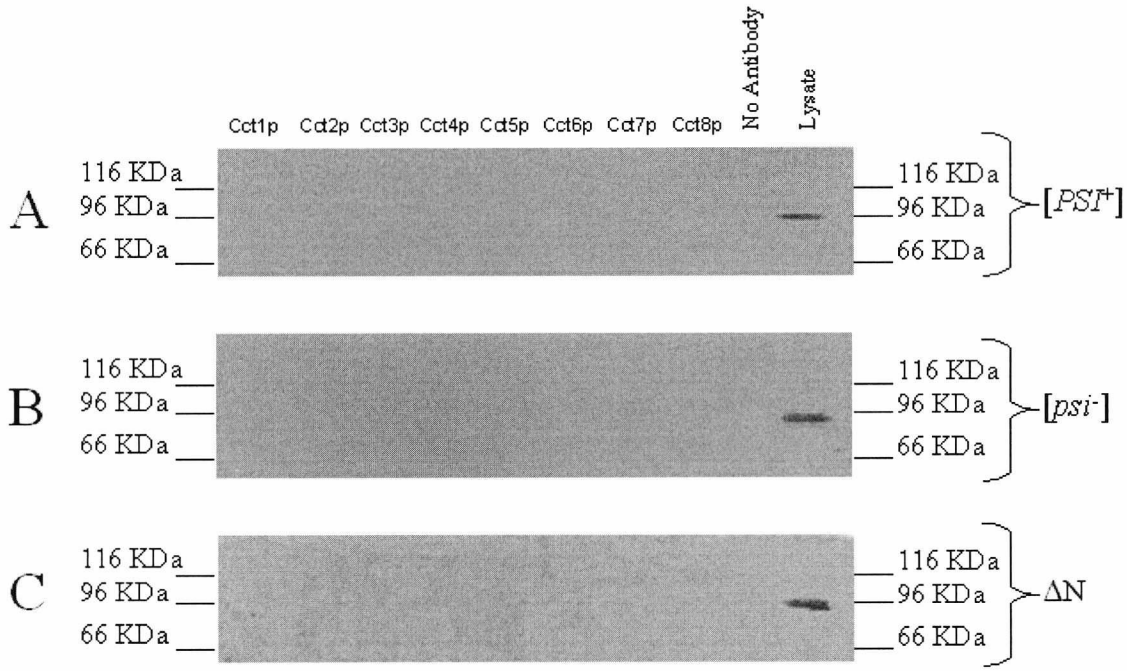

Figure 4.12 Western blots of immunoprecipitated CCT from both [*PSI*$^+$] **(A)**, [*psi*$^-$] **(B)** and ΔN **(C)** yeast cell lysates. Rabbit antibodies raised against the C-terminus of the yeast CCT subunits were used to immunoprecipitate the CCT complex from whole cell lysate in the presence of RIPA conditions (0.5% Triton-X100, 1% Na deoxycholate, 1% nonidet P40 and 0.1% SDS). The immunoprecipitate was then electrophoresed by SDS-PAGE (30mA, 1hr), western blotted (750mA, 1hr, 4°C) and probed with a guinea pig antibody raised against the C-terminus of Sup35p.

Figure 4.12 again shows that there is no interaction between CCT subunits and Sup35p, this time under RIPA conditions as no Sup35p is detectable on the immunoblots.

This data suggests that the CCT interaction with Sup35p is not a substrate-like interaction even though the ATP conformer of CCT does not bind Sup35p either. This suggests that Sup35p is a CCT associated protein rather than a substrate and that the whole complex has to be present in order for the interaction to occur.

4.2.4 Distribution of Sup35p and the CCT subunits when fractionated on a sucrose gradient.

Sucrose gradients can be used to separate proteins according to their size without disrupting stable interactions that may be taking place. As Sup35p aggregates form in *[PSI$^+$]* yeast cells they get larger and larger and should, therefore, be able to move through the more concentrated sucrose layers of a gradient. If CCT is associated with these large Sup35p aggregates then it seems reasonable to expect that some CCT will also move down a sucrose gradient and appear in heavier fractions than when Sup35p in not aggregated.

Both [PSI+] and [psi-] yeast cell lysates were loaded onto 10-40% sucrose gradients and centrifuged (85000g, 4°C, 18hr, acceleration setting 7, deceleration setting 0, Beckman SW40 or SW28 swing out rotor, Beckman L8-70M ultracentrifuge). The gradients were then fractionated into 22 fractions and the pellet resuspended. Each of these fractions were electrophoresed by SDS-PAGE and western blotted. These blots were then probed with antibodies against the CCT subunits and Sup35p.

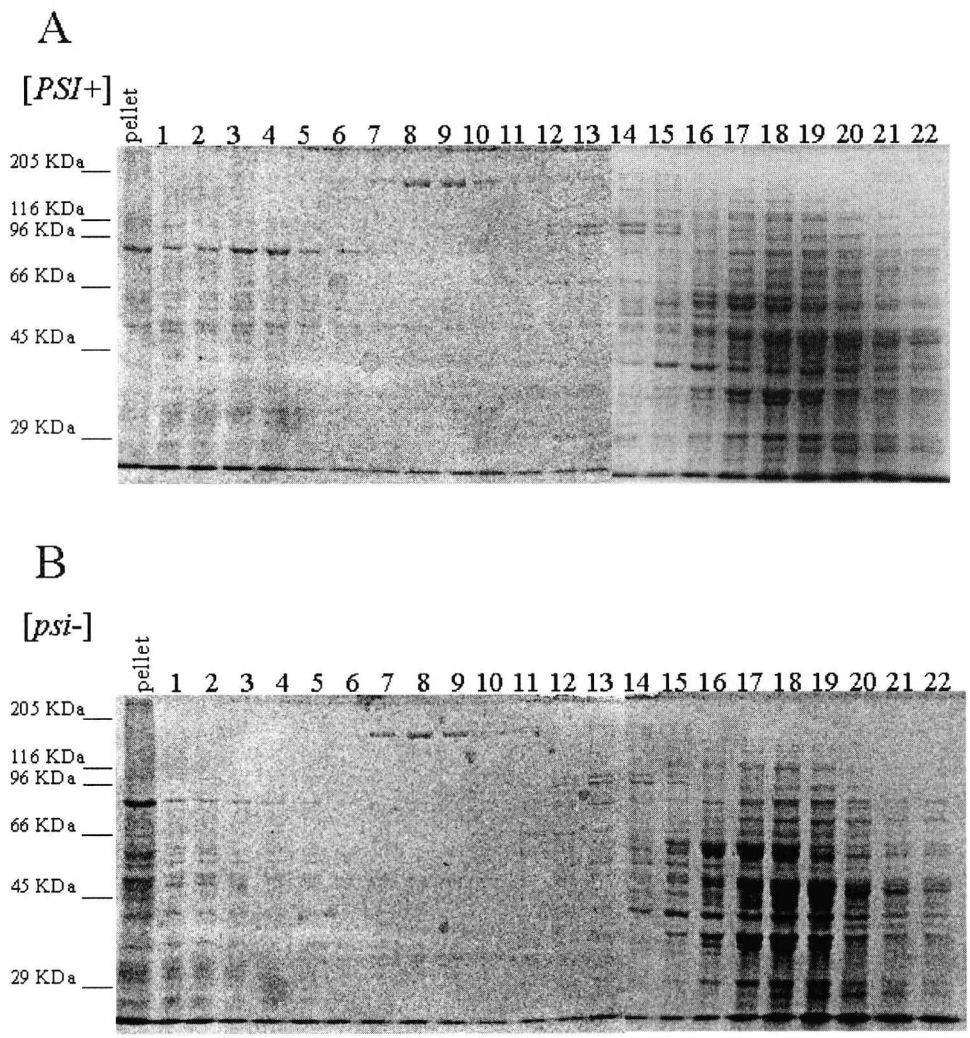

Figure 4.13 Coomassie stained SDS-PAGE gels of sucrose gradient fractions of yeast cell lysate from both *[PSI$^+$]* **(A)** and *[psi$^-$]* **(B)** cells. Yeast cell lysate was centrifuged (85000g, 4°C, 18hr, acceleration setting 7, deacceleration setting 0, Beckman SW40 or SW28 swing out rotor, Beckman L8-70M ultracentrifuge) through a 10-40% sucrose gradient. The gradients were then fractionated and electrophoresed by SDS-PAGE (30mA, 1hr), stained with coomassie brilliant blue and photographed using the BioRad GelDoc Bioimaging system.

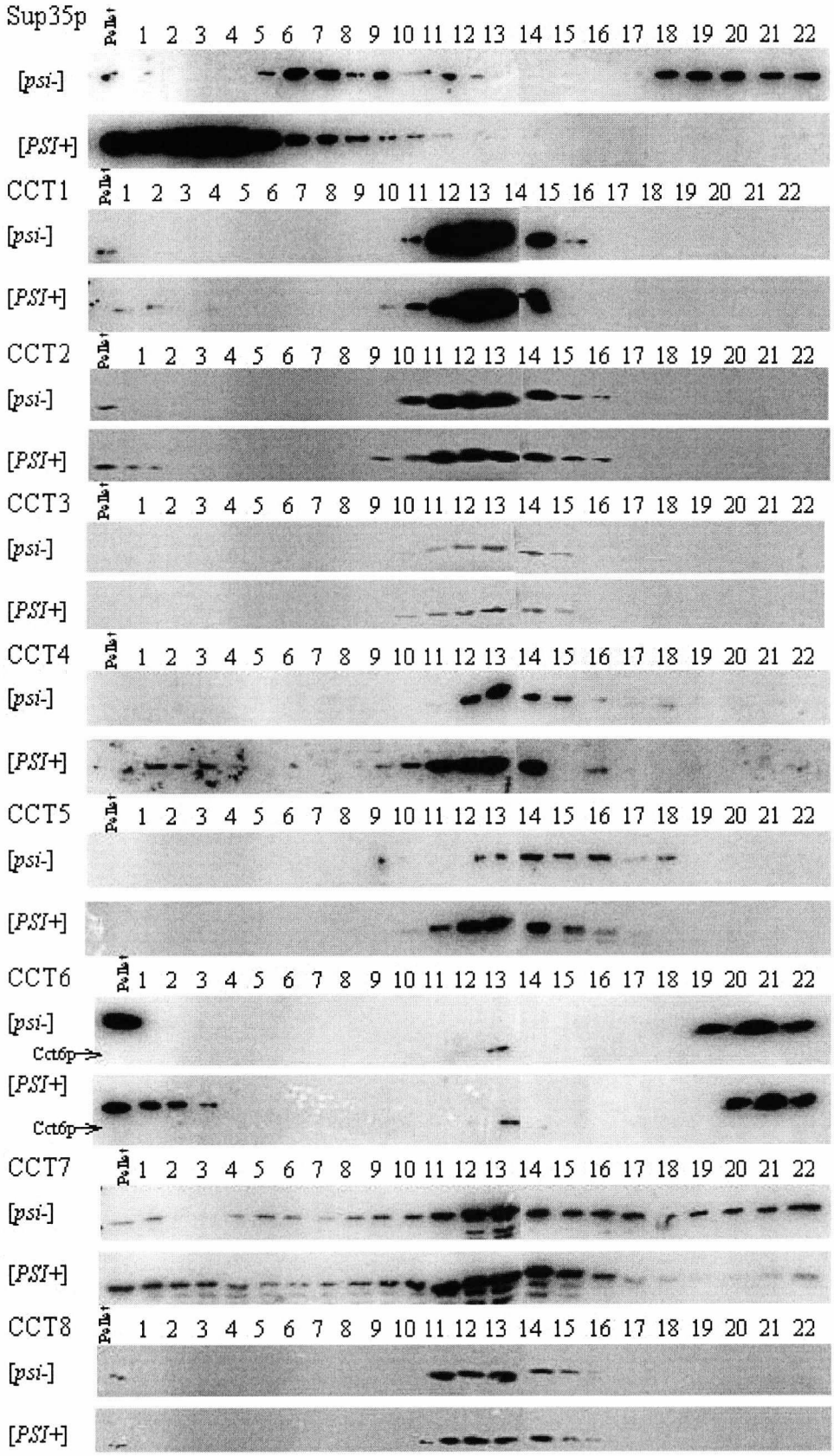

Figure 4.14 Western blots of sucrose gradient fractions of yeast cell lysate from both *[PSI$^+$]* and *[psi$^-$]* cells. Yeast cell lysate was centrifuged (25000rpm, 4°C, 18hr, acceleration setting 7, deceleration setting 0, Beckman SW40 or SW28 swing out rotor, Beckman L8-70M ultracentrifuge) through a 10-40% sucrose gradient. The gradients were then fractionated and electrophoresed by SDS-PAGE (30mA, 1hr); western blotted (750mA, 1hr, 4°C) and probed with antibodies raised against the C-terminus of Sup35p and yeast CCT subunits.

Figure 4.14 shows the distribution of the CCT subunits and Sup35p in sucrose gradients of both [*PSI*+] and [*psi*-] yeast cell lysates. When sucrose gradient analysis of a mammalian cell lysate was carried out, the CCT can be found in the central, 26S, fractions (see section 2.5.2). Some of the lighter fractions also contain individual subunits (see chapter 5) and some of the heavier fractions contain CCT in complex with cytoskeletal elements or ribosomes (McCallum *et al*, 2000). In the case of the yeast gradients I would expect to see the CCT subunits in fractions 11-14 as in the mammalian system, however the distribution of some of the subunits was quite unexpected. In both [*psi*-] and [*PSI*+] cell lysates the CCT subunits can be seen in the expected fractions, however, there are remarkable differences between the CCT content of both the heavier and lighter fractions when the prion positive and negative profiles are compared.

In [*psi*-] cells the Sup35p is found near the top of the gradient, as would be expected for a protein of its size. Sup35p is also found in some of the heavier fractions, including the CCT complex range of fractions. The presence of Sup35p in some of the heavier fractions could be as a result of the translation termination complex binding to other proteins or ribosomes (Gavin *et al*, 2002, Ho *et al*, 2002) or in association with cytoskeletal elements such as actin (see chapter 5). In the [*PSI*+] cells the Sup35p is only found in the heavier fractions and the pellet, with the amount of Sup35p detected decreasing down the gradient. This is as a result of the aggregation of the Sup35p into large complexes of increasing size and complexity.

In the [*psi*-] gradient some of the CCT subunits, especially Cct5p and Cct7p, can be found in the lighter fractions and the profile of micro complexes and individual subunit sized proteins is greatly increased. Whereas in the [*PSI*+] gradient the CCT found in the heavier fractions is increased, especially Cct1p, Cct4p and Cctp7. This

could indicate a change in the nature of the interaction between Sup35p and CCT in the prion positive and negative state.

The result from the Cct6p antibody cross-reactant shows a striking movement down the gradient in [*PSI*$^+$] cells, and is found in the lighter fractions in the [*psi*$^-$] cell gradient. This indicates that the cross reactant may itself be an interacting protein of Sup35p and could be closely associated with Sup35p, whatever its aggregation state. This cross-reactant could be one of several Hsp70p proteins from yeast as these are well documented to have a functional interaction with Sup35p (Chernoff *et al*, 1995, Newman *et al*, 1999, Chacinska *et al*, 2001).

4.2.5 Apportionment of Sup35p and CCT subunits when Sup35p aggregates are pelleted.

In [*PSI*$^+$] yeast cells Sup35p forms large aggregates and very little soluble Sup35p is left. In contrast in [*psi*$^-$] yeast cells all Sup35p remains soluble and no aggregates form. When centrifuged at high speed, aggregated and soluble Sup35p can be separated. If proteins are associated with the Sup35p aggregates then the proportion of these proteins found in the soluble and insoluble fractions of yeast cell lysate would change when [*PSI*$^+$] and [*psi*$^-$] cell lysates are compared.

Cell lysate from both [*PSI*$^+$] and [*psi*$^-$] yeast cells were centrifuged at high speed (50 000rpm, 4°C, 15min, Beckman TL 100.3 rotor, Beckman TL 100 ultra centrifuge), the supernatant removed and the pellet resuspended in an equal volume of buffer. Samples (10µl) of supernatant, resuspended pellet and total lysate were electrophoresed by SDS-PAGE, western blotted and probed with antibodies raised against the C-terminus of Sup35p and yeast CCT subunits.

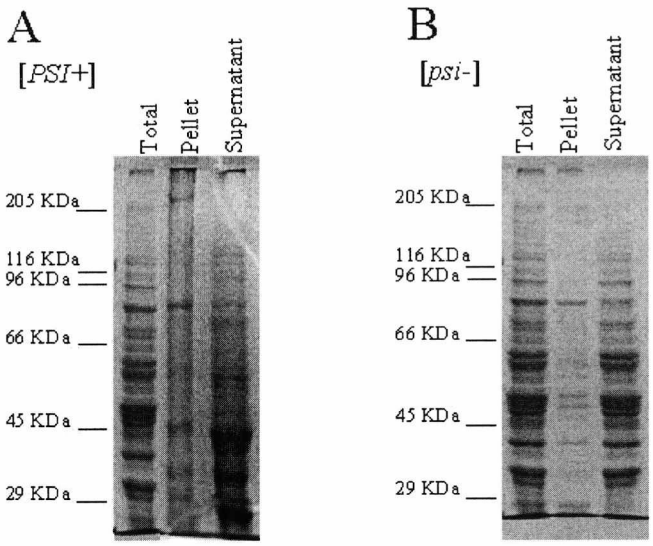

Figure 4.15 Coomassie stained SDS-PAGE gels of yeast cell lysate, from both [PSI^+] **(A)** and [psi^-] **(B)** cells, centrifuged to separate soluble and insoluble proteins. Yeast cell lysate was centrifuged (50 000rpm, 4°C, 15min, Beckman TL 100.3 rotor, Beckman TL 100 ultra centrifuge) and the supernatant, resuspended pellet and total lysate were electrophoresed by SDS-PAGE (30mA, 1hr), stained with coomassie brilliant blue and photographed using the BioRad GelDoc Bioimaging system.

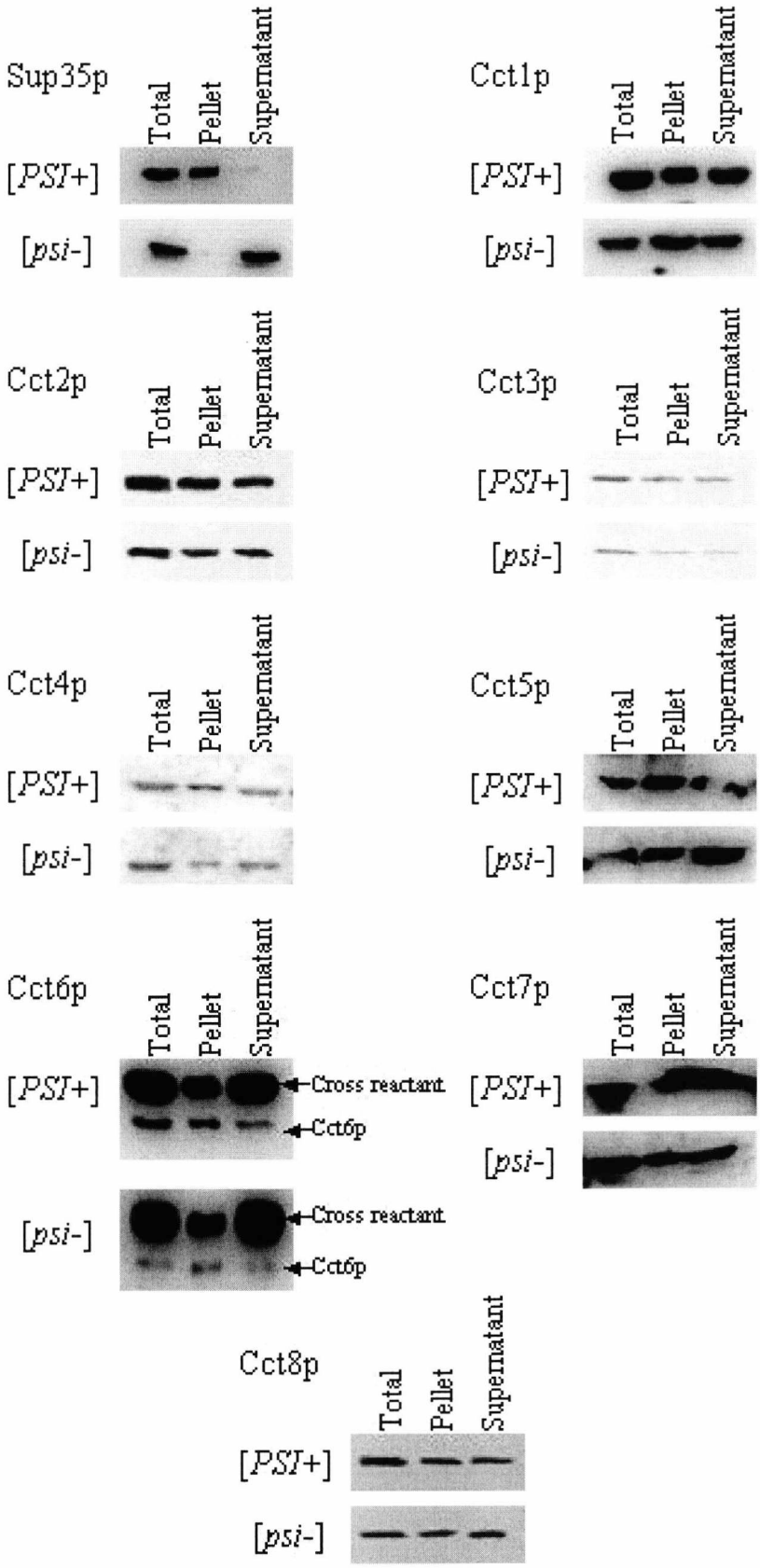

Figure 4.16 Western blots of yeast cell lysate from both [*PSI*$^+$] and [*psi*$^-$] cells, centrifuged to separate soluble and insoluble proteins. Yeast cell lysate was centrifuged (50 000rpm, 4°C, 15min, Beckman TL 100.3 rotor, Beckman TL 100 ultra centrifuge) and the supernatant, resuspended pellet and total lysate were electrophoresed by SDS-PAGE (30mA, 1hr), western blotted (750mA, 1hr, 4°C) and probed with antibodies raised against the C-terminus of Sup35p and yeast CCT subunits.

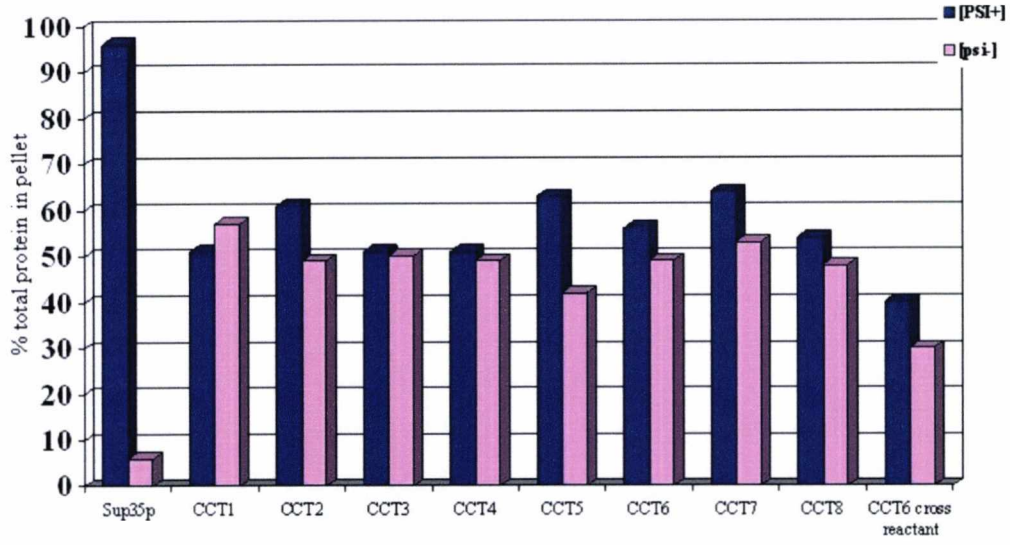

Figure 4.17 Graph to show percentage of total protein found in insoluble fraction of protein in [*PSI*$^+$] and [*psi*$^-$] yeast cell lysates.

The results represented in figures 4.16 and 4.17 show that there is a difference in the amount of CCT subunits found in the pellet of yeast lysate samples centrifuged at high speed. When subjected to these conditions, almost 100% of Sup35p is pelleted from [*PSI*+] yeast cell lysate, whereas in the [*psi*-] cell lysate almost 100% of Sup35p is soluble. The graph in figure 4.15 shows that in the majority of instances, but especially noticeable in the case of Cct5p and Cct7p, more of the CCT subunits are found in the pellet of [*PSI*+] than in [*psi*-] samples. The exception to this appears to be Cct1p, which becomes more soluble in [*PSI*+] cells. This offers further evidence of a difference in the interaction between aggregated and non-aggregated Sup35p and CCT.

This difference can also be seen in the Cct6p cross-reacting protein, indicating that this protein also decreases in solubility in [*PSI*$^+$] cells.

4.2.6 *In vitro* transcription/translation of wild type and mutant (ΔN) Sup35p.

In order to study protein interactions with CCT it is useful to produce them under controlled conditions. The rabbit reticulocyte in vitro translation system has become a useful tool. The reticulocyte is produced as an intermediate step between stem cell and red blood cell. It has all of the machinery, including CCT, required to make functional proteins but lacks any endogenous DNA and mRNA. This means that when the lysed cells are 'seeded' with exogenous DNA or mRNA the protein encoded by it is produced.

In order to use the rabbit reticulocyte *in vitro* translation system (Promega) the gene to be translated must be under the control of either a T3 or T7 promoter. The original plasmids coding for the N-terminally depleted Sup35p and wild-type Sup35p do not contain either of these promoters and therefore the gene had to be sub-cloned into an appropriate plasmid. The plasmids were digested with BamHI and XbaI restriction enzymes and re-ligated into the digested pBluescript plasmid behind the T7 promoter (see figure 4.18) and the modified pBluescript transformed into DH5α *E. coli* and selected on solid LB media containing ampicillin.

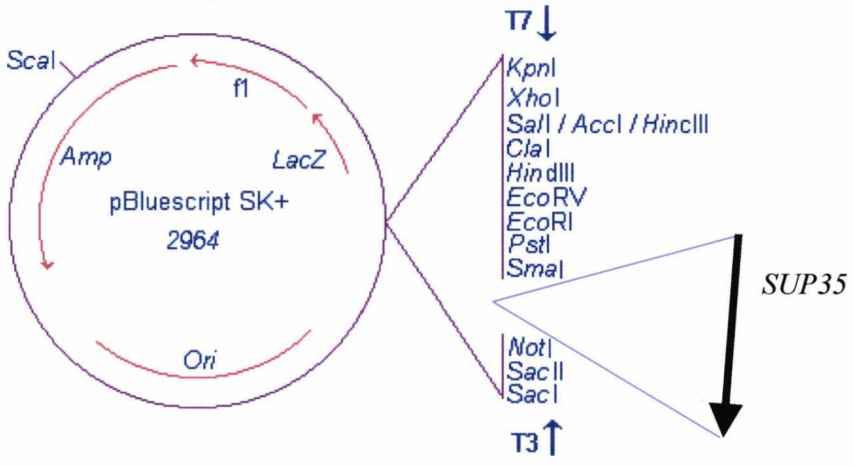

Figure 4.18 Map of pBluescript plasmid containing the GSPT2 full length gene under the control of the T7 promotor (pUKC2300). With DN plasmid denoted pUKC2301.

The plasmid was then re-isolated and re-digested to make sure it contained the correct sized insert.

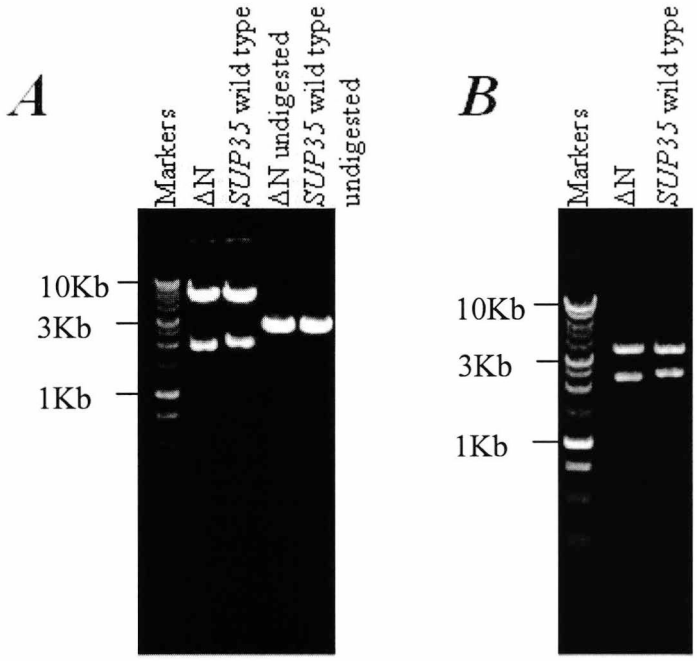

Figure 4.19 A Gel to show the products of the digestion of the *ΔN* and *SUP35* plasmids. *ΔN* and *SUP35* plasmids were digested with BamHI and XbaI restriction enzymes and the products electrophoresed on a 1% agarose TAE gel containing 0.5mg/ml ethidium bromide and photographed using the BioRad GelDoc Bioimaging system.

B Gel to show the products of the digestion of the re-isolated, sub-cloned *ΔN* and *SUP35* plasmids. The plasmids were digested with BamHI and XbaI restriction enzymes and the products electrophoresed on a 1% agarose TAE gel containing 0.5mg/ml ethidium bromide and photographed using the BioRad GelDoc Bioimaging system

Figure 4.19 shows the successful digestion of the *SUP35* and *ΔN* plasmids by BamHI and XbaI restriction enzymes showing the 2105bp and 1775bp products respectively. It also shows the successful ligation into and re-isolation of the pBluescript plasmids, demonstrated by the correct sized products (2105bp and 1775bp respectively) being digested out of the re-isolated plasmids. These plasmids could then be used in the *in vitro* transcription/translation experiments.

By adding radiolabelled amino acids to the reticulocyte system the protein produced can be located by autoradiography. Due to its oligomeric size, CCT can easily be

identified on a gel electrophoresed under native conditions and if the radiolabelled protein being produced is interacting with CCT then the CCT band on a native PAGE gel will show up on the autoradiograph. Such interactions can be further studied by the introduction of a 'chase'. If the interacting protein is a substrate then, following the chase, the CCT band on the autoradiograph can be seen to decrease in intensity over time. However, if the protein is associated with CCT in some other way then the band will not decrease. Instead of using the traditional cold chase, which can cause half labeled proteins to be produced, aurintricarboxylic acid (ATC) was used. This is an azo dye that has a number of effects on living cells but is useful as it inhibits initiation of translation (Stewart *et al*, 1971, Huang & Grollman, 1972). This means that proteins already being translated continue to completion but no new proteins are produced. This creates a cleaner cut off point and no half-labeled proteins are produced.

The transcription/translation reaction was initiated by plasmid addition and warming to 30°C and allowed to continue for 30min before the addition of 8μM ATC to half of the reaction mixture. Samples were taken every 10 min for 80min and then electrophoresed over both SDS PAGE and native PAGE. The gels were stained with Coomassie brilliant blue and dried before being autoradiographed.

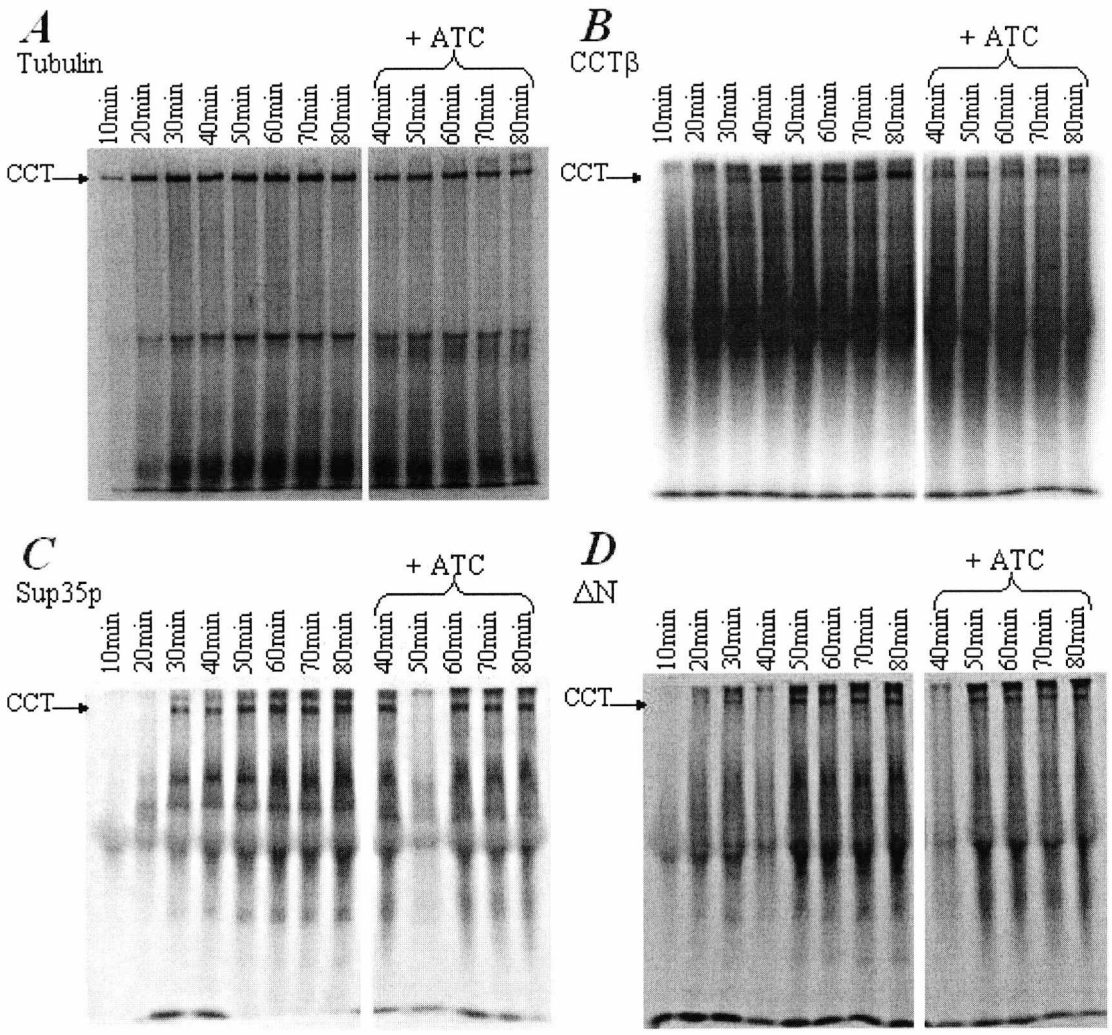

Figure 4.20 Autoradiographs of native PAGE gels of *in vitro* transcription/translation reaction samples of beta tubulin **(A)**, mammalian CCTβ **(B)**, Sup35p **(C)** and ΔN **(D)**. T7 driven plasmids were used in rabbit reticulocyte in vitro transcription/translation reactions, after 30 min half the reaction was made 8μM with respect to aurintricarboxylic acid and the reaction continued for a further 50min. Samples (taken every 10min) were then electrophoresed by native PAGE, stained with coomassie brilliant blue, dried and autoradiographed.

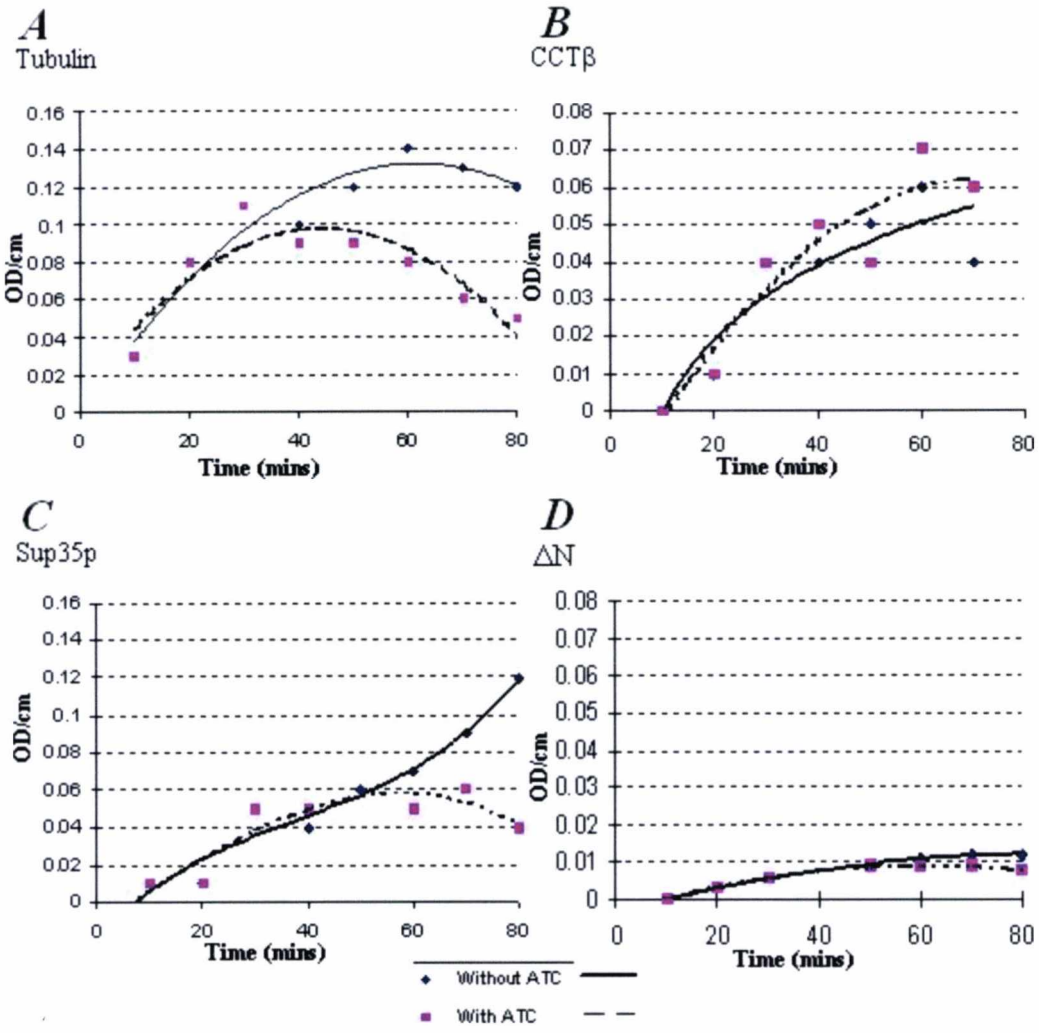

Figure 4.21 Graph of the densitometry of the CCT band on autoradiographs of native PAGE gels of *in vitro* transcription/translation reaction samples of beta tubulin **(A)**, mammalian CCTβ **(B)**, Sup35p **(C)** and ΔN **(D)**. T7 driven plasmids were used in rabbit reticulocyte in vitro transcription/translation reactions, after 30 min half the reaction was made 8μM with respect to aurintricarboxylic acid and the reaction continued for a further 50min. Samples (taken every 10min) were then electrophoresed by native PAGE, stained with coomassie brilliant blue, dried and autoradiographed. The autoradiographs were analyzed using the BioRad GelDoc Bioimaging system and a graph of the density of the CCT bands produced.

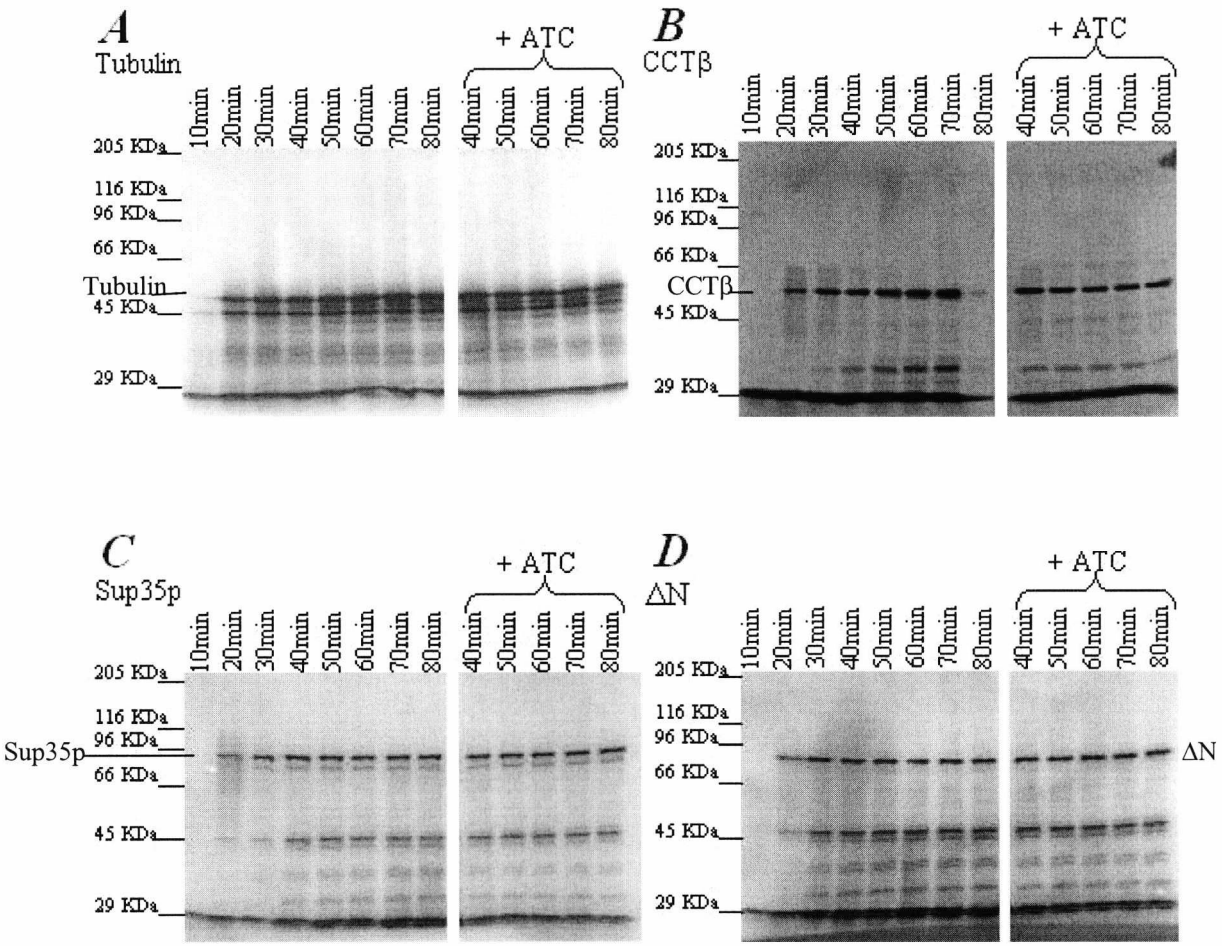

Figure 4.22 Autoradiographs of SDS-PAGE gels of *in vitro* transcription/translation reaction samples of beta tubulin **(A)**, mammalian CCTβ **(B)**, Sup35p **(C)** and ΔN **(D)**. T7 driven plasmids were used in rabbit reticulocyte in vitro transcription/translation reactions, after 30 min half the reaction was made 8μM with respect to aurintricarboxylic acid and the reaction continued for a further 50min. Samples (taken every 10min) were then electrophoresed by SDS PAGE, stained with coomassie brilliant blue, dried and autoradiographed.

It can be seen from figures 4.20 and 4.21 that the behavior of substrate (beta tubulin) and associated protein (mammalian CCTβ), when subjected to the conditions outlined are very different. While both tubulin and CCTβ increase in their association with the CCT complex, when translation initiation is halted the amount of association between the CCT complex and tubulin dramatically decreases, indicating that the tubulin is removed from the complex quite rapidly, whereas the amount of CCTβ association remains the same, showing that the CCT subunit is permanently associated with the complex. It can also be noted that the CCT band becomes evident before the appearance of fully folded tubulin, whereas the CCT subunit

appears before the CCT complex band becomes evident. This indicates that only the fully mature subunit is able to associate with CCT whereas the unfolded tubulin is associated with the complex.

The pattern of association for the wild type and mutant Sup35p interaction is remarkably different to either the substrate or subunit association. Wild type Sup35p appears on the autoradiograph before the CCT complex becomes evident, indicating that only the mature protein is interacting, and therefore not a chaperone-substrate interaction. However, the association between the Sup35p and CCT complex decreases when translation initiation is stopped, indicating that the association between the proteins is only transient. This points to a short-lived association between the two proteins.

The mutant, ΔN Sup35p does not appear to interact very well with the CCT complex (the scale is halved on the graph in figure 4.20 when compared to wild type Sup35p), although the pattern of association is similar to the wild type protein. This could mean that the CCT complex interacts with the N-terminus of Sup35p, or that the N-terminus stabilizes the interaction and therefore, when it is removed; the interaction is so unstable as to be practically immeasurable by this method.

Figure 4.22 shows the proteins produced by the *in vitro* translation are of the expected size. A number of smaller proteins can be seen and these relate to internal methionine residues acting as start signals for translation. Both the wild type and ΔN Sup35p translations show a major smaller band of the same size and this indicates the C-terminal region, as there is an internal methionine at the beginning of this region. The wild type Sup35p also shows a major band corresponding to the M-C domain of the protein as there is also an internal methionine at the beginning of the

M domain and this is also the same size as the ΔN mutant. These smaller bands do not affect the native gel result as overall the only difference between the two is the absence, in the mutant, of the N-domain, meaning any difference in the profile is due only to this absence.

4.3 Discussion

The evidence presented here clearly confirms an interaction between the CCT complex and Sup35p. This interaction has only been predicted by functional algorithmic analysis (Eisenberg *et al,* 2000) but has never been demonstrated experimentally, despite analyses of the yeast proteome (Gavin *et al*, 2002, Ho *et al*, 2002).

Results from the immunoprecipitations show a strong interaction between the CCT subunits and Sup35p in its prion state; however, this interaction is shown to be disrupted by ATP and strong detergent. This interaction is also decreased somewhat when Sup35p is not aggregated and when the N-terminal portion of the Sup35p is missing, however an interaction is still present, in a subunit specific manner. This indicates that Sup35p is not a substrate of CCT, as detergent is known to only disrupt non-substrate interactions (Hynes & Willison, 2000). This also points to the relationship being between Sup35p and the whole CCT complex as this is disrupted into its component subunits under these conditions (Roobol & Carden, 1999). ATP hydrolysis is a property of the CCT subunits and this process causes major conformational changes within the protein (Llorca *et al,* 1998). This could easily interrupt any interaction between CCT and Sup35p. Sup35p also has GTPase

activity when bound to Sup45p and the ribosome (Nakamura & Ito, 1998) and this may also cause the disruption of the relationship.

The interaction is demonstrated further by *in vitro* translation of wild type and mutant (ΔN) Sup35p in rabbit reticulocyte lysate, where the CCT band is visible on a native gel autoradiograph. This interaction is severely reduced in the case of the mutant and does not compare well with a substrate interaction or that of a permanently associated protein (see figure 4.21). The interaction appears to be transient but again not substrate-like in nature. The Sup35p produced in this instance should be non-aggregated as no 'seeds', required for the prionisation of the protein, are present. This can be seen from the native gel as no large aggregates are found at the top of the lanes, showing that the non-aggregated protein interacts with the CCT complex. The reduction in interaction when the N-terminus is missing may indicate that this region of Sup35p is required for stabilization of the relationship, or contains the binding site.

The sucrose gradient analysis does demonstrate that Sup35p is found in the same fractions as the CCT subunits and also shows an increase in the number of micro-complexes and individual subunits in [*psi-*] cell lysate when compared to that from [*PSI+*] cells, and conversely the amount of subunits found in the heavier fractions also increases in [*PSI+*] cell lysate. This could mean that some CCT is associated with Sup35p and thus follows Sup35p as its position changes in the sucrose gradient depending on its aggregation state. Similarly, sedimentation analysis shows that more CCT is found in the pellet from [*PSI+*] cell lysate than that from [*psi-*] cells. Again indicating a difference in solubility of the CCT between prion positive and negative cells.

Taken separately, these pieces of evidence provide intriguing clues as to the nature of the interaction between Sup35p and CCT. But together they can offer a model for the association between these two important proteins. It is tempting to think that the chaperone is somehow responsible, in part, for the misfolding event of Sup35p leading to its prionisation, and indeed this would be a very important finding. It is not without precedent for a chaperone to be involved in this process as it is well documented that other chaperones are necessary for this eventuality, especially Hsp104p (Chernoff *et al*, 1995). The class I chaperonin GroEL has also been implicated in prion formation *in vitro* (DeBurman *et al*, 1997). However, neither of these proteins are found in mammalian cells and only one homologue, of GroEL, CCT, has been found. Nevertheless the evidence presented here does not implicate CCT in the folding of Sup35p; it does indicate that these two proteins associate for another, more intriguing, reason.

Both proteins have been implicated to have a role in the cell cycle (Yokota *et al*, 2001, Kikuchi *et al*, 1988); however, this seems unlikely as an explanation for their interaction as there is now debate over the involvement of Sup35p in this process (Parham S. N. PhD Thesis, 2001). It does seem strange that no ill effects have been reported on the cell division cycle when Sup35p is in its inactive aggregated form (Chernoff *et al*, 1998, Eaglestone *et al*, 1999).

The only other cellular process both proteins could have reason to interact is that of protein synthesis. Convention dictates that these two proteins should not come into contact with each other during this process as Sup35p is associated with newly synthesized, unfolded, proteins in its role as part of the translation termination complex (Frolova et al, 1994, Zhouravleva et al, 1995), and CCT is associated with more mature, partially folded, proteins (Llorca *et al*, 1999). However there have

been reports that CCT does associate with nascent peptide chains (McCallum *et al*, 2000; Dunn *et al*, 2001).

I propose that Sup35p interacts with the CCT complex in a subunit specific manner, during protein synthesis, to facilitate the binding of nascent polypeptide chains to CCT for folding. The native immunoprecipitation of the ΔN Sup35p mutant cell lysate shows a strong interaction with Cct1p and Cct7p and a much weaker interaction with Cct2, Cct5 and Cct6. When organized into a ring conformation with the same order of subunits proposed for the mammalian complex (Liou & Willison, 1997), these subunits lie next to each other (see figure 4.22).

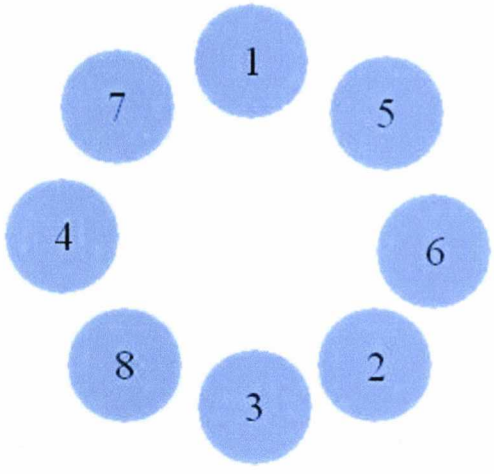

Figure 4.23 Order of CCT subunits in the yeast complex, based on that proposed for the mammalian complex by Liou & Willison, (1997)

I believe that these subunits represent the normal binding sites of Sup35p and that the presence of the 'free' N-terminus in the prion negative cells inhibits this interaction. Nevertheless an interaction in the [*psi*-] cells does take place, but only with Cct2. I therefore propose that Cct2 acts as an anchor for Sup35p and that it is this subunit that is involved in the stabilization of the interaction by binding at the N/M domain junction of Sup35p. This is proposed because the interaction still occurs in the ΔN IP and is the only subunit found to bind Sup35p with a free N-terminus in the [psi-]

IP, but also when the N-terminus is missing, the interaction is much depleted (from figure 4.17), implicating a role for this region in the stabilization of the interaction. It seems, from the IP evidence, that Sup35p binds strongly to Cct1 and Cct7 and much more weakly to Cct5 and Cct6, indicating that Sup35p binds across the ring complex. It is feasible to assume that the free N-terminal region of Sup35p could interfere with this binding, maybe in response to the ATPase induced conformational changes in the CCT or the GTPase activity of Sup35p. This also brings in another factor to the model. Sup35p only exhibits GTPase activity in the presence of Sup45p and the ribosome (Nakamura & Ito, 1998) and one or both of these may also be present in the CCT/Sup35p complex. The other evidence for at least a third component of the complex is that only the free N-terminus is able to inhibit the interaction, as when it is missing the interaction still occurs but less stably. This indicates that the N-terminus may have to be bound to a third component of the complex in order for full cooperation to occur between CCT and Sup35p. Though the functional component of Sup35p has been identified as the C-terminal domain (Ter-Avanesyan *et al*, 1993, 1994, Wilson & Culbertson, 1988), it has been shown recently that the poly (A)-binding protein (Pab1p) is also able to bind the N and M domains of Sup35p (Cosson *et al*, 2002). This could indicate that Pab1p brings Sup35p into close proximity with the poly (A) region of the mRNA being translated, thus bringing the entire translation termination complex into the correct position to initiate translation termination (Cosson *et al*, 2002), and thus allowing CCT to interact with Sup35p and hence carry out its function as protein folding chaperone.

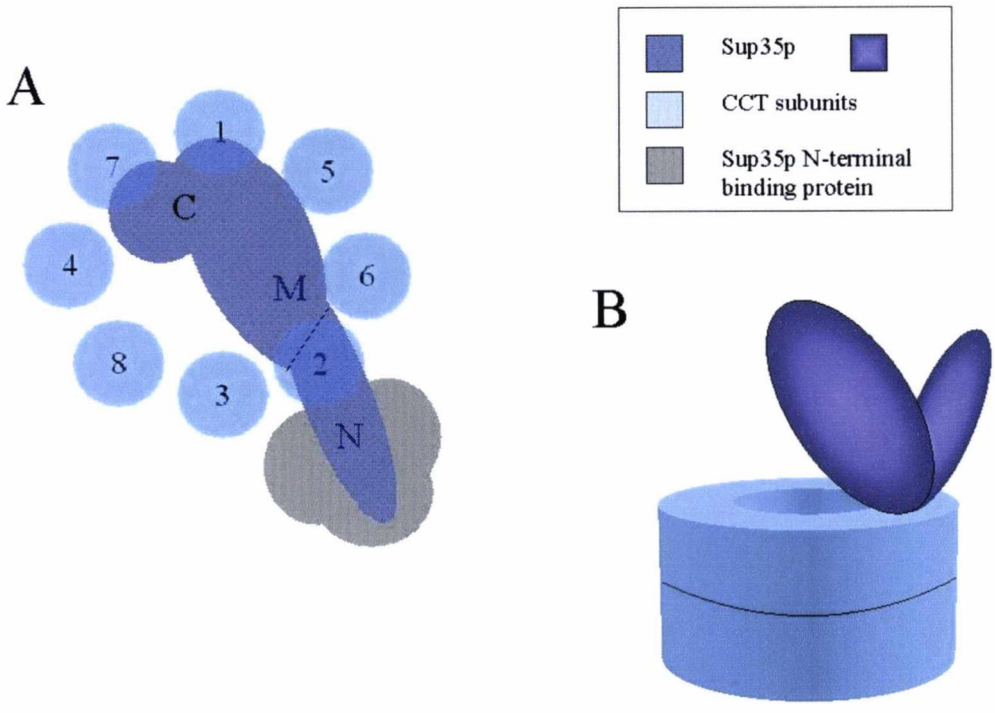

Figure 4.24 Diagram showing the possible orientation of interaction between Sup35p and CCT. When the N-terminus of Sup35p is bound to another component of the complex then the interaction is stabilized and Sup35p interacts with Cct1, Cct7, Cct5, Cct6 and Cct2 **(A).** When the N-terminus of Sup35p is unbound then the interaction is destabilized and Sup35p is only bound to Cct2 **(B).**

This model can also explain why the aggregated Sup35p interacts with all of the CCT subunits. In the prion state the N-terminal domains have a β-sheet conformation (Cohen *et al*, 1994) allowing them to bind closely to each other, thus the N-terminal domains are no longer free and are unable to inhibit the interaction. With the Sup35p molecules in close proximity to each other, an interaction with any bound CCT is likely to be enhanced and is therefore liable to be detected in all native IPs.

Chapter 5: CCT/eRF3 (GSPT1/2) interaction

5.1 Introduction

5.1.1 GSPT1/2

The yeast Sup35p protein is a translational release factor, namely eRF3 (see section 4.1.2). Its mammalian homologues have now been identified during Human genome sequencing but initially they were identified in complementation experiments in yeast. G_1 to S phase transition proteins 1 and 2 (GSPT1/2) are two mouse proteins said to be homologous to the yeast Sup35p/eRF3 protein (Hoshino *et al*, 1998). However, the first yeast homologue found in mammalian cells was called GST1-Hs (renamed GSPT1) and was isolated from human DNA (Hoshino *et al*, 1989). It was found that this homologue was able to complement the *gst1* mutation of *S. cerevisiae* (Hoshino *et al*, 1989), which had been earlier found to be in the *SUP35* gene (Kikuchi *et al*, 1988), and had led to the assumption that Sup35p had a role in G to S phase transition (Kikuchi *et al*, 1988), hence the name of the mammalian proteins, although this is now thought not to be the case (Parham S.N. PhD thesis, 2001). Subsequent chromosome mapping identified the location of the *GSPT1* gene to be on human chromosome 16p13.1 (Ozawa *et al*, 1992), but interestingly a homologous gene was also found on the X chromosome (Ozawa *et al*, 1992), later mapped to chromosomal band Xp11.23 (Hansen *et al*, 1999), indicating that more than one *GSPT* gene was present in the human genome. It was not until six years later that work on isolating the mouse homologue of *GSPT1* yielded a second gene, named *GSPT2* (Hoshino *et al*, 1998). The predicted amino acid sequence generated from these genes shows that they share a high amount of identity with each other and with both human GSPT1 and yeast Sup35p (Hoshino *et al*, 1998) (see figure 5.1). In fact

the two mouse proteins are practically identical for most of their length only differing in the N-terminal third of their sequence. The human protein also shares its C-terminal sequence with the mouse proteins, and high homology with the N-terminus of mouse GSPT1, indicating a high degree of conservation between this family of proteins (Hoshino *et al*, 1998).

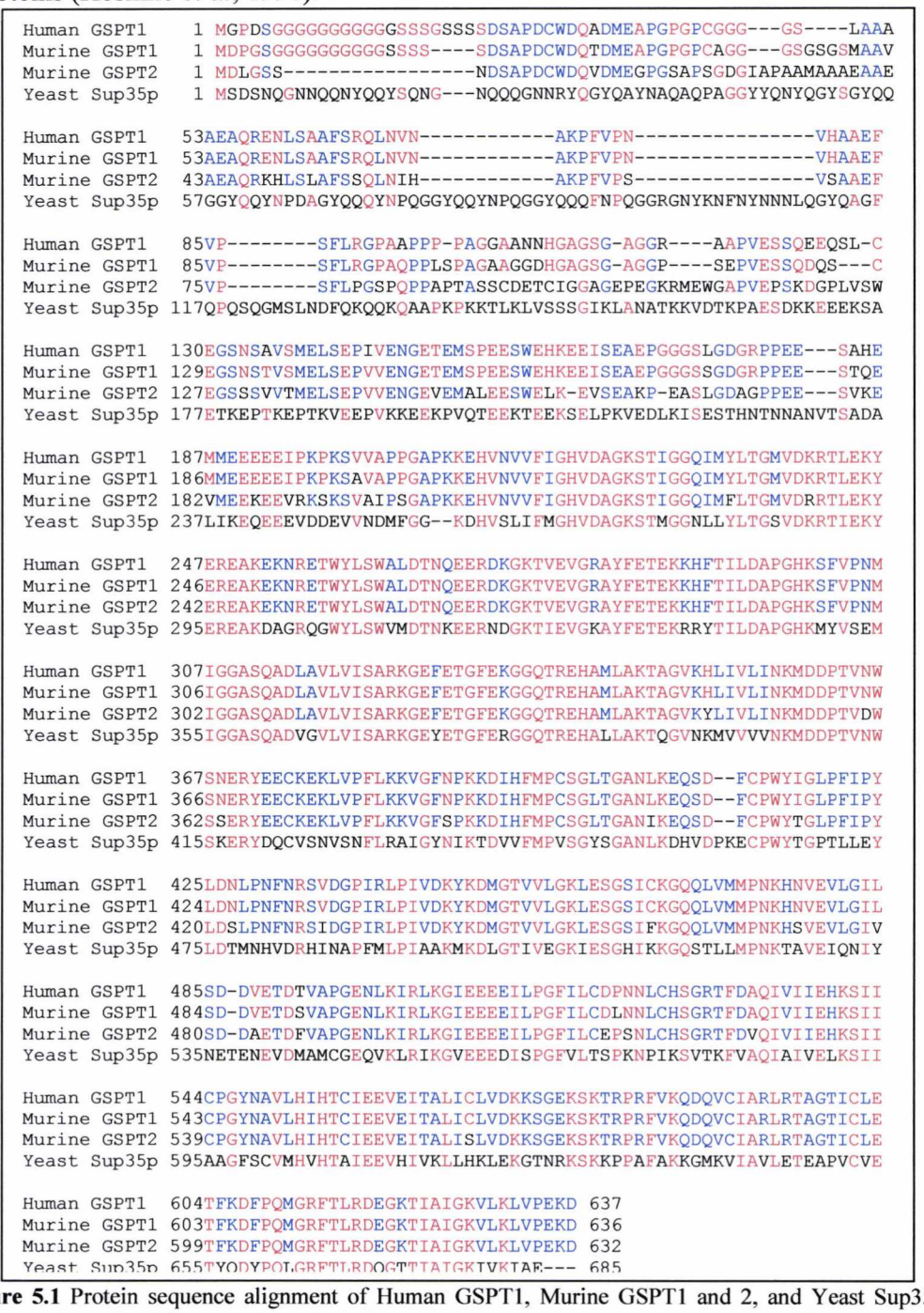

Figure 5.1 Protein sequence alignment of Human GSPT1, Murine GSPT1 and 2, and Yeast Sup35p. Identical residues are shown in red and those only identical in the GSPTs are in blue.

The similarity between the yeast and the mammalian proteins has led to the assumption that these proteins have a similar function in both organisms. A number of conserved domains involved in GTP binding have been identified as well as an EF-1α-like domain (Hoshino *et al*, 1998). Further to this, both GSPT1 and GSPT2 have been shown to interact with eRF1 by immunoprecipitation and yeast two-hybrid assay, with a more significant interaction detected between GSPT2 and eRF1 (Hoshino *et al*, 1998). This interaction was later seen to involve the C-terminal domain of GSPT2 (Hoshino *et al*, 1999), which is similar to the yeast system where eRF1 (Sup45p) associates with only the C-terminal region of Sup35p (Ito *et al*, 1998, Ebihara & Nakamura, 1999). It was later shown that mouse *GSPT2* but not *GSPT1* could functionally replace yeast *SUP35* (Le Goff *et al*, 2002). This study also demonstrated that the N-terminal region of GSPT1 was responsible, but not sufficient, for the lack of complementarity between Sup35p and GSPT1 (Le Goff *et al*, 2002).

Further evidence for GSPT1 and 2 being involved in the translation termination is that they associate with poly(A)-binding protein (PABP) (Hoshino *et al*, 1999) and, in the case of GSPT2, this interaction is through the N-terminal domain associating with the C-terminal domain of PABP (Hoshino *et al*, 1999). Again this is similar to the interaction observed between yeast Sup35p and PABP (Cosson *et al*, 2002). A further role for GSPT2 has been hypothesized to be in the translation cycle as a whole (Uchida *et al*, 2002). Inhibition of the interaction between GSPT2 and PABP significantly attenuated translation of capped/poly(A)-tailed mRNA (Uchida *et al*, 2002). This is thought to be because PABP is required to facilitate the binding of GSPT2 to the cap binding factor eEIF4G resulting in a circularization of mRNA being translated (Uchida *et al*, 2002). Although this interaction has been shown not

to be necessary for the initial formation of the 80s ribosome (Uchida *et al*, 2002) it may have a role in ribosome recycling (for review see Sonenberg & Dever, 2003), a role also put forward for Sup35p (Nakamura & Ito, 1998).

One of the major differences between the mammalian and yeast proteins is in their N-terminal domain. The mammalian proteins lack the repeat regions found in Sup35p, which are required for the prionisation of the protein (Ter-Avanesyan *et al*, 1994, Parham *et al*, 2001). However, the N-terminal domain of GSPT1, especially, is very unusual in that it contains a very high number of glycine residues and GSPT2 contains a region of alanine residues at the N-terminus. These curious N-terminal regions may have no significance whatsoever but may have evolved to form specific structures necessary for function or to prevent prionisation of the proteins, but as these proteins have not yet been solved structurally we shall have to wait and see.

5.1.2 Evidence for an interaction

At the start of my work, evidence for an interaction between GSPT1/2 and CCT was speculative at best. As figure 4.1 (chapter 4) shows, only the yeast proteins have been linked by computer analysis (Eisenberg *et al*, 2000) and as the mammalian proteome has not yet undergone such in-depth analysis, an interaction has not been predicted. However, as shown in chapter 4 of this study, the yeast proteins have now been shown to interact and so it seems logical that, as homologues of these proteins exist in mammals, they should interact in mammalian cells as well, especially if the function of the interaction is as fundamental as proposed for yeast, linking translation termination and protein folding. One of the major rationales for investigating an interaction between the mammalian proteins was to determine whether the

interaction in yeast owed more to a yeast-specific role in prionisation-related behaviour or instead to a more general role in translation. The evidence presented in chapter 4 points to the latter as the N-terminal, prion-forming domain, has been shown not to be required for the interaction and although some differences were observed in the interaction in [*PSI*$^+$] (prion positive) and [*psi*$^-$] (prion negative) cells, the interaction does not appear to be one of chaperonin/substrate.

Further to this, it has also been shown that CCT subunits peak in expression during early S-phase of the cell cycle (Yokota *et al*, 2001) and the name of the GSPT proteins are G to S-phase transition proteins because of their similarity to yeast Sup35p, which has been implicated in the G to S phase transition (Kikuchi *et al*, 1988), indicating that a role for an interaction may be implied in this process.

5.1.3 I.M.A.G.E.

For the purpose of this study it was necessary to obtain clones of both *GSPT1* and *GSPT2*. After numerous PCR-based attempts at cloning these genes from various sources and using several methods, I was unsuccessful. In an attempt to confirm the published sequence, I mined the mouse EST (expressed sequence tag) database and came across references to the I.M.A.G.E consortium.

An Integrated Molecular Analysis of Genomes and their Expression (I.M.A.G.E.) consortium was set up between four academic groups in 1993 to efficiently analyse the vast amounts of sequence data generated by the Human Genome Mapping Project (HGMP) (Lennon *et al*, 1996). This has been extended to include sequence data from cDNA libraries from mouse and zebrafish.

The cDNA libraries are directionally cloned, using oligo(dT)-primers so that the 3' end represents each gene, into plasmid vectors in endA bacterial hosts (Lennon *et al*, 1996). These clones are arrayed in 384-well microtiter plates using an automated colony picker and maintained in glycerol stocks. These arrays are then sent to laboratories around the world and sequenced, often with only one round of sequencing at the 5' end. This information is then posted on public databases (Lennon *et al*, 1996). The clones are given unique identification numbers and are then available, for a nominal fee, to any researcher who wants them from a number of companies around the world and directly from the HGMP resource centre in Cambridge (England).

5.1.4 Aims and objectives

The aims of the studies described in this chapter were very similar to those in chapter 4. The main objectives were to discover whether mammalian CCT subunits and eRF3 (GSPT1/2) interact and, if so, to elucidate something of the nature of this interaction.

Finally a comparison between the yeast and mammalian system can hence be made.

5.2 Results

5.2.1 Tissue distribution of GSPT1/2

The differentiation of cells into different types, within mammalian tissues, means that proteins are expressed at varying levels in each tissue type. It is logical to assume, therefore, that if two proteins interact, then they must be expressed in the same tissues. Thus, western blot analysis of cell lysates from different rat tissues was performed with antibodies to GSPT1/2 (see Chapter 3) and CCT (a kind gift from Dr. Roobol).

Various tissues were dissected from a euthanased male rat and placed into liquid nitrogen (dissection kindly carried out by Dr. Anne Roobol). Samples were then ground to a fine powder under liquid nitrogen, resuspended in lysis buffer and debris removed by centrifugation (see section 2.3.1). Equal quantities of protein were then electrophoresed by 9% SDS-PAGE and blotted. Blots were probed with antibodies against GSPT1/2 (see chapter 3) and CCT subunit γ, chosen as a representative CCT subunit.

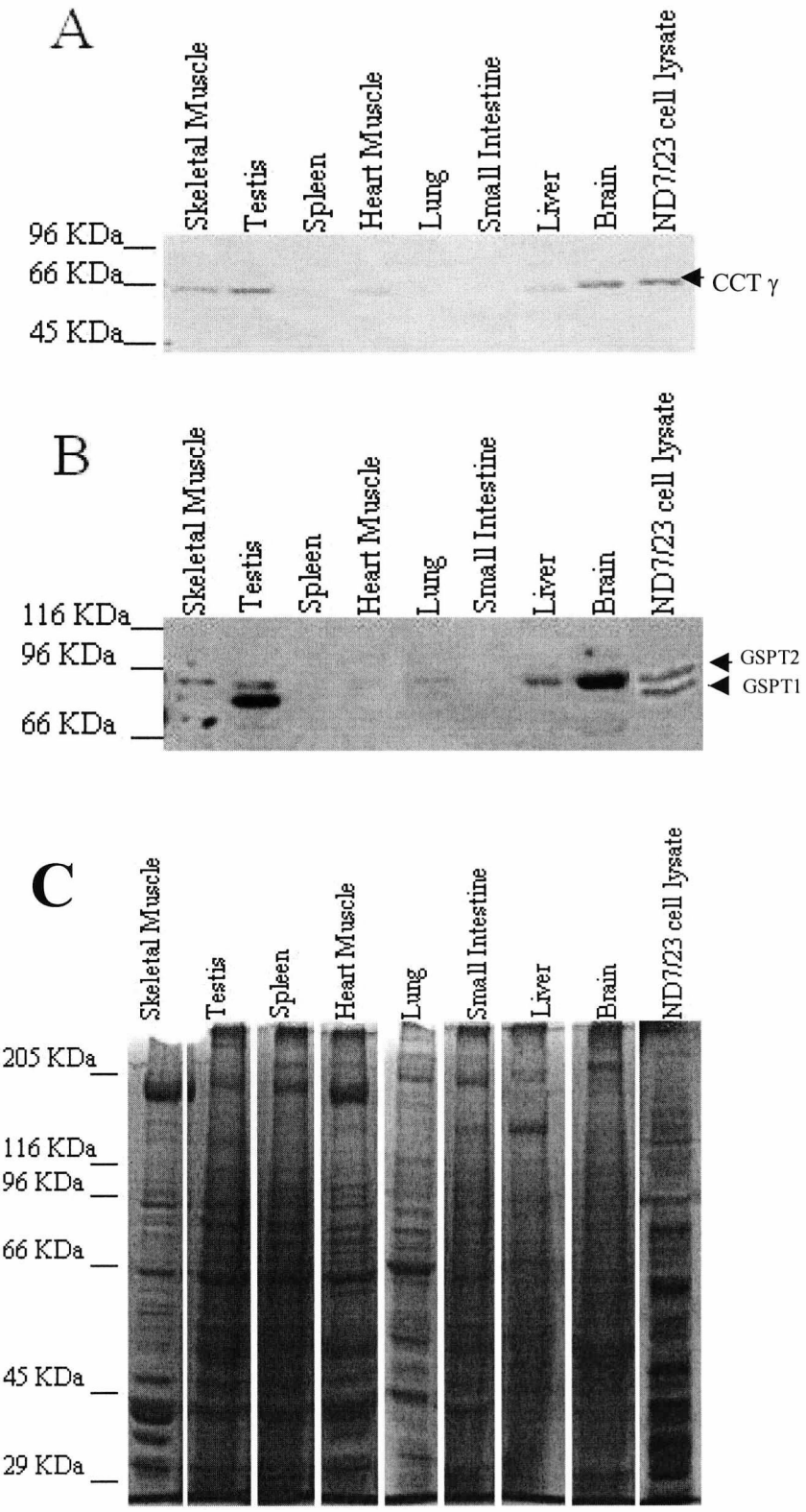

Figure 5.2 Western blots of various tissue samples from a euthanised male rat. Tissues were ground under liquid nitrogen, resuspended in lysis buffer and centrifuged to remove debris. The lysates (30μg) were then electrophoresed by SDS-PAGE (30mA, 1hr), western blotted (750mA, 1hr, 4°C) and probed with guinea pig antibodies raised against the C-terminus of CCTγ (**A**) and rabbit antibodies raised against the C-terminus of GSPT1/2 (**B**).
(**C**) SDS-PAGE of various tissue samples from a euthanised male rat. Tissues were ground under liquid nitrogen, resuspended in lysis buffer and centrifuged to remove debris. The lysates (30μg) were then electrophoresed by SDS-PAGE (30mA, 1¼hr) and stained with Coomassie brilliant blue.

Figure 5.2C shows the Coomassie stained SDS-PAGE of various tissue samples of a euthanised male rat. The amount of protein detected in the samples appears to be different despite equal loading. This is due to the differential amounts of various proteins synthesised in the various cell types, for example, in both the heart and skeletal muscle samples a large band can be seen at the top of the gel, which is only present in smaller quantities in the other tissue samples, this corresponds to myosin which is expected to be present in large quantities in these tissues.

Figures 5.2A and 5.2B show the western blots of the various tissue samples probed with both anti-CCTγ and anti-GSPT1/2 antibodies. It can clearly be seen that CCT γ is present in the skeletal muscle, testis, heart muscle, liver, brain and ND7/23 cell samples in varying quantities, with the most detected in testis, brain and ND7/23 cell samples. The GSPT1/2 displays a similar expression pattern to CCT γ; however, the difference between the expression levels of GSPT1 and GSPT2 are striking. GSPT2 (the larger band) appears to be predominant in the skeletal muscle, heart muscle, lung, liver, brain and ND7/23 cell samples and GSPT1 is predominant in the testis sample although still detected in some of the other tissues. This pattern of expression for GSPT2 corresponds to the published analysis of mRNA levels detected in different tissues (Hoshino *et al*, 1998). These data indicate that both CCT and GSPT1/2 are expressed in the same tissue types as CCT, a positive indicator that these proteins could come into physical contact with each other *in vivo*.

5.2.2 Demonstration of a physical interaction between CCT subunits and GSPT1/2

As in chapter 4, immunoprecipitation was used as a means to demonstrate a direct interaction between CCT and GSPT1/2. In this instance, the CCT antibodies were raised in guinea pig and antibody against GSPT1/2 was raised in rabbit (see chapter 3). Again this was to prevent antibody bands from being detected on the resultant blots.

Antibodies were raised in guinea pig against KLH-coupled synthetic peptides with the sequence of the C-terminus of the mouse CCT subunits. These were used to IP the CCT complex from ND7/23 cell lysate. Samples were electrophoresed (on SDS-PAGE), western blotted and the blots probed for GSPT1/2 with antibody raised in rabbit against the C-terminus of GSPT1/2 (see section 2.7). In the same way, IPs from radiolabelled cell lysate were produced in order to show the diversity, sizes and numbers of other proteins co-immunoprecipitated with the CCT subunits.

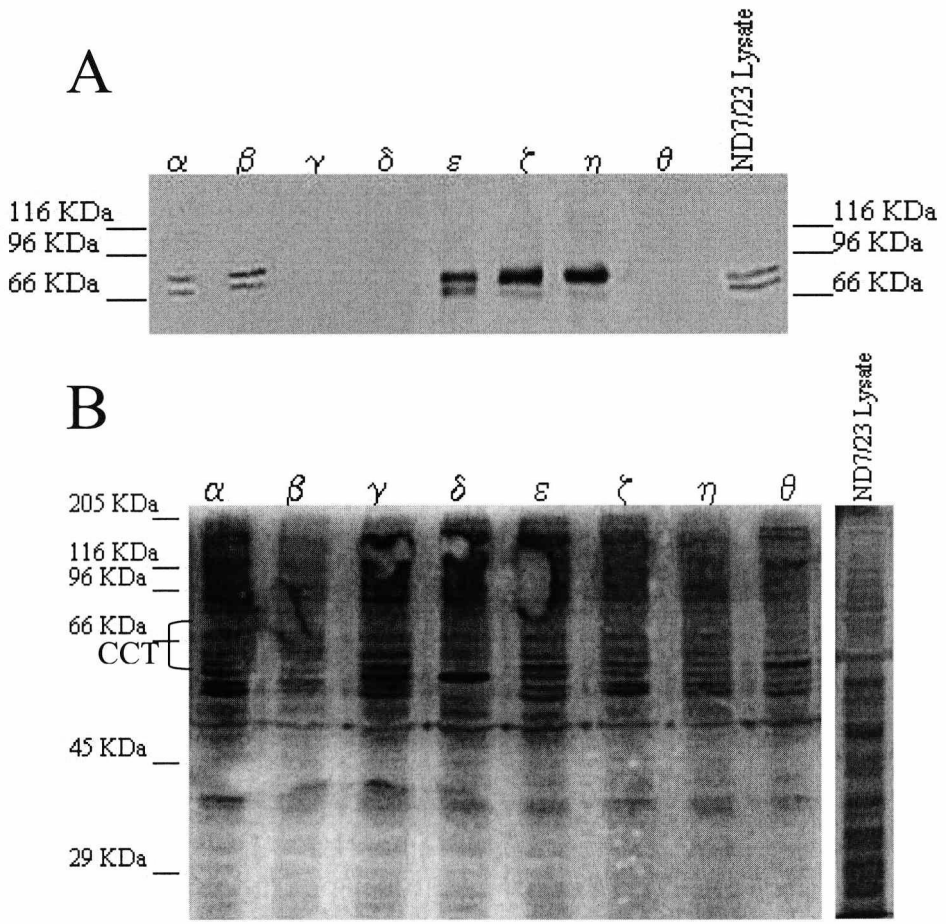

Figure 5.4 (**A**) Western blots of immunoprecipitated CCT from ND7/23 cell lysates. Guinea pig antibodies raised against the C-terminus of the mouse CCT subunits were used to immunoprecipitate CCT from whole cell lysate. The immunoprecipitate was then electrophoresed by SDS-PAGE (30mA, 1hr), western blotted (750mA, 1hr, 4°C) and probed with a rabbit antibody raised against the C-terminus of GSPT1/2.
(**B**) Autoradiographs of immunoprecipitated CCT from ND7/23 cell lysates. Guinea pig antibodies raised against the C-terminus of the mouse CCT subunits were used to immunoprecipitate the CCT complex from whole cell lysate labeled with [^{35}S] methionine and [^{35}S] cysteine. The immunoprecipitate was then electrophoresed by SDS-PAGE (30mA, 1hr), stained with Coomassie brilliant blue, dried (70°C, 90min, medium ramp) and incubated with autoradiography film (7 days, room temperature).

Figure 5.4B shows an autoradiograph of immunoprecipitated CCT from [^{35}S] radiolabelled ND7/23 cell lysate. The typical CCT ladder is clearly visible in all of the immunoprecipitations except when the anti-CCT δ antibody is used. This antibody is known to only precipitate the CCT δ subunit and not the entire complex (Roobol & Carden, 1999). This is likely because the C-terminus of the δ subunit is buried when the subunit is in the complex and this may be because the C-terminus of the δ subunit is the shortest of the CCT subunits when an alignment is performed

(using Multalign; http://cbrg.inf.ethz.ch/Server/MultAlign.html, data not shown). Several other bands can be seen in all of the immunoprecipitations, which could represent both substrate and interacting proteins.

Figure 5.4A shows the western blot of immunoprecipitated CCT subunits from ND7/23 cell lysate. The blot was probed with the anti-GSPT1/2 antibody. It can clearly be seen that both GSPT1 and GSPT2 are detected in some of the IPs. It is also noted that although these two proteins are detected at clearly different levels they are both present in all of the positive IPs. GSPT2 appears to be the more abundant of the two proteins and this is especially evident in the ε, ζ and η targeted Ips. Interestingly these data are similar to those in chapter 4, where the yeast CCT proteins are immunoprecipitated and probed with anti-Sup35p antibodies, in that the eRF3 is detected in the equivalent subunit targeted IPs (i.e. Cct1p, Cct2p, Cct5p, Cct6p and Cct7p). However, this is only the case when the N-terminal domain of the Sup35p protein is missing.

Further these data suggest that GSPT1/2 are not interacting with the whole CCT complex since it should appear in all of the IPs, except CCTδ where the antibodies do not precipitate the whole complex due to epitope accessibility, but only access free subunits. Alternatively the binding of the anti-CCTγ and θ antibodies may displace GSPT1/2 from the CCT complex.

5.2.3 Influence of ATP on CCT subunit/GSPT1/2 interaction.

As previously stated, in the presence of physiological concentrations of potassium and ATP it has been shown that the CCT complex undergoes partial disassembly in mammalian systems (Roobol *et al*, 1999) and it is generally agreed that bound

substrate is released in the presence of ATP (Quaite-Randall *et al*, 1995). Therefore the immunoprecipitations were carried out as above in the presence of 2mM ATP and 140mM KCl to determine if the interaction between mammalian CCT and GSPT1/2 was substrate-like or whether it was similar to that in the yeast system (see chapter 4).

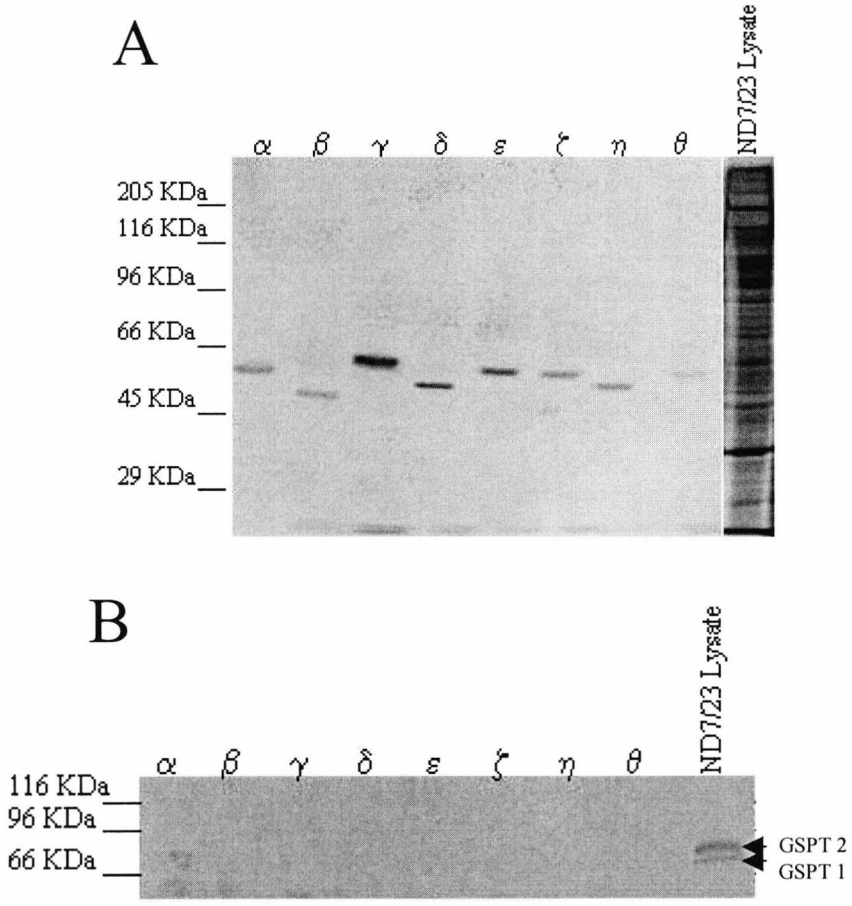

Figure 5.4 (**A**) Autoradiographs of immunoprecipitated CCT from ND7/23 cell lysate. Guinea pig antibodies raised against the C-terminus of the mouse CCT subunits were used to immunoprecipitate the CCT complex from whole cell lysate labeled with [^{35}S] methionine and [^{35}S] cysteine, in the presence of 2mM ATP and 140mM KCl. The immunoprecipitate was then electrophoresed by SDS-PAGE (30mA, 1hr), stained with Coomassie brilliant blue, dried (70°C, 90min, medium ramp) and incubated with autoradiography film (7 days, room temperature).
(**B**) Western blots of immunoprecipitated CCT from ND7/23 cell lysates. Guinea pig antibodies raised against the C-terminus of the mouse CCT subunits were used to immunoprecipitate the CCT complex from whole cell lysate in the presence of 2mM ATP and 140mM KCl. The immunoprecipitate was then electrophoresed by SDS-PAGE (30mA, 1hr), western blotted (750mA, 1hr, 4°C) and probed with a rabbit antibody raised against the C-terminus of GSPT1/2.

Figure 5.4A shows the autoradiograph of CCT subunits precipitated from whole cell lysate in the presence of ATP. This clearly shows that only individual CCT subunits are precipitated in the presence of ATP although the amount of subunit brought down varies from subunit to subunit with CCT γ being the most efficiently precipitated.

As can clearly be seen from figure 5.4B, when ATP is present in the IP mixture, no GSPT1/2 is detected, even though, under these conditions, targeted CCT subunits of CCT IP (figure 5.4A; Roobol *et al*, 1999). This is as chapter 4 and indicates that the presence of ATP and potassium disrupts the interaction of CCT and GSPT1/2, as seen in figure5.4B, and indicates the interaction in the two systems may be similar in that either GSPT1/2 is a substrate of CCT and in the presence of ATP and potassium it is released as the CCT complex disassembles, or, that the major conformational changes that occur in the CCT complex during ATP hydrolysis (Llorca *et al,* 1998) may simply disrupt any interaction. This also indicates that, like Sup35p, GSPT1/2 likely makes contact with the CCT subunits in their apical domains, as their conformational changes are the greatest during the hydrolysis of ATP (Llorca *et al,* 1998).

5.2.4 Influence of RIPA detergents on CCT subunit/GSPT1/2 interaction.

As in chapter 4 the IPs were carried out under mildly denaturing (RIPA) conditions. As previously stated, in the presence of RIPA conditions, in mammalian cells, it has been shown that the CCT complex is disrupted into its individual subunits (Roobol & Carden, 1999). However, the subunit-subunit interaction is weaker than the subunit-substrate interaction and therefore substrate can remain bound to specific CCT subunits and it is thought that these are the specific subunits to which that substrate

binds in the whole complex (Hynes & Willison, 2000). The presence of GSPT1/2 in these IPs would infer that the interaction is a strong one and may indicate GSPT1/2 as a substrate of CCT.

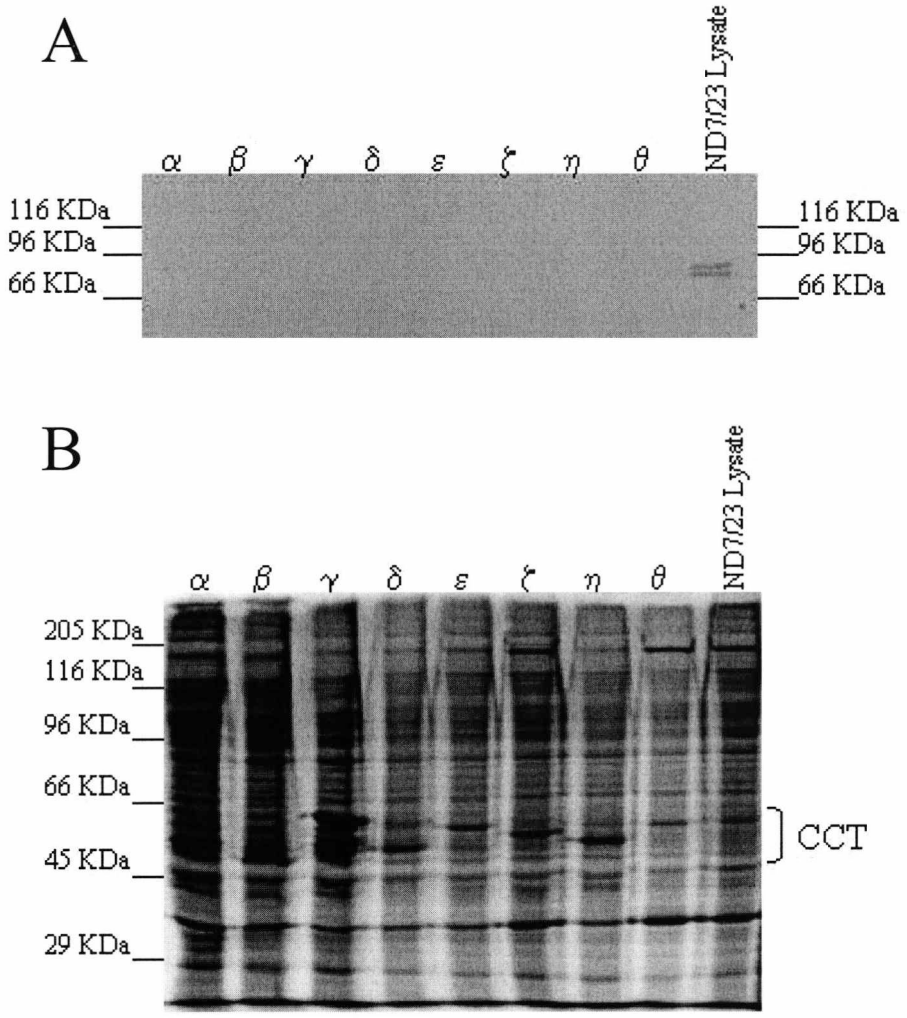

Figure 5.5 (**A**) Western blots of immunoprecipitated CCT from ND7/23 cell lysate. Guinea pig antibodies raised against the C-terminus of the mouse CCT subunits were used to immunoprecipitate the CCT complex from whole cell lysate in the presence of RIPA conditions (1% Triton-X100, 1% Na deoxycholate and 0.1% SDS). The immunoprecipitate was then electrophoresed by SDS-PAGE (30mA, 1hr), western blotted (750mA, 1hr, 4°C) and probed with a rabbit antibody raised against the C-terminus of GSPT1/2.
(**B**) Autoradiographs of immunoprecipitated CCT from ND7/23 cell lysate. Guinea pig antibodies raised against the C-terminus of the mouse CCT subunits were used to immunoprecipitate the CCT complex from whole cell lysate labeled with [^{35}S] methionine and [^{35}S] cysteine, in the presence of RIPA conditions (1% Triton-X100, 1% Na deoxycholate and 0.1% SDS). The immunoprecipitate was then electrophoresed by SDS-PAGE (30mA, 1hr), stained with coomassie brilliant blue, dried (70°C, 90min, medium ramp) and incubated with autoradiography film (7 days, room temperature).

Figure 5.5B shows the resultant autoradiograph when whole, labelled, ND7/23 cell lysate is immunoprecipitated in the presence of RIPA conditions (1% Triton-X100, 1% Na deoxycholate and 0.1% SDS). Again single subunits are present in the samples, however, there are also a number of other bands present on the autoradiograph. This is especially noticeable in the α, β, and γ samples where there also appears to be the presence of other CCT subunits. This may indicate that these subunits remain bound to a number of proteins, including other CCT subunits, under these conditions.

Once again, figure 5.5A shows that there is no interaction between CCT subunits and GSPT1/2 under RIPA conditions, as no GSPT1/2 is detectable on the immunoblots when carried out under these conditions.

These data suggest that the GSPT1/2 interaction with CCT is not a substrate-like interaction even though the ATP conformation of CCT does not bind GSPT1/2 either. As is the case of Sup35p, GSPT1/2 appears to be a CCT-associated protein rather than a substrate and the evidence is more consistent with the interaction being with CCT micro-complexes or ribosome associated CCT. This evidence implies that the interaction in both yeast and mammalian cells is similar and serves a similar purpose.

5.2.5 Sucrose gradient analysis

Sucrose gradients are an important first step in the purification of the CCT complex from crude cell lysates. The CCT is easily identified in the 26S (the central 3-4 fractions) part of the gradient. However when western blots of sucrose gradient fractions are probed with antibody against CCT subunits, a signal is also detected in

both lighter and heavier fractions due to sub-16mer assemblies (micro-complexes), 'free' subunits and larger complexes e.g. with ribosomes or cytoskeleton. It was therefore decided to probe sucrose gradient fractions for CCT subunits and GSPT1/2 to identify fractions that contained both these proteins.

ND7/23 cell lysate was loaded onto 10-40% sucrose gradients and centrifuged (85000g, 4°C, 18hr, acceleration setting 7, deceleration setting 0, Beckman SW40 or SW28 swing out rotor, Beckman L8-70M ultracentrifuge). The gradients were then fractionated into 24 fractions and the pellet resuspended. Each of these fractions were electrophoresed by SDS-PAGE and western blotted. These blots were then probed with antibodies against the CCT subunits α, β and γ and GSPT1/2.

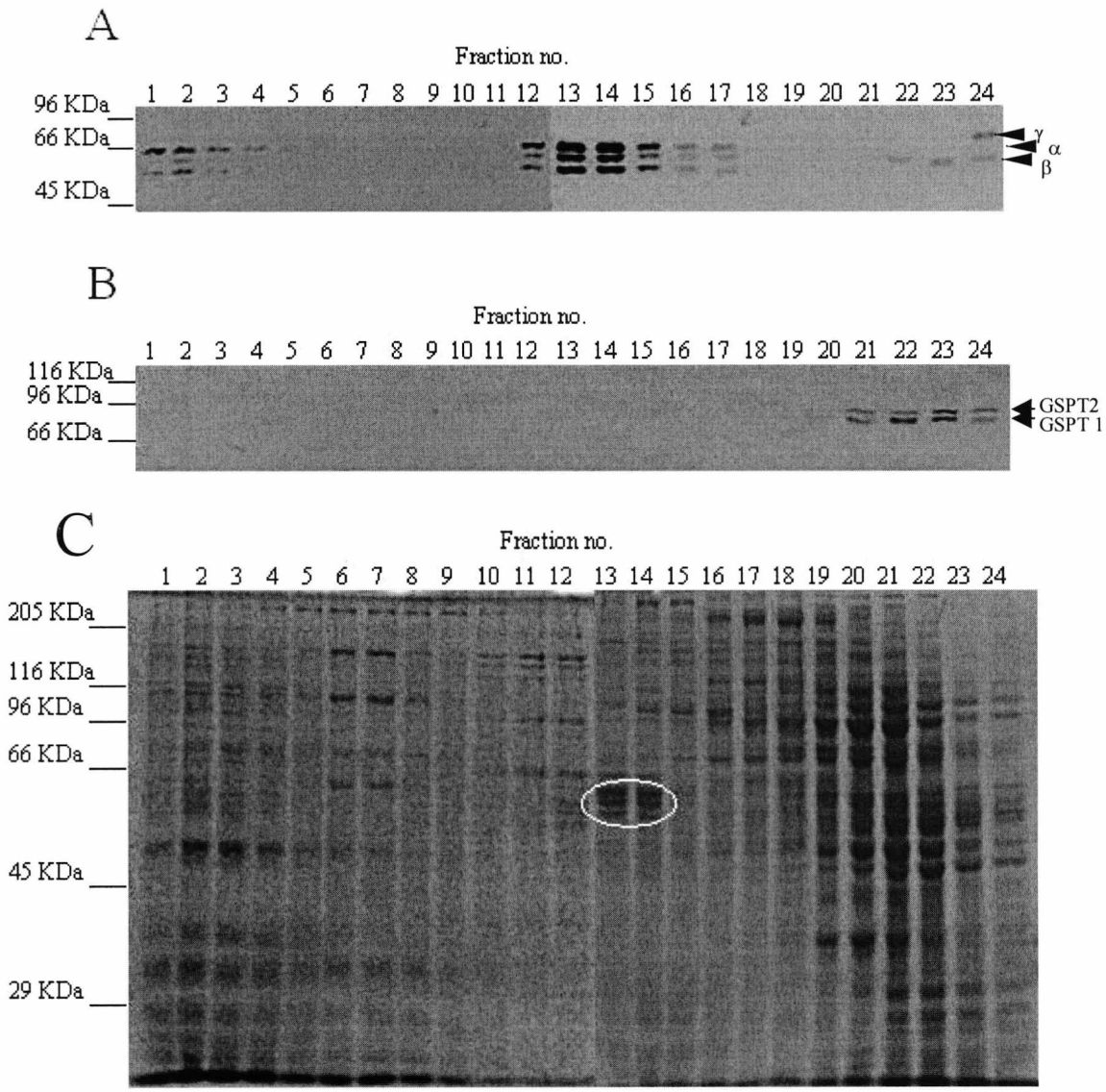

Figure 5.6 Western blots of sucrose gradient fractions of ND7/23 cell lysate. ND7/23 cell lysate was centrifuged (25000rpm, 4°C, 18hr, acceleration setting 7, deceleration setting 0, Beckman SW40 or SW28 swing out rotor, Beckman L8-70M ultracentrifuge) through a 10-40% sucrose gradient. The gradients were then fractionated and electrophoresed by SDS-PAGE (30mA, 1hr); western blotted (750mA, 1hr, 4°C) and probed with antibodies raised against the C-terminus of mouse CCTα, β and γ subunits **(A)** and C-terminus of GSPT1/2 **(B)**.
(**C**) Coomassie Stained SDS-PAGE gels of sucrose gradient fractions of ND7/23 cell lysate. ND7/23 cell lysate was centrifuged (85000g, 4°C, 18hr, acceleration setting 7, deceleration setting 0, Beckman SW40 or SW28 swing out rotor, Beckman L8-70M ultracentrifuge) through a 10-40% sucrose gradient. The gradients were then fractionated and electrophoresed by SDS-PAGE (30mA, 1hr), stained with coomassie brilliant blue and photographed using the BioRad GelDoc Bioimaging system. The CCT 'ladder' has been circled.

Figure 5.6A shows a coomassie stained SDS-PAGE gels of the fractions obtained from fractionating ND7/23 cell lysate over a 10-40% sucrose gradient, with fraction 1 corresponding to the heaviest fraction. The CCT fractions can clearly be seen in

the central portion of the gradient. This represents the whole complex (Lewis *et al*, 1992). The fractions were then blotted and probed for representative CCT subunits and GSPT1/2.

As can be seen from figure 5.6A and 5.6B, the representative CCT subunits (α, β, and γ), chosen as they are easily distinguishable from each other, can be found in lighter fractions, indicating the presence of single subunits and micro-complexes. The figure also shows that both GSPT1 and GSPT2 are present in the lighter fractions indicating that it is found in the same fractions as the single subunits and micro-complexes of CCT but could not be detected where the whole complex is present. However, the proteosome inhibitor MG-132 was not present in these samples, therefore, although leupeptin (a proteosome inhibitor) was present, the GSPT1/2 may have been degraded.

Having identified fractions containing both CCT subunits and GSPT1/2 and the subunits with which GSPT1/2 interacts, IPs were carried out using antibodies raised in guinea pig against the C-terminus of those CCT subunits to 'pull down' the CCT subunits from the identified fractions. The samples were then electrophoresed and western blotted and probed with antibody raised in rabbit against the C-terminus of GSPT1/2.

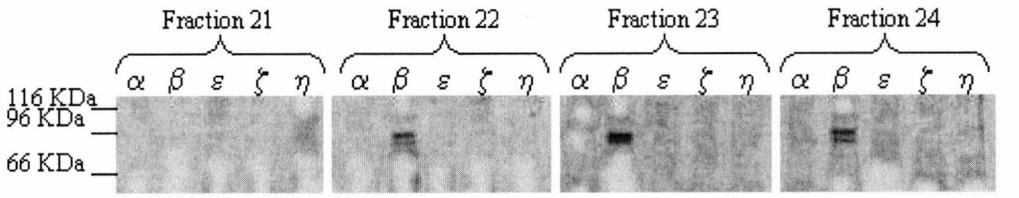

Figure 5.7 Western blots of immunoprecipitated CCT from sucrose gradient fractions containing both CCT subunits and GSPT1/2. Guinea pig antibodies raised against the C-terminus of the mouse CCT subunits were used to immunoprecipitate CCT subunits from sucrose gradient fractions. The immunoprecipitate was then electrophoresed by SDS-PAGE (30mA, 1hr), western blotted (750mA, 1hr, 4°C) and probed with a rabbit antibody raised against the C-terminus of GSPT1/2.

It can be seen from figure 5.7 that an interaction between only the β subunit of CCT and GSPT1 and 2 was detected in the lighter fractions of sucrose gradient fractionated ND7/23 cell lysate. This is surprising as when IPs are performed on whole lysate an interaction is detected with five different subunits, although the sucrose gradient fractions were only probed for the α, β and γ subunits, therefore it is possible that the other subunits were not present in the fractions tested and the data for the α subunit supports this. It is possible that only small amounts of GSPT1 and 2 are present in heavier fractions but are beyond the detection system used for immunoblots of whole fractions; when IPs from whole lysate are performed, the GSPT1/2 interacting with the complex is concentrated and therefore detectable. With hindsight, IPs should have been performed on the ribosomal fractions as it is possible that some interaction may occur in these fractions, also, the sucrose gradient fractions should have been probed for all of the CCT subunits to give a full picture of where the all the subunits fractionate. It can also be noted from figure 5.7 that the interaction with the β subunit in the fractions seems to be more pronounced with GSPT2 (larger band). This is interesting as it has been shown that GSPT2 more closely resembles the function of Sup35p in yeast and can substitute for this protein in yeast mutants (Hoshino *et al*, 1998, 1999; Le Goff *et al*, 2002) and that as previously shown (in chapter 4), [*psi-*] *S. cerevisiae* Sup35p in stationary phase interacts only with Cct2p (CCT β homologue).

5.2.6 I.M.A.G.E. clone sequencing

In order to examine the interaction of GSPT1 and 2 with CCT in reticulocyte lysate it was necessary to obtain clones of the *GSPT1* and *GSPT2* genes. Numerous attempts

were made to this end, including reverse transcription PCR (RTPCR) and 5' and 3' RACE (rapid amplification of cDNA ends) from several mouse tissues and cultured cells including the addition of a number of supplements to the reaction, PCR from DNA isolated from both mouse tissue and cultured cells and the probing of cDNA libraries from heart, intestine and brain. None of these avenues yielded full-length clones, despite the use of several different primers (data not shown).

This process was not made straightforward as the sequences published on the databases (accession numbers AB003502 and AB003503) by Hoshino *et al* (1998) did not match the sequence published in the Journal of Biological Chemistry by the same group. I therefore made the assumption that the sequences in the paper were correct as they had extended N-termini and better matched the yeast Sup35p sequence. To this end I mined the mouse EST database for the missing N-terminal sequences, which were present in both the case of *GSPT1* and *GSPT2*. During this process I came across references to the I.M.A.G.E. consortium.

Two of the ESTs that matched the N-terminal sequences (one for each gene) had I.M.A.G.E. numbers (GSPT1; 533932 and GSPT2; 586105) meaning that they were available from the consortium. As the I.M.A.G.E. clones are originally isolated from cDNA libraries via olig(dT)-priming and sequenced from the 5' end when submitted to the databases, it seemed logical to assume that these clones could be the full length genes. These clones were then ordered and sequenced.

```
1       GAGATCCTTTCGCACACACGAGGAGGGTTGAGCCGCTGTCGACCTGGTCTCGAGTGTACT
61      GTCTGGACTGTAGCTGCTGCCCAGGACGCCGGCGAGTGAGTCATTGACTGTCAGCTCCCC
121     AGTCTTGCCGTCCTCCCCGGGTCAGCGCGGCCTGCTCCTCCCCGGTCGGCCGCCCCCGCC
181     TCCATTTCCCGCCCTCTCTTCACCACACACACGGCCCCCCCGATCATGGATCCTAGCAGC
241     GGCGGTGGCGGCGGTGGCGGCGGCGGCGGGAGCAGCAGCAGCGACTCTGCGCCCGAC
301     TGCTGGGACCAGACGGATATGGAGGCCCCCGGGCCCGGGCCTTGCGGCGGCGGCGGGAGC
361     GGCAGCGGCTCCATGGCCGCGGTGGCCGAGGCCCAGCGTGAGAACCTCAGCGCGGCTTTC
421     AGCCGGCAACTCAACGTCAACGCCAAGCCTTTCGTCCCCAACGTCCACGCCGCTGAATTC
481     GTGCCGTCCTTCCTGCGGGGTCCGGCCCAGCCGCCGCTATCCCCAGCTGGCGCAGCCGGA
541     GGCGACCACGGAGCAGGCAGCGGCGCGGGAGGCCCTTCGGAACCTGTAGAGTCCTCTCAA
601     GACCAGTCGTGTGAAGGTTCAAATTCTACTGTTAGCATGGAACTTTCAGAACCTGTTGTA
661     GAAAATGGAGAGACAGAAATGTCCCCAGAAGAATCATGGGAGCACANAGAANAAATAAGT
721     GAAAAAAAAAAAA
```

Figure 5.8 Sequence of the I.M.A.G.E. clone 533932. This clone is identical (when translated) to the N-terminus (long) of GSPT1. Sequencing primers are shown highlighted. Start codon is coloured blue and areas rich in adenine bases are shown in green.

Figure 5.8 shows the sequence of I.M.A.G.E. clone 533932, which has the same N-terminus (when translated) as the long form of mouse GSPT1. This sequence is the full length of the insert and this is not the full-length gene. The 3'end of the original mRNA must contain a region rich in adenine bases (see figure 5.8) which could have caused oligo(deoxyThymine)-primer binding at this internal site rather than at the poly(A) tail in the initial generation of the mouse macrophage cDNA library.

```
1     CCGCGGTGGCGGCCGCTCTAGAACTAGTGGATCCCCCGGGCTGCAGGAATTCGGACGAGG
61    CAGCATCTGCGCTTAGCTGCCTCCGCGCCGCTAAGGTTCGCGTCGCTCGCCCGTGGCCCG
121   TGGCTGTTCCTGCCTTACTACCACCGGTAGAACCCTCTCCTCCTGACCTGCCTACCTCGC
181   TCCTTCTCCGCCGCACCCCGGCTGCTCACACCATGGATCTCGGCAGCAGCAGCGACTCGG
241   CTCCCGACTGCTGGGATCAGGTGGACATGGAAGCCCCGGGTTCGGCTCCGAGCGGGGATG
301   GAATCGCCCCCGCAGCCATGGCAGCGGCTGAGGCCGCGGAAGCCGAGGCCCAGCGCAAGC
361   ATCTCAGCTTGGCCTTCAGCAGTCAGCTCAACATCCACGCCAAACCTTTCGTGCCTAGCG
421   TAAGCGCAGCGGAGTTCGTGCCGTCCTTCCTGCCTGGATCGGCCCAGCCGCCCGCCCCCA
481   CAGCCTCCAGCTGCGACGAAACCTGCATCGGTGGCGCCGGGGAGCCTGAAGGTAAACGGA
541   TGGAATGGGGAGCACCTGTAGAACCTTCCAAAGATGGCCCTTTAGTGTCGTGGGAGGGTT
601   CCAGTTCAGTTGTTACCATGGAACTTTCAGAACCTGTTGTAGAAAATGGAGAGGTGGAGA
661   TGGCCCTAGAAGAATCTTGGGAGCTTAAAGAAGTGAGTGAAGCAAAGCCTGAGGCTTCTT
721   TGGGAGATGCAGGGCCCCCAGAAGAAAGTGTCAAGGAAGTGATGGAGGAGAAAGAGGAAG
781   TAAGGAAATCAAAATCTGCGTCCATACCATCAGGTGCACCTAAGAAAGAACACGTAAATG
841   TGGTCTTCATTGGGCATGTGGATGCTGGCAAGTCAACCATTGGAGGACAAATAATGTTTT
901   TGACAGGAATGGTTGACAGAAGGACACTTGAGAAATACGAACGAGAAGCTAAGGAGAAGA
961   ATAGAGAGACCTGGTACTTGTCCTGGGCCTTAGATACAAACCAGGAAGAACGAGACAAGG
1021  GTAAAACAGTGGAAGTGGGCCGTGCGTATTTTGAAACGGAAAAGAAGCATTTCACAATCC
1081  TAGATGCCCCTGGCCACAAGAGTTTTGTCCCAAATATGATTGGCGGTGCCTCTCAAGCCG
1141  ATTTAGCTGTGCTGGTGATCTCTGCCAGGAAAGGGGAATTTGAGACTGGATTTGAAAAAG
1201  GTGGACAGACAAGAGAACATGCAATGCTGGCCAAAACAGCAGGGGTAAAATACTTAATAG
1261  TGCTTATTAATAAGATGGATGACCCCACAGTAGATTGGAGCAGTGAGCGATATGAAGAAT
1321  GTAAAGAAAAACTGGTGCCCTTTTTGAAAAAAGTTGGTTTCAGTCCAAAAAAGGACATTC
1381  ACTTTATGCCCTGCTCAGGACTGACTGGAGCAAATATTAAAGAGCAATCTGATTTCTGTC
1441  CTTGGTACACCGGATTACCATTTATTCCGTATTTGGATAGTTTGCCAAACTTCAACAGAT
1501  CAATTGATGGGCCAATTAGGTTGCCAATTGTGGATAAGTACAAGGATATGGGCACTGTGG
1561  TCCTGGGTAAGCTGGAATCAGGATCCATTTTTAAAGGCCAGCAGCTTGTGATGATGCCAA
1621  ACAAGCACAGTGTGGAAGTTCTAGGAATCGTTTCTGATGATGCCGAGACTGATTTTGTAG
1681  CTCCAGGTGAAAACCTCAAAATCAGACTGAAAGGGATTGAAGAGGAAGAGATTCTTCCAG
1741  GCTTCATACTTTGTGAACCCAGTAATCTTTGCCATTCCGGACGCACATTTGATGTTCAGA
1801  TAGTGATCATTGAGCACAAGTCTATCATCTGCCCAGGTTATNATGCGGTGCGGCACATTC
1861  ATACTTGTATTGAGGAGGTTGAAATAACAGCCTTGATCTCCTTAGTAGACAAAAAGTCAG
1921  GAGAAAAAAGCAAGACACGGCCCCGCTTTGTGAAGCAAGACCAAGTGTGCATTGCCCGGT
1981  TAAGGACAGCAGGAACTATCTGCCTGGAGACATTTAAAGATTTTCCTCAGATGGGTCGTT
2041  TTACTTTAAGAGATGAGGGTAAAACAATCGCCATTGGAAAAGTTCTGAAGCTGGTCCCAG
2101  AGAAGGACTAAGCAATCTCTTTTGATGCCTCTGCACCATAATGTGTGAAAGATTGACCGC
2161  AACCTACTGCCCATTGACAAACTTGTGCCCATATTTTGCAGAGAAATTTCACAGCAAAAA
2221  TCCACGTGTTGTCAGCTTTCTCATGTTGAGACTTCAGTCGTGTCACTCCTGAATGCATAC
2281  TCCAGTTTCCTCCCTCTATAGCACTCTGCTTCCTTGGACAAATCAGTAATAGCTTTGTAA
2341  GTGATGTGTGTGTAATTGCCTACAGTCCTAAAAAGAATATATTTTAAAGTTTTCATTTCC
2401  GTTTGGGATATCTAGACATCCTTTGTTCTGTGGGGAACAGTCAGTGTTGGTGTGTGTATA
2461  TGTTGAAGATAACTAACATGTAAATAAAACGTTGCGTTTGAAACTTCAAAAAAAAAAAAA
2521  AAAAACTCGAGGGGGGCCCGGNCCCAATTG
```

Figure 5.9 Sequence of the I.M.A.G.E. clone 586105. This clone is identical (when translated) to the full length (long) GSPT2. Sequencing primers are shown highlighted. Start codon is coloured blue and the stop codon is shown in red, with the poly(A)-signal sequence in pink.

Figure 5.9 shows the sequence of I.M.A.G.E. clone 586105, which has the same N-terminus (when translated) as the long form of mouse GSPT2. This sequence is the full length of the insert and is the full-length gene obtained from mouse heart cDNA library, containing both start and stop codons as well as poly(A)-signal sequence and partial poly(A)-tail.

When originally cloned into pBluescript SK- vector, the expression of the clone was under T3 promotor control and in order to carry out *in vitro* transcription/translation analysis the gene was sub-cloned into pBluescript KS- utilising the Xho1 and EcoR1 restriction sites (data not shown) so that the clone was under T7 promotor control (pUKC2302).

5.2.7 *In vitro* transcription/translation

The rabbit reticulolysate system is another useful tool for determining interactions with CCT. As shown in chapter 4, yeast Sup35p shows an interaction with mammalian CCT present in reticulocyte lysate. Therefore an interaction between the mammalian GSPT2 and CCT in the lysate seemed likely. If the GSPT2 protein is a substrate then, following the chase with ATC (see chapter 4), the CCT band on the autoradiograph would be seen to decrease in intensity over time. However, if the GSPT2 is associated with CCT in some other way then the band will not decrease.

The transcription/translation reaction was initiated by plasmid addition and warming to 30°C and allowed to continue for 30min before the addition of 8μM ATC to half of the reaction mixture. Samples were taken every 10 min for 80min and then electrophoresed over both SDS PAGE and native PAGE. The gels were stained with coomassie brilliant blue and dried before being autoradiographed.

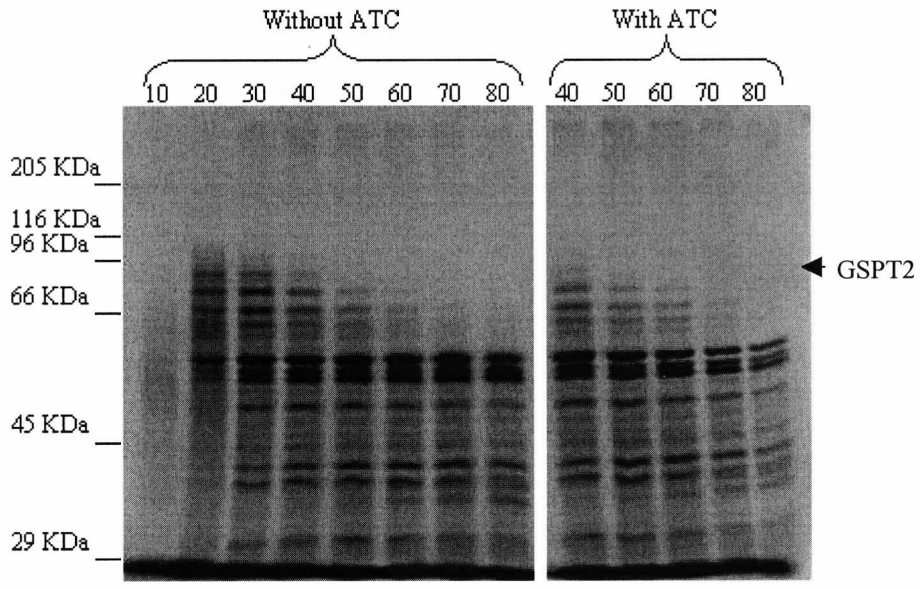

Figure 5.10 Autoradiograph of SDS-PAGE gel of *in vitro* transcription/translation reaction samples of GSPT2. T7 driven plasmid was used in a rabbit reticulocyte in vitro transcription/translation reaction, after 30 min half the reaction was made 8μM with respect to aurintricarboxylic acid and the reaction continued for a further 50min. Samples (taken every 10min) were then electrophoresed by SDS PAGE, stained with coomassie brilliant blue, dried and autoradiographed.

As can be seen from figure 5.10, the protein produced in this reaction decreased in size over time in a manner that suggests that it is being broken down. The reaction was therefore repeated containing 10μg/ml Leupeptin, a protease inhibitor efficient against the proteosome, in order to prevent breakdown of the protein in the reticulocyte lysate, as MG-132, another proteosome inhibitor, was found to prevent the breakdown of Sup35p in [*psi-*] yeast. However, the addition of Leupeptin resulted in the complete inhibition of the transcription/translation reaction. When the experiment was repeated containing 200μM MG-132, similarly the reaction was inhibited completely. However, without either of the inhibitors present an interaction with CCT can be seen on the native gel, although these data cannot be used to determine flux through CCT due to the breakdown of the sample seen in figure 5.10.

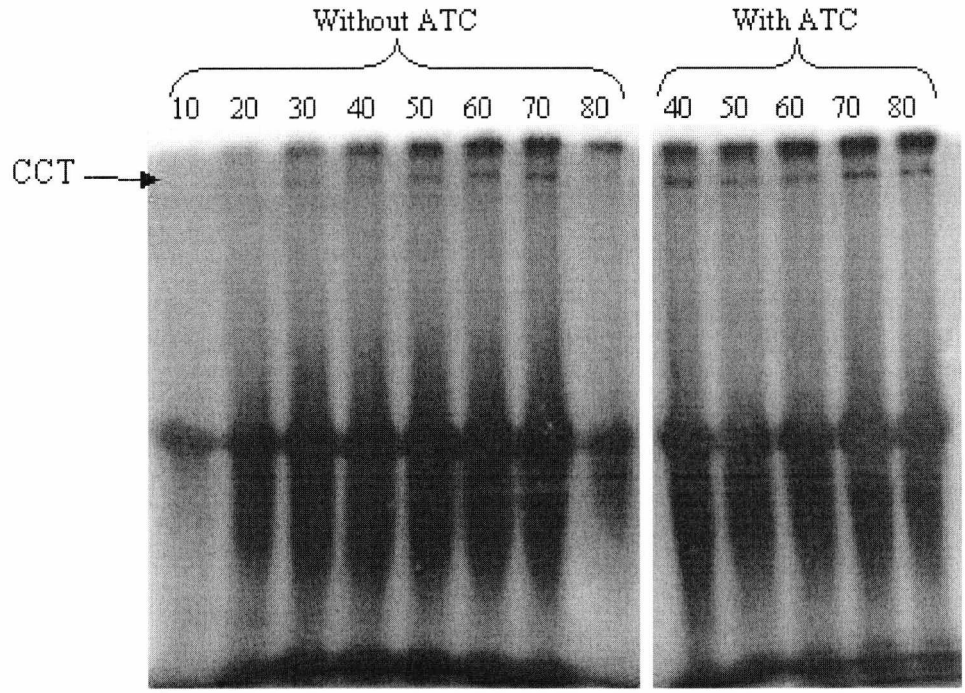

Figure 5.11 Autoradiograph of native PAGE gels of *in vitro* transcription/translation reaction samples of GSPT2. T7 driven plasmids were used in rabbit reticulocyte *in vitro* transcription/translation reactions, after 30 min half the reaction was made 8μM with respect to aurintricarboxylic acid and the reaction continued for a further 50min. Samples (taken every 10min) were then electrophoresed by native PAGE, stained with coomassie brilliant blue, dried and autoradiographed.

As can be seen from figure 5.11, the GSPT2 protein does interact with CCT in reticulocyte lysate. What is not clear is whether this interaction is with the full-length protein or breakdown products. Although as the CCT band is still visible when no full length GSPT2 is detected it is suggestive that the CCT is interacting with breakdown products of GSPT2 and this could also suggest that a particular region or sequence of GSPT2 interacts with the CCT or simply that the breakdown products of GSPT2 are recognised by CCT as misfolded protein.

5.2.8 Immunocytochemistry

Immunocytochemistry allows the location of proteins to be determined within a cell and by using two different fluorophores attached to the secondary antibodies it allows the location of two proteins to be determined within the same cell and areas of co-localisation to be determined.

ND7/23 cells were grown on glass cover slips before being fixed, permeabilised, blocked in BSA and incubated with a combination of either CCTβ (guinea pig) and GSPT1/2 (rabbit) or actin (mouse) antibodies. The secondary antibodies used had either rhodamine (anti-rabbit) or fluorescein (anti-guinea pig and anti-mouse) conjugated to them to distinguish between the labelling of the two proteins.

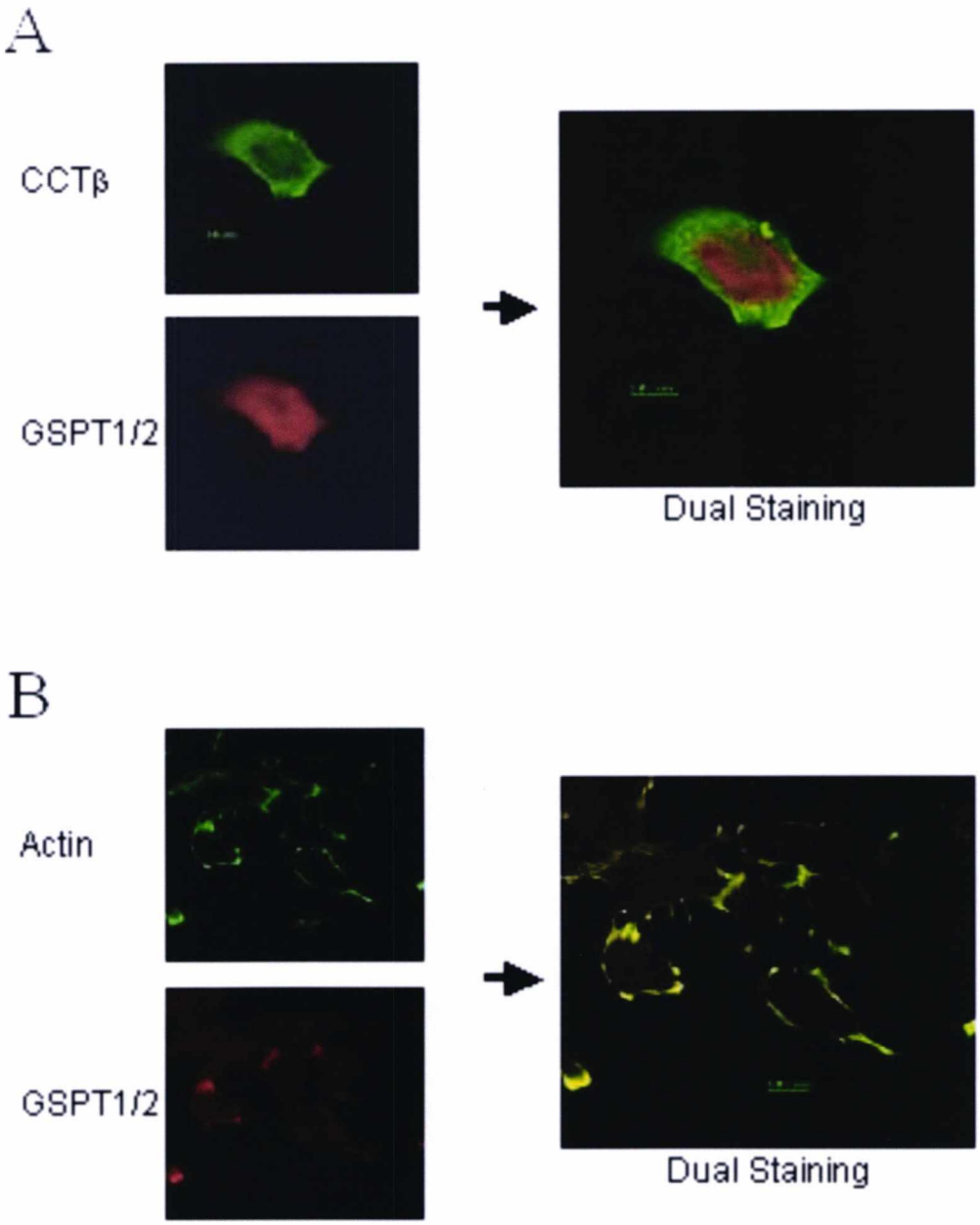

Figure 5.12 Immunocytochemistry of GSPT1/2 and either CCTβ (A) or actin **(B)**. ND7/23 cells were grown on glass cover slips in 24 well Costar plates. The cells were then fixed, permeabilisedblocked in BSA and incubated with either a combination of CCTβ antibody raised against the C-terminus in guinea pig and GSPT1/2 antibody raised against the C-terminus in rabbit or actin monoclonal (AC15) antibody raised in mouse and GSPT1/2 antibody raised against the C-terminus in rabbit. After incubation with secondary antibody conjugated to either rhodamine (anti-rabbit) or fluorescein (anti-guinea pig and anti-mouse), cells were viewed and recorded using a confocal microscope (Leica TCS 4D) (Leica, Bensheim, Germany).

Figure 5.12 shows immunostaining of ND7/23 cells with antibodies directed against the C-terminus of GSPT1/2 and CCT β subunit and actin monoclonal antibody (clone AC15). It can be seen that there are areas of dual staining (yellow in the dual stain) indicating some co-localisation of the two proteins within the cell. This is important as it indicates that in living cells the two proteins come into close proximity with each other giving them a chance to interact in vivo. It is also evident that most of the dual staining for GSPT1/2 and CCTβ occurs around the periphery of the nucleus and GSPT1/2 also shows obvious staining in the nucleus, which in these cells is horseshoe shaped and easily recognisable. Originally, the actin stain was used as a positive control to ensure that the method was successful, however, as can be seen from the dual stain, the actin also indicated some co-localisation with GSPT1/2 at the periphery of the cell. This has previously not been shown and led to the possibility that actin mediates the dual stains of CCT and GSPT1/2. However, this was considered unlikely as the interaction between GSPT1/2 and actin was in a completely different part of the cell when compared to the GSPT1/2/CCTβ dual stain. It has been shown that ribosomes programmed with actin mRNA are located to the actin rich edge of cells (Sundell & Singer, 1990) and this could indicate that GSPT1/2 may associate with ribosomes engaged in actin/tubulin synthesis and this could therefore tie in with the proposed cell cycle role of GSPT1/2 (Kikuchi *et al*, 1988).

In order to define whether actin was a mediatory protein, IPs with the CCT subunits were performed, western blotted and probed for actin. If actin was acting as an mediatory protein then it would be expected that actin would be detected in the same IPs as GSPT1/2.

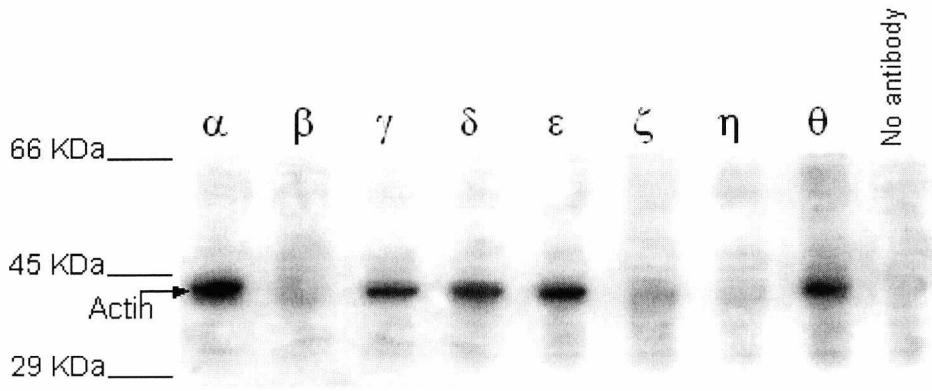

Figure 5.13 Western blots of immunoprecipitated CCT from ND7/23 cell lysates. Guinea pig antibodies raised against the C-terminus of the mouse CCT subunits were used to immunoprecipitate the CCT from whole cell lysate under non-denaturing conditions. The immunoprecipitate was then electrophoresed by SDS-PAGE (30mA, 1hr), western blotted (750mA, 1hr, 4°C) and probed with a mouse monoclonal antibody raised against actin (clone C4).

As can be seen from figure 5.13, actin is not detected in all of the IPs that GSPT1 and 2 are detected in. Actin is detected in the CCT α, γ, δ, ε and θ Ips, whereas GSPT1 and 2 are detected in CCT α, β, ε, ζ and η IPs. It could be argued that actin could mediate the interaction between CCT α and ε as both proteins are detected in these IPs, however, it seems from the data presented, that CCT β is the most important subunit associated with GSPT1/2 and actin is not detected in this IP. It is also indicated here that actin is interacting with micro-complexes of CCT since, under these conditions, the β, ζ and η antibodies IP the whole complex and therefore actin would be expected in all of these IPs if its interaction with the whole complex were detected. Indeed it has been shown by Dr. Anne Roobol (unpublished data) that tubulin also interacts with micro-complexes of CCT, in that tubulin is detected in IPs of the CCT subunits in sucrose gradient fractions between where the 16mer and monomer proteins are detected. This is the case even when tubulin is not detected in immunoblots of the whole fractions indicating that it is concentrated in the IP.

5.3 Discussion

The evidence presented here clearly confirms an interaction between the CCT complex and GSPT1 and 2, with a more pronounced interaction occurring with GSPT2 rather than GSPT1. This interaction has not been predicted in mammalian cell but an interaction between the yeast homologues of these proteins has been predicted by functional algorithmic analysis (Eisenberg *et al,* 2000) and confirmed in this study (chapter 4).

Results from the immunoprecipitations show a strong interaction between some CCT subunits and GSPT1/2; however, this interaction was shown to be disrupted by ATP and strong detergent. The interaction with the CCT subunits is similar to that demonstrated between yeast CCT and Sup35p in that the interaction is detected under native conditions with the α (1), β (2), ε (5), ζ (6) and η (7) CCT subunits and not in the presence of ATP or strong detergents. This could mean that this interaction is not only conserved in evolution but that it may have a similar function in both species. These IP data also point to the relationship being between GSPT1/2 and CCT micro-complexes as the interaction does not include subunits which IP the whole CCT complex, this is supported when lysate is subjected to analysis by sucrose gradient fractionation, GSPT1/2 was not found in the central portion of the gradient which contains the whole CCT complex, but appears further up where micro-complexes and monomers are located. The IP data also indicates that GSPT1 and 2 are not substrates of CCT, as detergent is known to only disrupt non-substrate interactions (Hynes & Willison, 2000). ATP hydrolysis is a property of the CCT subunits and this process causes major conformational changes within the protein (Llorca *et al,* 1998). This could easily interrupt any interaction between CCT and GSPT1/2. A number of conserved domains involved in GTP binding have been

identified in GSPT1 and 2 (Hoshino *et al*, 1998), and it therefore seems that these proteins may have a similar GTPase activity to Sup35p (Nakamura & Ito, 1998), although Sup35p GTPase activity is only present when bound to Sup45p and the ribosome (Nakamura & Ito, 1998), and this may also cause the disruption of the interaction between CCT and GSPT1/2. This is using the assumption that ATP could substitute for GTP in these proteins. There is a precedent for these two molecules to be exchangeable in that GTP will replace ATP in CCT disassembly but greater quantities are required (Roobol *et al*, 1999).

The sucrose gradient analysis does demonstrate that GSPT1 and 2 are found in the some of the same fractions as the CCT subunits, although this is only in the lighter fractions containing only single subunits and micro-complexes. Of course small amounts of GSPT1/2 may be present in the heavier fractions but were just not identified by the method of detection (E.C.L.) used. When these lighter fractions were subjected to IP analysis using antibodies to the subunits shown to interact with GSPT1/2 in the previous IP analysis, GSPT1 and 2 were only detected in the CCT β IP indicating that GSPT1 and 2 associate only with this subunit when it is free of the complex and that interaction with the other subunits occurs when this subunit is included in sub-16mer complexes. Incidentally this evidence also indicates that the interaction between CCT β and GSPT1/2 is possibly through hydrophobic residues, as this interaction is not detected when CCT β is separated from the complex by detergent.

Detection of both CCT β and GSPT1/2 in cells by immunocytochemistry also indicates that these two proteins interact *in vivo*. The areas of co-localisation appear to be confined to an area surrounding the nucleus, where the rough endoplsmic reticulum is situated, this indicates that the interaction may have a role in protein

synthesis in this organelle. Interestingly an interaction between actin, one of CCTs substrates (Gao *et al*, 1992), and GSPT1/2 is also detected by immunostaining but only at the periphery of the cell. This developed the intriguing idea that actin acts as a mediatory protein between CCT and GSPT1/2. However, this interaction appeared in a different part of the cell when compared to the CCT β/GSPT1/2 interaction and when IPs of the CCT subunits were analysed for the presence of actin, it was seen that actin interacted with different subunits to GSPT1/2. The co-localisation with actin at the periphery of the cell adds further evidence that GSPT1/2 has a role in protein synthesis as it has been shown that ribosomes programmed with actin mRNA are located to the actin rich edge of cells (Sundell & Singer, 1990). This could indicate that GSPT1/2 may associate with ribosomes engaged in actin/tubulin synthesis and this could therefore tie in with the proposed cell cycle role of GSPT1/2 (Kikuchi *et al*, 1988) and may offer a reason for its interaction with CCT as a way of targeting the correct ribosomes for actin and tubulin production.

The interaction between GSPT1/2 and CCT has such parallels with the interaction detected in yeast that it is tempting to assume that the purpose of the interaction is the same. It seems then that the cellular process both proteins could have reason to interact in both organisms is that of protein synthesis. As previously stated, these proteins should not come into contact with each other as GSPT1/2 and especially GSPT2 as it has been shown to complement Sup35p mutations in yeast (Le Goff *et al*, 2002), would be associated with newly synthesized, unfolded, proteins in its role as part of the translation termination complex (Hoshino *et al*, 1998, 1999), and CCT is associated with more mature, partially folded, proteins (Llorca *et al*, 1999). However there have been reports based on cross-linking experiments that CCT associates with nascent peptide chains (McCallum *et al*, 2000; Dunn *et al*, 2001).

As for Sup35p, the evidence suggests that GSPT1/2 interacts with the CCT complex in a subunit specific manner, during protein synthesis, to facilitate the binding of nascent polypeptide chains to CCT for folding. The native IP of the ND7/23 cell lysate shows an interaction with CCT α, β, ε, ζ and η, when organized into a ring conformation with the order of subunits proposed for the complex (Liou & Willison, 1997), these subunits lie next to each other (see figure 5.14).

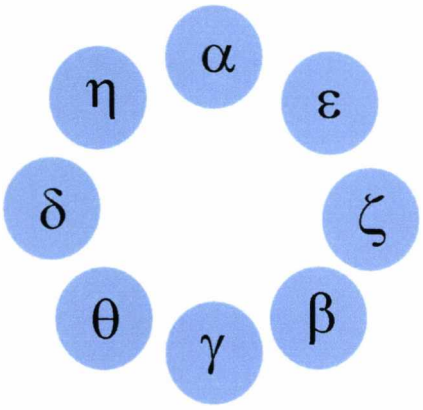

Figure 5.14 Order of subunits in the CCT complex as proposed by Liou & Willison, (1997)

This is the same orientation of subunits detected to interact with Sup35p in yeast and could therefore interact in a similar way to that proposed in chapter 4. In chapter 4 it was proposed that the binding of these subunits was inhibited by the presence of the free N-terminus of Sup35p and that binding to the whole complex was only possible when the N-terminus was either missing or bound to either itself (in the case of the aggregated [*PSI*$^{+}$] form of the protein) or to another, unidentified binding partner. In the absence of these conditions only binding to Cct2p (CCT β homologue) was found. This model still fits with the data presented in this chapter as the interaction between GSPT1/2 and the same CCT subunits is detected when the whole lysate is present, however, when fractionated, GSPT1/2 is only detected in the lighter fractions and is only found to interact with the CCT β subunit. This implies that only

a tiny amount of the GSPT1/2 present in the cell interacts with whole complex, binding in a similar manner to that in the ΔN Sup35p mutant of yeast but that the majority is interacting with CCT β alone. The proposal that Cct2p/CCT β acts as an anchor for Sup35p/GSPT1/2 and that it is this subunit that is involved in the stabilization of the interaction still holds true, although it now seems that the interaction with this subunit does not involve the whole CCT complex and that the interaction may be mediated by hydrophobic residues. The free N-terminal region of Sup35p/GSPT1/2 could still interfere with binding to the whole complex or may interfere with the binding of other subunits to Cct2p/CCT β to form the complete CCT complex, possibly in response to the ATPase induced conformational changes in the CCT or the GTPase activity of eRF3. As Sup35p only exhibits GTPase activity in the presence of Sup45p (eRF1) and the ribosome (Nakamura & Ito, 1998), it can be assumed that a similar system operates in the case of GSPT1/2, and one or both of these may also be present in the CCT/eRF3 complex. The involvement of the N-terminal domain of GSPT1/2 in the interaction also goes some way to explain the differences in the interaction between CCT and the two proteins as they differ maximally at their N-terminus and are relatively identical for the rest of their length (Hoshino *et al*, 1998). Just like Sup35p, GSPT1/2 have been shown to interact with poly(A)-binding protein (PABP) (Hoshino *et al*, 1999) and, in the case of GSPT2, this interaction is through the N-terminal domain associating with the C-terminal domain of PABP (Hoshino *et al*, 1999), similar to the interaction observed between yeast Sup35p and PABP (Cosson *et al*, 2002). This could indicate that PABP brings eRF3 into close proximity with the poly (A) region of the mRNA being translated, thus bringing the entire translation termination complex into the correct position to initiate translation termination (Cosson *et al*, 2002) in both yeast and mammalian

cells, and thus allowing CCT to interact with eRF3 and hence carry out its function as protein folding chaperone.

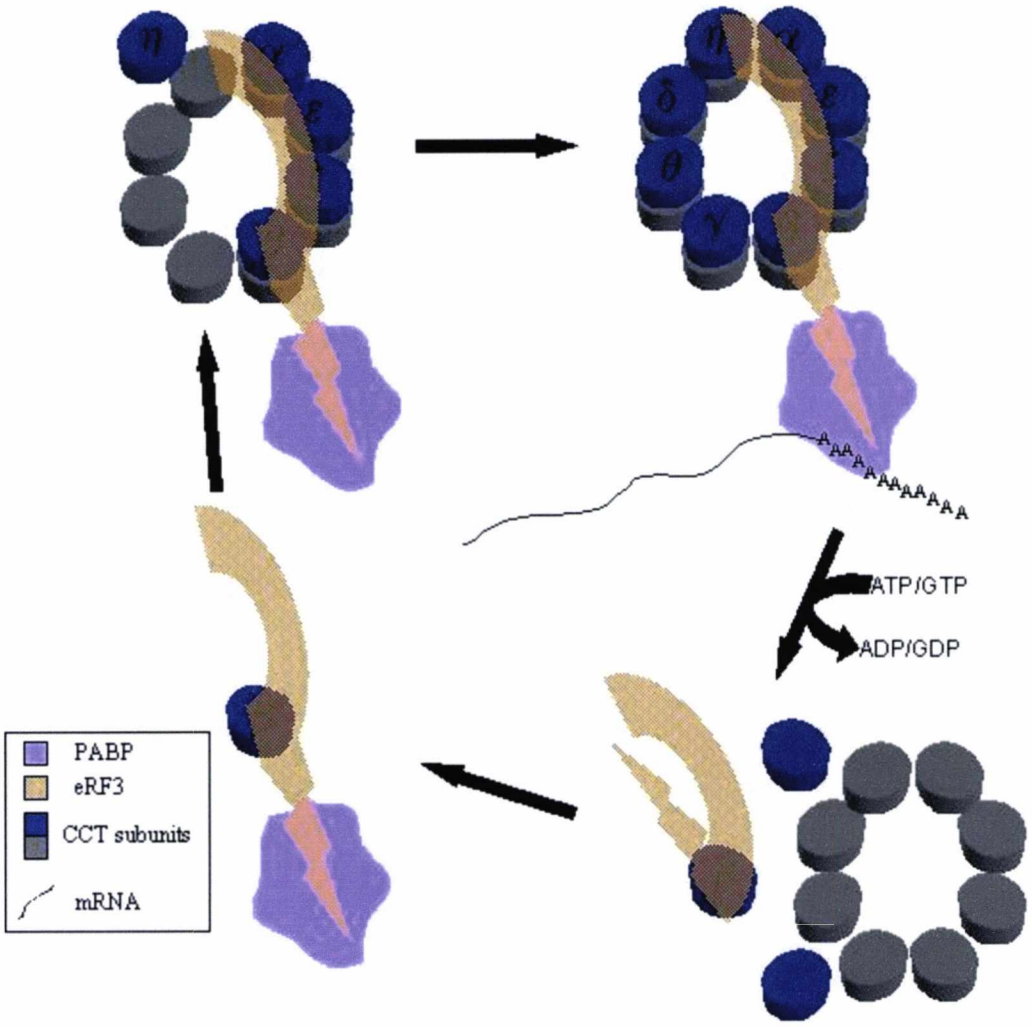

Figure 5.15 Diagram of the proposed model for CCT/eRF3 interaction.

In the model proposed in figure 5.15, eRF3 is bound to the single CCT β subunit until the N-terminal domain of the eRF3 is bound by PABP. The binding of this partner allows the binding of other CCT subunits to complete the complex. The PABP then binds to the poly(A) tail of mRNA to facilitate the termination of translation and folding of the native polypeptide. Either once folded or once termination is complete ATP is hydrolysed by the CCT facilitating its disassembly

and eRF3 hydrolyses GTP providing its release from the termination complex and ribosome. At this point eRF3 is not detected in IPs (with ATP present) and therefore could be released from the β subunit and then rebinds the freed subunit, thus beginning the cycle again.

Chapter 6: CCT Disassembly

6.1 Introduction

6.1.1 The Disassembly of CCT

The ATPase activity of CCT is highly dependant upon K^+ levels and an interesting phenomenon occurs when both ATP and K^+ are at physiological levels. Not only is the substrate released but also the complex falls apart into smaller, oligomeric, structures and individual subunits (Roobol *et al,* 1999). This process is dependent upon ATP hydrolysis and can be reversed when ATP is removed (Roobol *et al,* 1999). It has also been shown that ATP and K^+ are not the only elements in the disassembly of CCT, but that additional, unidentified, factors are also required for this process to occur (Roobol *et al,* 1999).

It also seems that there is a hierarchy within the CCT subunit population on the basis of the ease with which the subunits are able to leave the complex. This appears to be related to the size of a variable length loop in the ascending limb of the intermediate domain of the subunits; the smaller the loop the more readily the subunit can leave the complex (Roobol *et al,* 1999) (see figure 6.1).

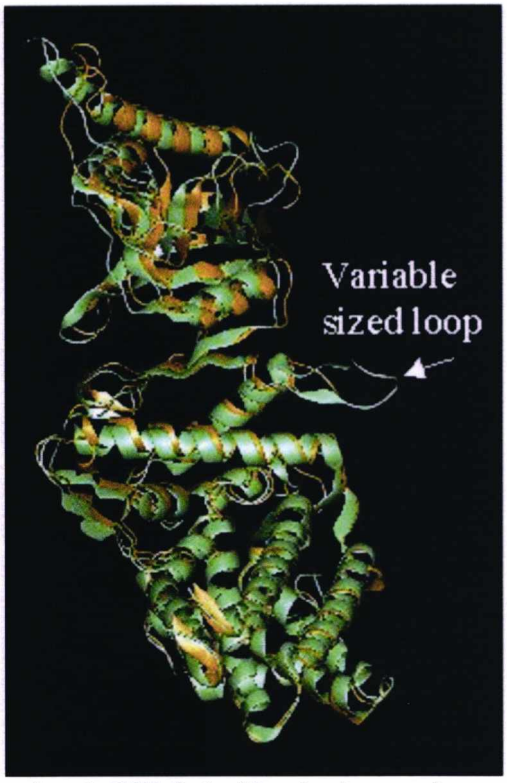

Figure 6.1 CCTα (*green*) and CCT β (*gold*) subunits superimposed to demonstrate the differences in size of the variable sized loop on different subunits. This is thought to play a role in the ease with which subunits can leave the complex when disassembly occurs (Roobol *et al*, 1999a).

This hierarchy could also be related to the ATPase activity of the individual subunits. It has been shown in yeast that there is a particular hierarchy in the ATPase activity of the subunits (Lin *et al,* 1997) and this is likely to be the case in mammalian CCT. Although the order of ATPase activity proposed for the yeast system does not correspond to the ease with which subunits leave the complex in the presence of ATP and K^+ ions (Roobol et al, 1999) (see figure 6.2). This could be because a number of factors are involved in this process including, relative ATPase activity, relative loop length, interaction with disassembly factors or the phosphorylation state of a putative site on the lateral loop (Lin *et al*, 1997).

Cct1p → Cct7p → Cct4p → Cct8p → Cct3p → Cct2p → Cct6p → Cct5p → (yeast)
Cctβ → Cctη → Cctθ → Cctζ → Cctε → Cctδ → Cctα → Cctγ → (mammalian)

Figure 6.2 Comparison between the order of ATPase activity found amongst the yeast CCT subunits and the ease with which mammalian subunits are able to leave the complex. Order of ATPase activity is shown in red (this also represents the order of the subunits proposed by Liou & Willison (1997)) and order of leaving the complex shown in black.

Additionally, it has been shown that large conformational changes occur in both the equatorial and apical domains of the subunits, within one of the rings only, upon ATP binding (Llorca *et al,* 1998), this could lead to a weakening of the interaction between the rings and between the subunits within the affected ring, thus making dissociation more favourable.

6.1.2 Function of CCT disassembly

There could be a number of reasons why the CCT complex disassembles so readily. The disassembly of the complex appears to occur only in one ring at a time, suggesting that the single remaining ring could act as a template for the semi-conservative replication of the CCT complex (Liou *et al*, 1998). Alternatively, the disassembly of a single ring could be an integral part of the CCT folding cycle and may be necessary for the release of substrate from the complex (Quaite-Randall *et al*, 1995). A more likely scenario would be the combination of these theories, where the disassembly of a single ring releases the substrate and then the intact ring acts as a template for the reassembly of the whole complex.

However, the disassembly of the complex leaves the intriguing possibility that the individual subunits or micro-complexes have a function outside that of the intact chaperonin. Upon immunoprecipitation under native conditions it has been noted that the number and size of associated proteins brought down with the individually targeted CCT subunits differs from subunit to subunit (Roobol & Carden, 1999; Roobol *et al*, 1999a). This suggests that the individual subunits have differing affinities for proteins found in the cell and that the subunits may have individual functions. This is further supported by the early observation that all but one of the subunits are equimolar within the cell (Rommelaere *et al*, 1993; Kubota *et al*, 1994;

Creutz *et al*, 1994; Hynes *et al*, 1996); this is surprising if the CCT complex always uniformly consists of, and functions as, two eight membered rings containing one each of the subunits, in a particular order, as suggested (Liou & Willison, 1997). If this were the case, it would be expected in this case for all of the subunits to be present at all times in the same quantities. However it has been shown that the composition of the CCT complex changes during the cell division cycle with mitotic CCT being deficient in some subunits (mainly α and δ) and unable to fold actin (Yokota *et al*, 2001).

If it is assumed then that the subunits and micro-complexes have individual functions, the question remains of what these could be. It has previously been shown that the Cctβ subunit interacts with synapsin (Roobol, unpublished data), in this study, the translation termination factor, eRF3, from yeast, also Cctβ and Cctε interact with the ribosomal L7a protein (Roobol & Carden, 1999) and CFTR protein (Meacham *et al*, 1999). This evidence suggests that individual subunits are capable of interacting with target proteins alone or as part of a micro-complex of different CCT subunits. It has also been demonstrated that the CCT subunits β, δ and η alone are able to suppress the lethality of overexpressed cyclin E in yeast (Won *et al*, 1998), it was then confirmed that cyclin E was a folding substrate of CCT (Won *et al*, 1998). This evidence may afford a clue as to the function of these sub-16mer-complex subunits in that their function may be to 'collect' substrate proteins and await the construction of the whole complex around them to facilitate folding. Alternatively, their function could be to remain bound to substrate proteins once they are released from the rest of the CCT complex in order to facilitate further rounds of CCT-mediated folding and prevent partially folded proteins being released into the

cytosol or to release the substrate protein when the correct signal is received, hence acting as a regulatory mechanism.

Other cellular roles for CCT subunits are also proposed in higher plants, where the α subunit has been found to be sufficient to confer tolerance to salt and osmotic-stress (Yamada *et al*, 2002), and the α and ε subunits are found to fluctuate with the prevailing light conditions (Himmelspach *et al*, 1997), suggesting a regulatory role for these subunits, although no mechanism has been proposed, and that CCTε and α may be involved in ciliate formation in *Tetrahymena pyriformis* (Casalou *et al*, 2001)

6.1.3 Aims and objectives

The previous work done in this project has demonstrated a possible role for micro-complexes and individual subunits in a complex with eRF3 from both yeast and mammalian cells. Interactions between micro-complexes and actin (chapter 5) and tubulin (Dr. Anne Roobol, unpublished data) have also been alluded to.

Therefore, the overall aim of this study was to investigate the disassembly of the CCT complex and to try and deduce the properties of the individual subunits by either isolating them from the whole complex or expressing them recombinantly. A study of the conditions and outcomes of CCT complex disassembly has been carried out.

6.2 Results

6.2.1 Demonstration of CCT complex disassembly

As has been shown previously, immunoprecipitation is a means of isolating a target protein as well as any interacting proteins. In the case of CCT, usually when one subunit is targeted the entire complex is immunoprecipitated. However, under conditions of physiological K^+ and ATP, it has been shown that the whole complex is no longer precipitated (Roobol *et al*, 1999a).

This key experiment was therefore repeated using an increasing concentration of ATP in the IP reaction. Antibodies raised against the C-terminus of mouse CCT subunits were used to immunoprecipitate the CCT complex from [^{35}S] labelled ND7/23 cell lysate (see section 2.3.3). Samples were electrophoresed (on SDS-PAGE), stained with Coomassie brilliant blue, destained and dried. The dried gels were then autoradiographed.

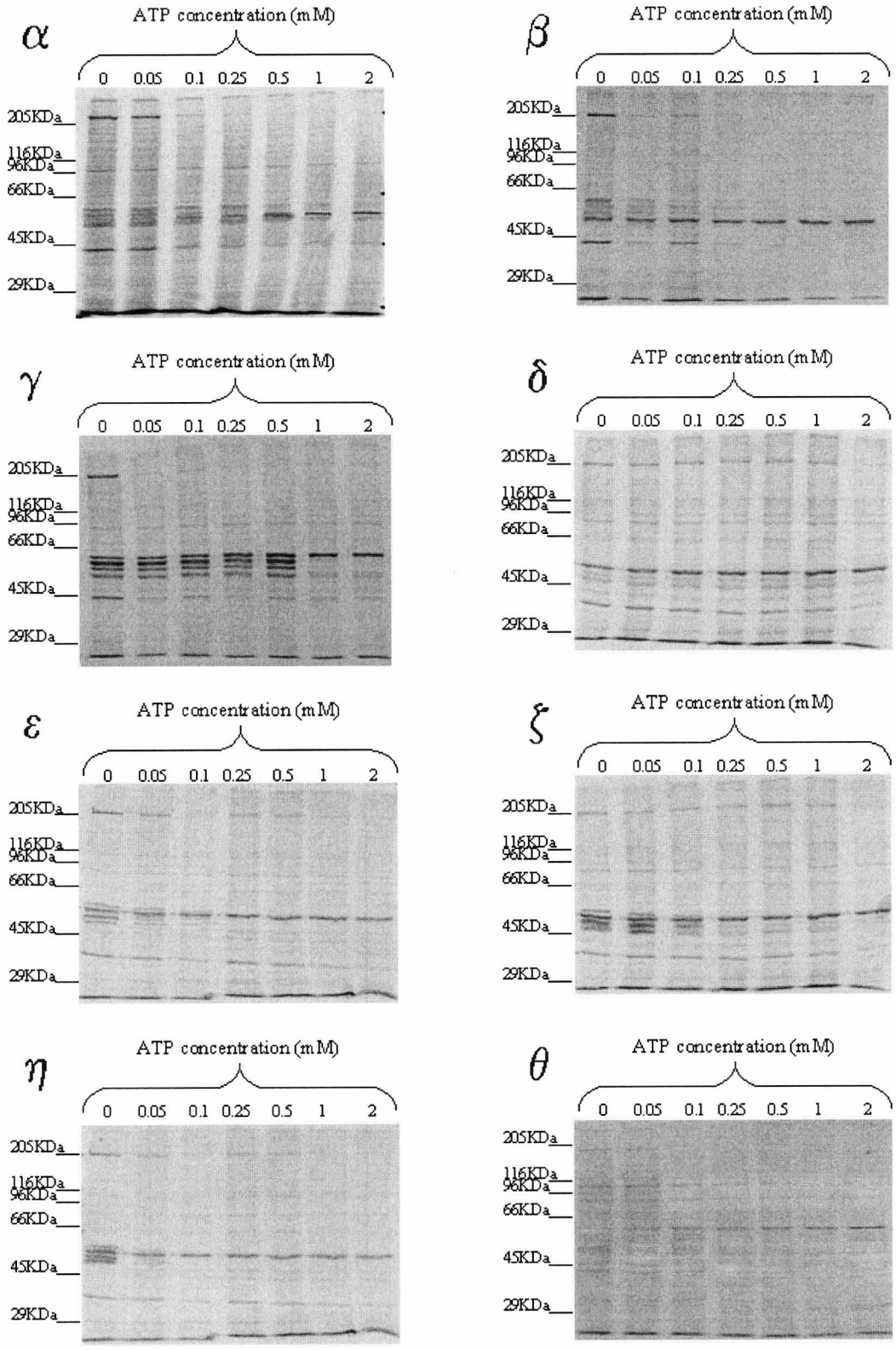

Figure 6.3 Autoradiographs of immunoprecipitated CCT from ND7/23 cell lysate. Rabbit antibodies raised against the C-termini of the mouse CCT subunits were used to immunoprecipitate the CCT complex from whole cell lysate labelled with [^{35}S] methionine and [^{35}S] cysteine with varying concentrations of ATP in the presence of 140mM K^+ ions. The immunoprecipitate was then electrophoresed by SDS-PAGE (30mA, 1hr), stained with coomassie brilliant blue, dried (70°C, 90min, medium ramp) and incubated with autoradiography film (7 days, room temperature).

As can be seen from figure 6.3, the CCT complex disassembles upon the addition of ATP, with each subunit varying in the ease with which it leaves the complex. It can be seen that the Cctη subunit is the most easily released as the whole complex is no longer brought down after the addition of 50μM ATP, followed by Cctε, Cctβ, Cctζ, Cctα and Cctγ, which requires 1mM ATP before it is liberated from the complex. It should also be noted that when the Cctδ and θ subunits are targeted, the whole complex is not precipitated; this is as expected and has been reported (Roobol *et al*, 1999). What should be noted is that the amount of subunit precipitated in these two cases increases as the concentration of ATP increases indicating that the C-terminal epitope of these two subunits is not accessible in the intact complex but as CCT disassembles more subunit is released from the complex exposing this epitope and therefore an increase in the amount of available subunit for precipitation is also increased.

As mentioned earlier, this disassembly phenomenon only occurs in the presence of physiological levels of K^+ ions and the complex remains whole if this is replaced by an equal concentration of Na^+ ions (see figure 6.4).

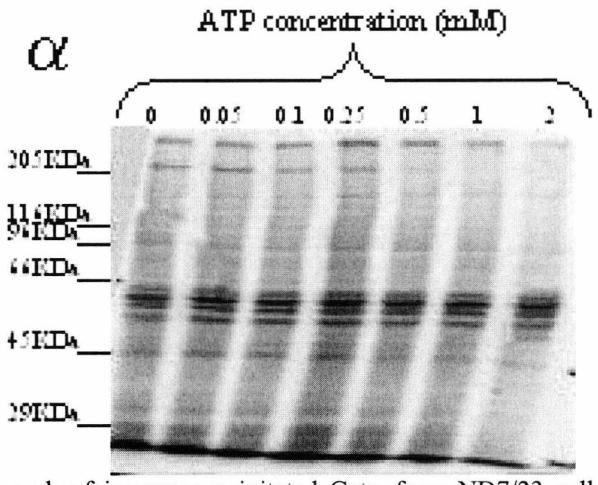

Figure 6.4 Autoradiograph of immunoprecipitated Cctα from ND7/23 cell lysate. Rabbit antibodies raised against the C-terminus of the mouse Cctα subunit were used to immunoprecipitate the CCT complex from whole cell lysate labelled with [^{35}S] methionine and [^{35}S] cysteine with varying concentrations of ATP in the presence of 140mM Na^+ ions. The immunoprecipitate was then electrophoresed by SDS-PAGE (30mA, 1hr), stained with coomassie brilliant blue, dried (70°C, 90min, medium ramp) and incubated with autoradiography film (7 days, room temperature).

Figure 6.4 shows that the complex does not disassemble when Na^+ ions are used in place of K^+ indicating that it is the K^+ ions themselves and not just any mono-ionic species that is required for the disassembly process.

In view of the conformational changes found within the apical region of the CCT subunits during ATP binding and hydrolysis (Llorca *et al,* 1998), it was interesting to investigate the ability of antibodies raised against this region to precipitate the complex in increasing concentrations of ATP. Therefore the IP experiment was repeated using antibodies raised against a peptide, which lies at the base of the apical domain region of the Cctα subunit, in the presence of 140mM K^+ ions and increasing concentrations of ATP.

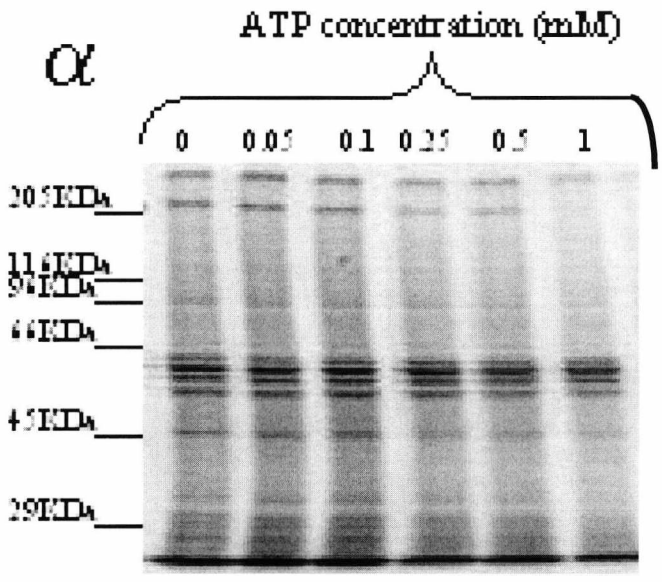

Figure 6.5 Autoradiograph of immunoprecipitated Cctα from ND7/23 cell lysate. Rabbit antibodies raised against the apical domain region of the mouse Cctα subunit were used to immunoprecipitate the CCT complex from whole cell lysate labelled with [^{35}S] methionine and [^{35}S] cysteine with varying concentrations of ATP in the presence of 140mM K^+ ions. The immunoprecipitate was then electrophoresed by SDS-PAGE (30mA, 1hr), stained with coomassie brilliant blue, dried (70°C, 90min, medium ramp) and incubated with autoradiography film (7 days, room temperature).

As figure 6.5 shows, an increasing concentration of ATP approximately halves the amount of CCT Iped as ATP concentration reaches 1mM. Furthermore, this antibody did not detect the population of free α subunits detected by the antibody directed to the CCTα C-terminus (figure 6.3). These data are explicable if it is postulated that firstly, the apical domain antibody can access its epitope in both CCT rings but is not able to access its epitope in the free subunit and secondly, that the C-terminal antibody can access its epitope in free subunits and in one ring of the complex (the disassembling ring) but not the oligomer remaining after disassembly (verified in Roobol *et al*, 1999). It therefore became necessary to investigate the nature of the disassembled CCT species and to detect whether single rings are indeed present as previously suggested (Quaite-Randall *et al*, 1995; Liou *et al*, 1998; Roobol *et al*, 1999).

6.2.2 Analysis of disassembled CCT complex

In order to analyse the disassembled state of CCT, various samples were subjected to size analysis using a superose 6-gel filtration column. It has previously been shown that the CCT β subunit is most readily liberated from the chaperonin complex; therefore, this subunit was depleted from a whole cell lysate sample. Immunoprecipitation, in the presence of ATP and K^+ ions, depleted whole cell lysate of the CCT β subunit and the remaining supernatant split into two samples, one of which was depleted of ATP by incubation with apyrase. These two samples together with whole lysate were loaded onto the column and eluted with lysis buffer, fractions were collected and analysed by SDS-PAGE and silver staining.

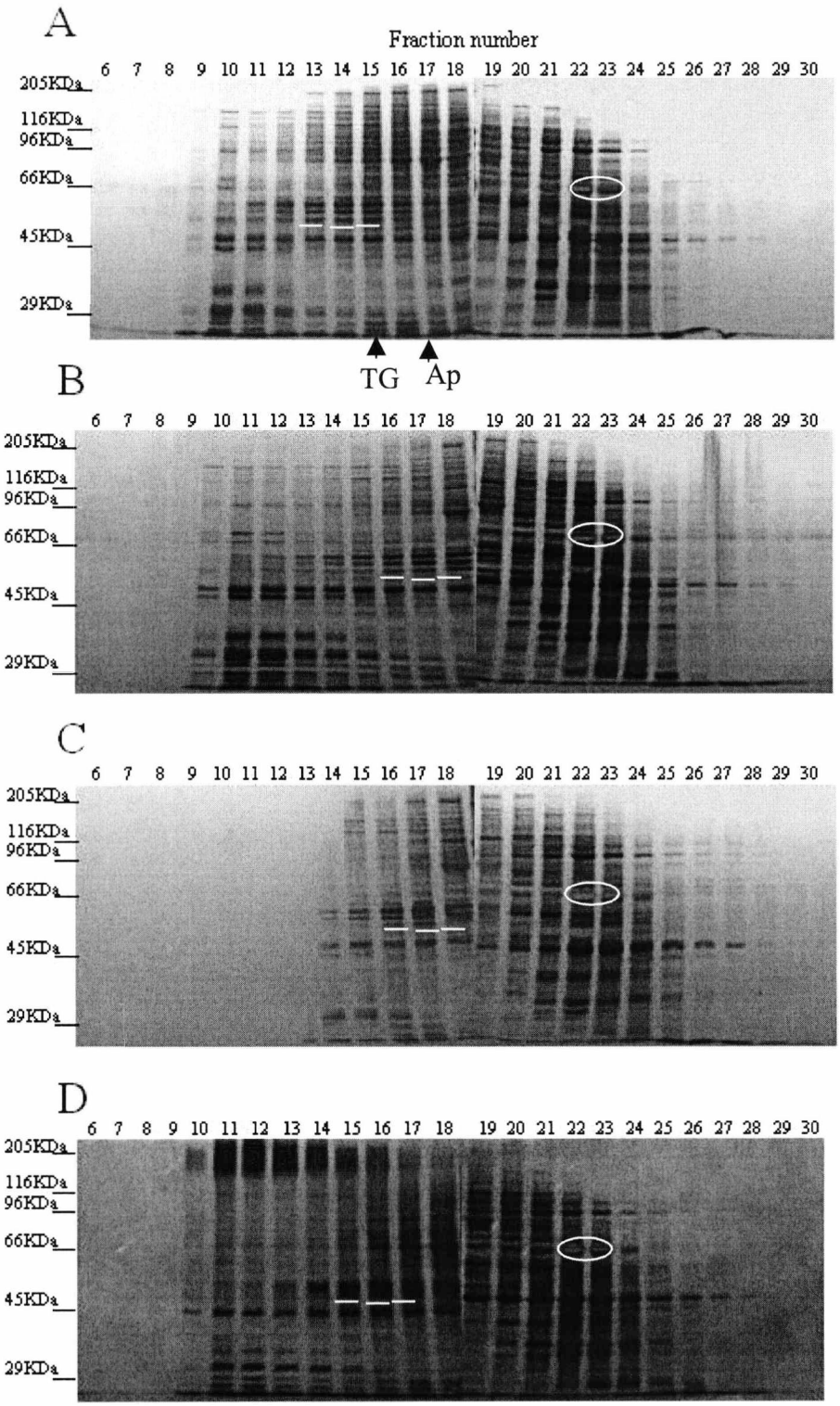

Figure 6.6 Silver stains of fractions eluted from a Superose 6 gel filtration column. Either whole lysate (**A**), whole lysate with 2mM ATP added (**B**), whole lysate depleted of the Cctβ subunit by IP with anti-C-terminal Cctβ antibodies in the presence of 2mM ATP (**C**) or whole lysate depleted of the Cctβ subunit by IP with anti-C-terminal Cctβ antibodies in the presence of 2mM ATP and subsequent addition of 1mM Apyrase (**D**), were loaded onto a Superose 6 column (1ml/min) and eluant (1ml) collected, electrophoresed by 9% SDS-PAGE and silver stained. Markers were Thyroglobulin (TG) (669Kda) and Apoferritin (Ap) (443Kda). The CCT ladder position is marked by white lines and representative proteins which remain in constant fraction positions are circled.

Figure 6.6 shows the silver stains of the collected eluant from the four different samples loaded onto a Superose 6 column. Samples included whole ND7/23 cell lysate and whole cell lysate containing 2mM ATP together with whole lysate depleted of the CCTβ subunit by immunoprecipitation with anti-CCTβ C-terminus, polyclonal antibody and the CCTβ depleted lysate pre-incubated (5min, room temperature) with 1mM apyrase to remove the ATP.

Examination of the profiles in figure 6.6 show many proteins to have a constant elution position across the four profiles. For example, the heavy band circled consistently appears in fraction 22 and to a lesser extent in fraction 23. CCT complex components were clearly identified from their characteristic appearance in all four profiles. CCT in whole extract eluted in fractions 13-15 (underlined) slightly before a thyroglobulin marker (669Kda). In samples containing ATP both whole extract and CCTβ depleted extract profiles show a shift in CCT elution to fractions 16-18 in a similar position to that which apoferritin (443KDa) eluted. CCTβ depleted extract in the absence of ATP (apyrase depleted) eluted at a position (fractions 15-17) equivelent to oligomers clearly smaller than the whole complex. These data are consistent with exposure to ATP and depletion of the CCTβ subunit resulting in a smaller sized oligomer, most likely a single ring (predicted size of 450KDa). The species resulting from β depletion followed by apyrase treatment may be a partly reassembled oligomer lacking CCTβ or may be a single ring which has undergone conformational change on removal of ATP. These possibilities could be resolved by examining the subunit content of IPs from the elution fractions obtained with either the α apical domain antibody or the α C-terminal antibody.

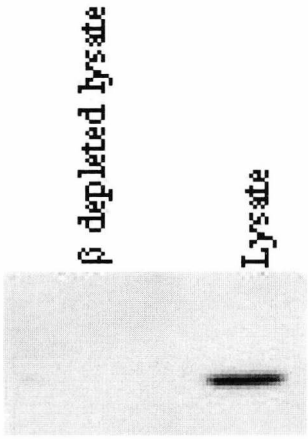

Figure 6.7 Western blots whole lysate and CCTβ depleted lysate were also probed for the presence of CCTβ to ensure complete clearance.

As can be seen from figure 6.7, the depletion of CCTβ from the samples was completely successful.

6.2.3 Purification of individual CCT subunits

In order to study the properties of individual CCT subunits it is necessary to isolate them from the whole complex without destroying their structure. It has been demonstrated that the CCT complex dissociates upon ATP hydrolysis in the presence of K^+ ions in a subunit dependant manner (Roobol *et al*, 1999a) and that, in yeast, the subunits displayed a hierarchy in their hydrolysis of ATP (Lin *et al,* 1997). Taking these two pieces of information together it was decided to try and separate the subunits from each other using an ATP column. The affinity of CCT for ATP was used in the past as a means of purification for the complex, once isolated from whole extract by sucrose gradient fractionation (Lewis *et al*, 1992). One of the observed problems of this method of purification was that, after storage, the CCT oligomer could no longer be observed by EM of negatively stained samples (Roobol, unpublished data), in essence the high concentrations of ATP (10mM) had caused the

complex to disassemble. It was also observed that CCT would elute from the column over a very wide range of ATP concentrations and therefore high concentrations were used to ensure maximal elution. It therefore seemed feasible that the elution of CCT from the ATP column occurred in a subunit specific manner with those subunits most easily released from the complex being eluted at lower concentrations to the other subunits. Therefore, a shallow gradient of ATP concentrations might result in fractions enriched for particular subunits and this would make purification of the individual subunits possible.

A 10mm x 100mm advanced purification glass column (WAT021901, Waters, Massachusetts, USA) containing ATP immobilised using a C_8 linkage on cross-linked 4% beaded agarose with a 9 atom spacer (SIGMA, A-2767) was made and sucrose gradient fractions containing CCT were loaded onto the column and eluted over a 0mM – 10mM linear ATP gradient (see figure 6.8). Fractions were analysed by dot blotting 50µl onto nitro-cellulose and treating this as a western blot as in section 2.6.6.

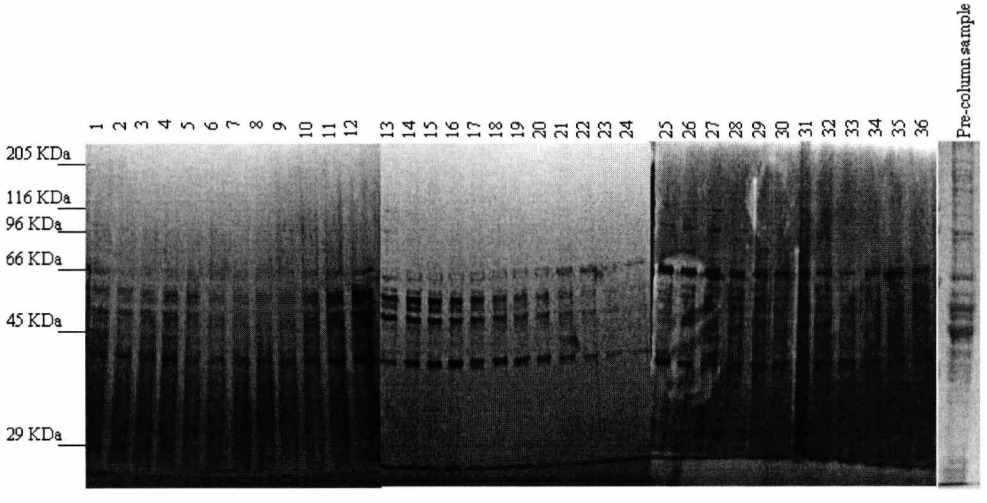

Figure 6.8 Silver stain of CCT containing sucrose gradient fractions passed over an ATP column. A 10mm x 100mm advanced purification glass column (WAT021901, Waters, Massachusetts, USA) containing ATP immobilised on cross-linked 4% beaded agarose with a 9 atom spacer (SIGMA, A-2767) was made and sucrose gradient fractions containing CCT were loaded onto the column and eluted over a 0mM – 10mM linear ATP gradient. Samples (20µl) were separated by SDS-PAGE (9% gel, 30mA, 1¼hr), transferred to nitrocellulose membrane (750mA, 4°C, 1¼hr), and then silver stained.

Figure 6.8 shows the elution profile of CCT from the ATP column in the absence of K^+ ions. The elution profile changes when K^+ ions are present and the best way to see this is with dot blots. It appears that when K^+ ions are present the majority of the CCT is eluted quickly from the column in the first few fractions and then the amount detected tails off. However, when K^+ ions are replaced by Na^+ ions the elution profile is different in that the CCT appears to elute from the column over a much wider range of ATP concentrations with the majority being eluted when the ATP concentration is approximately 3.6 - 4.7mM (fractions 13-17). This implies that the affinity for the ATP column is reduced in the presence of K^+ ions.

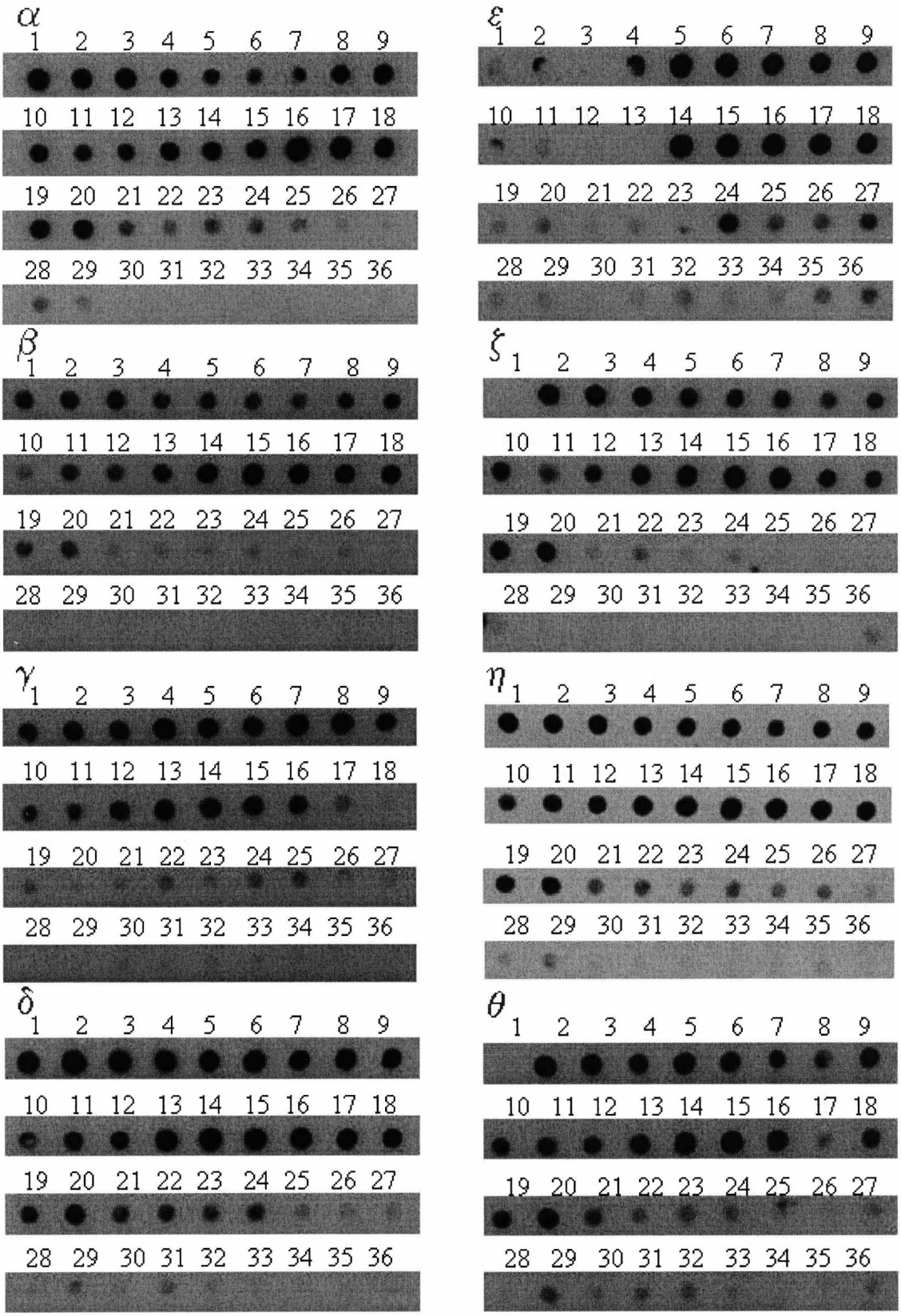

Figure 6.9 Dot blots of CCT containing sucrose gradient fractions resolved over an ATP column in the presence of K^+ ions. A 10mm x 100mm advanced purification glass column (WAT021901, Waters, Massachusetts, USA) containing ATP immobilised on cross-linked 4% beaded agarose with a 9 atom spacer (SIGMA, A-2767) was made and sucrose gradient fractions containing CCT were loaded onto the column and eluted over a 0mM – 10mM linear ATP gradient. Samples (50μl) were dotted onto nitrocellulose and the blots probed with the appropriate anti-CCT antibody.

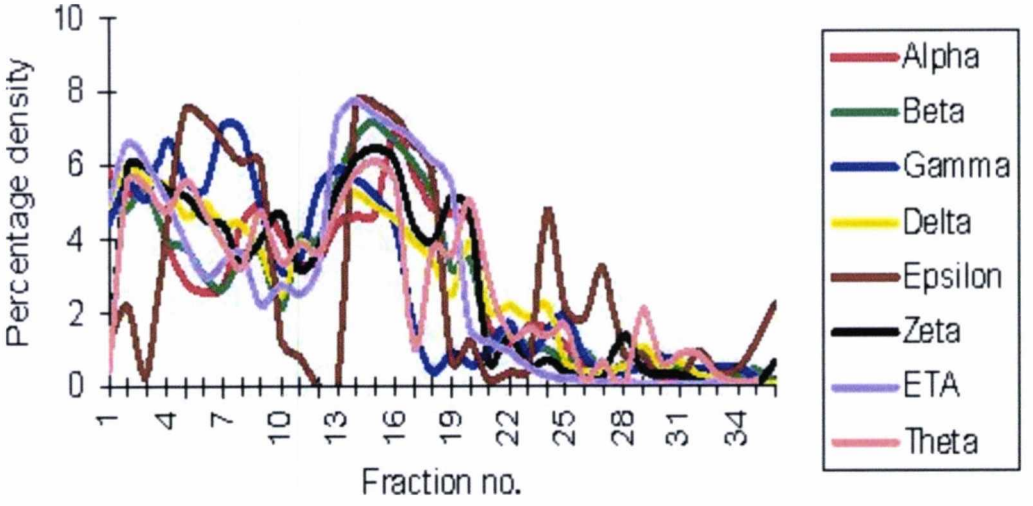

Figure 6.10 Percentage density of each fraction eluted from the ATP column when probed for the different CCT subunits.

As can be seen from figures 6.9 and 6.10, the elution properties for the different subunits in the presence of K^+ ion are different, however these profiles are not sufficiently dissimilar to enable the isolation of individual subunits. The elution shows a definite double peak of CCT subunits. The first peak appears to be when the ATP concentration is approximately 0.8 – 2.8mM (fractions 3 – 10) and the second at approximately 3.6 – 5.3 mM ATP (fractions 13 – 19). This is an interesting observation in that it demonstrates that CCT subunits may have differing affinities for ATP dependant on their oligomeric states. The first peak occurs at a relatively physiological ATP level whilst the second peak occurs at a much higher ATP concentration. This is interesting because if the disassembly of CCT occurs in a single ring whilst the other remains intact as has been suggested by others (Quaite-Randall *et al*, 1995; Liou *et al*, 1998; Llorca *et al,* 1998; Roobol *et al,* 1999a) and in this study, then these data would indicate that the first peak is generated by subunits which have disassembled from the complex at a physiological ATP concentration, while the second peak is the remaining single ring complex eluting as such (or also as disassembled subunits). It is noteworthy that in the absence of K^+, CCT elutes in

the same set of fractions as the second CCT peak observed in the presence of K^+, substantiating the notion that in the ring format (either single or double), CCT subunits have an overall higher affinity for ATP than do the free subunits. The oligomeric status of the fractions could be resolved by negative stain EM. A further diagnostic test would be IP of the relevant fractions with CCTα apical and C-terminal antibodies, a single ring format should be precipitated by the apical but not C-terminal antibodies and vice versa.

Unfortunately the attempts to purify individual subunits using the ATP column were unsuccessful; therefore an attempt to express the individual subunits in the *Pichia pastoris* expression system (Invitrogen) was made. Over-expression studies have shown that an increased amount of one CCT subunit within a cell creates problems for the cell and this can lead to a failure to divide and can ultimately be lethal. In order to overcome these problems I decided to artificially express the subunits as secretory proteins in *P. pastoris*, hence avoiding contact between native and over-expressed subunits. This process, whilst on paper seeming simple, proved extremely difficult as the vector required for expression, and the restriction enzymes it was necessary to use, were difficult to work with and the recombination event, required for expression, was very rare. Success was garnered in expressing the CCT ζ subunit however; but the protein ran erroneously on SDS-PAGE and was heavily glycosylated (data not shown). Further attempts to express subunits in this way, with a His-tag to aid purification, failed and due to time constraints these attempts were abandoned.

6.2.4 ATPase activity of individual CCT subunits

Due to the failure of purification attempts, both by isolation of individual CCT subunits from whole complex and expression of functional subunits in *P. pastoris*, it was decided to try and study the individual subunits by immobilising the CCT complex on beads. Whole ND7/23 extract was incubated with an anti-C-terminal, CCT subunit specific, antibody in the presence of both ATP and K^+ ions, to promote disassembly of the CCT complex. The antibody/subunit complex was then bound to protein A beads and isolated from the rest of the lysate by washing, a process that also resulted in the removal of excess ATP.

The amount of protein present was estimated by electrophoresis of a known quantity of beads by SDS-PAGE and comparison to a known quantity of BSA electrophoresed on the same gel and analysed using the BioRad GelDoc Bioimaging system. Initially the targeted CCT subunit was eluted from the antibody by the addition of acidic (0.1M glycine, 0.15M NaCl, pH2.8) buffer to the beads and isolation of the supernatant, however, this was found to denature the CCT subunit to such an extent that further analysis was not possible. Therefore, the targeted subunit was left bound to the antibody and protein A beads during the further analysis.

The isolated subunits were then subjected to ATPase analysis using a modification of the ATP-Lite™ Luminescence ATP detection assay system and readings made using the Wallac luminometer (see section 2.3.9).

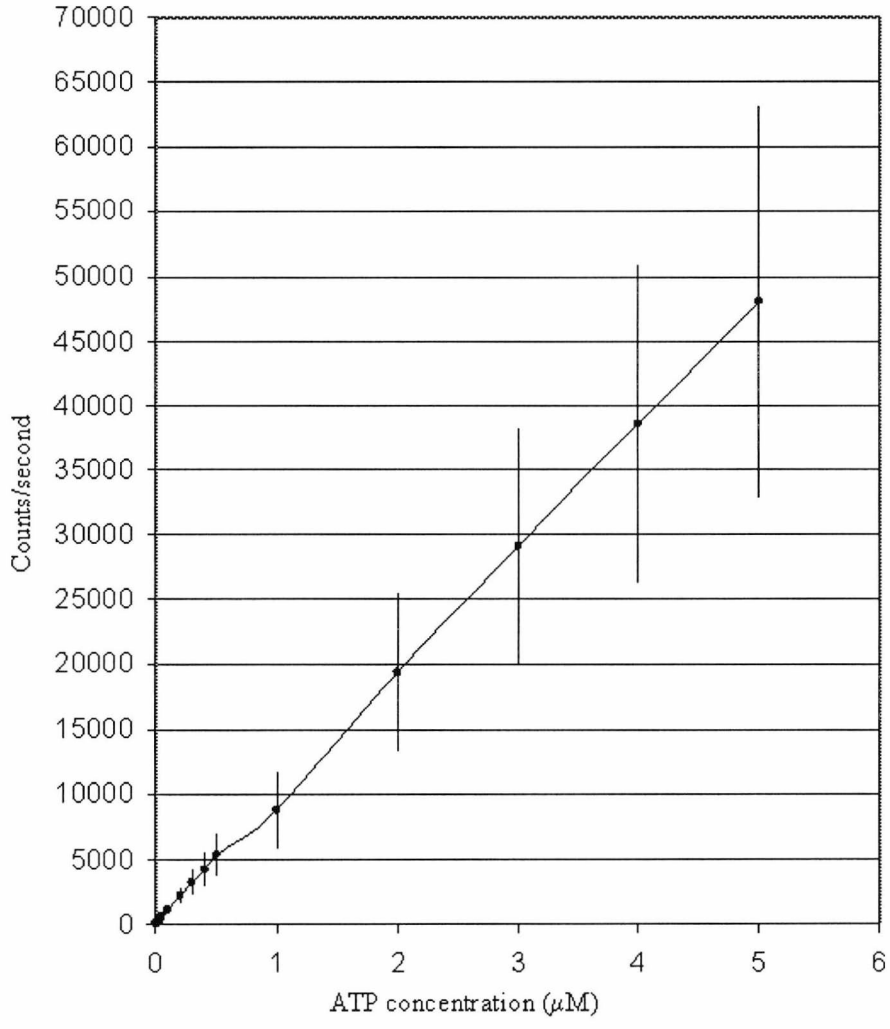

Figure 6.11 Graph of luminescence counts per second for differing concentrations of ATP using the ATP-Lite™ Luminescence ATP detection assay system and readings made using the Wallac luminometer. Error bars represent standard deviation from n=20.

Figure 6.11 shows a standard curve for the ATP-Lite™ Luminescence ATP detection assay system. The graph shows that the detection of ATP is linear for a very large range of concentrations of ATP from nanomolar to millimolar. This indicated that the system used be accurate for the detection of small changes in ATP concentration required for ATPase activity measurement.

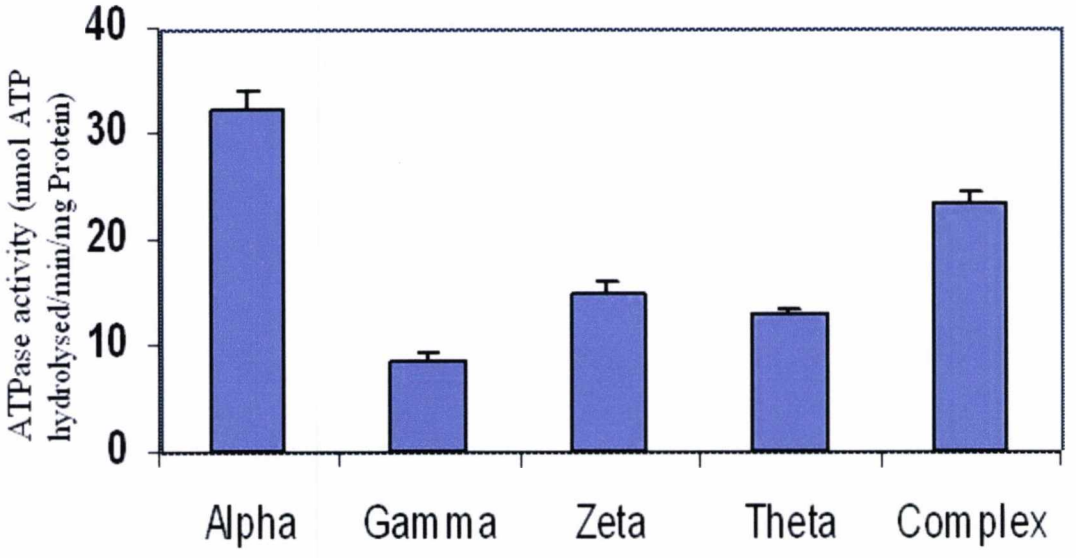

Figure 6.12 Bar chart to show the different ATPase activities of four of the CCT subunits and the whole complex. Individual subunits were targeted for Ip in the presence of ATP and K+ ions to facilitate disassembly of the CCT complex and isolation of individual subunits. After washing, the subunits were incubated with ATP and the concentration of ATP taken at different time points using the ATP-Lite™ Luminescence ATP detection assay system and readings made using the Wallac luminometer. The ATPase activity could then be calculated.

Figure 6.12 shows the difference in ATPase activity amongst four of the CCT subunits and the whole complex. Unfortunately attempts to measure the ATPase activity of the other subunits was unsuccessful, either due to difficulties in measuring the amount of protein present or an ATPase activity that was too low to be measured. The four subunits for which results are available gave consistently similar results over all assays carried out (n=50).

The order of activity does not correspond with either the predicted order of subunits in the CCT ring (Liou & Willison, 1997) or the ATPase hierarchy of CCT subunits in yeast cells (Lin *et al,* 1997), however the ATPase activities were never measured and indeed the CCTζ subunit was predicted to have no ATPase activity at all which is disproved here. There is some correspondence with the order of size of variable loop as described by Roobol *et al* (1999a) in that the θ, ζ and α subunits form an order where the harder it is for them to leave the complex and the larger the variable loop,

the higher the ATPase activity. However, the γ subunit, which has the largest lateral loop, does not fit this pattern in that, of the four subunits measured, it has the lowest activity of all. But if relative ATPase has some role in disassembly hierarchy, the slowest disassembling subunit would be predicted to have the slowest ATPase; in this case the results for CCTα are the anomaly.

It is most interesting to note, however, that from the data available, the average ATPase activity of the individual subunits is slightly lower than that of the whole complex. This would further support the suggestion that the early eluting peak from the ATP column, run in the presence of K+, represents free CCT subunits having a lower affinity for ATP than the oligomeric format eluting in the second peak.

The differences in ATPase activity for each of the subunits are quite large (α = 32.4, γ = 8.7, ζ = 15 and θ = 12.8 nmoles ATP hydrolysed/min/mg protein), indicating that the differences serve some purpose in the functioning of each of the subunits either within the complex or alone or in the disassembly or reassembly of the CCT complex.

One problem with looking at ATPase activities of isolated subunits is if in their normal oligomeric state they function cooperatively, however, as stated in the introduction, a function for lone subunits *in vivo* is emerging, overcoming this problem somewhat.

6.3 Discussion

The evidence presented here demonstrates the disassembly of the CCT complex under conditions of physiological ATP and K^+ ion concentrations, thus confirming the findings of Roobol *et al* (1999).

The immunoprecipitation data clearly shows that the whole CCT (16mer) complex is no longer isolated when individual CCT subunits are targeted under conditions of increasing ATP concentrations only the presence of K^+ ions, as figure 6.4 shows that the whole complex is still isolated at high ATP concentrations when K^+ ions are replaced by Na^+ ions. However, the concentration of ATP at which this disassembly occurs varies with the subunit targeted, inferring that there is a difference in the ability of each subunit to leave the complex. The order of the ease with which subunits can leave the complex is shown in figure 6.13.

$$\eta \rightarrow \varepsilon \rightarrow \beta \rightarrow \zeta \rightarrow \alpha \rightarrow \gamma$$

Figure 6.13 The order of ease with which CCT subunits are able to leave the 16mer complex, as determined by immunoprecipitation of targeted subunits with increasing concentrations of ATP in the presence of 140mM K+ ions.

The order shown in figure 6.13 mostly corresponds with order proposed in Roobol *et al* (1999), in that the order of leaving the complex is related to the size of a variable sized loop, indicated in figure 6.1, where the smaller the loop the easier it is for the subunit to leave the complex. It is noted that the CCTδ and θ subunits are not included in the order determined above; this is because these antibodies do not precipitate the entire complex, only the targeted, free subunit (Roobol *et al*, 1999).

However, these Ips show an increasing amount of free subunit available for precipitation, indicating that these subunits also leave the complex.

This defined order of leaving the 16mer complex indicates that intermediate, sub-16mer complexes of subunits, or micro-complexes, are present within cells at any one time. This is also inferred by data presented in chapters 4 and 5 where eRF3 from both yeast and mammalian cells are interpreted to interact with a sub-16mer CCT complex. Also this is indicated by Ips carried out using peptide antibodies raised against the apical domain of the CCTα subunit, where the typical CCT oligomeric subunit composition is maintained through increasing concentrations of ATP.

A single ring mode of disassembly shown by the data obtained from the ATP column where a distinctive double peak of elution is found for all subunits with the first peak being seen at around physiological ATP concentrations and the second at a much higher concentration. The difference in the ability of the two rings of CCT to disassemble indicates that the properties of the two rings differ in some way and that the single ring format is more stable conformation than the double ring format. This could be due to the conformation of one ring being more stable than the other at any one point or maybe due to other binding partners either stabilising or destabilising one ring. Indeed it has been hinted at that other factors are required for the disassembly of the CCT complex (Roobol *et al*, 1999) as purified CCT has been shown to be stable in that it does not disassemble unless unidentified factors found in the lighter fractions of a sucrose gradient fractionation are added (Roobol *et al*, 1999). Figure 6.14 shows a proposed cycle of disassembly and reassembly of the CCT chaperonin with one ring disassembling, one subunit at a time and the other remaining intact to act as a template for the rebuilding of the double ring structure.

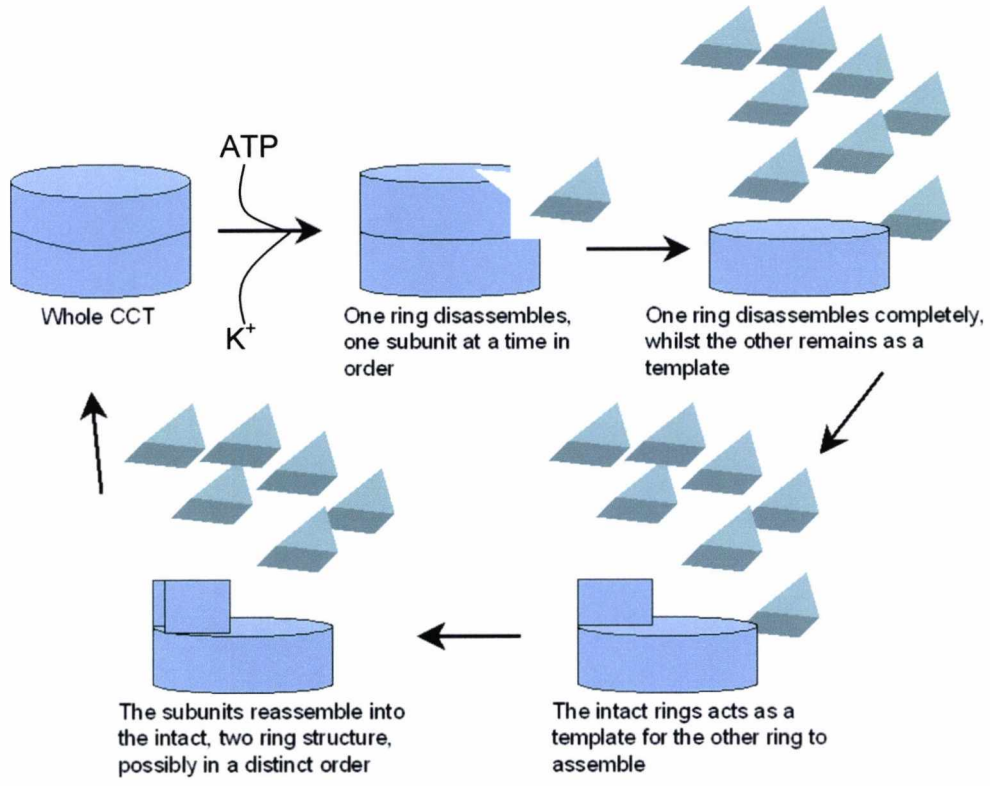

Figure 6.14 Schematic diagram of the proposed disassembly cycle of the CCT double ring complex. One ring disassembles, one subunit at a time until the eight free subunits and one intact ring remain. The Single intact ring then acts as a template for the reassembly of the second ring and the formation of the double ring form.

The ordered disassembly of the CCT complex also indicates that the subunits themselves have different properties. Whilst the ATP column data served to indicate a dual stage disassembly process, it unfortunately did not serve the purpose of purifying the individual CCT subunits. Other methods employed for trying to obtain individual subunits were of limited success. Expression in *Pichia pastoris* was unsuccessful although with more time this may work in the future and purification by IP was partially successful. Some ATPase activity data were obtained from the IP purified subunits and this shows a striking difference between the activities of each subunit. The highest ATPase activity was displayed by the α subunit and the lowest by γ. This appears to bear no relation to the order with which the subunits are able to

leave the complex, which as shown earlier indicates that α and γ leave the complex with more or less equal difficulty. The ATPase activity of the ζ subunit lies between α and γ and leaves the complex with only slightly more ease but unfortunately the other subunit for which ATPase data is available, θ, does not have disassembly data available since the θ antibody epitope appears to be inaccessible in the CCT oligomeric format. The order of ATPase activity described here does not fully concur with that published for the yeast CCT subunits (Lin *et al,* 1997), but with only the ζ subunit activity differing in the order proposed for that of yeast (Lin *et al,* 1997). However, the full picture of how the ATPase activities of the individual CCT subunits fits into the disassembly process will remain elusive until activities for the remaining subunits can be determined.

The data presented in this chapter serve to confirm data published before in that the disassembly of CCT is confirmed (Roobol *et al*, 1999) and the single ring mode of disassembly is also demonstrated (Quaite-Randall *et al*, 1995: Liou *et al*, 1998). The data also show that sub-16mer complexes can also be formed by the CCT subunits and that the CCT subunits have differing ATPase activity, although the relationship between ATPase activity and ease with which the subunit can leave the complex remains unknown as does the issue of whether the second ring can disassemble at higher ATP concentrations and why one of the rings is more stable than the other. These questions can be left for future studies.

Chapter 7: Discussion

7.1 The use of antibodies in research

Much of this project relies on the specificity of antibodies used. Unfortunately this specificity cannot be guaranteed as antibodies do not recognise specific peptide sequences but more the fold and shape of a peptide within a protein (Kuby, 1997), thus the use of a peptide outside its context of a surrounding protein can promote cross reactivity and non-specificity. Other approaches for the detection and characterisation of protein interactions, such as yeast two hybrid screening or tagged proteins could have been used. However these methods do add an artificial element to the interaction in that they often involve artificial expression of proteins, elevated numbers of false positives or changes in the native state of the proteins under investigation.

Due to their highly specific nature, antibodies have become useful tools in biological research. They are used for several techniques to both identify proteins and help elucidate their structure and function. The most common techniques used are immunoblotting, enzyme linked immunosorbant assay (ELISA) and immunofluorescence, several of which have been used in this study. The use of peptide specific antibodies combines the specificity of monoclonal antibodies with the ease of production of polyclonal antibodies. They also provide a quick and easy method of purification.

The antibodies used in this study have been used carefully and the data interpreted taking into account non-specific cross-reactivities, although when subjected to experimental conditions the specific nature of these antibodies for their targets has been demonstrated.

This study has resulted in the production of ten peptide antibodies. These antibodies have been used to determine an interaction between CCT and Sup35p in yeast and between CCT and GSPT1/2 in mammals. Much of this study then relies on the use of these specific antibodies.

These antibodies mostly produce single bands on western blots and where this is not the case other bands are not visible when the antibodies are used to probe two-dimensional blots, where a lower concentration of lysate used. The exception is the antibody raised against the C-terminus of Cct6p. This antibody exhibits very strong cross reactivity with another protein of approximately 70KDa. This was taken into account when these antibodies were used in further studies especially when using the antibodies for IP studies, although IP data suggests that this cross-reacting protein is not bound by the antibody in its native state and hence is not targeted in IPs.

The efficacy of the purified antibodies varies enormously and some are used at very high concentrations (e.g. anti-Cct2p is used at a 1/20 dilution). This could be a result of the purification procedure, however, even at such high concentrations, cross-reactivity is minimal showing that the antibody is at least extremely pure and as such is usable for further studies.

7.2 Do CCT and eRF3 interact?

The evidence presented in this thesis clearly confirms an interaction between the CCT complex and Sup35p and GSPT1 and 2, with a more pronounced interaction occurring with GSPT2 rather than GSPT1. This interaction has only been predicted in yeast by functional algorithmic analysis (Eisenberg *et al,* 2000) but has never been

demonstrated experimentally, despite analyses of the entire yeast proteome (Gavin *et al*, 2002, Ho *et al*, 2002).

Results from the immunoprecipitations show a strong interaction between some CCT subunits and Sup35p and GSPT1/2, however, ATP and strong detergent disrupt this interaction. The interaction with the CCT subunits is similar in both mammalian and yeast in that the interaction is detected under native conditions with the α (1), β (2), ε (5), ζ (6) and η (7) CCT subunits. This could mean that this interaction is not only conserved in evolution but that it may have a similar function in both species.

The interaction is demonstrated further by *in vitro* translation of wild type and mutant (ΔN) Sup35p and GSPT2 in rabbit reticulocyte lysate, where the CCT band is visible on a native gel autoradiograph.

Detection of both CCT β and GSPT1/2 in cells by immunocytochemistry also indicates that these two proteins interact *in vivo*.

7.3 What is the nature of the eRF3-CCT interaction?

The fact that detergents easily disrupt the interaction between CCT and eRF3 indicates that eRF3 is not a substrate of CCT, as detergent is known to only disrupt non-substrate interactions (Hynes & Willison, 2000). Also, because the interaction is disrupted by the addition of ATP, a relationship is indicated between eRF3 and the whole CCT complex or a sub-16mer variant as CCT is disrupted into its component subunits under these conditions (Roobol & Carden, 1999) (see chapter 6). ATP hydrolysis is a property of the CCT subunits and this process causes major conformational changes within the protein (Llorca *et al,* 1998). This could easily interrupt any interaction between CCT and eRF3. Sup35p also has GTPase activity

when bound to Sup45p and the ribosome (Nakamura & Ito, 1998) and this may also cause the disruption of the relationship. A number of conserved domains involved in GTP binding have been identified in GSPT1 and 2 (Hoshino *et al*, 1998), and it therefore seems that these proteins may have a similar GTPase activity to Sup35p (Nakamura & Ito, 1998), and this may also cause the disruption of the interaction between CCT and GSPT1/2. This is using the assumption that ATP could substitute for GTP in these proteins. There is a precedent for these two molecules to be exchangeable in that GTP will replace ATP in CCT disassembly but greater quantities are required (Roobol *et al*, 1999).

IP data does point to the relationship in yeast being between Sup35p and CCT micro-complexes as the interaction does not include subunits which immunoprecipitate the whole CCT complex e.g Cct1p. In the mammalian system, sucrose gradient fractionation analysis of cell lysate shows that GSPT1/2 was not found in the central portion of the gradient, which contains the whole CCT complex, but appears further up where micro-complexes and monomers are located and this is also the case for yeast Sup35p. When these lighter fractions were subjected to IP analysis using antibodies to the subunits shown to interact with GSPT1/2 in the previous IP analysis, GSPT1 and 2 were only detected in the CCT β IP indicating that GSPT1 and 2 associate only with this subunit when it is free of the complex and that interaction with the other subunits occurs when this subunit is included in sub-16mer complexes. Incidentally this evidence also indicates that the interaction between CCT β and GSPT1/2 is possibly through hydrophobic residues, as this interaction is not detected when CCT β is separated from the complex by detergent. The presence of sub-16mer CCT complexes was also indicated by IPs carried out using peptide antibodies raised against the apical domain of the CCTα subunit, where the typical CCT 'ladder' is still

detected despite increasing concentrations of ATP, whereas when the C-terminal antibody is used this is not the case, also the presence of a hierarchy of subunits able to leave the complex also points to the existence of sub-16mer complexes.

The interaction is demonstrated further by *in vitro* translation of wild type and mutant (ΔN) Sup35p and GSPT2 in rabbit reticulocyte lysate, where the CCT band is visible on a native gel autoradiograph. This interaction is severely reduced in the case of the mutant and does not compare well with a substrate interaction or that of a permanently associated protein (see figure 4.20). The interaction appears to be transient but again not substrate-like in nature. The Sup35p produced in this instance should be non-aggregated as no 'seeds', required for the prionisation of the protein, are present. This can be seen from the native gel as no large aggregates are found at the top of the lanes, showing that the non-aggregated protein interacts with the CCT complex. The reduction in interaction when the N-terminus is missing may indicate that this region of Sup35p is required for stabilization of the relationship, or contains the binding site. Unfortunately the data from the GSPT2 *in vitro* tranlation was inconclusive as the protein was quickly broken down, however and interaction was seen.

7.4 What could be the function of the eRF3-CCT interaction?

One of the properties of Sup35p is that it is prone to self-seeded aggregation and as such is a model prion protein (Glover *et al,* 1997). Interestingly, the interaction with yeast Sup35p changes with its aggregation state, with its aggregated form showing a strong interaction with all CCT subunits but the interaction is decreased somewhat when Sup35p is not aggregated and when the N-terminal portion of the Sup35p is

missing when the interaction is in a subunit specific manner, in a similar way to that with GSPT1/2. Sedimentation analysis of yeast cells shows that more CCT is found in the pellet from [*PSI*$^+$] cell lysate than that from [*psi*$^-$] cells, indicating a difference in solubility of the CCT between prion positive and negative cells. The sucrose gradient analysis also demonstrates that the CCT subunits show an increase in the number of micro-complexes and individual subunits in [*psi*$^-$] cell lysate when compared to that from [*PSI*$^+$] cells, and conversely the amount of subunits found in the heavier fractions also increases in [*PSI*$^+$] cell lysate. This could mean that some CCT is associated with Sup35p and thus follows Sup35p as its position changes in the sucrose gradient depending on its aggregation state. However as stated earlier Sup35p does not appear to be a substrate protein of CCT and hence this interaction does not appear to have any bearing on the prionisation process.

The interaction between CCT and eRF3 is further indicated *in vivo* by the detection of both CCT β and GSPT1/2 in cells by immunocytochemistry. The areas of co-localisation appear to be confined to an area surrounding the nucleus, where the rough endoplasmic reticulum is situated, this indicates that the interaction may have a role in protein synthesis in this organelle. Interestingly an interaction between actin, one of CCTs substrates (Gao *et al*, 1992), and GSPT1/2 is also detected by immunostaining but only at the periphery of the cell. This indicates that actin may act as a mediatory protein between CCT and GSPT1/2. However, this interaction appeared in a different part of the cell when compared to the CCT β/GSPT1/2 interaction and when IPs of the CCT subunits were analysed for the presence of actin, it was seen that actin interacted with different subunits to GSPT1/2.

Taken separately, these pieces of evidence provide intriguing clues as to the nature of the interaction between eRF3 and CCT. But together they can offer a model for the association between these two important proteins.

Both eRF3 and CCT have been implicated to have a role in the cell cycle (Yokota *et al*, 2001, Kikuchi *et al*, 1988); however, this seems unlikely as an explanation for their interaction as there is now debate over the involvement of Sup35p in this process (Tuite M. F. personal communication). It does seem strange that no ill effects have been reported on the cell division cycle when Sup35p is in its inactive, aggregated form (Chernoff *et al*, 1998, Eaglestone *et al*, 1999) and from observations in this study the prion positive cells seem to grow faster than their prion negative relatives.

It seems then that the only other cellular process both proteins could have reason to interact is that of protein synthesis. Convention dictates that these two proteins should not come into contact with each other during this process as eRF3 is associated with newly synthesized, unfolded, proteins in its role as part of the translation termination complex (Frolova et al, 1994, Zhouravleva et al, 1995), and CCT is associated with more mature, partially folded, proteins (Llorca *et al*, 1999). However there have been reports that CCT does associate with nascent peptide chains (McCallum *et al*, 2000; Dunn *et al*, 2001). GSPT2 has been shown to complement Sup35p mutations in yeast (Le Goff *et al*, 2002) and would also be associated with newly synthesized, unfolded, proteins in its role as part of the translation termination complex in mammals (Hoshino *et al*, 1998, 1999).

I propose that eRF3 interacts with the CCT complex in a subunit specific manner, during protein synthesis, to facilitate the binding of nascent polypeptide chains to CCT for folding. The native immunoprecipitation of the ΔN Sup35p mutant cell lysate shows a strong interaction with Cct1p and Cct7p and a much weaker interaction

with Cct2, Cct5 and Cct6. When organized into a ring conformation with the same order of subunits proposed for the mammalian complex (Liou & Willison, 1997), these subunits lie next to each other (see figure 7.1).

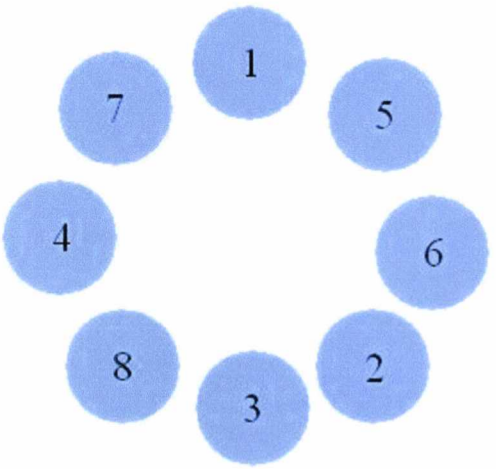

Figure 7.1 Order of CCT subunits in the yeast complex, based on that proposed for the mammalian complex by Liou & Willison, (1997)

It seems that these subunits represent the normal binding sites of eRF3 and that the presence of the 'free' N-terminus in the yeast prion negative cells inhibits this interaction. Nevertheless an interaction in the [*psi⁻*] cells does take place, but only with Cct2p. Therefore, it seems possible that Cct2p acts as an anchor for Sup35p and that it is this subunit that is involved in the stabilization of the interaction by binding at the N/M domain junction of Sup35p. This is proposed because the interaction still occurs in the ΔN IP and is the only subunit found to bind Sup35p with a free N-terminus in the [*psi⁻*] IP, but also when the N-terminus is missing, the interaction is much depleted (from figure 4.17), implicating a role for this region in the stabilization of the interaction. The interaction between GSPT1/2 and the same CCT subunits is detected when the whole lysate is present, however, when fractionated by sucrose gradient; GSPT1/2 is only detected in the lighter fractions and is only found to interact with the CCT β subunit. This implies that only a tiny amount of the GSPT1/2

present in the cell interacts with whole complex, binding in a similar manner to that in the ΔN Sup35p mutant of yeast but that the majority is interacting with CCT β alone. From the IP evidence, it seems that Sup35p binds strongly to Cct1 and Cct7 and much more weakly to Cct5 and Cct6, indicating that Sup35p binds across the ring complex. It is reasonable to assume that the free N-terminal region of Sup35p could interfere with this binding, maybe in response to the ATPase induced conformational changes in the CCT or the GTPase activity of Sup35p. This also brings in another factor to the model. Sup35p only exhibits GTPase activity in the presence of Sup45p and the ribosome (Nakamura & Ito, 1998) and one or both of these may also be present in the CCT/Sup35p complex. The other evidence for at least a third component of the complex is that only the free N-terminus is able to inhibit the interaction, as when it is missing the interaction still occurs but less stably. This indicates that the N-terminus may have to be bound to a third component of the complex in order for full cooperation to occur between CCT and Sup35p. Though the functional component of Sup35p has been identified as the C-terminal domain (Ter-Avanesyan *et al*, 1993, 1994, Wilson & Culbertson, 1988), it has been shown recently that the poly (A)-binding protein (Pab1p) is also able to bind the N and M domains of Sup35p (Cosson *et al*, 2002). The involvement of the N-terminal domain of GSPT1 and 2 in the interaction also goes some way to explain the differences in the interaction between CCT and these two proteins as they differ maximally at their N-terminus and are relatively identical for the rest of their length (Hoshino *et al*, 1998). Just like Sup35p, GSPT1/2 have been shown to interact with poly(A)-binding protein (PABP) (Hoshino *et al*, 1999) and, in the case of GSPT2, this interaction is through the N-terminal domain associating with the C-terminal domain of PABP (Hoshino *et al*, 1999), similar to the interaction observed between yeast Sup35p and PABP (Cosson *et al*,

2002). This could indicate that PABP brings eRF3 into close proximity with the poly (A) region of the mRNA being translated, thus bringing the entire translation termination complex into the correct position to initiate translation termination (Cosson *et al*, 2002) in both yeast and mammalian cells, and thus allowing CCT to interact with eRF3 and hence carry out its function as a protein folding chaperone.

.

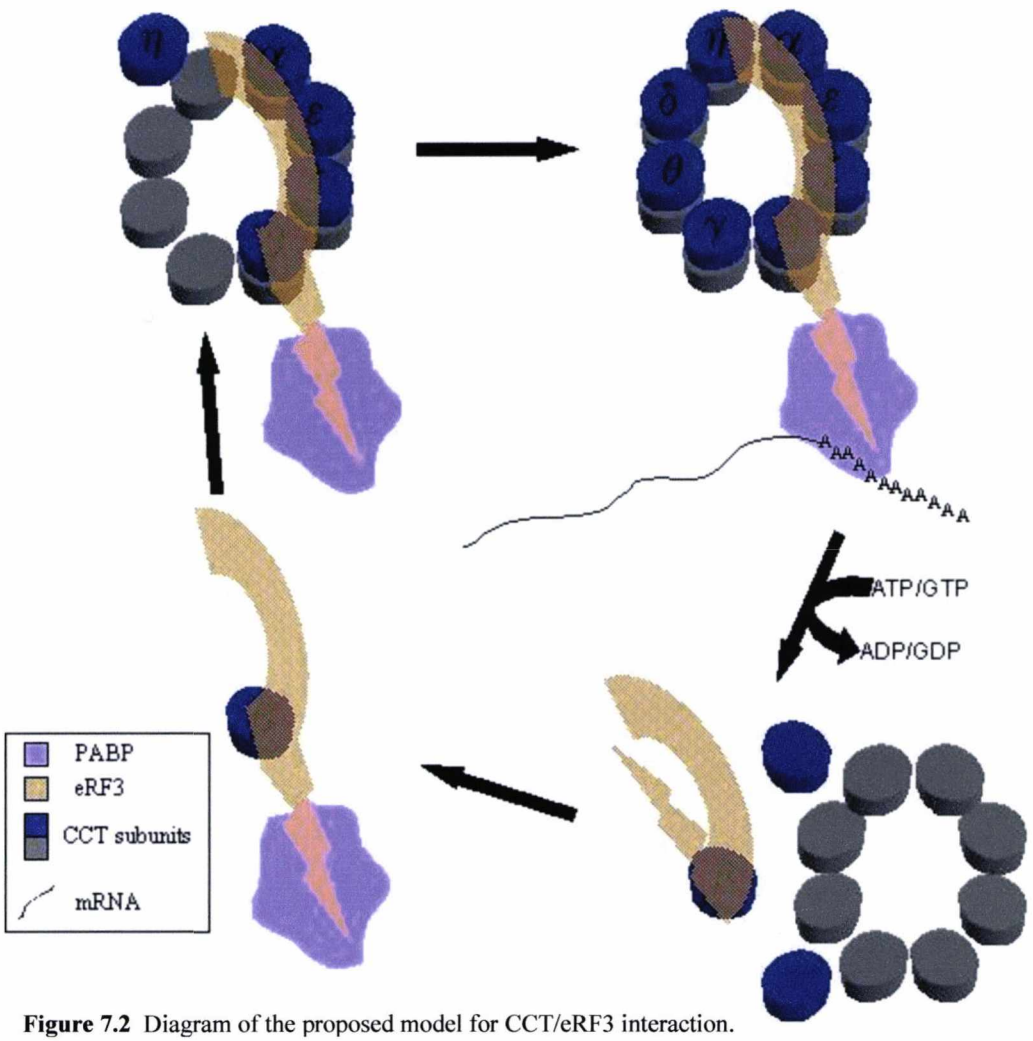

Figure 7.2 Diagram of the proposed model for CCT/eRF3 interaction.

In the model proposed in figure 7.2, eRF3 is bound to the single CCT β subunit until the N-terminal domain of the eRF3 is bound by PABP. The binding of this partner allows the binding of other CCT subunits to complete the complex. The PABP then binds to the poly(A) tail of mRNA to facilitate the termination of translation and

folding of the native polypeptide. Either once folded or once termination is complete ATP is hydrolysed by the CCT facilitating its disassembly and eRF3 hydrolyses GTP providing its release from the termination complex and ribosome. At this point eRF3 is not detected in Ips (with ATP present) and therefore could be released from the β subunit and then rebinds the freed subunit, thus beginning the cycle again. This model can also explain why the aggregated Sup35p interacts with all of the CCT subunits. In the prion state the N-terminal domains have a β-sheet conformation (Cohen *et al*, 1994) allowing them to bind closely to each other, thus the N-terminal domains are no longer free and are unable to inhibit the interaction. With the Sup35p molecules in close proximity to each other, an interaction with any bound CCT is likely to be enhanced and is therefore liable to be detected in all native IPs.

7.5 Does CCT disassemble?

Evidence is also presented here to demonstrate the disassembly of the CCT complex under conditions of physiological ATP and K^+ ion concentrations, thus confirming the findings of Roobol *et al* (1999).

The whole CCT (16mer) complex is no longer isolated when individual CCT subunits are targeted under conditions of increasing ATP concentrations only the presence of K^+ ions, as the whole complex is still when K^+ ions are replaced by Na^+ ions. However, the concentration of ATP at which this disassembly occurs varies with the subunit targeted, inferring a hierarchy in the ability of each subunit to leave the complex. The order of the ease with which subunits can leave the complex is shown in figure 7.3.

$$\eta \rightarrow \varepsilon \rightarrow \beta \rightarrow \zeta \rightarrow \alpha \rightarrow \gamma$$

Figure 7.3 The order of ease with which CCT subunits are able to leave the 16mer complex, as determined by immunoprecipitation of targeted subunits with increasing concentrations of ATP in the presence of 140mM K+ ions.

This order mostly corresponds with the order proposed in Roobol *et al* (1999), in that it is related to the size of a variable sized loop, indicated in figure 6.1, where the smaller the loop the easier it is for the subunit to leave the complex. CCTδ and θ subunits are not included in the order determined above because these antibodies do not precipitate the entire complex, only the targeted, free, subunit (Roobol *et al*, 1999). However, these IPs show an increasing amount of free subunit, indicating these subunits also leave the complex.

7.6 What is the nature of the disassembled products?

This defined order of leaving the 16mer complex indicates that intermediate, sub-16mer complexes of subunits, or micro-complexes, are present within cells at any one time. This is also inferred by data presented in chapters 4 and 5 where eRF3 from both yeast and mammalian cells are interpreted to interact with a sub-16mer CCT complex. This points to a single ring mode of disassembly, however, when the ATP concentration becomes very high CCT is no longer present in the IPs, indicating that at high concentrations of ATP the entire complex disassembles into its component subunits.

This is further shown by the data obtained from the ATP column where a distinctive double peak of elution is found. The difference in the ability of the two rings of CCT to disassemble indicates that the properties of the two rings differ in some way and that the single ring format is a more stable conformation than the double ring, this maybe due to other binding partners either stabilising or destabilising one ring. Other factors have been found to be required for the disassembly of the CCT complex (Roobol *et al*, 1999) as purified CCT does not disassemble unless unidentified factors

found in the lighter fractions of a sucrose gradient fractionation are added (Roobol *et al*, 1999).

When the disassembled product is applied to a superose 6 column CCT subunits are detected in fractions containing single ring sized proteins, indicating a single ring mode of disassembly, but also in fractions containing slightly larger and smaller proteins indicating that both sub-16mer and sub-8mer CCT complexes are present when the complex is disassembled.

7.7 What are the properties of the individual CCT subunits?

The ordered disassembly of the CCT complex also indicates that the subunits themselves have different properties. Some ATPase activity data was obtained from the IP purified subunits and this shows a striking difference between the activities of each subunit. This data appears to bear no relation to the order with which the subunits are able to leave the complex. The order of ATPase activity described here does not fully concur with that published for the yeast CCT subunits (Lin *et al,* 1997), However, the full picture of how the ATPase activities of the individual CCT subunits fits into the disassembly process will remain elusive until activities for the remaining subunits can be found.

7.8 Conclusion

CCT and eRF3 have been shown to interact in both yeast and mammalian cells in a similar way both *in vivo* and *in vitro*. This interaction does not appear to be that of chaperonin-substrate but more that of two interacting proteins. The data also indicates that the interaction takes place between sub-16mer CCT complexes and

eRF3. It is proposed here that the reason for this interaction is to couple translation termination and protein folding in the cytosol, a process not previously put forward involving these two proteins.

The disassembly of the CCT complex is also confirmed (Roobol *et al*, 1999), as is the single ring mode of disassembly (Quaite-Randall *et al*, 1995: Liou *et al*, 1998). The data also shows that sub-16mer complexes can also be formed by the CCT subunits and that the CCT subunits have differing ATPase activity.

7.9 Further Work

Further work on this project should include an investigation into what other proteins may be involved in the CCT/eRF3 interaction, especially the effects of the presence of eRF1. Indeed it may be found later that either eRF1 mediates the interaction or that eRF3 can only interact with CCT in the absence of sufficient eRF1. Further work should also be carried out on the involvement of the ribosome in this process. It may be the case that CCT binds eRF3 and releases it in the presence of the ribosome and/or eRF1 much in the same way as it does in the VHL complex (Feldman *et al*, 1999) and the APC (Camasses *et al*, 2003), acting as a regulator of translation termination. It may also be found that the chaperonin does have some role in the prionisation of Sup35p and this could be tested by augmenting the expression of the CCT subunits and looking for curing of the prion or causing it to develop from prion negative cells much as HSP104 does (Chernoff *et al*, 1995).

Further work should be done into the factors involved in the CCT disassembly process. Work also needs to be done to ascertain whether disassembly occurs in living cells and this could be carried out by live cell imaging techniques, involving the

labelling of two or more CCT subunits. The properties of the individual CCT subunits also need to be investigated further and this may involve either the expression or isolation of individual subunits. Until this is possible then separating the properties and activities of the individual subunits may prove virtually impossible.

With the advent of major works into proteins interacting within the cell (Gavin *et al*, 2002, Ho *et al*, 2002) it also seems that the work of characterising these interactions has begun and will continue. Perhaps the age of the genome is over and the age of the 'interactome' has begun.

References

Advisory Committee on Dangerous Pathogens (ACDP). (1998). Transmissible Spongiform Encephalopathy Agents: Safe working and the prevention of infection. The Stationery Office. ISBN 0-11-322166-5.

Alexandru G., Zachariae W., Schleiffer A., and Nasmyth K. (1999). Sister chromatid separation and chromosome re-duplication are regulated by different mechanisms in response to spindle damage. *EMBO J.* **18**, 2707-2721

Altschul, S.F., Gish, W., Miller, W., Myers, E.W. & Lipman, D.J. (1990). Basic local alignment search tool. *J. Mol. Biol.* **215**, 403-410.

Anfinsen C. B. (1973). Principles that govern the folding of protein chains. *Science.* **181**, 223-230.

Barhite S., Thibault C., and Miles M. F. (1998). Phosducin-like protein (PhLP), a regulator of G beta gamma function, interacts with the proteasomal protein SUG1. *Biochem. Biophys. Acta.* **1402**, 95-101.

Bauer P. H., Muller S., Puzicha M., Pippig S., Obermaier B., Helmreich E. J., and Lohse M. J. (1992). Phosducin is a protein kinase-a-regulated g-protein regulator. *Nature.* **358**, 73-76.

Bellotti V., Mangione P., and Stoppini M. (1999). Biological activity and pathological implications of misfolded proteins. *Cell. Mol. Life. Sci.* **55**, 977-991.

Boisvert D. C., Wang J., Otwinowski Z., Horwich A. L., and Sigler P. B. (1996). The 2.4Å crystal structure of the bacterial chaperonin GroEL complexed with ATPγS. *Nature Struct. Biol.* **3**, 170-177.

Bourke G.J., El Alami W., Wilson S.J., Yuan A.D., Roobol A., and Carden M.J. (2002). Slow axonal transport of the cytosolic chaperonin CCT with Hsc73 and actin in motor neurons. *J. Neur. Res.* **68**, 29-35.

Boyle, M. D. P. and Reis K. J. (1987). Bacterial Fc Receptors. *Biotech* **5,** 697-703.

Bradford, N. (1976). A refined and sensitive method for the quatification of microgram quantities of protein utilising the principle of protein-dye binding. *Analytical Biochemistry,* **72**, 248.

Braig K., Otwinowski Z., Hedge R., Boisvert D. C., Joachimiak A., Horwich A. L., and Sigler B. P. (1994). The crystal structure of the bacterial chaperonin GroEL at 2.8Å. *Nature*, **371**, 578-586.

Buchner J., Schmidt M., Fuchs M., Jaenicke R., Rudolph R., Schmid F. X., and Kiefhaber T. (1991). GroE facilitates refolding of citrate synthase by suppressing aggregation. *Biochem.* **30**, 1586-1591.

Buckle A. M., Zahn R., and Fersht A. R. (1997). A structural role for GroEL-polypeptide recognition. *Proc. Natl. Acad. Sci. USA.* **94,** 3571-3575.

Burland T. G., Gull K., Schedl T., Boston R. S., and Dove W. F. (1983). Cell type dependant expression of tubulins in *Physarum. J. Cell. Biol.* **97**, 1852-1859.

Burston S. G., Ranson N. A., and Clarke A. R. (1995). The origins and consequences of asymmetry in the chaperonin reaction cycle. *J. Mol. Biol.* **249**, 138-152.

Camasses A., Bogdanova A., Shevchenko A., and Zachariae W. (2003). The CCT chaperonin promotes activation of the anaphase-promoting complex through the generation of functional Cdc20. *Mol. Cell.* **12**, 87-100.

Casalou C., Cyrne L., Rosa M.R., and Soares H. (2001). Microtubule cytoskeleton perturbation induced by taxol and colchicine affects chaperonin containing TCP-1 (CCT) subunit gene expression in Tetrahymena cells. *Biochim. Biophys. Acta.* **1522**, 9-21

Caughey B., and Chesebro B. (1997). Prion protein and the transmissible spongiform encephalopathies. *Trends. Cell. Biol.* **7**, 56-62.

Chacinska A., Szczesniak B., Kochneva-Pervukhova N. V., Kushnirov V. V., Ter-Avanesyan M. D., and Boguta M. (2001). Ssb1 chaperone is a [*PSI+*] prion-curing factor. *Curr. Genet.* **39**, 62-67.

Chaudhuri T. K., Farr G.W., Fenton W.A., Rospert S., and Horwich A.L. (2001). GroEL/GroES-mediated folding of a protein too large to be encapsulated. *Cell.* **107**, 235-246.

Chen F., Kishida T., Yao M., Hustard T., Glavac D., Dean M., Gnarra J. R., Orcutt M. L., Duh F. M., Glenn G., Green J., Hsia Ye., Lamiell J., Li H., Wei Mh., Schmidt L., Tory K., Kuzmin I., Stackhouse T., Latif F., Linehan Wm., Lerman M., and Zbar B. (1995). Germline mutations in the von Hippel-Lindau disease tumour suppressor gene: Correlations with phenotype. *Hum. Mutat.* **5**, 66-75.

Chen S., Roseman A. M., Hunter A. S., Wood S. P., Burston S. G., Ranson N. A., Clarke A. R., and Saibil H. R. (1994). Location of a folding protein and shape changes in GroEL-GroES complexes imaged by cryo-electron microscopy. *Nature*, **371**, 261-264.

Chen X., Sullivan D. S., and Huffaker T. C. (1994). Two yeast genes with a similarity to TCP-1 are required for microtubule and actin function *in vivo. Proc. Natl. Acad. Sci. USA.* **91**, 9111-9115.

Chernoff Y. O., Derkach I. L., and Inge-Vechtomov S. (1993). Multicopy SUP35 gene induces de novo appearance of psi-like factors in the yeast *Saccharomyces cerevisiae*. *Curr. Genet.* **24**, 268-270.

Chernoff Y. O., Galkin A. P., Lewitin E., Chernova T. A., Newnam G. P., and Belenkiy S. M. (2000). Evolutionary conservation of prion-forming abilities of the yeast Sup35 protein. *Molec. Microbiol.* **35**, 865-876.

Chernoff Y. O., Lindquist S. L. Ono B., Inge-Vechtomov S. G., and Liebman S. W. (1995). Role of the chaperone protein Hsp104 in propagation of the yeat prion-like factor [*PSI*+]. *Science.* **268**, 880-884.

Chernoff Y., Derkatch I., Dagkesamanskaya A., Tikhomironva V., Ter-Avanesyan M., and Inge-Vechtomov S. (1988). Nonsense-suppression by amplification of translational protein factor gene. *Dokl. Akad. SSSR.* **301**, 1227-1229.

Clurmanhress B. E., Sheaff R. J., Thress K., Groudine M., and Roberts J. M. (1998). Turnover of cyclin E by the ubiquitin/proteasome pathway is regulated by Cdk2 binding and cyclin phosphorylation. *Genes. Dev.* **10**, 1979-1990.

Cohen F. E. (1999). Protein misfolding and prion diseases. *J. Mol. Biol.* **293**, 313-320.

Cohen F. E., Pan M., Fletterick K. M., Huang Z., Baldwin R. J., and Prusiner S. B. (1994). Structural clues to prion replication. *Science.* **264**, 530-531.

Corpet F. (1988). Multiple sequence alignment with hierarchical clustering. *Nucl. Acids. Res.* **16**, 10881-10890.

Cosson B., Couturier A., Chabelskaya S., Kiktev D., Inge-Vechtomov S., Philippe M., and Zhouravleva G. (2002). Poly(A)-binding protein acts in translation termination via eukaryotic release factor 3 interaction and does not influence *[PSI+]* propagation. *Mol. Cell. Biol.* **22,** 3301-3315.

Cox B. (1965). [PSI], a cytoplasmic suppressor of super-suppression in yeast. *Heredity.* **20**, 505-521.

Creutz C. E., Liou A., Snyder S. L., Brownawell A., and Willison K. R. (1994). Identification of the major chromaffin granule-binding protein, chromabindin A, as the cytosolic chaperonin CCT (Chaperonin containing TCP-1). *J. Biol. Chem.* **269**, 32035-32038.

DebBurman S.K., Raymond G.J., Caughey B., and Lindquist S. (1997). Chaperone-supervised conversion of prion protein to its protease-resistant form. *Proc. Nat. Acad. Sci.USA* **94**, 13938-13943.

Ditzel L., Lowe J., Stock D., Stetter K. O., Huber H., Huber R., and Steinbacher S. (1998). Crystal structure of the thermosome, the archaeal chaperonin and homologue of CCT. *Cell.* **93**, 125-138.

Doel S. M., McCready S. J., Nierras C. R., and Cox B. S. (1994). The dominant PNM2-mutation which eliminates the psi factor of *Saccharomyces cerevisiae* is the result of a missense mutation in in the SUP35 gene. *Genetics*. **137**, 659-670.

Dudley K., Potter J., and Willison K. R. (1984). Analysis of male sterile mutations in the mouse using haploid stage expressed cDNA probes. *Nucleic Acids Res.* **12**, 4281-4293.

Dunn A. Y., Melville M. W., and Frydman J. (2001). Review: Cellular substrates of the eukaryotic chaperonin TriC/CCT. *J. Struct. Biol.* **135**, 176-184.

Eaglestone S. S., Cox B. S., and Tuite M. F. (1999). Translation termination efficiency can be regulated in *Saccharomyces cerevisiae* by environmental stress through a prion mediated mechanism. *EMBO. J.* **18**, 1974-1981.

Ebihara K., and Nakamura Y. (1999). C-terminal interaction of translational release factors eRF1 and eRF3 of fission yeast: G-domain uncoupled binding and the role of conserved amino acids. *RNA*. **5,** 739-750.

Edelman G. M. (1973). Antibody structureand molecular immunology. *Science*. **180,** 830-840.

Eisenberg D., Marcotte E.M., Xenarios I., and Yeates T.O. (2000). Protein function in the post-genomic era. *Nature*. **405,** 823-826.

Elble R. (1992). A simple and efficient procedure for transformation of yeasts. *Biotechniques*. **13**, 18-20.

Ellis R. J. (1996). Chaperonins: Introductory perspective. In The Chaperonins, (Ellis R. J. editor). Academic Press, London, pp1-27.

Ellis R. J., and Hartl F. U. (1999). Principles of protein folding in the cellular environment. *Curr. Op. Strut. Biol.* **9**, 102-110.

Ellis R. J., and Hemmingsen S. M. (1989). Molecular Chaperones: Proteins essential for the biogenesis of some macromolecular structures. *Trends Biochem. Sci.* **14**, 339-342.

Farr G. W., Furtak K., Rowland M. B., Ranson N. A., Saibil H. R., Kirchausen T., and Horwich A. L. (2000). Multivalent binding of non-native substrate proteins by the chaperonin GroEL. *Cell*. **100**, 561-573.

Farr G. W., Scharl E. C., Schumacher R. J., Sondek S., and Horwich A. L. (1997). Chaperonin-mediated folding in the eukaryotic cytosol proceeds through rounds of release of native and non-native forms. *Cell*. **89**, 927-937.

Fayet O., Zeigelhoffer T., and Georgopoulos C. (1989). The groES and groEL heat shock gene products of *Escherichia coli* are essential for bacterial growth at all temperatures. *J. Bacteriol.* **171**, 1379-1385.

Feldman D. E., Thulasiraman V., Ferreya R. G., and Frydman J. (1999). Formation of the VHL-elongin BC tumour suppressor complex is mediated by the chaperonin TriC. *Mol. Cell.* **4**, 1051-1061.

Fenton W. A., Kashi Y., Furtak K., and Horwich A. L. (1994). Residues in chaperonin GroEL required for polypeptide binding and release. *Nature.* **371**, 614-619.

Flores, K.H., Senger, M., T., Glatting, P. Ernst, A. Hotz-Wagenblatt, and S. Suhai. (1998). W2H: WWW Interface to the GCG Sequence Analysis Package. *Bioinformatics,* **14**, 452-457

Frőlich K-U., and Madeo F. (2000). Apoptosis in yeast – a monocellular organism exhibits altruistic behaviour. *FEBS. Letts.* **473**, 6-9.

Frolova L., Le Goff X., Zhouravleva G., Davydova E., Philippe M., and Kisselev L. (1996). Eukaryotic polypeptide chain release factor eRF3 is an eRF1- and ribosome-dependant guanosine triphosphate. *RNA.* **2**, 334-341.

Frydman J., Nimmesgern E., Erdjument-Bromage H., Wall J. S., Tempst P., and Hartl F. U. (1992). Function in protein folding of TriC, a cytosolic ring complex containing TCP-1 and structurally related subunits. *EMBO J.* **11**, 4767-4778.

Gao Y., Thomas J. O., Chow R. L., Lee G. H., and Cowan N. J. (1992). A cytoplasmic chaperonin that catalyses β-actin folding. *Cell.* **69**, 1043-1050.

Gao Y., Vainberg I. E., Chow R. L., and Cowan N. J. (1993). Two cofactors and cytosolic chaperonin are required for the folding of α and β tubulin. *Mol. Cell. Biol.* **13**, 2478-2485.

Gavin A. C., Bosche M., Krause R., Grandi P., Marzioch M., Bauer A., Schultz J., Rick J. M., Michon A. M., Cruciat C. M., Remor M., Hofert C., Schelder M., Brajenovic M., Ruffner H., Merino A., Klein K., Hudak M., Dickson D., Rudi T., Gnau V., Bauch A., Bastuck S., Huhse B., Leutwein C., Heurtier M. A., Copley R. R., Edelmann A., Querfurth E., Rybin V., Drewes G., Raida M., Bouwmeester T., Bork P., Seraphin B., Kuster B., Neubauer G., and Superti-Furga G. (2002). Functional organization of the yeast proteome by systematic analysis of protein complexes. *Nature.* **415**, 141-147.

Georgopoulos G. C., Hendrix R. W., Casjens S., and Kaiser A. (1973). Host participation in bacteriophage lambda head assembly. *J. Mol. Biol.* **76**, 45-60.

Glockshuber R., Hornemann S., Riek R., Wider G., Billeter M., and Wuthrich K. (1997). Three-dimensional NMR structure of a self-folding domain of the prion protein PrP(121-231). *TIBS.* **22**, 241-242.

Gnarra J. R., Tory K., Weng Y., Schmidt L., Wei M. H., Li H., Latif F., Liu S., Chen F., Duh F. M., Lubensky I., Duan Dr. Florence C., Pozzatti R., Walther Mm., Bander Nh., Grossman Hb., Brauch H., Pomer S., Brooks Jd., Isaacs Wb., Lerman Mi., Zbar B., and Linehan Wm. (1994). Mutations of the VHL tumour suppressor gene in renal carcinoma. *Nat. Genet.* **7**, 85-90.

Goda S., Takano K., Yamagata Y., Maki S., Namba K., and Yutani K. (2002). Elongation in a beta-structure promotes amyloid-like fibril formation of human lysozyme. *J. Biochem.* **132,** 655-661.

Grossberger R., Gieffers C., Zachariae W., Podtelejnikova A.V., Schleiffer A., Nasmyth K., Mann M., and Peters J.M. (1999). Characterization of the DOC1/APC10 subunit of the yeast and the human anaphase-promoting complex. *J. Biol. Chem.* **274**, 14500-14507

Hansen L. L., Jakobsen C. G., and Justesen J. (1999). Assignment of the human chain release factor 3 (GSPT2) to Xp11.23 → p11.21 and of the distal marker DXS1039 by radiaton hybrid mapping. *Cytogenet. Cell. Genet.* **86**, 250-251.

Harlow E., and Lane D. (1988). Antibodies: A laboratory manual. Cold Spring Harbour, New York.

Harris B. (1991). Magic Bullets. *Chem. Ind.* **18**, 656-659.

Harrison Lavoie K. J., Lewis V. A., Hynes G. M., Collison K. S., Nutland E., and Willison K. R. (1993). A 102 kda subunit of a golgi-associated particle has homology to beta-subunits of trimeric g-proteins. *EMBO. J.* **12**, 2847-2853.

Hawes B. E., Touhara K., Kurose H., Lefkowitz R. J., and Inglese J. (1994). Determination of the g-beta-gamma-binding domain of phosducin - a regulatable modulator of g-beta-gamma signalling. *J. Biol. Chem.* **269,**29825-29830.

Hekman M., Bauer P. H., Sohlemann P., and Lohse M. J. (1994). Phosducin inhibits receptor phosphorylation by the beta-adrenergic-receptor kinase in a pka-regulated manner. *FEBS. Lett.* **343**, 120-124.

Hemmingsen S. M., Woolford C., Van Der Vies S. M., Tilly K., Dennis D. T., Georgopoulos G. C., Hendrix R. W., and Ellis R. J. (1988). Homologous plant and bacterial proteins chaperone oligomeric protein assembly. *Nature.* **333**, 330-334.

Himmelspach R., Nick P., Schäfer E., and Ehmann B. (1997). Developmental and light dependant changes of the cytosolic chaperonin containing TCP-1 (CCT) subunits in maize seedlings, and the localisation in coleoptiles. *Plant. J.* **12**, 1299-1310.

Hloden R., and Hartl F. U. (1994). How the protein folds in the cell. In Mechanisms of protein folding. Ed: Pain R. H. pp194-228. Oxford University Press, Oxford.

Ho L., Carmichael J., Swartz J. E., Wyttenbach A., Rankin J., and Rubinsztein D. C. (2001). The molecular biology of Huntington's disease. *Psychol. Med.* **31**, 3-14.

Ho Y., Gruhler A., Heilbut A., Bader G. D., Moore L., Adams S-L., Millar A., Taylor P., Bennett K., Boutilier K., Yang L., Wolting C., Donaldson I., Schandorff S., Shewnarane J., Vo M., Taggart J., Goudreault M., Muskat B, Alfarano C, Dewar D., Lin Z., Michalickova K., Willems A. R., Sassi H., Nielsen P. A., Rasmussen K. J., Andersen J. R., Johansen L. E., Hansen L. H., Jespersen H., Podtelejnikov A., Nielsen E., Crawford J., Poulsen V., Sørensen B. D., Matthiesen J., Hendrickson R. C., Gleeson F., Pawson T., Moran M. F., Durocher D., Mann M., Hogue C. W. V., Figeys D., and Tyers M. (2002). Systematic identification of protein complexes in *Saccharomyces cerevisiae* by mass spectrometry. *Nature* **415**, 180 - 183 .

Hohfield J., and Hartl F. U. (1994). Role of the chaperonin cofactor Hsp10 in protein folding and sorting in yeast mitochondria. *J. Cell. Biol.* **126**, 305-315.

Hoshino S-i., Imai M., Kobayashi T., Uchida N., and Katada T. (1999). The eukaryotic polypeptide chain releasing factor (eRF3/GSPT) carrying the translation termination signal to the 3'-Poly(A) tail of mRNA. *J. Biol. Chem.* **274**, 16677-16680.

Hoshino S-i., Imai M., Mizutani M., Kikuchi Y., Hanaoka F., Ui M., and Katada T. (1998). Molecular cloning of a novel member of the eukaryotic polypeptide chain-releasing factors (eRF). *J. Biol. Chem.* **273**, 22254-22259.

Hoshino S-i., Miyazawa H., Enomoto T., Hanaoka F., Kikuchi Y., Kikuchi A., and Ui M. (1989). A human homolog of the yeast gst1-gene codes for a gtp-binding protein and is expressed in a proliferation-dependent manner in mammalian-cells. *EMBO J.* **8**, 3807-3814.

Houry W. A., Frishman D., Eckerskorn C., Lottspeich F. and Hartl F. U. (1999). Identification of in vivo substrates of the chaperonin GroEL. *Nature.* **402**, 147-154.

Huang M-T., and Grollman A. P. (1972). Effects of aurintricarboxylic acid on ribosomes and the biosynthesis of globin in rabbit reticulocytes. *Mol. Pharm.* **8**, 111-127.

Hunt J. F., and Deisenhofer J. (1997). The structure of *Escherichia coli* GroES. In Guidebook to molecular chaperones and protein folding catalysts. Ed; Gething M. pp179-182, Oxford University Press, Oxford.

Hutchingson E. G., Tichelaar W., Hofhaus G., Weiss H., and Leonard K. R. (1989). Identification and electron microscopic analysis of a chaperonin oligomer from *Neurosprora crassa* mitochondria. *EMBO J.* **8**, 1485-1490.

Huynen M., Snell B., Lathe W., 3rd and Bork P. (2000). Predicting protein function by genomic context: quantitative evaluation and qualitative inferences. *Genome. Res.* **10**, 1204-1210.

Hynes G. M., and Willison K. R. (2000). Individual subunits of the eukaryotic cytosolic chaperonin mediate interactions with binding sites located on subdomains of beta-actin. *J. Biol. Chem.* **275,** 18985-18994.

Hynes G., Sutton C. W., and Willison K. R. (1996). Peptide mass fingerprinting of chaperonin-containing TCP-1 (CCT) and copurifying enzymes. *Faseb J.* **10**, 137-147.

Ito K., Ebihara K., and Nakamura Y. (1998). The stretch of C-terminal acidic amino acids of translational release factor eRF1 is a primary binding site for eRF3 of fission yeast. *RNA.* **4**, 958-972.

Ito K., Ebihara K., Uno M., and Nakamura Y. (1996). Conserved motifs of prokaryotic and eukaryotic polypeptide release factors: tRNA-protein mimicry hypothesis. *Proc. Natl. Acad. Sci. USA.* **93**, 5443-5448.

Ito T., Chiba T., Ozawa R., Yoshida M., Hattori M., and Sakaki Y. (2001). A comprehensive two hybrid analysis to explore the yeast protein interactome. *Proc. Natl. Acad. Sci. USA.* **98**, 4569-4574.

Jackson G. S., Staniforth R. A., Halsall D. J., Atkinson T., Holbrook J. J., Clarke A. R., and Burston S. G. (1993). Binding and hydrolysis of nucleotides in the chaperonin catalytic cycle: implications for the mechanism of assisted protein folding. *Biochem.* **32**, 2554-2563.

Jaenicke R. (1998). Protein self-organisation *in vitro* and *in vivo*: partitioning between physical biochemistry and cell biology. *Biol. Chem.* **379**, 237-243.

Johnston J. A., Ward C. L., Kopito R. R. (1998). Aggresomes: A cellular response to misfolded proteins. *J. Cell Biol.* **143**, 1883-1898.

Kad N. M., Ranson N.A., Cliff M.J., and Clarke A.R. (1998). Asymmetry, commitment and inhibition in the GroE ATPase cycle impose alternating functions on the two GroEL rings. *J. Mol. Biol.* **278**, 267-278.

Kashuba E., Pokrovskaja K., Klein G., and Szekely L. (1999). Epstein-Barr virus-encoded nuclear protein EBNA-3 interacts with the epsilon subunit of the T-complex protein 1 chaperonin complex. *J. Hum. Virol.* **2**, 33-37.

Kibel A., Iliopoulos O., DeCaprio J. A., and Kaelin W. G. (1995). Binding of the von Hippel-Lindau tumour suppressor protein to elongin B and C. *Science.* **269**, 1444-1446.

Kikuchi C., Shimatake H., and Kikuchi A. (1988). 'A yeast gene required for the G_1-to-S transition encodes a protein containing an A-kinase target site and GTPase domain.' *EMBO J.* **7**, 1175-1182.

Kim S., Willison K. R., and Horwich A. L. (1994). Cytosolic chaperonin subunits have a conserved ATPase domain but diverged polypeptide-binding domains. *TIBS.* **19**, 543-548.

King C. Y., Tittmann P., Gross H., Gerbert R., Aebi M., and Wuthrich K. (1997). Prion-inducing domain 2-114 of yeast Sup35 protein transforms *in vitro* into amyloid-like filaments. *Proc. Natl. Acad. Sci. USA.* **94**, 6618-6622.

Kirchoff C., and Willison K. R. (1990). Nucleotide and amino acid sequence of human testis-derived *TCP1*. *Nucleic Acids Res.* **18**, 4247.

Köhler G., and Milstein C. (1975). Continuous cultures of fused cells secreting antibody of predefined specificity. *Nature.* **256**, 495-497.

Kubota H., and Willison K. R. (1997). Cytosolic chaperonins. In Guidebook to molecular chaperones and protein folding catalysts. Ed; Gething M. pp 207-227. Oxford University Press, Oxford.

Kubota H., Hynes G. M., Kerr S. M., and Willison K. R. (1997). Tissue specific subunit of the mouse chaperonin-containing TCP-1. *FEBS Lett.* **402**, 53-56.

Kubota H., Hynes G., Carne A., Ashworth A., and Willison K. R. (1994). Identification of six *Tcp-1* related genes encoding divergent subunits of the TCP-1 containing chaperonin. *Curr. Biol.* **4**, 89-99.

Kubota H., Willison K. R., Ashworth A., Nozaki M., Miyamoto H., Yamamoto H., Matsushiro A., and Morita T. (1992). Structure and expression of the gene encoding t-complex polypeptide 1 (*Tcp-1*). *Gene.* **120**, 207-215.

Kuby J. (1997). Immunology, 3rd Ed, W. H. Freeman and company, New York.

Kushnirov V. V., Kryndushkin D. S., Boguta M., Smirnov V. N., and Ter-Avanesyan M. D. (2000). Chaperones that cure yeast artificial [PSI+] and their prion-specific effects. *Curr. Biol.* **10,** 1443-1446.

Laemmli U. K. (1970). Cleavage of structural proteins during the assembly of the bacteriophage T4. *Nature.* **277**, 680-685.

Laskey R. A., Honda B. M., Mills A. D., and Finch J. T. (1978). Nucleosomes are assembled by an acidic protein which binds histones and transfers them to DNA. *Nature.* **275**, 416.

Latif F., Tory K., Gnarra J., Yao M., Duh F. M., Orcutt M. L., Stackhouse T., Kuzmin I., Modi W., Geil L., Schmidt L., Zhou Fw., Li H., Wei Mh., Chen F, Glenn G.,

Choyke P., Walther Mm., Weng Yk., Duan D.s.r, Dean M., Glavac D., Richards Fm., Crossey Pa., Fergusonsmith Ma., Lepaslier D., Chumakov I., Cohen D., Chinault Ac., Maher Er., Linehan Wm., Zbar B., and Lerman Mi. (1993). Identification of the von Hippel-Lindau disease tumour suppressor gene. *Science.* **260**, 1317-1320.

Lazarov M.E., Martin M.M., Willardson B.M., and Elton T.S. (1999). Human phosducin-like protein (hPhLP) messenger RNA stability is regulated by cis-acting instability elements present in the 3 '-untranslated region. *Biochem. Biophys. ACTA.* **1446**, 253-264.

Le Goff C., Zemlyanko O., Moskalenko S., Berkova N., Inge-Vechtomov S., Philippe M., and Zhouravleva G. (2002). Mouse GSPT2, but not GSPT1, can substitute for yeast eRF3 in vivo. *Genes to Cells.* **7**, 1043-1054.

Lee R. H., Ting T. D., Leiberman B. S., Tobias D. E., Lolley R. N., and Ho Y. K. (1992). Regulation of retinal cgmp cascade by phosducin in bovine rod photoreceptor cells - interaction of phosducin and transducin. *J. Biol. Chem.* **267**, 25104-25112.

Lennon G., Auffray C., Polymeropoulos M. and Soares M.B. (1996). 'The I.M.A.G.E. Consortium: An Integrated Molecular Analysis of Genomes and their Expression.' *Genomics.* **33**, 151-152.

Lennon G., Auffray C., Polymeropoulos M., and Soares M. B. (1996). The I.M.A.G.E. consortium: an integrated molecular analysis of genomes and their expression. *Genomics.* **33**, 151-152.

Lewis V. A., Hynes G. M., Zheng D., Saibil H., and Willison K. R. (1992). T-complex polypeptide 1 is a subunit of a heteromeric particle in the eukaryotic cytosol. *Nature.* **358**, 249-252.

Lewis V. A., Hynes G. M., Zhong D., Saibil H., and Willison K. (1992). T-complex polypeptide-1 is a subunit of a heteromeric particle in the eukaryotic cytosol. *Nature.* **358**, 249-252.

Li W-Z., Lin P., Frydman J., Boal T. R., Cardillo T. S., Richard L. M., Toth D., Lichtman L. A., Hartle F-U., Sherman F., and Segel G. B. (1994). Tcp20, a subunit of the eukaryotic TriC chaperonin from humans and yeast. *J. Biol. Chem.* **269**, 18616-18622.

Lin P., and Sherman F. (1997). The unique hetero-oligomeric nature of the subunits in the catalytic cooperativity of the yeast Cct chaperonin complex. *Proc. Natl. Acad. Sci. USA.* **94,** 10780-10785.

Lin P., Cardillo T. S., Richard L. M., Segel G. B., and Sherman F. (1997). Analysis of mutationally altered forms of the Cct6 subunit of the chaperonin from *Saccharomyces cerevisiae. Genetics.* **147**, 1609-1633

Lindquist S. (1997). Mad cows meet psi-chotic yeast: the expansion of the prion hypothesis. *Cell.* **89**, 495-498.

Linehan W. M., Lerman M. I., and Zbar B. (1995). Identification of the von Hippel-Lindau (VHL) gene: its role in renal cancer. *J. Am. Med. Assoc.* **273**, 564-570.

Lingpappa J. R., Martin R. L., Wong M. L., Ganem D., Welch W. J., and Lingpappa V. R. (1994). A eukaryotic cytosolic chaperonin is associated with high molecular weight intermediate in the assembly of hepatitis B virus capsid, a multimeric particle. *J. Cell. Biol.* **125**, 99-111.

Liou A. K. F., and Willison K. R. (1997). Elucidation of the subunit orientation in CCT (chaperonin containing TCP1) from the subunit composition of micro-complexes. *EMBO J.* **16**, 4311-4316.

Liou A. K. F., McCormack E. A., and Willison K. R. (1998). The chaperonin containing TCP-1 (CCT) displays a single ring mediated disassembly and reassembly cycle. *Biol. Chem.* **379**, 311-319.

Llorca O., Martin-benito J., Grantham J., Ricto-Vonsovici M., Willison K. R., Carrascosa J. L., and Valpuesta J. M. (2001). The 'sequential allosteric ring' mechanism in the eukaryotic chaperonin-assisted folding of actin and tubulin. *EMBO. J.* **20**, 4065-4075.

Llorca O., Martin-Benito J., Ritco-Vonsovici M., Grantham J., Hynes G., Willison K. R., Carrascosa J. L., and Valpuesta J. M. (2000). Eukaryotic chaperonin CCT stabilizes actin and tubulin folding intermediates in open quasi-native conformations. *EMBO. J.* **19**, 5971-5979.

Llorca O., McCormack E., Hynes G., Grantham J., Cordell J., Carrascosa J. L., Willison K. R., Fernandez J. J., and Valpuesta J. M. (1999). Eukaryotic type II chaperonin CCT interacts with actin through specific subunits. *Nature.* 402, 693-696.

Llorca O., Smyth M. G., Marco S., Carrascosa J. L., Willison K. R., and Valpuesta J. M. (1998). ATP binding induces large conformational changes in the apical and equatorial domains of the eukaryotic chaperonin containing TCP-1 complex. *J. Biol. Chem.* **273**, 10091-10094.

Maher E. R., and Kaelin W. G. (1997). Von Hippel-Lindau disease. *Medicine.* **76**, 381-391.

Marcotte E. M., Pellegrini M., Thompson M. J., Yeates T. O., and Eisenberg D. (1999). *Nature.* **402**, 83-86.

Martin J., Langer T., Boteva R., Schramel A., Horwich A. L., and Hartl F. U. (1991). Chaperonin-mediated protein folding at the surface of groEL through a 'molten globule'-like intermediate. *Nature.* **352**, 36-42.

Martin J., Mayhew M., Langer T., and Hartl F. U. (1993). The reaction cycle of GroEL and GroES in chaperonin-assisted protein folding. *Nature*. **366**, 228-233.

Maynard Smith J., and Szathmary E. (1995). The major transitions in evolution. W.H. Freeman and company, New York. (Eds; Morimoto R. I., Tissiéres A., and Georgopoulos C.) pp299-312.

McCallum C. D., Do H., Johnson A. E., and Frydman J. (2000). The interaction of the chaperonin tailless complex polypeptide 1 (TCP1) ring complex (TRiC) with ribosome-bound nascent chains examined using photo-cross-linking. *J. Cell. Biol.* **149**, 591-601.

McLoughlin J. N., Thulin C. D., Hart S. J., Resing K. A., Ahn N. G., and Willardson B. M. (2002). Regulatory interaction of the phosducin-like protein with the cytosolic chaperonin complex. *Proc. Natl. Acad. Sci. USA*. **99**, 7962-7967.

Meacham G., Lu Z., King S., Sorscher E., Tousson A., and Cyr D. (1999). The Hdj-2/Hsc70 chaperone pair facilitates early steps in CFTR biogenesis. *EMBO J.* **18**, 1492-1505.

Melki R., Vainberg I. E., Chow R. L., and Cowan N. J. (1993). Chaperonin-mediated folding of vertebrate actin-related protein and γ-tubulin. *J. Cell. Biol.* **122,** 1301-1310.

Miklos D., Caplan S., Mertens D., Hynes G., Pitluk Z., Kashi Y., Harrison-Lavoie K., Stevenson S., Brown C., Barrell B., Horwich A. L., and Willison K. (1994). Primary structure and function of a second essential member of the heterooligomeric TCP1 chaperonin complex of yeast, TCP1β. *Proc. Natl. Acad. Sci. USA*. **91**, 2743-2747.

Miles M.F., Barhite S., Sganga M., and Elliott M. (1993). Phosducin-like protein - an ethanol-responsive potential modulator of guanine-nucleotide-binding protein function. *Proc. Nat. Acad. Sci.USA*. **90**, 10831-10835.

Newman G. P., Wegrzyn R. D., Lindquist S. L., and Chernoff Y. L. (1999). Antagonistic interactions between yeast chaperones Hsp104 and Hsp70 in prion curing. *Mol. Cell. Biol.* **19**, 1325-1333.

O'Farrell P. H. (1975). High resolution two dimensional electrophoresis of proteins. *J. Biol. Chem.* **250**, 4007-4021.

Ohh M., Yauch R. L., Lonergan K. M., Whaley J. M., Stemmerrachaminov A. O., Louis D. N., Gavin B. J., Kley N., Kaelin W. G., and Iliopoulos O. (1998). The Von Hippel-Lindau tumour-suppressor protein is required for proper assembly of an extracellular fibronectin matrix. *Mol. Cell.* **1**, 959-968.

Overbeek R., Fonstein M., D'Souza M., Pusch G. D., and Maltsev N. (2000). The use of gene clusters to infer functional coupling. *Proc. Natl. Acad. Sci. USA.* **96**, 2896-2901.

Ozawa K., Murakami Y., Eki T., Yokoyama K., Soeda E., Hoshino S., Ui M., and Hanaoka F. (1992). Mapping of the human GSPT1 gene, a human homolog of the yeast yeast GST1 gene, to chromosomal band 16p13.1. *Som. Cell. Mol. Genet.* **18**, 189-194.

Pappenberger G., Wilsher J. A., Roe S. M., Counsell D. J., Willison K. R., and Pearl L. H. (2002). Crystal structure of the CCTγ apical domain: Implications for substrate binding to the eukaryotic cytosolic chaperonin. *J. Mol. Biol.* **318**, 1367-1379.

Parham S.N., Resende C.G. and Tute M.F. (2001). 'Oligopeptide repeats in the yeast protein Sup35p stabilize intermolecular prion interactions.' *EMBO J.* **20**, 2111-2119.

Pause A., Lee S., Lonergan K. M., and Klausner R. D. (1998). The von Hippel-Lindau tumour suppressor gene is required for cell cycle exit upon serum withdrawal. *Proc. Natl. Acad. Sci. USA.* **95**, 993-998.

Peters J.M., King R.W., Hoog C., and Kirschner M.W. (1996). Identification of BIME as a subunit of the anaphase-promoting complex. *Science.* **274**, 1199-1201.

Phipps B. M., Hoffman A., Stetter K. O., and Baumeister W. (1991). A novel ATPase complex selectively accumulated upon heat shock is a major cellular component of thermophilic archaebacteria. *EMBO J.* **10**, 1711-1722.

Phipps B. M., Typke D., Hegerl R., Volker S., Hoffman A., Stetter K. O., and Baumeister W. (1993). Structure of a molecular chaperone from a thermophilic archaebacterium. *Nature.* **361**, 475-477.

Prusiner S. B. (1982). Novel proteinaceous infectious particles cause scrapie. *Science.* **216,** 136-144.

Quaite-Randall E., Trent J. D., Josephs R., and Joachimiak A. (1995). Conformational cycle of the archaeosome, a TCP1-like chaperonin from *Sulfolobus-shibatae*. *J. Biol. Chem.* **270**, 28818-28823.

Rasmussen S. W. (1995). A 37.5kb region of yeast chromosome X includes the *SME1, MEF2, GSH1* and *CSD3* genes, a TCP-1-related gene, an open reading frame similar to the *DAL80* gene, and a $tRNA^{Arg}$. *Yeast* **11**, 873-883.

Rodrigues P. (2001). 'An affordable way to reveal peroxidase activity without expensive kits.' http://www.mbshortcuts.com/cgi-bin/protocshow.cgi?pt006.htm

Rommelaere H., De Neve M., Melki R., Vandekerckhove J., and Ampe C. (1993). Eukaryotic cytosolic chaperonin contains t-complex polypeptide 1 and seven related subunits. *Proc. Natl. Acad. Sci. USA.* **90**, 11975-11979.

Roobol A., and Carden M. J. (1993). Identification of chaperonin particles in mammalian brain cytosol and t-complex polypeptide 1 as one of their components. *J. Neurochem.* **60**, 2327-2330.

Roobol A., and Carden M. J. (1999). Subunits of the eukaryotic cytosolic chaperonin CCT do not always behave as components of a uniform hetero-oligomeric particle. *Eur. J. Cell. Biol.* **78,** 21-32.

Roobol A., Grantham. J., Whitaker H. C., and Carden M. J. (1999). Disassembly of the cytosolic chaperonin in mammalian cell extracts at intracellular levels of K^+ and ATP. *J. Biol. Chem.* **27**, 19220-19227.

Roobol A., Holmes F. E., Hayes N. V. L., Baines A. J., and Carden M. J. (1995). Cytoplasmic chaperonin complexes enter neuritis developing *in vitro* and differ in subunit composition within single cells. *J. Cell. Sci.* **108**, 1477-1488.

Rye H.S., Burston S.G., Fenton W.A., Beechem J.M., Xu Z.H., Sigler P.B., and Horwich A.L. (1997). Distinct actions of cis and trans ATP within the double ring of the chaperonin GroEL. *Nature.* **388**, 792-798.

Saibil H. R., Zheng D., Roseman A. M., Hunter A. S., Watson G. M. F., Chen S., Auf Der Mauer A., O' Hara B. P., Wood S. P., Mann N. H., Barnett L. K., and Ellis R. J. (1993). ATP induces large quaternary rearrangements in a cage-like chaperonin structure. *Curr. Biol.* **3**, 265-273.

Schroeder S., and Lohse M. J. (1996). Inhibition of G-protein beta gamma-subunit functions by phosducin-like protein. *Proc. Natl. Acad. Sci. USA.* **93**, 2100-2104.

Schuster B., Neidig M., Alving B. M., and Alving C. R. (1979). Production of antibodies against phosphocholine, phosphotidylcholine, sphingomyelin and lipid A by injection of liposomes containing lipid A. *J. Immun.* **122**, 900-905.

Seixas C., Casalou C., Melo L.V., Nolasco S., Brogueira P., and Soares H. (2003). Subunits of the chaperonin CCT are associated with *Tetrahymena* microtubule structures and are involved in cilia biogenesis. *Exp. Cell Res.* **290**, 303-321.

Serio T. R., and Lindquist S. L. (1999). [PSI+]: An epigenetic modulator of translation termination efficiency. *Annu. Rev. Cell. Dev. Biol.* **15**, 661-703.

Shirayama M., Zachariae W., Ciosk R., and Nasmyth K. (1998). The polo-like kinase Cdc5p and the WD-repeat protein Cdc20p/fizzy are regulators and substrates of the anaphase promoting complex in *Saccharomyces cerevisiae. EMBO. J.* **17**, 1336-1349.

Shuin T., Kondo K., Torigoe S., Kishida T., Kubota Y., Hosaka M., Nagashimi Y., Kitamura H., Latif F., Zbar B., Lerman M.I., Yao M. (1994). Frequent somatic mutations and loss of heterozygosity of the von Hippel-Lindau tumour suppressor gene in primary human renal cell carcinomas. *Cancer. Res.* **54**, 2852-2855.

Shuler K.R., Dunham R.G., & Kanda P. (1992). 'A simplified method for determination of peptide-protein molar ratios using amino-acid-analysis.' *J. Immunol. Methods*. **156,** 137-149.

Siegers K., Waldmann T., Leroux M. R., Grein K., Shevchenko A., Schiebel E., and Hartl F. U. (1999). Compartmentation of protein folding *in vivo*: sequestration of non-native polypeptide by the chaperonin-GimC system. *EMBO. J.* **18**, 75-84.

Silver L. M., Kleen K. C., Distel R. J., and Hecht N. B. (1987). Synthesis of mouse t-complex proteins during haploid stages of spermatogenesis. *Dev. Biol.* **119**, 605-608.

Sonenberg N., and Dever T. E. (2003). Eukaryotic translation initiation factors and regulators. *Curr. Op. Struc. Biol.* **13**, 56-63.

Song H., Mugnier P., Das A.K., Webb H.M., Evans D.R., Tuite M.F., Hemmings B.A. and Barford D. (2000). The crystal structure of human eukaryotic release factor eRF1 – mechanism of stop codon recognition and peptidyl-tRNA hydrolysis. *Cell.* **100**, 311-321.

Soues S., Kann M.L., Fouquet J.P., and Melki R. (2003). The cytosolic chaperonin CCT associates to cytoplasmic microtubular structures during mammalian spermiogenesis and to heterochromatin in germline and somatic cells. *Exp. Cell Res*. **288**, 363-373.

Srikakulam R., and Winkelmann D. A. (1999). Myosin II folding is mediated by a molecular chaperonin. *J. Biol. Chem*. **274**, 27265-27273.

Stansfield I., and Tuite M. F. (1994). Polypeptide chain termination in *Saccharomyces cerevisiae. Curr. Genet.* **25,** 385-395.

Stansfield I., Jones K. M., Kushnirov V. V., Dagkesamanskaya A. R, Poznyakovski A.I., Paushkin S.V., Nierras C.R., Cox B.S., Teravanesyan M.D., and Tuite M.F. (1995). The products of the SUP45 (eRF1) and SUP35 genes interact to mediate translation termination in *Saccharomyces cerevisiae. EMBO. J.* **14**, 4365-4373.

Sternberg N. (1973). Properties of a mutant of *Escherichia coli* defective in bacteriophage lambda head formation (groE). II. The propagation of phage lambda. *J. Mol. Biol*. **76**, 25-44.

Stewart M. L., Grollman A. P., and Huang M-T. (1971). Aurintricarboxylic acid: Inhibitor of initiation of protein synthesis. *Proc. Natl. Acad. Sci.* **68**, 97-101.

Stoldt V., Rademacher F., Kehren V., Ernst J. F., Pearce D. A., and Sherman F. (1996). Review: The Cct eukaryotic chaperonin subunits of *Saccharomyces cerevisiae* and other yeasts. *Yeast*, **12**, 523-529.

Sundell C. L., and Singer R. H. (1990). Actin messenger-RNA localizes in the absence of protein-synthesis. *J. Cell Biol.* **111,** 2397-2403.

Telling G. C., Parchi P., DeArmond S. J., Cortelli P., Montagna P., Gabizon R., Mastrianni J., Lugaresi E., Gambetti P., and Prusiner S. B. (1996). Evidence for the conformation of the pathologic isoform of the prion protein enciphering and propagating prion diversity. *Science.* **274,** 2079-2082.

Ter-Avanesyan M. D., Dagkesamanskaya A. R., Kushnirov V. V., and Smirnov V. N. (1994). The SUP35 omnipotent suppressor gene is involved in the maintenance of the non-Mendelian determinant *[PSI+]* in the yeast *Saccharomyces cerevisiae. Genetics.* **137**, 671-676.

Ter-Avanesyan M. D., Kushnirov V. V., Dagkesamanskaya A. R., Didichenko S. A., Chernoff Y. O., Inge-Vechtomov S. G., and Smirnov V. N. (1993). Deletion analysis of the *SUP35* gene of the yeast *Saccharomyces cerevisiae* reveals two non-overlapping functional regions in the encoded protein. *Mol. Microbiol.* **7**, 683-692.

Thibault C., Sganga M. W., and Miles M. F. (1997). Interaction of phosducin-like protein with G protein beta gamma snbunits. *J. Biol. Chem.* **272**, 12253-12256.

Thompson, J.D., Higgins, D.G. and Gibson, T.J. (1994) CLUSTAL W: improving the sensitivity of progressive multiple sequence alignment through sequence weighting, positions-specific gap penalties and weight matrix choice. *Nucleic Acids Research*, **22**, 4673-4680.

Thulasiraman V., Yang C. F., and Frydman J. (1999). In vivo newly translated polypeptides are sequestered in a protected folding environment. *EMBO. J.* **18**, 85-95.

Thulin C. D., Howes K., Driscoll C. D., Savage J. R., Rand T. A., Baehr W., and Willardson B. M. (1999). The immunolocalization and divergent roles of phosducin and phosducin-like protein in the retina. *Mol. Vis.* **5**, 40.

Todd M. J., Vitanen P. V., and Lorimer G. H. (1993). Hydrolysis of adenine 5'-triphosphate by *Escherichia coli* GroEL: effects of GroES and potassium ion. *Biochem.* **32**, 8560-8567.

Tong A. H., Evangelista M., Parsons A.B., Xu H., Bader G.D., Page N., Robinson M., Raghibizadeh S., Hogue C.W.V., Bussey H., Andrews B., Tyers M., and Boone

C. (2001). Systematic genetic analysis with ordered arrays of yeast deletion mutants. *Science*. **294**, 2364-2368.

Towbin H., Staehelin T., and Gordon J. (1979). Electrophoretic transfer of proteins from polyacrylamide gels to nitrocellulose sheets: procedure and some applications. *Proc. Nat. Acad. Sci. USA*. **76**, 4350-4353.

Trent J. D., Nimmesgern E., Wall J. S., Hartl F. U., and Horwich A. L. (1991). A molecular chaperone from a thermophilic archaebacterium is related to the eukaryotic protein t-complex polypeptide 1. *Nature*. **354**, 490-493.

Uchida N., Hoshino S., Imataka H., Sonenberg N., and Katada T. (2002). A novel role of the mammalian GSPT/eRF3 associating with poly(A)-binding protein in cap/poly(A)-dependent translation. *J. Biol. Chem.* **277,** 50286-50292.

Uetz P., Giot L, Cagney G, Mansfield TA, Judson RS, Knight JR, Lockshon D, Narayan V, Srinivasan M, Pochart P, Qureshi-Emili A, Li Y, Godwin B, Conover D, Kalbfleisch T, Vijayadamodar G, Yang MJ, Johnston M, Fields S, Rothberg JM. (2000). A comprehensive analysis of protein-protein interactions in *Saccharomyces cerevisiae. Nature.* **403,** 623-627.

Ursic D., and Culbertson M. R. (1991). The yeast homologue to mouse *Tcp-1* affects microtubule-mediated processes. *Mol. Cell. Biol.* **11**, 2629-2640.

Ursic D., Sedbrook J. C., Himmel K. L., and Culbertson M. R. (1994). The essential yeast Tcp1 protein affects actin and microtubules. *Mol. Biol. Cell.* **5**, 1065-1080.

Vainberg I. E., Lewis S. A., Rommelaere H., Ampe C., Vandekerckove J., Klein H. L., Cowan N. J. (1998). Prefoldin, a chaperone that delivers unfolded proteins to cytosolic chaperonin. *Cell.* **93**, 863-873.

Van D., Perea J., Jacq C. (1995). Submitted to the protein sequence database, September 1995.

Vinh D. B-N., and Drubin D. G. (1994). A yeast TCP-1 like protein is required for actin function *in vivo. Proc Natl. Acad. Sci. USA*. **91**, 9116-9120.

Visintin R., Prinz S., and Amon A. (1997). CDC20 and CDH1: A family of substrate-specific activators of APC-dependent proteolysis. *Science.* **278**, 460-463.

Vitanen P. V., Donaldson G. K., Lorimer G. H., Lubben T. H., and Gatenby A. A. (1991). Complex interactions between the chaperonin 60 molecular chaperone and dihydrofolate reductase. *Biochem.* **30**, 9716-9723.

Vitanen P., Lubben T., Reed J., Goloubinoff P., O'Keefe D., and Lorimer G. (1990). Chaperonin-facilitated refolding of ribulosebisphosphate carboxylase and ATP

hydrolysis by chaperonin 60 (groEL) are K^+ dependent. *Biochem.* **29**, 5665-5671.

Wainer B. H., and Heller A. (1992). 'Neuronal hybrid cell lines: generation, characterisation, and utility.' Neuronal Cell Lines A Practical Approach, Ed Wood J. N. Chapter 1, Oxford university press, Oxford, England.

Wang J. D., and Weissman J. S. (1999). Thinking outside the box: new insights into the mechanism of GroEL-mediated protein folding. *Nature Struct. Biol.* **6**, 597-600.

Weiss R. B., Murphy J. P., and Gallant J. A. (1984). Genetic screen for cloned release factor genes. *J. Bacteriol.* **158**, 362-364.

Weissman J. S., Fenton W. A., Braig K., Adams P. D., and Horwich A. (1997). *Escherichia coli* GroEL, structure and function. In Guidebook to molecular chaperones and protein folding catalysts. Ed; Gething M. pp173-178, Oxford University Press, Oxford.

Werner G., & McCray J. (1989), 'Production and properties of site-specific antibodies to synthetic peptide antigens related to potential cell surface receptor sites for rhinovirus.' *Methods. Enzymol.* **178**, 676-692.

Werner-Washburne M., Stone D. E., and Craig E. A. (1987). Complex interactions among members of an essential subfamily of hsp70 genes in *Saccharomyces cerevisiae. Mol. Cell. Biol.* **7**, 2568-2577.

Wickner R. B. (1994). [URA3] as an altered URE2 protein: evidence for for a prion analog in *Saccharomyces cerevisiae. Science.* **264**, 566-569.

Willison K. R., and Grantham J. (2001). The roles of the cytosolic chaperonin, CCT, in normal ekaryotic cell growth. In Molecular Chaperones: frontiers in molecular biology (Ed; Lund P.). pp90-118. Oxford university press, Oxford.

Willison K. R., and Horwich A. L. (1996). Chaperonins in archaebacteria and eukaryotic cytosol. In The Chaperonins. Ed; Ellis R. J. pp 107-136. Academic Press, London.

Willison K. R., Dudley K., and Potter J. (1986). Molecular cloning and sequence analysis of a haploid expressed gene encoding t-complex polypeptide 1. *Cell.* **44**, 727-738.

Willison K. R., Dudley K., Goodfellow P., Spurr N., Groves V., Gorman P., Sheer D., and Trowsdale J. (1987). The human homologue of the mouse t-complex gene, *TCP-1*, is located on chromosome 6 but is not near the HLA region. *EMBO J.* **6**, 621-632.

Willison K. R., Hynes G., Davies P., Goldsborough A., and Lewis V. A. (1990). Expression of three t-complex genes, *Tcp-1, D17Leh117c3* and *D17Leh66,* in purified murine spermatogenic cell populations. *Gent. Res. Camb.* **56**, 193-201.

Wilson P. G., and Culbertson M. R. (1988). *SUF12* suppressor protein of yeast. A fusion protein related to the EF-1 family of elongation factors. *J. Mol. Biol.* **199**, 559-573.

Wittinghofer A. (1994). The structure of transducin-G(Alpha-T): More to view than just Ras. *Cell.* **76**, 201-204.

Won K. A., Schumacher R. J., Farr G. W., Horwich A. L., and Reed S. I. (1998). Maturation of human cyclin E requires the function of eukaryotic chaperonin CCT. *Mol. Cell. Biol.* **18**, 7584-7589.

Wray W., Boulikas T., Wray V. P., and Hancock P. (1981). Silver staining of proteins in polyacrylamide gels. *Anal. Biochem.* **18**, 197-203.

Xu Z., Horwich H. L., and Sigler P. B. (1997). The crystal structure of the asymmetric GroEl-GroES-(ADP)7 chaperonin complex. *Nature.* **388**, 741-750.

Yaffe M. B., Farr G. W., Mikolos D., Horwich A. L., Sternlicht M. L., and Sternlicht H. (1992). TCP1 complex is a molecular chaperone in tubulin biogenesis. *Nature*, **358**, 245-248.

Yamada A., Sekiguchi M., Milmura T., and Ozeki Y. (2002). The role of plant CCTα in salt- and osmotic-stress tolerance. *Plant Cell. Physiol.* **43**, 1043-1048.

Yifrach O., and Horovitz A. (1994). Two lines of allosteric communication in the oligomeric chperonin GroEL are revealed by the single mutation Arg 196→ Ala. *J. Mol. Biol.* **243**, 397-401.

Yifrach O., and Horovitz A. (1995). Nested co-operativity in the ATPase activity of the oligomeric chaperonin GroEL. *Biochem.* **34**, 5303-5308.

Yokota S., Yanagi H., Yura T., and Kubota H. (2001). Cytosolic chaperonin CCT changes contents of particular subunit species concomitant with substrate binding and folding activities during the cell cycle. *Eur. J. Biochem.* **268**, 4664-4673.

Yoshida T., Willardson B. M., Wilkins J. F., Jensen G. J., Thornton B. D., and Bitensky M. W. (1994). The phosphorylation state of phosducin determines its ability to block transducin subunit interactions and inhibit transducin binding to activated rhodopsin. *J. Biol. Chem.* **269**, 24050-24057.

Zachariae W., and Nasmyth K. (1999). Whose end is destruction:cell division and the anaphase promoting complex. *Genes Dev.* **13**, 2039-2058.

Zhu X., and Craft C. M. (1998). Interaction of Phosducin and Phosducin Isoforms with a 26S Proteasomal Subunit, SUG1. *Mol. Vis.* **4**, 13.

Zwickl P., Pfeifer G., Lottspeich F., Kopp F., Dahlmann B., and Baumeister W. (1990). Electron microscopy and image analysis reveal common principles of organisation in two large protein complexes: groEL-type proteins and proteosomes. *J. Struct. Biol.* **103**, 197-203.

Cct1p (TCP1)

CCT2 chaperonin of the TCP1 ring complex, cytosolic

CCT3 chaperonin of the TCP1 ring complex, cytosolic

CCT5 T-complex protein 1, epsilon subunit

CCT6 component of chaperonin-containing T-complex (zeta subunit)

YLR030w hypothetical protein

YHR033w strong similarity to glutamate 5-kinase

DUN1 protein kinase

COR1 ubiquinol--cytochrome-c reductase 44K core protein

QCR2 ubiquinol--cytochrome-c reductase 40KD chain II

YJR072c strong similarity to C.elegans hypothetical protein and similarity to YLR243w

HCH1 strong similarity to YDR214w

YDR214w similarity to hypothetical protein YNL281w

RPT3 26S proteasome regulatory subunit

GCD11 translation initiation factor eIF2 gamma chain

SEC53 phosphomannomutase

RNR2 ribonucleoside-diphosphate reductase, small subunit

RFC3 DNA replication factor C, 40 kDa subunit

CPR6 member of the cyclophilin family

TPK3 cAMP-dependent protein kinase 3, catalytic chain

FET4 low affinity Fe(II) iron transport protein

AYR1 1-Acyldihydroxyacetone-phosphate reductase

PDA1 pyruvate dehydrogenase (lipoamide) alpha chain precursor

DHH1 putative RNA helicase of the DEAD box family

ARP2 actin-like protein

RFC5 DNA replication factor C, 40 KD subunit

YCK2 casein kinase I isoform

YBR025c strong similarity to Ylf1p

SNF1 carbon catabolite derepressing ser/thr protein kinase

CFT1 pre-mRNA 3'-end processing factor CF II

CLU1 translation initiation factor eIF3 (p135 subunit)

CTR1 copper transport protein

SEC18 vesicular-fusion protein, functional homolog of NSF

BTN2 Gene/protein whose expression is elevated in a btn1 minus/Btn1p lacking yeast strain

TPK1 cAMP-dependent protein kinase 1, catalytic chain

SEC28 epsilon-COP coatomer subunit

MKK2 protein kinase of the map kinase kinase (MEK) family

PCT1 cholinephosphate cytidylyltransferase

ENT2 clathrin binding protein, required for endocytosis

GAL7 UDP-glucose--hexose-1-phosphate uridylyltransferase

YER049w strong similarity to hypothetical S.pombe protein YER049W

PRB1 protease B, vacuolar

SOF1 involved in 18S pre-rRNA production

RNQ1 prion, epigenetic modifier of protein function

WTM1 transcriptional modulator

PGM2 phosphoglucomutase, major isoform

YKR007w weak similarity to Streptococcus protein M5 precursor

YIL136W protein of the outer mitochondrial membrane

SRP54 signal recognition particle subunit

HEM15 ferrochelatase precursor

TPD3 ser/thr protein phosphatase 2A, regulatory chain A

YGR086c strong similarity to hypothetical protein YPL004c

IME2 ser/thr protein kinase

YER160C Function unknown TyB Gag-Pol protein

SIP2 dominant suppressor of some ts mutations in RPO21 and PRP4

KAP95 karyopherin-beta

SEC26 coatomer complex beta chain of secretory pathway vesicles

OSH7 similarity to KES1P

EAP1 translation initiation factor 4E-associated protein

PPH21 protein ser/thr phosphatase PP2A-1

GSY1 UDP glucose--starch glucosyltransferase, isoform 1

RFC2 DNA replication factor C, 41 KD subunit

NAP1 nucleosome assembly protein I

YJU2/CWC16 function unknown (but essential)

BRX1 strong similarity to C.elegans K12H4.3 protein

TIF35 translation initiation factor eIF3 (p33 subunit)

ARG4 arginosuccinate lyase

YJR070c similarity to C.elegans hypothetical protein C14A4.1

VPS13 involved in regulating membrane traffic

YLR326w hypothetical protein

STE4 GTP-binding protein beta subunit of the pheromone pathway

RAD28 protein involved in the same pathway as RAD26P, has beta-transducin (WD-40) repeats

CCT4 component of chaperonin-containing T-complex

DED81 asparaginyl-tRNA-synthetase

DIA4 strong similarity to seryl-tRNA synthetases

TUB1 alpha-1 tubulin

CAF4 CCR4 associated factor

EGD1 GAL4 DNA-binding enhancer protein

GPA1 GTP-binding protein alpha subunit of the pheromone pathway

RVS161 similarity to human amphiphysin and RVS167P

STE12 transcriptional activator

PWP1 similarity to human IEF SSP 9502 protein

COP1 coatomer complex alpha chain of secretory pathway vesicles

CDC28 cyclin-dependent protein kinase

BCY1 cAMP dependent protein kinase, regulatory subunit

YNL181w similarity to hypothetical S. pombe protein

isocitrate dehydrogenase (NAD+) subunit 1, mitochondrial

WTM2 transcriptional modulator

HGH1 weak similarity to human HMG1P and HMG2P

MDH1 malate dehydrogenase precursor, mitochondrial

YDL204w similarity to hypothetical protein YDR233c

RRP5 processing of pre-ribosomal RNA

YCR076c weak similarity to latent transforming growth factor beta binding protein 3' H. sapiens

YBL029w hypothetical protein

YKR046c hypothetical protein

ATP3 F1F0-ATPase complex, F1 gamma subunit

MAE1 malic enzyme

NMD5 NAM7P interacting protein

STI1 stress-induced protein

RPN7 subunit of the regulatory particle of the proteasome

PRO3 delta 1-pyrroline-5-carboxylate reductase

ARC35 subunit of the ARP2/3 complex

SNF4 nuclear regulatory protein

MET10 sulfite reductase flavin-binding subunit

YBR187w similarity to mouse putative transmembrane protein FT27

SOD1 copper-zinc superoxide dismutase

SEC27 coatomer complex beta' chain (beta'-cop) of secretory pathway vesicles

PRP19 non-snRNP sliceosome component required for DNA repair

KRE33 similarity to A.ambisexualis antheridiol steroid receptor

PPH3 protein ser/thr phosphatase

LEM3 similarity to Ycx1p

YNL201c weak similarity to pleiotropic drug resistance control protein PDR6

PFS2 polyadenylation factor I subunit 2 required for mRNA 3'-end processing, bridges two mRNA 3'-end processing factors

MAD3 spindle-assembly checkpoint protein

GPT2 strong similarity to SCT1P

IDH2 isocitrate dehydrogenase (NAD+) subunit 2, mitochondrial

RAD24 cell cycle checkpoint protein

SNU66 component of U4/U6.U5 snRNP

PET9 ADP/ATP carrier protein (MCF)

PRE10 20S proteasome subunit C1 (alpha7)

TAF90 TFIID and SAGA subunit

TPK2 cAMP-dependent protein kinase 2, catalytic chain

CDC55 ser/thr phosphatase 2A regulatory subunit B

CDC20 cell division control protein

RIM15 protein kinase involved in expression of meiotic genes

TIF2 translation initiation factor eIF4A

YBL046w weak similarity to hypothetical protein YOR054c

YNK1 nucleoside diphosphate kinase

SEC21 coatomer complex gamma chain (gamma-COP) of secretory pathway vesicles

YHR198c strong similarity to hypothetical protein YHR199c

YHR199c strong similarity to hypothetical protein YHR198c

GCN1 translational activator

RET2 coatomer complex delta chain

YKL187c strong similarity to hypothetical protein YLR413w

YLR413w strong similarity to YKL187c

HXT7 high-affinity hexose transporter

RPN1 26S proteasome regulatory subunit

PPH22 protein ser/thr phosphatase PP2A-2

NMD3 nonsense-mediated mRNA decay protein

TIF34 translation initiation factor eIF3, p39 subunit

GAL83 glucose repression protein

ERG27 3-keto sterol reductase

ADE17 5-aminoimidazole-4-carboxamide ribotide transformylase

Cct2p

CCT3 chaperonin of the TCP1 ring complex, cytosolic

TCP1 component of chaperonin-containing T-complex

CCT6 component of chaperonin-containing T-complex (zeta subunit)

CCT5 T-complex protein 1, epsilon subunit

YHR033w strong similarity to glutamate 5-kinase

NAP1 nucleosome assembly protein I

BRX1 strong similarity to C.elegans K12H4.3 protein

YJR070c similarity to C.elegans hypothetical protein C14A4.1

STE12 transcriptional activator

YJR072c strong similarity to C.elegans hypothetical protein and similarity to YLR243w

KRE33 similarity to A.ambisexualis antheridiol steroid receptor

RPN6 subunit of the regulatory particle of the proteasome

RVB1 RUVB-like protein

SEN2 tRNA splicing endonuclease beta subunit

MDS3 negative regulator of early meiotic expression

YBL049w strong similarity to hypothetical protein - human

RNR2 ribonucleoside-diphosphate reductase, small subunit

CPR6 member of the cyclophilin family

SEC26 coatomer complex beta chain of secretory pathway vesicles

OSH7 similarity to KES1P

EAP1 translation initiation factor 4E-associated protein

CLU1 translation initiation factor eIF3 (p135 subunit)

HTB1 histone H2B

PPH21 protein ser/thr phosphatase PP2A-1

HSP60 heat shock protein - chaperone, mitochondrial

CDC25 GDP/GTP exchange factor for RAS1P and RAS2P

FZO1 required for biogenesis of mitochondria

YDR239c hypothetical protein

YCL039w similarity to TUP1P general repressor of RNA polymerase II transcription

UBI4 ubiquitin

YDL156w weak similarity to Pas7p

TIF35 translation initiation factor eIF3 (p33 subunit)

ARG4 arginosuccinate lyase

UBR1 ubiquitin-protein ligase

HAS1 helicase associated with SET1P

YOL078w similarity to stress activated MAP kinase interacting protein S. pombe

STE4 GTP-binding protein beta subunit of the pheromone pathway

RAD28 protein involved in the same pathway as RAD26P, has beta-transducin (WD-40) repeats

CCT4 component of chaperonin-containing T-complex

VID28 similarity to S. pombe SPAC26H5.04 protein of unknown function

DIA4 strong similarity to seryl-tRNA synthetases

RPN10 26S proteasome regulatory subunit

SAP190 SIT4P-associated protein

CLB2 cyclin, G2/M-specific

DIG2 MAP kinase-associated protein, down-regulator of invasive growth and mating

YNL187w hypothetical protein

QCR2 ubiquinol--cytochrome-c reductase 40KD chain II

CAF4 CCR4 associated factor

GPA1 GTP-binding protein alpha subunit of the pheromone pathway

RVS161 similarity to human amphiphysin and RVS167P

FET4 low affinity Fe(II) iron transport protein

PWP1 similarity to human IEF SSP 9502 protein

KSS1 ser/thr protein kinase of the MAP kinase family

YNL101w similarity to YKL146w

NEW1 similarity to translation elongation factor eEF3

STE7 ser/thr/tyr protein kinase of MAP kinase kinase family

COP1 coatomer complex alpha chain of secretory pathway vesicles

CDC28 cyclin-dependent protein kinase

VID30 weak similarity to human RANBPM NP_005484.1

SSD1 involved in the tolerance to high concentration of Ca2+

IME2 ser/thr protein kinase

YNL181w similarity to hypothetical S. pombe protein

SIK1 involved in pre-rRNA processing

IDH1 isocitrate dehydrogenase (NAD+) subunit 1, mitochondrial

FAB1 phosphatidylinositol 3-phosphate 5-kinase

WTM2 transcriptional modulator

MRPL3 ribosomal protein of the large subunit, mitochondrial

AYR1 1-Acyldihydroxyacetone-phosphate reductase

THI3 positive regulation factor of thiamin metabolism

HGH1 weak similarity to human HMG1P and HMG2P

MDH1 malate dehydrogenase precursor, mitochondrial

YDL204w similarity to hypothetical protein YDR233c

HCH1 strong similarity to YDR214w

YDR214w similarity to hypothetical protein YNL281w

YPR034W component of SWI-SNF global transcription activator complex and RSC chromatin remodeling complex

RRP5 processing of pre-ribosomal RNA

YCR076c weak similarity to latent transforming growth factor beta binding protein 3' H. sapiens

PIM1 ATP-dependent protease, mitochondrial

YBL029w hypothetical protein

YKR046c hypothetical protein

YBR025c strong similarity to Ylf1p

ATP3 F1F0-ATPase complex, F1 gamma subunit

STI1 stress-induced protein

YNL047c similarity to probable transcription factor ASK10P and hypothetical protein YPR115w, and strong similarity to hypothetical protein YIL105c

YPR115w similarity to probable transcription factor ASK10P, and to YNL047c and YIL105c

RPN7 subunit of the regulatory particle of the proteasome

YER049w strong similarity to hypothetical S.pombe protein YER049W

HIR1 histone transcription regulator

YJL109c weak similarity to ATPase DRS2P

YGL041c weak similarity to YJL109c

FYV8 weak similarity to Tetrahymena acidic repetitive protein ARP1

PDA1 pyruvate dehydrogenase (lipoamide) alpha chain precursor

DHH1 putative RNA helicase of the DEAD box family

GIM4 Gim complex component

PEX7 peroxisomal import protein - peroxin

ARP2 actin-like protein

BCK2 suppressor of mutations in protein kinase C pathway components

YCK2 casein kinase I isoform

CFT1 pre-mRNA 3'-end processing factor CF II

MSE1 glutamyl-tRNA synthetase, mitochondrial

YNL085w required for propagation of M2 dsRNA satellite of L-A virus

CTR1 copper transport protein

SEC18 vesicular-fusion protein, functional homolog of NSF

Gene/protein whose expression is elevated in a btn1 minus/Btn1p lacking yeast strain

SEC28 epsilon-COP coatomer subunit

MKK2 protein kinase of the map kinase kinase (MEK) family

PCT1 cholinephosphate cytidylyltransferase

ENT2 clathrin binding protein, required for endocytosis

GAL7 UDP-glucose--hexose-1-phosphate uridylyltransferase

YOR267c similarity to ser/thr protein kinases

PRB1 protease B, vacuolar

YKE2 Gim complex component

STE11 ser/thr protein kinase of the MEKK family

RNQ1 prion, epigenetic modifier of protein function

STV1 H+-ATPase V0 domain 102 KD subunit, not vacuolar

SOF1 involved in 18S pre-rRNA production

YKR007w weak similarity to Streptococcus protein M5 precursor

PGM2 phosphoglucomutase, major isoform

WTM1 transcriptional modulator

POL5 DNA polymerase V

BEM2 GTPase-activating protein

SIT4 ser/thr protein phosphatase

SEC53 phosphomannomutase

YIL136W protein of the outer mitochondrial membrane

DUN1 protein kinase

SRP54 signal recognition particle subunit

YGL068w strong similarity to Cricetus mitochrondial ribosomal L12 protein

HEM15 ferrochelatase precursor

CDH1 substrate-specific activator of APC-dependent proteolysis

TPD3 ser/thr protein phosphatase 2A, regulatory chain A

NAN1 weak similarity to fruit fly TFIID subunit p85

YER160C Function unknown TyB Gag-Pol protein

YGR086c strong similarity to hypothetical protein YPL004c

KRE31 similarity to M.sexta steroid regulated MNG10 protein

COR1 ubiquinol--cytochrome-c reductase 44K core protein

LAP4 aminopeptidase yscI precursor, vacuolar

PRO3 delta 1-pyrroline-5-carboxylate reductase

MYO2 myosin heavy chain

UBP15 similarity to human ubiquitin-specific protease

YBR187w similarity to mouse putative transmembrane protein FT27

SEC27 coatomer complex beta' chain (beta'-cop) of secretory pathway vesicles

PPH3 protein ser/thr phosphatase

YNL201c weak similarity to pleiotropic drug resistance control protein PDR6

PFS2 polyadenylation factor I subunit 2 required for mRNA 3'-end processing, bridges two mRNA 3'-end processing factors

SEN1 positive effector of tRNA-splicing endonuclease

ACC1 acetyl-CoA carboxylase

MAD3 spindle-assembly checkpoint protein

GFA1 glucosamine--fructose-6-phosphate transaminase

GPT2 strong similarity to SCT1P

YMR135c weak similarity to conserved hypothetical protein S. pombe

RPT3 26S proteasome regulatory subunit

PYC1 pyruvate carboxylase 1

CIN8 kinesin-related protein

PET9 ADP/ATP carrier protein (MCF)

SNU66 component of U4/U6.U5 snRNP

ACO1 aconitate hydratase

PRE10 20S proteasome subunit C1 (alpha7)

GCD11 translation initiation factor eIF2 gamma chain

TIF4631 mRNA cap-binding protein (eIF4F), 150K subunit

SAP185 SIT4P-associating protein

TAF90 TFIID and SAGA subunit

YKL056c strong similarity to human IgE-dependent histamine-releasing factor

CDC55 ser/thr phosphatase 2A regulatory subunit B

YKL195w similarity to rabbit histidine-rich calcium-binding protein

PHO84 high-affinity inorganic phosphate/H+ symporter

RPA135 DNA-directed RNA polymerase I, 135 KD subunit

PMA1 H+-transporting P-type ATPase, major isoform, plasma membrane

BUD3 budding protein

YDR255c weak similarity to hypothetical S.pombe hypothetical protein SPBC29A3

CDC20 cell division control protein

SAP155 SIT4P-associated protein

CYS4 cystathionine beta-synthase

YBL046w weak similarity to hypothetical protein YOR054c

SEC21 coatomer complex gamma chain (gamma-COP) of secretory pathway vesicles

YBL059w weak similarity to hypothetical protein YER093c-a

YER093c weak similarity to S.epidermidis PepB protein

YER093c-a similarity to hypothetical protein YBL059w

YGR090w similarity to PIR:T40678 hypothetical protein SPBC776.08c S. pombe

SEC6 protein transport protein

RET2 coatomer complex delta chain

TEC1 Ty transcription activator

HXT6 high-affinity hexose transporter

RRP12 hypothetical protein

PPH22 protein ser/thr phosphatase PP2A-2

TIF34 translation initiation factor eIF3, p39 subunit

ERG27 3-keto sterol reductase

BEM3 GTPase-activating protein for CDC42P and RHO1P

ADE17 5-aminoimidazole-4-carboxamide ribotide transformylase

YGL245w strong similarity to glutamine--tRNA ligase

DIG1 MAP kinase-associated protein, down-regulator of invasive growth and mating

YLR154c hypothetical protein

Cct3p

CCT2 chaperonin of the TCP1 ring complex, cytosolic

TCP1 component of chaperonin-containing T-complex

CCT5 T-complex protein 1, epsilon subunit

CCT6 component of chaperonin-containing T-complex (zeta subunit)

YHR033w strong similarity to glutamate 5-kinase

YJR072c strong similarity to C.elegans hypothetical protein and similarity to YLR243w

CLU1 translation initiation factor eIF3 (p135 subunit)

BRX1 strong similarity to C.elegans K12H4.3 protein

SRP54 signal recognition particle subunit

MKK2 protein kinase of the map kinase kinase (MEK) family

HCH1 strong similarity to YDR214w

YDR214w similarity to hypothetical protein YNL281w

ATP3 F1F0-ATPase complex, F1 gamma subunit

KRE33 similarity to A.ambisexualis antheridiol steroid receptor

YBL049w strong similarity to hypothetical protein - human

YKR051w similarity to C.elegans hypothetical protein

YER077c hypothetical protein

YGR266w hypothetical protein

DHH1 putative RNA helicase of the DEAD box family

ARP2 actin-like protein

FOL2 GTP cyclohydrolase I

TPS1 alpha,alpha-trehalose-phosphate synthase, 56 KD subunit

PRE1 20S proteasome subunit C11(beta4)

OYE2 NADPH dehydrogenase (old yellow enzyme), isoform 1

ILV2 acetolactate synthase

ENT2 clathrin binding protein, required for endocytosis

RPN6 subunit of the regulatory particle of the proteasome

YKE2 Gim complex component

PGM2 phosphoglucomutase, major isoform

WTM1 transcriptional modulator

POL5 DNA polymerase V

HEM15 ferrochelatase precursor

APT1 adenine phosphoribosyltransferase

TPD3 ser/thr protein phosphatase 2A, regulatory chain A

YNLPOR1 mitochondrial outer membrane porin

KRE31 similarity to M.sexta steroid regulated MNG10 protein

YKU80 component of DNA end-joining repair pathway

LAP4 aminopeptidase yscI precursor, vacuolar

YML020w hypothetical protein

UBP15 similarity to human ubiquitin-specific protease

MAD3 spindle-assembly checkpoint protein

CCT2 chaperonin of the TCP1 ring complex, cytosolic

SNU66 component of U4/U6.U5 snRNP

CIN8 kinesin-related protein

RVB1 RUVB-like protein

TAF90 TFIID and SAGA subunit

CDC55 ser/thr phosphatase 2A regulatory subunit B

YDR255c weak similarity to hypothetical S.pombe hypothetical protein SPBC29A3

CDC20 cell division control protein

ACC1 acetyl-CoA carboxylase

YBL046w weak similarity to hypothetical protein YOR054c

YKL187c strong similarity to hypothetical protein YLR413w

YLR413w strong similarity to YKL187c

GIM4 Gim complex component

ADR1 zinc-finger transcription factor

MET16 3'-phosphoadenylylsulfate reductase

OSH7 similarity to KES1P

MYO2 myosin heavy chain

HTB1 histone H2B

PPH21 protein ser/thr phosphatase PP2A-1

RAD24 cell cycle checkpoint protein

RFC2 DNA replication factor C, 41 KD subunit

FZO1 required for biogenesis of mitochondria

LYS12 homo-isocitrate dehydrogenase

RRP12 hypothetical protein

NAP1 nucleosome assembly protein I

PUP3 20S proteasome subunit (beta3)

YCL039w similarity to TUP1P general repressor of RNA polymerase II transcription

PHO86 inorganic phospate transporter

GPH1 glycogen phosphorylase

YDL156w weak similarity to Pas7p

YER160C Function unknown TyB Gag-Pol protein

DPB2 DNA-directed DNA polymerase epsilon, subunit B

YNL201c weak similarity to pleiotropic drug resistance control protein PDR6

RPN12 26S proteasome regulatory subunit

UBR1 ubiquitin-protein ligase

SIP1 multicopy suppressor of SNF1

YNL108c strong similarity to YOR110w TFC7 TFIIIC (transcription initiation factor) subunit, 55 kDa

YOL078w similarity to stress activated MAP kinase interacting protein S. pombe

TIF4631 mRNA cap-binding protein (eIF4F), 150K subunit

VID31 similarity to glutenin, high molecular weight chain proteins and SNF5P

STE4 GTP-binding protein beta subunit of the pheromone pathway

SOF1 involved in 18S pre-rRNA production

CCT4 component of chaperonin-containing T-complex

YBT1 yeast bile transporter

YMR226c similarity to ketoreductases

VID28 similarity to S. pombe SPAC26H5.04 protein of unknown function

DIA4 strong similarity to seryl-tRNA synthetases

CLB2 cyclin, G2/M-specific

QCR2 ubiquinol--cytochrome-c reductase 40KD chain II

CAF4 CCR4 associated factor

LST8 required for transport of permeases from the golgi to the plasma membrane

YGR090w similarity to PIR:T40678 hypothetical protein SPBC776.08c S. pombe

GPA1 GTP-binding protein alpha subunit of the pheromone pathway

SEC6 protein transport protein

DUN1 protein kinase

SIS1 heat shock protein

STE12 transcriptional activator

PPH22 protein ser/thr phosphatase PP2A-2

RFC5 DNA replication factor C, 40 KD subunit

PWP1 similarity to human IEF SSP 9502 protein

NOG2 strong similarity to human breast tumor associated autoantigen

TEM1 GTP-binding protein of the RAS superfamily

PDX1 pyruvate dehydrogenase complex protein X

NEW1 similarity to translation elongation factor eEF3

YPR003c similarity to sulphate transporter proteins

CPA2 arginine-specific carbamoylphosphate synthase, large chain

PUF3 transcript-specific regulator of mRNA degradation

COP1 coatomer complex alpha chain of secretory pathway vesicles

CDC28 cyclin-dependent protein kinase

FYV10 weak similarity to erythroblast macrophage protein EMP Mus musculus

RPT3 26S proteasome regulatory subunit

SEC53 phosphomannomutase

VID30 weak similarity to human RANBPM NP_005484.1

YDR453c strong similarity to thiol-specific antioxidant proteins

RNQ1 prion, epigenetic modifier of protein function

YKL056c strong similarity to human IgE-dependent histamine-releasing factor

SSD1 involved in the tolerance to high concentration of Ca2+

GCD11 translation initiation factor eIF2 gamma chain

ARC40 ARP2/3 protein complex subunit, 40 kilodalton

PST2 strong similarity to S.pombe obr1 brefeldin A resistance protein

VMA8 H+-ATPsynthase V1 domain 32 KD subunit, vacuolar

SIK1 involved in pre-rRNA processing

PPH3 protein ser/thr phosphatase

PHO85 cyclin-dependent protein kinase

IDH1 isocitrate dehydrogenase (NAD+) subunit 1, mitochondrial

RFC3 DNA replication factor C, 40 kDa subunit

WTM2 transcriptional modulator

CDH1 substrate-specific activator of APC-dependent proteolysis

BUD3 budding protein

MDH1 malate dehydrogenase precursor, mitochondrial

ECM10 heat shock protein of HSP70 family

YGL068w strong similarity to Cricetus mitochrondial ribosomal L12 protein

LSC1 succinate-CoA ligase alpha subunit

ARO1 arom pentafunctional enzyme

PEX7 peroxisomal import protein - peroxin

RRP3 required for maturation of the 35S primary transcript

NAN1 weak similarity to fruit fly TFIID subunit p85

SLC1 fatty acyltransferase

RRP5 processing of pre-ribosomal RNA

FUN12 general translation factor eIF2 homolog

YCK2 casein kinase I isoform

SEN2 tRNA splicing endonuclease beta subunit

ADE17 5-aminoimidazole-4-carboxamide ribotide transformylase

YBL029w hypothetical protein

YBR025c strong similarity to Ylf1p

MSU1 3'-5' exonuclease for RNA 3' ss-tail, mitochondrial

GAL7 UDP-glucose--hexose-1-phosphate uridylyltransferase

SLX1 similarity to hypothetical A.thaliana protein

SOD2 superoxide dismutase (Mn) precursor, mitochondrial

STI1 stress-induced protein

YMR135c weak similarity to conserved hypothetical protein S. pombe

YDR128w weak similarity to SEC27P, YMR131c and human retinoblastoma-binding protein

HIR1 histone transcription regulator

YJL109c weak similarity to ATPase DRS2P

YGL041c weak similarity to YJL109c

Cct4p

AAC3 ADP/ATP carrier protein (MCF)

GUT1 glycerol kinase

CCT2 chaperonin of the TCP1 ring complex, cytosolic

GCD2 translation initiation factor eIF2B, 71 kDa (delta) subunit

CHC1 clathrin heavy chain

SAC6 actin filament bundling protein, fimbrin

GCD6 translation initiation factor eIF2b epsilon, 81 kDa subunit

TCP1 component of chaperonin-containing T-complex

GCD1 translation initiation factor eIF2bgamma subunit

GCD11 translation initiation factor eIF2 gamma chain

SRV2 adenylate cyclase-associated protein, 70kDa

ACT1 actin

GCN20 positive effector of GCN2P

SLC1 fatty acyltransferase

RPT1 26S proteasome regulatory subunit

FAS1 fatty-acyl-CoA synthase, beta chain

ECM29 involved in cell wall biogenesis and architecture

KAP123 RAN-binding protein

GCD7 translation initiation factor eIF2b, 43 kDa subunit

GCN1 translational activator

GCN3 translation initiation factor eIF2B, 34 KD, alpha subunit

SUI3 translation initiation factor eIF2 beta subunit

RGR1 DNA-directed RNA polymerase II holoenzyme subunit

SEC7 component of non-clathrin vesicle coat

CCT3 chaperonin of the TCP1 ring complex, cytosolic

Cct5p

ACC1 acetyl-CoA carboxylase

ARP2 actin-like protein

TCP1 component of chaperonin-containing T-complex

CCT3 chaperonin of the TCP1 ring complex, cytosolic

CCT2 chaperonin of the TCP1 ring complex, cytosolic

CCT6 component of chaperonin-containing T-complex (zeta subunit)

YHR033w strong similarity to glutamate 5-kinase

QCR2 ubiquinol--cytochrome-c reductase 40KD chain II

YJR072c strong similarity to C.elegans hypothetical protein and similarity to YLR243w

ATP3 F1F0-ATPase complex, F1 gamma subunit

GCD11 translation initiation factor eIF2 gamma chain

MKK2 protein kinase of the map kinase kinase (MEK) family

SRP54 signal recognition particle subunit

RPN12 26S proteasome regulatory subunit

YKR051w similarity to C.elegans hypothetical protein

ARC18 subunit of the ARP2/3 complex

YER077c hypothetical protein

YGR266w hypothetical protein

DHH1 putative RNA helicase of the DEAD box family

RRP3 required for maturation of the 35S primary transcript

PEX7 peroxisomal import protein - peroxin

YCK2 casein kinase I isoform

FOL2 GTP cyclohydrolase I

YBR025c strong similarity to Ylf1p

MET16 3'-phosphoadenylylsulfate reductase

CFT1 pre-mRNA 3'-end processing factor CF II

TPS1 alpha,alpha-trehalose-phosphate synthase, 56 KD subunit

PRE1 20S proteasome subunit C11(beta4)

CLU1 translation initiation factor eIF3 (p135 subunit)

PRP46 strong similarity to A.thaliana PRL1 and PRL2 proteins

OYE2 NADPH dehydrogenase (old yellow enzyme), isoform 1

ILV2 acetolactate synthase

YNL108c strong similarity to YOR110w

TFC7 TFIIIC (transcription initiation factor) subunit, 55 kDa

ENT2 clathrin binding protein, required for endocytosis

GAL7 UDP-glucose--hexose-1-phosphate uridylyltransferase

RPN6 subunit of the regulatory particle of the proteasome

VID31 similarity to glutenin, high molecular weight chain proteins and SNF5P

RNQ1 prion, epigenetic modifier of protein function

SOF1 involved in 18S pre-rRNA production

LST8 required for transport of permeases from the golgi to the plasma membrane

SIT4 ser/thr protein phosphatase

SEC53 phosphomannomutase

DUN1 protein kinase

HEM15 ferrochelatase precursor

TPD3 ser/thr protein phosphatase 2A, regulatory chain A

APT1 adenine phosphoribosyltransferase

YER160C Function unknown TyB Gag-Pol protein

YLR386w similarity to hypothetical S. pombe protein

POR1 mitochondrial outer membrane porin

YKU80 component of DNA end-joining repair pathway

COR1 ubiquinol--cytochrome-c reductase 44K core protein

LAP4 aminopeptidase yscI precursor, vacuolar

ARC35 subunit of the ARP2/3 complex

PFK1 6-phosphofructokinase, alpha subunit

ADR1 zinc-finger transcription factor

OSH7 similarity to KES1P

PPH21 protein ser/thr phosphatase PP2A-1

FZO1 required for biogenesis of mitochondria

LYS12 homo-isocitrate dehydrogenase

NAP1 nucleosome assembly protein I

YKL095W YJU2/CWC16 function unknown (but essential)

BRX1 strong similarity to C.elegans K12H4.3 protein

PHO86 inorganic phospate transporter

DPB2 DNA-directed DNA polymerase epsilon, subunit B

UBR1 ubiquitin-protein ligase

SIP1 multicopy suppressor of SNF1

YOL078w similarity to stress activated MAP kinase interacting protein S. pombe

STE4 GTP-binding protein beta subunit of the pheromone pathway

DED81 asparaginyl-tRNA-synthetase

YBT1 yeast bile transporter

YMR226c similarity to ketoreductases

CAF4 CCR4 associated factor

EGD1 GAL4 DNA-binding enhancer protein

GPA1 GTP-binding protein alpha subunit of the pheromone pathway

PWP1 similarity to human IEF SSP 9502 protein

NOG2 strong similarity to human breast tumor associated autoantigen

PDX1 pyruvate dehydrogenase complex protein X

NEW1 similarity to translation elongation factor eEF3

COP1 coatomer complex alpha chain of secretory pathway vesicles

ARP3 actin related protein

PST2 strong similarity to S.pombe obr1 brefeldin A resistance protein

ARC40 ARP2/3 protein complex subunit, 40 kilodalton

VMA8 H+-ATPsynthase V1 domain 32 KD subunit, vacuolar

ARC19 subunit of the ARP2/3 complex

IDH1 isocitrate dehydrogenase (NAD+) subunit 1, mitochondrial

PHO85 cyclin-dependent protein kinase

HGH1 weak similarity to human HMG1P and HMG2P

MDH1 malate dehydrogenase precursor, mitochondrial

ECM10 heat shock protein of HSP70 family

HCH1 strong similarity to YDR214w

YDR214w similarity to hypothetical protein YNL281w

LSC1 succinate-CoA ligase alpha subunit

RRP5 processing of pre-ribosomal RNA

YBL029w hypothetical protein

YLR271w weak similarity to hypothetical protein T04H1.5 C. elegans

MSU1 3'-5' exonuclease for RNA 3' ss-tail, mitochondrial

SLX1 similarity to hypothetical A.thaliana protein

SOD2 superoxide dismutase (Mn) precursor, mitochondrial

STI1 stress-induced protein

MYO2 myosin heavy chain

YML020w hypothetical protein

SOD1 copper-zinc superoxide dismutase

PRP19 non-snRNP sliceosome component required for DNA repair

KRE33 similarity to A.ambisexualis antheridiol steroid receptor

PFS2 polyadenylation factor I subunit 2 required for mRNA 3'-end processing, bridges two mRNA 3'-end processing factors

MAD3 spindle-assembly checkpoint protein

SNU66 component of U4/U6.U5 snRNP

SIS1 heat shock protein

CCT8 component of chaperonin-containing T-complex

PUF3 transcript-specific regulator of mRNA degradation

YDR453c strong similarity to thiol-specific antioxidant proteins

TAF90 TFIID and SAGA subunit

SLC1 fatty acyltransferase

FUN12 general translation factor eIF2 homolog

CDC55 ser/thr phosphatase 2A regulatory subunit B

ARC15 subunit of the ARP2/3 complex

SEN2 tRNA splicing endonuclease beta subunit

CDC20 cell division control protein

TIF2 translation initiation factor eIF4A

PUP3 20S proteasome subunit (beta3)

YNK1 nucleoside diphosphate kinase

CPA2 arginine-specific carbamoylphosphate synthase, large chain

SEC6 protein transport protein

PPH22 protein ser/thr phosphatase PP2A-2

NMD3 nonsense-mediated mRNA decay protein

YPR003c similarity to sulphate transporter proteins

ARO1 arom pentafunctional enzyme

TEM1 GTP-binding protein of the RAS superfamily

ADE17 5-aminoimidazole-4-carboxamide ribotide transformylase

YDR128w weak similarity to SEC27P, YMR131c and human retinoblastoma-binding protein

Cct6p

RNQ1 prion, epigenetic modifier of protein function

TAP42 component of the Tor signaling pathway

CCT2 chaperonin of the TCP1 ring complex, cytosolic

TCP1 component of chaperonin-containing T-complex

CCT3 chaperonin of the TCP1 ring complex, cytosolic

CCT5 T-complex protein 1, epsilon subunit

BRX1 strong similarity to C.elegans K12H4.3 protein

YHR033w strong similarity to glutamate 5-kinase

RNR2 ribonucleoside-diphosphate reductase, small subunit

ARP2 actin-like protein

WTM1 transcriptional modulator

CPR6 member of the cyclophilin family

RVB1 RUVB-like protein

SEC53 phosphomannomutase

WTM2 transcriptional modulator

KRE33 similarity to A.ambisexualis antheridiol steroid receptor

ATP3 F1F0-ATPase complex, F1 gamma subunit

MAE1 malic enzyme

THI21 similarity to B.subtilis transcriptional activator tenA, and strong similarity to hypothetical proteins YOL055c and YPR121w

YGL111w weak similarity to hypothetical protein S. pombe

DHH1 putative RNA helicase of the DEAD box family

CFT1 pre-mRNA 3'-end processing factor CF II

CTR1 copper transport protein

ENT2 clathrin binding protein, required for endocytosis

PRB1 protease B, vacuolar

RPN6 subunit of the regulatory particle of the proteasome

PGM2 phosphoglucomutase, major isoform

POL5 DNA polymerase V

MUB1 involved in budding

YER002w weak similarity to chicken microfibril-associated protein

YBR187w similarity to mouse putative transmembrane protein FT27

THR1 homoserine kinase

PFS2 polyadenylation factor I subunit 2 required for mRNA 3'-end processing, bridges two mRNA 3'-end processing factors

CIN8 kinesin-related protein

PET9 ADP/ATP carrier protein (MCF)

PRE10 20S proteasome subunit C1 (alpha7)

YGL245w strong similarity to glutamine--tRNA ligase

ERB1 weak similarity to A.thaliana PRL1 protein

YER006w similarity to P.polycephalum myosin-related protein mlpA

CAF130 hypothetical protein

MDJ1 heat shock protein - chaperone

NPR2 nitrogen permease regulator

SEC26 coatomer complex beta chain of secretory pathway vesicles

SEC26 coatomer complex beta chain of secretory pathway vesicles

PFK1 6-phosphofructokinase, alpha subunit

YDR412w similarity to hypothetical protein SPAC29A4.09 - S. pombe

COR1 ubiquinol--cytochrome-c reductase 44K core protein

OSH7 similarity to KES1P

EAP1 translation initiation factor 4E-associated protein

CLU1 translation initiation factor eIF3 (p135 subunit)

MYO2 myosin heavy chain

LAP4 aminopeptidase yscI precursor, vacuolar

HTB1 histone H2B

PPH21 protein ser/thr phosphatase PP2A-1

SAH1 S-adenosyl-L-homocysteine hydrolase

RET2 coatomer complex delta chain

HXT5 member of the hexose transporter family

FZO1 required for biogenesis of mitochondria

CIC1 adaptor protein specifically linking the 26S proteasome to its substrate, the SCF component CDC4

RRP12 hypothetical protein

NOP2 nucleolar protein

ADO1 strong similarity to human adenosine kinase

SEH1 nuclear pore protein

GND1 6-phosphogluconate dehydrogenase

YDR1SRP54 signal recognition particle subunit

RRP13 similarity to zebrafish essential for embryonic development gene pescadillo

SIT4 ser/thr protein phosphatase

MRT4 mRNA turnover 4

TPD3 ser/thr protein phosphatase 2A, regulatory chain A

TIF6 translation initiation factor 6 (eIF6)

YOR283w weak similarity to phosphoglycerate mutases

GLT1 glutamate synthase (NAPDPH) (GOGAT)

PRP46 strong similarity to A.thaliana PRL1 and PRL2 proteins

SEC21 coatomer complex gamma chain (gamma-COP) of secretory pathway vesicles

SEC27 coatomer complex beta' chain (beta'-cop) of secretory pathway vesicles

ACO1 aconitate hydratase

AYR1 1-Acyldihydroxyacetone-phosphate reductase

ERG27 3-keto sterol reductase

TIF35 translation initiation factor eIF3 (p33 subunit)

FAA4 long-chain-fatty-acid--CoA ligase

ARG4 arginosuccinate lyase

RMT2 N-delta-arginine methyltransferase

NDH1 mitochondrial cytosolically directed NADH dehydrogenase

CDC39 nuclear protein

GCN1 translational activator

FPR4 nucleolar peptidylprolyl cis-trans isomerase (PPIase)

SSQ1 mitochondrial heat shock protein 70

UBR1 ubiquitin-protein ligase

HAS1 helicase associated with SET1P

YJR070c similarity to C.elegans hypothetical protein C14A4.1

YER182w similarity to hypothetical protein SPAC3A12.08 - S. pombe

HXT7 high-affinity hexose transporter

DPM1 dolichyl-phosphate beta-D-mannosyltransferase

NOG1 similarity to M.jannaschii GTP-binding protein

TIF4631 mRNA cap-binding protein (eIF4F), 150K subunit

CAF40 strong similarity to C.elegans hypothetical protein

CCT7 component of chaperonin-containing T-complex

STE4 GTP-binding protein beta subunit of the pheromone pathway

PRO3 delta 1-pyrroline-5-carboxylate reductase

GSF2 involved in glucose repression

RAD28 protein involved in the same pathway as RAD26P, has beta-transducin (WD-40) repeats

ACC1 acetyl-CoA carboxylase

SOF1 involved in 18S pre-rRNA production

POP2 required for glucose derepression

TIF34 translation initiation factor eIF3, p39 subunit

SAP190 SIT4P-associated protein

YMR196w strong similarity to hypothetical protein Neurospora crassa

HEM15 ferrochelatase precursor

EGD2 alpha subunit of the nascent polypeptide-associated complex

QCR2 ubiquinol--cytochrome-c reductase 40KD chain II

CAF4 CCR4 associated factor

PIB2 phosphatidylinositol 3-phosphate binding

KRE31 similarity to M.sexta steroid regulated MNG10 protein

YGR090w similarity to PIR:T40678 hypothetical protein SPBC776.08c S. pombe

GPA1 GTP-binding protein alpha subunit of the pheromone pathway

SEC6 protein transport protein

DUN1 protein kinase

PFK2 6-phosphofructokinase, beta subunit

NOC2 crucial for intranuclear movement of ribosomal precursor particles

SEC18 vesicular-fusion protein, functional homolog of NSF

RVS161 similarity to human amphiphysin and RVS167P

YKR007w weak similarity to Streptococcus protein M5 precursor

PPH22 protein ser/thr phosphatase PP2A-2

PWP1 similarity to human IEF SSP 9502 protein

CDC55 ser/thr phosphatase 2A regulatory subunit B

NEW1 similarity to translation elongation factor eEF3

POX1 acyl-CoA oxidase

BTN2 Gene/protein whose expression is elevated in a btn1 minus/Btn1p lacking yeast strain

COP1 coatomer complex alpha chain of secretory pathway vesicles

YJR072c strong similarity to C.elegans hypothetical protein and similarity to YLR243w

CDC33 translation initiation factor eIF4E

RPT3 26S proteasome regulatory subunit

SAP185 SIT4P-associating protein

YKL056c strong similarity to human IgE-dependent histamine-releasing factor

SSD1 involved in the tolerance to high concentration of Ca2+

GCD11 translation initiation factor eIF2 gamma chain

CYS3 cystathionine gamma-lyase

SAP155 SIT4P-associated protein

YNL181w similarity to hypothetical S. pombe protein

RPE1 D-ribulose-5-phosphate 3-epimerase

SPB4 ATP-dependent RNA helicase of DEAH box family

SIK1 involved in pre-rRNA processing

NOC3 required for maturation and intranuclear transport of pre-ribosomes

IDH1 isocitrate dehydrogenase (NAD+) subunit 1, mitochondrial

SEC28 epsilon-COP coatomer subunit

YTM1 microtubule-interacting protein

BUD3 budding protein

PCT1 cholinephosphate cytidylyltransferase

EBP2 required for pre-rRNA processing and ribosomal subunit assembly

UBR2 similarity to ubiquitin--protein ligase UBR1P

MET6 5-methyltetrahydropteroyltriglutamate--homocysteine methyltransferase

PDA1 pyruvate dehydrogenase (lipoamide) alpha chain precursor

SCS2 required for inositol metabolism

YNL110c weak similarity to fruit fly RNA-binding protein

YDL204w similarity to hypothetical protein YDR233c

HCH1 strong similarity to YDR214w

YDR214w similarity to hypothetical protein YNL281w

RPT4 26S proteasome regulatory subunit

YGL068w strong similarity to Cricetus mitochrondial ribosomal L12 protein

EXG1 exo-beta-1,3-glucanase (I/II), major isoform

ERV46 component of copii vesicles involved in transport between the ER and golgi complex

FAA1 long-chain-fatty-acid--CoA ligase

NAN1 weak similarity to fruit fly TFIID subunit p85

RRP5 processing of pre-ribosomal RNA

YGR086c strong similarity to hypothetical protein YPL004c

BGL2 endo-beta-1,3-glucanase of the cell wall

CCR4 transcriptional regulator

GSP1 GTP-binding protein of the ras superfamily

YCK2 casein kinase I isoform

YCR076c weak similarity to latent transforming growth factor beta binding protein 3' H. sapiens

PRP43 involved in spliceosome disassembly

SEN2 tRNA splicing endonuclease beta subunit

GPT2 strong similarity to SCT1P

ADE17 5-aminoimidazole-4-carboxamide ribotide transformylase

RLP7 strong similarity to mammalian ribosomal L7 proteins

YBL029w hypothetical protein

CDC14 dual specificity phosphatase

YKR046c hypothetical protein

GAL7 UDP-glucose--hexose-1-phosphate uridylyltransferase

CSR1 phosphatidylinositol transfer protein

STI1 stress-induced protein

YIL136W protein of the outer mitochondrial membrane

YDR128w weak similarity to SEC27P, YMR131c and human retinoblastoma-binding protein

RPN7 subunit of the regulatory particle of the proteasome

HCR1 component of translation initiation factor eIF3, has similarity to human eIF3 p35 subunit

YER049w strong similarity to hypothetical S.pombe protein YER049W

HIR1 histone transcription regulator

YJL109c weak similarity to ATPase DRS2P

YGL041c weak similarity to YJL109c

Cct7p

TAP42 component of the Tor signaling pathway

CCT6 component of chaperonin-containing T-complex (zeta subunit)

Cct8p

YHB1 flavohemoglobin

RVB2 RUVB-like protein

ARP2 actin-like protein

SMC3 required for structural maintenance of chromosomes

PFK1 6-phosphofructokinase, alpha subunit

EFT1 translation elongation factor eEF2

RPT5 26S proteasome regulatory subunit

ARO1 arom pentafunctional enzyme

ARC35 subunit of the ARP2/3 complex

SMC1 chromosome segregation protein

GCN1 translational activator

CCT5 T-complex protein 1, epsilon subunit

HSC82 heat shock protein

HHF2 histone H4

ARP3 actin related protein

EFT2 translation elongation factor eEF2

ARC40 ARP2/3 protein complex subunit, 40 kilodalton

RPT6 26S proteasome regulatory subunit

IDH2 isocitrate dehydrogenase (NAD+) subunit 2, mitochondrial

ARC18 subunit of the ARP2/3 complex

NOP12 weak similarity to M.sativa NUM1, hnRNP protein from C. tentans and D. melanogaster, murine/bovine poly(A) binding protein II, and NSR1P

ARC19 subunit of the ARP2/3 complex

ARC15 subunit of the ARP2/3 complex

GFA1 glucosamine--fructose-6-phosphate transaminase

RPT1 26S proteasome regulatory subunit

http://mips.gsf.de/proj/yeast/CYGD/interaction/